Konus catalog of short GRBs

E.P.Mazets, R.L. Aptekar, D.D. Frederiks, S.V. Golenetskii,
V.N. Il'inskii and V.D. Palshin

Ioffe Physico-Technical Institute, Russian Academy of Sciences

St.Petersburg, 194021, Russia

T.L.Cline and P.S. Butterworth

NASA Goddard Space Flight Center, Greenbelt, Maryland, 20771, USA

ABSTRACT

Observational data on the short GRBs obtained with the GGS-Wind Konus experiment in the period from 1994 to 2002 are presented. The catalog currently includes 130 events, detailing their appearance rate, time histories, and energy spectra. Evidence of an early X-ray and gamma-ray afterglow for some of the short GRBs is discussed.

1. INTRODUCTION

The gamma-ray burst (GRB) duration has a bimodal distribution (Mazets et al. 1981; Norris et al. 1984; Hurley 1992; Kouveliotou et al. 1993). This indicates the existence of two distinct morphological classes of events, namely short-duration (< 2 s) bursts and long-duration (> 2 s) bursts. Approximately 20 per cent of the observed bursts are short. Their energy spectra are usually harder than the spectra of long bursts (Kouveliotou et al. 1993).

The catalog contains data on 130 short GRBs observed with the Konus-Wind experiment on the Wind spacecraft in 1994–2002. The catalog presents time histories, energy spectra, fluences, peak fluxes, spectral parameters, and hardness ratios. Most of hardness ratios reveal spectral variability. The catalog is available electronically at http://www.ioffe.ru/LEA/shortGRBs/Catalog/.

Searches for the optical and radio afterglow of short GRBs have been carried out in only a few cases. Four GRBs were localized with high accuracy by the Interplanetary Network (IPN) (Hurley et al. 2002). No optical and radio afterglow emission was detected for these four events. No X-ray counterparts have been detected so far for the short bursts localized by Beppo-SAX (Gandolfi et al. 2000) or by HETE-2 (Lamb et al. 2002). The rapid follow-up observations have resulted in only upper limits on the brightness of the afterglows from these GRBs.

At the same time early X-ray and gamma-ray afterglows of short bursts were detected in a number cases by the GRB detectors themselves, in time intervals from seconds to tens of seconds after the trigger. BATSE observations showed that such a weak afterglow exists for some of the short bursts, lasting several tens seconds (Burenin, 2000; Lazatti et al. 2001; Connaughton, 2002). The afterglows of short GRBs were also detected by the Konus-Wind experiment. Afterglow emission in the energy range bellow 1 MeV is seen for about 10 per cent of events. These bursts are included in the catalog. A statistical analysis of burst sampling reveals that the afterglow is a more common feature of short GRBs. These results will be discussed in more detail elsewhere.

2. OBSERVATIONS

The Konus-Wind instrument is a gamma-ray spectrometer consisting of two identical gamma-ray detectors S1 and S2 which observe the southern and northern ecliptic hemispheres respectively in all-sky monitoring mode. Each detector contains a NaI(Tl) crystal, 5" in diameter and 3" in height, in a housing with an entrance window made of beryllium. The nominal energy range of gamma-ray measurements covers the interval from 12 keV up to 10 MeV. The instrument operates in two main modes: background measurements and triggered burst detections. While in the "background" mode, the count rates are recorded in three energy windows G1 (12–45 keV), G2 (45–190 keV), and G3 (190–770 keV). The time resolution of such observations is 2.94 s. When the count rate in the G2 window exceeds the 6σ trigger threshold the instrument is switched into the "burst" mode. The count rates in the three energy windows are recorded with time resolution from 2 ms up to 256 ms. These time histories, of total duration 230 s, also include 0.512 s of pre-trigger history. The spectral measurements are carried out in two energy intervals, 12–760 keV and 200 keV – 10 MeV, with 64 spectra being recorded for each interval over the 63-channel quasilog energy scale. The first four spectra are measured with a fixed accumulation time of 64 ms in order to study short bursts. An adaptive system varies the accumulation time for next spectra from 256 ms to 8.192 s depending on the current count rate in the G2 window. A detailed description of the Konus-Wind instrument and its operational modes is given in Aptekar et al. (1995). The gain of the Konus-Wind detectors has slowly decreased during the long period of operation. Instrumental control of the gain was exhausted in 1997. The low energy threshold grown to 20 keV for the S1 detector and to 17.5 keV for the S2 detector, from the original 12 keV. For convenience of comparison, the data for fluences and peak fluxes have been reduced to a 15 keV threshold. Results of the Konus-A experiments were used for the analysis of several short bursts in the absence of the Konus-Wind data. The spectrometric detectors of the Konus-A instruments are identical to the Konus-Wind detectors. The Konus-A experiments were carried out on board the low-orbiting spacecraft Kosmos-2326 (1995–1997) and Kosmos-2367 (1999–2001).

3. DATA PROCESSING

The process of gamma-ray photon spectral deconvolution from the count rate spectra is based on the Monte Carlo response function calculations and the results of the laboratory calibration described by Terekhov et al. (1998). The response functions of the Konus-Wind detectors were calculated in the energy range 5 keV – 10 MeV for angles of incidence in the 0°–90° range. The angles between the GRB direction and the detector's axis (GRB angles) have been determined using IPN or BATSE localizations. The ratio of the S1 and S2 detector count rates were used to estimate the GRB angle in those cases when GRBs were not localized. The dependence of the GRB angle on the S1/S2 ratio was derived from bursts with known localization. It allows the evaluation of the GRB angle for bursts with an unknown localization with an accuracy of 5°–20°. The deconvolution procedure (Terekhov et al. 1998) permits fits to the bursts spectra using different proposed models or their combinations. Most of the appropriate spectral models of GRBs were considered by Preece et al. (2000). For convenience, we follow their notation:

1. The power law model (PL):

$$f(E) = \mathrm{d}N(E)/\mathrm{d}E = A(E/100)E^{\alpha}$$

2. The broken power law model (BPL):

$$f(E) = \begin{cases} A(E/100)^{\alpha}, & \text{if } E \leq E_0 \\ A(E_0/100)^{\alpha}(E/E_0)^{\beta}, & \text{if } E > E_0 \end{cases}$$

3. The COMP model:

$$f(E) = A(E/100)\exp(-E/E_0)$$

4. The GRB model:

$$f(E) = \begin{cases} A(E/100)^{\alpha}\exp(-E/E_0), & \text{if } E \leq (\alpha-\beta)E_0 \\ A[(\alpha-\beta)E_0/100]^{(\alpha-\beta)}\exp(\beta-\alpha)(E/100)^{\beta}, & \text{if } E > (\alpha-\beta)E_0 \end{cases}$$

where: A is the intensity coefficient in photons $s^{-1}cm^{-2}keV^{-1}$, E_b is the break energy in keV, E_0 is the energy parameter in keV and α, β are the spectral indexes, E is the photon energy in keV.

4. CATALOG

4.1. Catalog Structure

The catalog contains tables, a set of figures with the time histories and energy spectra, and some statistical distributions.

Table 1 lists the main characteristics of the events. The first three columns specify burst order numbers, burst names according to the date of appearance, and trigger times T_0. The burst duration T_{90} measures the duration of the time interval during which 90% of the total observed counts in the energy windows G2+G3 were detected. The next two columns present values of peak fluxes and fluences. GRB fluences are calculated for emission observed above 15 keV. Peak fluxes are calculated using an average spectrum accumulated in the time interval around the peak. The seventh column presents the energy interval for which fluence and peak flux have been calculated. The last column presents information about the burst localization. The events localized by BATSE are marked "B" with the trigger number (Paciesas et al. 1999). The bursts localized by the IPN have the references on the Gamma-Ray Burst Coordinates Network (GCN) Circulars with the list of spacecraft or experiments which detected the burst (U—Ulysses, K—Konus ("Wind"), N—NEAR).

Table 2 contains the spectral data. The first two columns indicate the burst names and trigger times. The third and fourth columns indicate the start and stop times of the spectral measurements. The fifth column contains the energy interval in which the energy spectra were fitted. The sixth column indicates the type of spectral model used for fitting. The last four columns contain the parameters of spectral model [1]: A, α, E_0, β (in the notation of section 3).

A set of figures, from Fig. 1 up to Fig. 164, includes time histories and deconvolved background-subtracted photon spectra (panels "a" and "b"), respectively, for observed bursts. Time histories are usually given for the three energy windows G1, G2, and G3 together with the count rate ratios G2/G1 and G3/G2. Energy spectra were accumulated in the indicated time intervals. On the time history graphs, these intervals are marked by two vertical dotted lines.

[1] In case the error of paremeter is not given, the parameter was fixed when fitting

4.2. Afterglows of short bursts

The early afterglows of short GRBs are observed for 11 of 130 short bursts. These afterglows appear in time intervals from several seconds up to 100 seconds after the trigger. Characteristics of these bursts and their afterglows are collected in Tables 3 and 4.

Table 3 contains the data for fluences and peak fluxes. The first three columns specify burst names according to the date of appearance, the figure number on which time history and spectral data are displayed, and trigger times T_0. In the next columns, one of two lines presents characteristics of the burst. The other line contains characteristics of its afterglow. The energy intervals in which parameters of the burst and its afterglow have been determined are shown in the fourth column. The following columns present the time intervals of the fluence measurements, the fluences, the time intervals of the peak flux measurements and the peak fluxes.

Table 4 summarizes the spectral parameters of the bursts and their afterglows. Its first columns present burst names and trigger times T_0, starting and ending times of the spectral measurements, and energy range covered. The next columns indicate the spectral model used for fitting, and parameters α, β and E_0 (in the notation of section 3). The multichannel energy spectra were obtained only in the initial stage of the afterglow for five of the eleven events in Table 4. These spectra are shown in Figures 93, 99, 103, 117 and 131. In the other cases, the spectra were too weak for meaningful values to be obtained. In these cases, accumulated count rates in the energy windows G1, G2, and G3 were used to estimate spectra using the procedure developed for the analysis of fast spectral variability of GRB emission (Mazets et al. 2000). These estimates are also given in Table 4.

An early afterglow search for all the other short bursts has been carried out using the background mode data. Summing the time histories for numbers of events has permitted improved statistics which reveal the existence of an afterglow in 60 per cent of the strongest events at time interval up to 250 seconds after the burst trigger. This results, suggesting that an early afterglow is a typical feature of short bursts will be considered further elsewhere.

Here we discuss only two examples, which show that the distinguishing between short bursts with an afterglow and the more common long bursts may not always be easy. The event GRB 000727 begins with a typical short hard peak, but 7 seconds later a second short peak appears with a power law energy spectrum that is typical of the final stage in the evolution of long bursts. GRB 000218 may be either a short burst with an afterglow or a long burst with an intense initial stage.

5. CONCLUDING REMARKS

Some statistical distributions of the main characteristics of the short GRBs are presented in Figures 165–172. The electronic version of the catalog is available at http://www.ioffe.ru/LEA/shortGRBs/Catalog/. It contains detailed information about the characteristics of the short GRBs archived as ASCII files.

This work was supported by Russian Aviation and Space Agency Contract, and RFBR grant N 01-02-17808.

REFERENCES

Aptekar, R. L., et al. 1995, Space Sci. Rev., 71, 265

Burenin, R. A. 2001, Astronomy Letters, 26, 269

Connaughton, V. 2002, ApJ, 567, 1028

Gandolfi, G., et al. 2000, in AIP Conf.Proc. 526, Gamma-Ray Bursts, ed. R. Kippen, R. Mallozzi, & G. J. Fishman (N.Y.: AIP), 23

Hurley, K. 1992, in Gamma-Ray Bursts, Eds. W. Paciesas & G. Fishman, Huntswille, AL, AIP Conf. Proc. 265 (AIP Press-N.Y.), 304

Hurley, K., et al. 2002, ApJ, 567, 447

Kouveliotou, C., et al. 1993, ApJ, 413, L101

Lamb, D. Q., et al. 2002, ApJ(in press), astro-ph/0206151, v.2.

Lazzati, D., Ramirez-Ruiz, E. & Chisellini, G. 2001, A&A, 379, L39

Mazets, E. P., et al. 1981, Ap&SS, 80, 119

Mazets, E. P., et al. 2000, in Gamma-Ray Bursts in the Afterglow Era, Proc. of the International Workshop, Rome, Italy, October 2000, Eds. E. Costa, F. Frontera, & J. Hjorth (Berlin: Springer), 9

Norris, J., et al. 1984, Nature, 308, 434

Paciesas, W. S., et al. 1999, ApJS, 122, 465, http://www.batse.msfc.nasa.gov/batse/grb/catalog/

Preece, R. D., et al. 2000, ApJS, 126, 19

Terekhov, M., et al. 1998, in AIP Conf. Proc., 428, 4th Huntsville Symposium on Gamma-Ray Bursts, ed. C. Meegan, R. Preece, & T. Koshut (N.Y.: AIP), 894

Table 1. Short GRBs: basic data

N	Burst name	T_0 s UT	T_{90} s	Peak Flux erg cm^{-2} s^{-1}	Fluence erg cm^{-2}	Energy interval keV	Localization
1	950210	8424.148	0.14	7.2×10^{-6}	7.1×10^{-7}	15–2000	B (tr. 3410)
2	950211a	8697.749	0.12	6.4×10^{-5}	3.0×10^{-6}	15–5000	B (tr. 3412)
3	950414	40882.798	0.14	1.2×10^{-5}	8.2×10^{-7}	15–1000	···
4	950419a	8628.860	1.04	3.5×10^{-5}	1.8×10^{-5}	15–5000	···
5	950520	83271.404	1.10	9.5×10^{-6}	2.0×10^{-6}	15–5000	···
6	950610b	19096.034	0.07	1.6×10^{-5}	7.1×10^{-7}	15–1000	···
7	950726	51579.299	0.96	2.4×10^{-6}	1.7×10^{-6}	15–5000	B (tr. 3709)
8	950805b	13454.144	0.61	3.4×10^{-5}	1.8×10^{-6}	15–5000	B (tr. 3736)
9	951013	57097.299	0.04	1.6×10^{-5}	4.4×10^{-7}	15–1000	···
10	951014a	13108.167	1.51	7.3×10^{-5}	2.9×10^{-5}	15–5000	···
11	960312	51579.299	0.19	2.1×10^{-6}	4.1×10^{-7}	15–1000	···
12	960319	51992.828	0.36	1.7×10^{-5}	2.7×10^{-6}	15–1000	B (tr. 5277)
13	960420	17324.809	0.30	9.6×10^{-6}	1.5×10^{-6}	15–1000	···
14	960519	15966.283	0.60	1.3×10^{-4}	1.2×10^{-5}	15–3000	···
15	960602	42664.032	0.28	9.6×10^{-6}	1.6×10^{-6}	15–1000	···
16	960610	84502.254	0.47	2.3×10^{-5}	5.0×10^{-6}	15–6000	···
17	960614	67654.516	0.12	2.3×10^{-5}	2.7×10^{-6}	15–2000	···
18	960803	67525.033	0.05	2.1×10^{-5}	8.9×10^{-7}	15–5000	B (tr. 5561)
19	960902	58097.128	1.57	1.0×10^{-5}	5.0×10^{-6}	15–2000	···
20	960908	25028.442	0.36	6.7×10^{-5}	1.2×10^{-5}	15–5000	···
21	961113	80522.580	0.25	1.1×10^{-5}	9.8×10^{-7}	15–1000	···
22	961123	80522.580	0.26	1.8×10^{-5}	1.6×10^{-6}	15–1000	···
23	961212	14870.487	0.86	6.5×10^{-5}	2.7×10^{-5}	15–8000	B (tr. 5711)
24	970222	86006.565	0.85	7.8×10^{-5}	8.9×10^{-6}	15–3000	···
25	970315b	30064.853	0.13	2.0×10^{-5}	1.5×10^{-6}	15–1000	B (tr. 6123)
26	970330	43988.805	0.52	7.9×10^{-6}	2.3×10^{-6}	15–1000	···
27	970427	45723.327	0.06	1.0×10^{-5}	3.9×10^{-7}	15–1000	B (tr. 6211)
28	970428	13365.268	0.62	2.8×10^{-5}	4.9×10^{-6}	15–3000	···
28	970506	56603.264	1.59	5.5×10^{-6}	4.5×10^{-6}	15–1000	···
31	970521	49991.214	0.31	1.5×10^{-5}	2.0×10^{-6}	15–3000	···
30	970608	49032.954	0.98	7.7×10^{-6}	4.0×10^{-6}	15–2000	···
32	970625a	23681.548	0.03	3.8×10^{-5}	9.4×10^{-7}	15–3000	···
33	970626	6239.033	0.13	1.7×10^{-5}	1.8×10^{-6}	15–5000	···
34	970704	4097.025	0.09	1.5×10^{-3}	4.2×10^{-5}	15–10000	B (tr. 6293)
35	970803	66535.704	0.15	8.4×10^{-6}	9.5×10^{-7}	15–1000	B (tr. 6325)
36	970902a	27561.329	0.44	1.3×10^{-5}	3.6×10^{-6}	15–5000	···
37	970921	83828.200	0.06	1.0×10^{-4}	4.5×10^{-6}	15–8000	···
38	971015	30459.796	0.12	1.9×10^{-5}	1.7×10^{-6}	15–2000	B (tr. 6436)
39	971031	23420.942	0.16	8.0×10^{-6}	1.3×10^{-6}	15–1000	···
40	971118	29008.529	0.08	2.7×10^{-6}	1.7×10^{-7}	15–1000	B (tr. 6486)
41	971218b	52503.029	1.06	6.7×10^{-6}	5.1×10^{-6}	15–2000	B (tr. 6535)
42	971230	83750.187	0.32	1.8×10^{-5}	1.7×10^{-6}	15–5000	···
43	980205	19785.239	1.42	3.7×10^{-4}	5.9×10^{-6}	15–5000	···
44	980218b	54768.157	0.28	4.5×10^{-6}	1.2×10^{-6}	15–2000	B (tr. 6606)
45	980228a	24244.602	0.45	3.2×10^{-5}	7.6×10^{-6}	15–2000	B (tr. 6617)
46	980302b	29955.993	0.30	6.2×10^{-6}	1.1×10^{-6}	15–1000	···
47	980310a	50261.054	0.80	5.3×10^{-6}	2.0×10^{-6}	15–2000	B (tr. 6635)
48	980330a	96.711	0.10	5.2×10^{-5}	3.0×10^{-6}	15–5000	B (tr. 6668)

Table 1—Continued

N	Burst name	T_0 s UT	T_{90} s	Peak Flux erg cm^{-2} s^{-1}	Fluence erg cm^{-2}	Energy interval keV	Localization
49	980331	61078.449	0.17	6.7×10^{-6}	1.1×10^{-6}	15–2000	B (tr. 6671)
50	980429	20492.079	0.18	1.7×10^{-5}	1.8×10^{-6}	15–2000	···
51	980430	59702.214	0.30	3.2×10^{-5}	6.5×10^{-6}	15–4000	···
52	980605	51131.976	0.13	9.4×10^{-5}	2.5×10^{-6}	15–5000	···
53	980610a	71546.850	0.86	6.0×10^{-6}	3.3×10^{-6}	15–4000	···
54	980610b	86195.164	0.31	1.5×10^{-5}	3.0×10^{-6}	15–4000	···
55	980619	47530.372	0.11	7.0×10^{-5}	3.5×10^{-6}	15–4000	···
56	980706a	57586.277	0.32	1.7×10^{-4}	4.0×10^{-5}	15–6000	B (tr. 6904)
57	980904	31349.014	0.05	3.5×10^{-5}	1.3×10^{-6}	15–2000	B (tr. 7063)
58	980908	82263.835	0.45	5.5×10^{-6}	1.1×10^{-6}	15–1500	···
59	980925a	17571.284	0.45	4.4×10^{-6}	1.7×10^{-6}	15–1500	···
60	981005	64826.466	0.84	5.7×10^{-6}	2.8×10^{-6}	15–2000	B (tr. 7142)
61	981102	28554.533	0.58	4.2×10^{-5}	1.5×10^{-5}	15–4000	···
62	981107	781.395	0.37	6.7×10^{-4}	9.9×10^{-5}	15–8000	···
63	981218	62134.933	0.30	2.8×10^{-6}	7.7×10^{-7}	15–2000	···
64	981221	9057.150	0.13	9.4×10^{-6}	8.5×10^{-7}	15–1000	B (tr. 7273)
65	981226	38822.991	0.64	6.1×10^{-6}	2.7×10^{-6}	15–1000	B (tr. 7281)
66	990105	31789.507	0.52	1.2×10^{-5}	1.9×10^{-6}	15–1000	B (tr. 7305)
67	990126	51844.333	0.23	3.6×10^{-5}	3.0×10^{-6}	15–2000	B (tr. 7353)
68	990206c	57061.328	0.17	7.6×10^{-6}	7.7×10^{-7}	15–1000	B (tr. 7375)
69	990207	69675.009	0.39	1.8×10^{-5}	1.9×10^{-6}	15–1500	···
70	990208	15166.066	0.53	3.1×10^{-6}	8.5×10^{-7}	15–1000	B (tr. 7378)
71	990313	33712.652	0.27	1.8×10^{-5}	1.5×10^{-6}	15–1000	···
72	990327	22911.102	0.08	1.6×10^{-4}	1.4×10^{-5}	15–5000	···
73	990405b	30059.858	0.49	4.8×10^{-6}	8.3×10^{-7}	15–2000	···
74	990415	2297.309	0.17	7.1×10^{-6}	1.2×10^{-6}	15–1000	···
75	990504	67586.484	0.08	1.5×10^{-5}	1.2×10^{-6}	15–2000	···
76	990516	86065.136	0.31	2.1×10^{-4}	5.8×10^{-5}	15–5000	B (tr. 7569)
77	990619	46930.367	1.53	3.8×10^{-6}	1.8×10^{-6}	15–1500	B (tr. 7610)
78	990712a	27915.510	0.64	5.3×10^{-5}	2.5×10^{-5}	15–3000	B (tr. 7647)
79	990719	61135.420	0.06	1.0×10^{-5}	5.4×10^{-7}	15–1000	···
80	990720	75941.940	0.87	3.5×10^{-6}	1.8×10^{-6}	15–1000	B (tr. 7663)
81	990806b	60168.676	0.14	9.3×10^{-6}	1.1×10^{-6}	15–1000	···
82	990828	70020.016	1.12	5.9×10^{-6}	2.1×10^{-6}	15–500	···
83	990831	41835.091	0.08	5.9×10^{-6}	3.8×10^{-7}	15–1000	···
84	991001	4950.128	0.82	2.9×10^{-6}	2.2×10^{-6}	15–1000	B (tr. 7781)
85	991002	82143.664	0.25	3.7×10^{-6}	7.4×10^{-7}	15–1000	B (tr. 7784)
86	991226b	83339.767	0.08	7.7×10^{-6}	3.9×10^{-7}	15–1000	···
87	000108	60487.439	0.72	3.1×10^{-6}	2.2×10^{-6}	15–1000	B (tr. 7939)
88	000212	61592.339	0.17	4.3×10^{-6}	5.2×10^{-7}	15–1000	···
89	000218	58744.596	0.90	8.5×10^{-5}	4.7×10^{-5}	15–6000	···
90	000326	19134.798	0.96	5.2×10^{-6}	3.5×10^{-6}	15–1000	IPN (U-K-N; GCN 618), B (tr. 8053)
91	000412	42174.189	0.52	2.0×10^{-6}	5.7×10^{-7}	15–1000	B (tr. 8073)
92	000420a	42271.144	0.20	1.6×10^{-5}	2.1×10^{-6}	15–3000	···
93	000513	40894.793	0.35	4.1×10^{-6}	8.1×10^{-7}	15–1000	B (tr. 8104)
94	000526	84494.896	0.27	8.9×10^{-5}	1.5×10^{-5}	15–5000	···
95	000607	8689.115	0.09	1.2×10^{-4}	5.4×10^{-6}	15–3000	IPN (U-K-N; GCN 693)
96	000608	70497.255	0.18	1.7×10^{-5}	2.7×10^{-6}	15–1000	···

Table 1—Continued

N	Burst name	T_0 s UT	T_{90} s	Peak Flux erg cm^{-2} s^{-1}	Fluence erg cm^{-2}	Energy interval keV	Localization
97	000623	3887.359	0.17	5.9×10^{-6}	8.1×10^{-7}	15–3000	···
98	000701b	25961.013	0.94	2.6×10^{-5}	1.3×10^{-5}	15–3000	···
99	000707a	17372.072	0.21	5.1×10^{-6}	8.4×10^{-7}	15–1000	···
100	000727	70955.931	0.80	5.2×10^{-5}	1.9×10^{-5}	15–1000	IPN (U-K-N; GCN 754)
101	000818	72547.04	1.35	5.6×10^{-6}	2.3×10^{-6}	15–1000	···
102	000928	6285.374	0.22	2.4×10^{-5}	4.0×10^{-6}	15–3000	···
103	001022	20905.666	0.12	5.0×10^{-5}	3.5×10^{-6}	15–3000	···
104	001025c	71369.963	0.48	2.2×10^{-5}	5.9×10^{-6}	15–5000	IPN (U-N-K; GCN 865)
105	001204	28869.372	0.27	9.0×10^{-6}	1.7×10^{-6}	15–5000	IPN (U-N-S-K; GCN 895, 897)
106	001207a	8815.958	0.17	7.7×10^{-6}	7.4×10^{-7}	15–1000	···
107	001207b	34185.588	0.83	2.5×10^{-6}	2.2×10^{-6}	15–1000	···
108	010119	37179.556	0.18	3.6×10^{-5}	2.4×10^{-6}	15–5000	IPN (U-N-K; GCN 916)
109	010308	56338.468	0.85	9.6×10^{-6}	5.3×10^{-6}	15–2000	···
110	010420a	30786.674	0.01	1.2×10^{-5}	2.3×10^{-7}	15–1000	···
111	010427	67452.969	0.69	2.6×10^{-5}	5.4×10^{-6}	15–3000	···
112	010616	23724.028	0.10	1.8×10^{-5}	1.5×10^{-6}	15–1000	···
113	010624	48929.130	0.64	3.8×10^{-6}	1.7×10^{-6}	15–1000	···
114	010628a	4206.816	0.96	4.1×10^{-5}	1.3×10^{-5}	15–5000	···
115	011024	74609.296	0.61	4.1×10^{-6}	2.9×10^{-6}	15–1000	···
116	011101	34754.534	0.46	4.8×10^{-6}	2.2×10^{-5}	15–3000	···
117	020116	78766.919	0.08	···	···	···	···
118	020117	67773.429	0.47	2.0×10^{-4}	2.7×10^{-4}	15–1000	···
119	020218a	31263.113	0.09	···	···	···	···
120	020306	68280.713	0.15	3.8×10^{-5}	4.7×10^{-6}	15–6000	···
121	020326	39182.941	0.12	8.8×10^{-6}	9.3×10^{-7}	15–1000	···
122	020426	86171.048	0.19	···	···	···	···
123	020504	55835.141	1.05	···	2.8×10^{-5}	15–5000	···
124	020509	74.563	1.08	···	···	···	···
125	020525a	16014.630	0.18	1.5×10^{-5}	2.0×10^{-6}	15–2000	···
126	020602b	63030.315	0.46	8.0×10^{-6}	1.1×10^{-6}	15–1000	···
127	020715a	54866.135	0.43	9.0×10^{-6}	1.4×10^{-6}	15–2000	···
128	020731a	1635.905	0.12	2.4×10^{-5}	3.1×10^{-6}	15–2000	···
129	020731b	50231.739	0.29	3.4×10^{-6}	9.5×10^{-7}	15–1000	···
130	020828	20737.981	0.70	1.1×10^{-5}	4.0×10^{-6}	15–3000	···

Table 2. Short GRBs: spectral data

Burst name	T_0	Time interval Start	Stop	Energy interval	Model[1]	A photons	α	E_0	β
	s UT	s	s	keV		cm^{-2} s^{-1} keV^{-1}		keV	
950210	8424.148	0	0.128	15–2000	GRB	$(3.8 \pm 0.5) \times 10^{-1}$	-0.20	$(7.4 \pm 0.7) \times 10^{1}$	-2.95 ± 0.58
950211a	8697.749	0	0.128	15–5000	GRB	$(3.4 \pm 0.5) \times 10^{-1}$	-0.31 ± 0.14	$(1.7 \pm 0.3) \times 10^{2}$	-2.69 ± 0.38
950419a	8628.860	0	0.256	15–5000	GRB	$(1.7 \pm 0.1) \times 10^{-1}$	0.02 ± 0.17	$(2.4 \pm 0.4) \times 10^{2}$	-2.69 ± 0.38
		0.256	8.448	15–5000	GRB	$(1.8 \pm 0.3) \times 10^{-2}$	-0.29 ± 0.24	$(1.9 \pm 0.4) \times 10^{2}$	-2.70
950520	83271.404	0	0.064	15–5000	COMP	$(7.3 \pm 7.7) \times 10^{-2}$	-0.70 ± 0.25	$(4.5 \pm 2.1) \times 10^{2}$	···
950726	51579.299	0	0.256	15–5000	COMP	$(4.0 \pm 3.9) \times 10^{-2}$	-0.99 ± 0.27	$(2.4 \pm 1.2) \times 10^{2}$	···
950805b	13454.144	0	0.064	15–5000	COMP	$(9.6 \pm 5.3) \times 10^{-2}$	-0.93 ± 0.13	$(1.1 \pm 0.5) \times 10^{3}$	···
951014a	13108.167	0	0.256	15–5000	GRB	$(3.6 \pm 0.4) \times 10^{-1}$	-0.17 ± 0.13	$(2.1 \pm 0.3) \times 10^{2}$	-2.12 ± 0.12
		0.256	0.512	15–5000	GRB	$(4.8 \pm 0.4) \times 10^{-1}$	-0.55 ± 0.10	$(2.4 \pm 0.4) \times 10^{2}$	-2.25 ± 0.14
		0.512	7.936	15–3000	GRB	$(1.8 \pm 0.2) \times 10^{-2}$	-1.36 ± 0.12	$(4.5 \pm 1.8) \times 10^{2}$	-2.15 ± 0.10
960319	51992.828	0	0.256	15–3000	COMP	$(2.1 \pm 1.7) \times 10^{-2}$	-0.93 ± 0.17	$(1.6 \pm 1.3) \times 10^{3}$	···
960519	14766.283	0	8.448	15–3000	PL	$(3.5 \pm 1.5) \times 10^{-3}$	-1.24 ± 0.07	···	···
960610	84502.254	0	0.128	15–6000	COMP	$(4.1 \pm 0.5) \times 10^{-2}$	-0.50	$(9.4 \pm 1.6) \times 10^{2}$	···
960614	67654.516	0	0.064	15–2000	COMP	$(8.0 \pm 4.6) \times 10^{-2}$	-0.79 ± 0.14	1.0×10^{3}	···
960803	67525.033	0	0.064	15–5000	GRB	$(5.2 \pm 7.4) \times 10^{-1}$	-0.28 ± 0.82	$(5.8 \pm 5.2) \times 10^{1}$	-2.05 ± 0.23
960902	58097.128	0	0.128	15–2000	GRB	$(2.1 \pm 1.1) \times 10^{-1}$	-0.71 ± 0.38	$(1.4 \pm 1.0) \times 10^{2}$	-1.95 ± 0.18
		0.256	7.936	15–500	COMP	$(4.3 \pm 3.6) \times 10^{-2}$	-0.67 ± 0.26	$(6.7 \pm 1.5) \times 10^{1}$	···
960908	25028.442	0	0.128	15–3000	PL	$(1.3 \pm 0.2) \times 10^{-1}$	-1.32 ± 0.03	···	···
		0.128	0.256	15–3000	PL	$(1.7 \pm 0.2) \times 10^{-1}$	-1.62 ± 0.03	···	···
961212	14870.487	0	0.512	15–8000	GRB	$(1.7 \pm 0.1) \times 10^{-1}$	-0.89 ± 0.07	$(4.7 \pm 0.9) \times 10^{2}$	-2.05
		0.512	8.704	15–5000	COMP	$(7.3 \pm 1.5) \times 10^{-3}$	-1.58 ± 0.04	1.0×10^{3}	···
970222	86006.565	0	0.128	15–3000	GRB	$(1.7 \pm 0.4) \times 10^{-1}$	-0.51 ± 0.21	$(2.4 \pm 1.0) \times 10^{2}$	-1.85 ± 0.21
		0.256	8.448	15–3000	BPL	$(3.5 \pm 0.3) \times 10^{-3}$	-0.99 ± 0.09	3.6×10^{2}	-2.30
970428	13365.268	0	0.256	15–5000	COMP	$(6.1 \pm 2.6) \times 10^{-2}$	-0.82 ± 0.10	$(5.8 \pm 1.4) \times 10^{2}$	···
		0.256	8.448	15–5000	PL	$(2.6 \pm 1.1) \times 10^{-3}$	-1.29 ± 0.08	···	···
970506	56603.264	0	0.256	15–1000	GRB	1.2 ± 1.5	0.53 ± 0.87	$(3.8 \pm 1.8) \times 10^{1}$	-2.64 ± 0.25
		0.256	8.448	15–1000	PL	$(5.4 \pm 1.8) \times 10^{-3}$	-1.88 ± 0.08	···	···
970521	49991.214	0	0.256	15–3000	COMP	$(5.1 \pm 5.5) \times 10^{-2}$	-0.89 ± 0.25	$(4.8 \pm 2.3) \times 10^{2}$	···
970608	49032.954	0	0.256	15–2000	COMP	$(2.3 \pm 2.0) \times 10^{-2}$	-0.88 ± 0.19	$(1.5 \pm 1.2) \times 10^{3}$	···
970625a	23681.548	0	0.064	15–3000	COMP	$(6.0 \pm 3.2) \times 10^{-2}$	-1.32 ± 0.10	1.5×10^{3}	···
970626	6239.033	0	0.128	15–5000	COMP	$(5.3 \pm 4.5) \times 10^{-2}$	-1.14 ± 0.19	$(1.4 \pm 1.2) \times 10^{3}$	···
970704	4097.025	0	0.064	15–10000	COMP	$(5.3 \pm 1.4) \times 10^{-1}$	-0.76 ± 0.05	$(2.5 \pm 0.4) \times 10^{3}$	···
		0.064	0.128	15–5000	GRB	$(8.2 \pm 1.5) \times 10^{-1}$	-0.18 ± 0.20	$(1.5 \pm 0.3) \times 10^{2}$	-2.72 ± 0.34
		0.128	0.192	15–1000	COMP	$(2.9 \pm 3.4) \times 10^{-1}$	-0.82 ± 0.39	$(5.7 \pm 2.0) \times 10^{1}$	···
970902a	27561.329	0	0.256	15–5000	COMP	$(5.3 \pm 3.4) \times 10^{-2}$	-0.87 ± 0.14	$(8.1 \pm 3.0) \times 10^{2}$	···
970921	83828.200	0	0.064	15–8000	GRB	$(3.8 \pm 0.5) \times 10^{-1}$	0.14 ± 0.27	$(2.1 \pm 0.5) \times 10^{2}$	-2.30
971015	30459.796	0	0.064	15–2000	COMP	$(7.4 \pm 4.5) \times 10^{-2}$	-1.08 ± 0.15	$(1.7 \pm 1.6) \times 10^{3}$	···
971218b	52503.029	0	0.256	15–2000	PL	$(3.8 \pm 1.5) \times 10^{-2}$	-1.45 ± 0.09	···	···
		0.256	8.448	15–1000	PL	$(2.4 \pm 1.2) \times 10^{-3}$	-1.42 ± 0.11	···	···
971230	83750.187	0	0.128	15–2000	PL	$(2.1 \pm 1.1) \times 10^{-2}$	-1.18 ± 0.09	···	···
980205[2]	19785.239	0	0.256	15–5000	COMP+	$(3.5 \pm 2.0) \times 10^{-2}$	-0.88 ± 0.09	2.0×10^{3}	···
					PL	$(4.6 \pm 0.3) \times 10^{-2}$	-2.3	···	···
		0.256	8.448	15–1000	PL	$(1.3 \pm 1.1) \times 10^{-3}$	-2.21 ± 0.23	···	···
980228a	24244.602	0	0.256	15–5000	GRB	$(6.9 \pm 0.8) \times 10^{-1}$	-0.53 ± 0.13	$(1.5 \pm 0.2) \times 10^{2}$	-3.46 ± 0.46
		0.256	8.448	15–2000	COMP	$(7.0 \pm 6.3) \times 10^{-3}$	-1.71 ± 0.24	$(5.9 \pm 5.5) \times 10^{2}$	···
980310a	50261.054	0	0.256	15–2000	COMP	$(4.0 \pm 1.3) \times 10^{-2}$	-1.74 ± 0.08	5.0×10^{2}	···
		0.256	8.448	15–2000	COMP	$(4.2 \pm 1.7) \times 10^{-3}$	-1.80 ± 0.10	5.0×10^{2}	···
980330a	96.711	0	0.064	15–5000	GRB	$(4.4 \pm 0.7) \times 10^{-1}$	-0.53 ± 0.21	$(2.4 \pm 0.7) \times 10^{2}$	-2.60 ± 0.45
980331	61078.449	0	0.128	15–2000	COMP	$(3.4 \pm 1.7) \times 10^{-2}$	-1.18 ± 0.10	1.0×10^{3}	···
980429	20492.079	0	0.192	15–2000	COMP	$(1.8 \pm 0.1) \times 10^{-1}$	-0.20	$(1.7 \pm 0.1) \times 10^{2}$	···
980430	59702.214	0	0.256	15–4000	COMP	$(5.4 \pm 2.2) \times 10^{-2}$	-0.67 ± 0.07	1.0×10^{3}	···
980605	51131.976	0	0.064	15–5000	COMP	$(5.0 \pm 5.6) \times 10^{-2}$	-0.74 ± 0.25	$(1.0 \pm 0.8) \times 10^{3}$	···
980610a	71546.850	0	0.256	15–4000	COMP	$(3.4 \pm 5.2) \times 10^{-2}$	-0.18 ± 0.34	$(2.9 \pm 1.0) \times 10^{2}$	···
980610b	86195.164	0	0.192	15–4000	COMP	$(4.4 \pm 4.5) \times 10^{-2}$	-1.04 ± 0.23	$(1.2 \pm 0.9) \times 10^{3}$	···
980619	47530.372	0	0.064	15–4000	COMP	$(4.1 \pm 0.7) \times 10^{-2}$	0.00	$(5.9 \pm 0.9) \times 10^{2}$	···
980706a	57586.277	0	0.256	15–6000	COMP	$(2.6 \pm 0.4) \times 10^{-1}$	-0.75 ± 0.03	$(1.3 \pm 0.1) \times 10^{3}$	···

Table 2—Continued

Burst name	T_0	Time interval Start	Stop	Energy interval	Model[1]	A photons	α	E_0	β
	s UT	s	s	keV		cm^{-2} s^{-1} keV^{-1}		keV	
		0.256	8.448	15–3000	PL	$(4.2 \pm 1.2) \times 10^{-3}$	-1.26 ± 0.05	···	···
980904	31349.014	0	0.064	15–2000	PL	$(2.6 \pm 0.3) \times 10^{-2}$	-1.50	···	···
980908	82263.835	0	0.256	15–1500	COMP	$(4.5 \pm 7.0) \times 10^{-2}$	-0.29 ± 0.37	$(1.9 \pm 0.7) \times 10^2$	···
980925a	17571.284	0	0.256	15–1500	PL	$(3.0 \pm 1.4) \times 10^{-2}$	-1.85 ± 0.10	···	···
981005	64826.466	0	0.256	15–2000	COMP	$(1.6 \pm 1.1) \times 10^{-2}$	-0.95 ± 0.13	8.0×10^2	···
981102	28554.533	0	0.256	15–4000	COMP	$(5.0 \pm 2.8) \times 10^{-2}$	-0.74 ± 0.12	$(1.4 \pm 0.5) \times 10^3$	···
981107	781.395	0	0.128	15–8000	COMP	$(8.4 \pm 7.7) \times 10^{-2}$	-0.08 ± 0.16	$(8.0 \pm 1.3) \times 10^2$	···
		0.128	0.256	15–8000	COMP	$(1.5 \pm 0.6) \times 10^{-1}$	-0.29 ± 0.07	$(1.6 \pm 0.2) \times 10^3$	···
		0.256	0.512	15–8000	GRB	$(1.9 \pm 0.1) \times 10^{-1}$	-0.64 ± 0.04	$(1.1 \pm 0.1) \times 10^3$	-3.09 ± 0.60
981218	62134.933	0	0.256	15–2000	COMP	$(2.4 \pm 3.0) \times 10^{-1}$	-0.09 ± 0.38	$(6.1 \pm 1.7) \times 10^1$	···
981221	9057.150	0	0.064	15–1000	PL	$(3.2 \pm 2.0) \times 10^{-2}$	-1.20 ± 0.11	···	···
981226	38822.991	0	0.256	15–1000	COMP	$(1.1 \pm 0.9) \times 10^{-1}$	-1.21 ± 0.21	$(3.5 \pm 1.5) \times 10^2$	···
		0.256	8.448	15–500	PL	$(2.5 \pm 0.3) \times 10^{-3}$	-2.30 ± 0.50	···	···
990126	51844.333	0	0.064	15–2000	PL	$(3.7 \pm 2.9) \times 10^{-2}$	-1.05 ± 0.13	···	···
990207	69675.009	0	0.128	15–1500	COMP	$(6.7 \pm 3.4) \times 10^{-2}$	-0.66 ± 0.09	5.0×10^2	···
990313	33712.652	0	0.128	15–2000	GRB	$(1.8 \pm 0.5) \times 10^{-1}$	-1.08 ± 0.18	$(2.0 \pm 0.9) \times 10^2$	-2.43 ± 0.41
990327	22911.102	0	0.064	15–5000	COMP	$(1.7 \pm 0.9) \times 10^{-1}$	-0.86 ± 0.11	$(2.1 \pm 0.8) \times 10^3$	···
		0.256	16.640	15–5000	COMP	$(6.9 \pm 3.2) \times 10^{-3}$	-1.39 ± 0.11	$(1.2 \pm 0.7) \times 10^3$	···
990405b	30059.858	0	0.256	15–2000	COMP	$(3.8 \pm 2.0) \times 10^{-2}$	-1.64 ± 0.16	$(4.5 \pm 3.2) \times 10^2$	···
990415	2297.309	0	0.128	15–1000	COMP	$(5.6 \pm 9.9) \times 10^{-2}$	0.21 ± 0.40	$(2.0 \pm 0.6) \times 10^2$	···
990504	67586.484	0	0.064	15–2000	COMP	$(8.7 \pm 6.5) \times 10^{-2}$	-0.94 ± 0.18	$(6.6 \pm 3.8) \times 10^2$	···
990516	86065.136	0	0.064	15–5000	COMP	$(6.7 \pm 4.5) \times 10^{-2}$	-1.26 ± 0.16	$(1.9 \pm 2.4) \times 10^3$	···
		0.128	0.256	15–6000	COMP	$(1.7 \pm 0.6) \times 10^{-1}$	-0.60 ± 0.07	$(1.1 \pm 0.2) \times 10^3$	···
		0.256	8.448	15–5000	PL	$(3.8 \pm 1.5) \times 10^{-3}$	-1.60 ± 0.08	···	···
		8.448	33.024	15–5000	PL	$(2.8 \pm 0.8) \times 10^{-3}$	-1.72 ± 0.06	···	···
990619	46930.367	0	0.256	15–1500	COMP	$(6.0 \pm 6.4) \times 10^{-2}$	-0.59 ± 0.27	$(1.9 \pm 0.6) \times 10^2$	···
990712a	27915.510	0	0.256	15–5000	COMP	$(6.3 \pm 4.3) \times 10^{-2}$	-0.20 ± 0.13	$(6.1 \pm 1.0) \times 10^2$	···
		0.256	8.448	15–3000	COMP	$(5.4 \pm 2.2) \times 10^{-3}$	-0.97 ± 0.07	1.5×10^3	···
		24.832	41.216	15–1000	PL	$(3.1 \pm 1.6) \times 10^{-3}$	-1.98 ± 0.11	···	···
990719	61135.420	0	0.064	15–1000	COMP	$(1.1 \pm 1.5) \times 10^{-1}$	-0.76 ± 0.34	$(2.2 \pm 1.0) \times 10^2$	···
990720	75941.940	0	0.256	15–1000	COMP	$(4.0 \pm 3.1) \times 10^{-2}$	-1.01 ± 0.20	$(4.4 \pm 2.2) \times 10^2$	···
990806b	60168.676	0	0.128	15–1000	COMP	$(2.4 \pm 4.5) \times 10^{-2}$	-0.28 ± 0.38	$(5.2 \pm 2.6) \times 10^2$	···
990828	70020.016	0	0.256	15–500	COMP	$(2.5 \pm 3.1) \times 10^{-1}$	-0.49 ± 0.40	$(5.2 \pm 1.7) \times 10^1$	···
		0.256	8.448	15–500	PL	$(2.6 \pm 1.1) \times 10^{-3}$	-1.72 ± 0.10	···	···
991001	4950.128	0	0.256	15–1000	COMP	$(4.5 \pm 3.3) \times 10^{-2}$	-1.59 ± 0.21	$(4.7 \pm 3.8) \times 10^2$	···
		0.256	8.448	15–1000	PL	$(3.1 \pm 1.2) \times 10^{-3}$	-2.03 ± 0.09	···	···
000108	60488.072	0	0.256	15–1000	COMP	$(1.5 \pm 1.7) \times 10^{-1}$	-0.55 ± 0.30	$(1.1 \pm 0.3) \times 10^2$	···
000218	58744.596	0	0.256	15–6000	COMP	$(1.5 \pm 0.4) \times 10^{-1}$	-0.43 ± 0.05	$(9.0 \pm 0.8) \times 10^2$	···
		0.256	5.888	15–6000	COMP	$(2.3 \pm 0.5) \times 10^{-2}$	-0.95 ± 0.06	$(9.2 \pm 1.7) \times 10^2$	···
		5.888	13.568	15–2000	PL	$(7.2 \pm 1.9) \times 10^{-3}$	-1.46 ± 0.05	···	···
		13.568	29.696	15–2000	PL	$(4.8 \pm 1.1) \times 10^{-3}$	-1.59 ± 0.05	···	···
000326	19134.798	0	0.256	15–1000	GRB	1.9 ± 1.8	0.34 ± 0.61	$(3.2 \pm 1.0) \times 10^1$	-3.48 ± 0.52
		0.256	8.448	15–1000	GRB	$(7.3 \pm 5.1) \times 10^{-2}$	-0.31 ± 0.49	$(4.8 \pm 1.6) \times 10^1$	-3.50
000420a	42271.144	0	0.128	15–3000	COMP	$(4.8 \pm 3.7) \times 10^{-2}$	-1.03 ± 0.16	$(1.9 \pm 1.4) \times 10^3$	···
000513	40894.793	0	0.128	15–1000	COMP	$(3.0 \pm 0.5) \times 10^{-2}$	-1.00	$(4.7 \pm 1.2) \times 10^2$	···
000526	84494.896	0	0.256	15–5000	COMP	$(2.3 \pm 0.6) \times 10^{-1}$	-0.37 ± 0.05	$(4.9 \pm 0.4) \times 10^2$	···
000607	8689.115	0	0.064	15–5000	COMP	$(2.2 \pm 1.3) \times 10^{-1}$	-0.83 ± 0.13	$(1.2 \pm 0.4) \times 10^3$	···
000608	70497.255	0	0.128	15–3000	COMP	$(8.2 \pm 9.1) \times 10^{-2}$	-0.91 ± 0.24	$(7.0 \pm 3.6) \times 10^2$	···
000701b	25961.013	0	0.256	15–3000	COMP	$(2.8 \pm 2.3) \times 10^{-2}$	-0.35 ± 0.17	$(7.2 \pm 1.9) \times 10^2$	···
		0.256	8.448	15–1000	PL	$(4.0 \pm 1.4) \times 10^{-3}$	-1.18 ± 0.06	···	···
000727	70955.931	0	0.128	15–1000	COMP	1.2 ± 0.6	-0.55 ± 0.14	$(1.0 \pm 0.1) \times 10^2$	···
		0.256	0.768	15–3000	COMP	$(2.9 \pm 0.7) \times 10^{-1}$	-1.38 ± 0.06	$(3.0 \pm 0.4) \times 10^2$	···
		0.768	8.704	15–3000	PL	$(1.6 \pm 0.3) \times 10^{-2}$	-2.30 ± 0.04	···	···
000818	72547.040	0	0.256	15–1000	PL	$(2.4 \pm 0.9) \times 10^{-2}$	-1.19 ± 0.07	···	···
000928	6285.374	0	0.128	15–3000	COMP	$(4.9 \pm 0.6) \times 10^{-2}$	-0.30	$(6.1 \pm 0.7) \times 10^2$	···
001022	20905.666	0	0.064	15–3000	PL	$(3.2 \pm 1.5) \times 10^{-2}$	-0.93 ± 0.07	···	···

Table 2—Continued

Burst name	T_0	Time interval Start	Stop	Energy interval	Model[1]	A photons	α	E_0	β
	s UT	s	s	keV		cm^{-2} s^{-1} keV^{-1}		keV	
001025c	71369.963	0	0.192	15–5000	COMP	$(4.7 \pm 3.0) \times 10^{-2}$	-0.85 ± 0.13	$(1.4 \pm 0.6) \times 10^3$	···
001204	28869.372	0	0.128	15–2000	PL	$(5.4 \pm 2.4) \times 10^{-2}$	-1.69±0.09	···	···
001207b	34185.588	0	0.256	15–1000	COMP	$(6.3 \pm 4.0) \times 10^{-2}$	-1.15 ± 0.18	$(2.3 \pm 0.9) \times 10^2$	···
		0.256	8.448	15–500	COMP	$(3.0 \pm 2.9) \times 10^{-3}$	-1.62 ± 0.31	$(3.9 \pm 6.1) \times 10^2$	···
010119	37179.556	0	0.192	15–5000	COMP	$(1.1 \pm 0.3) \times 10^{-1}$	-0.59 ± 0.05	3.5×10^2	···
010308	56338.468	0	0.256	15–2000	COMP	$(1.8 \pm 0.7) \times 10^{-1}$	-0.76 ± 0.10	$(2.4 \pm 0.4) \times 10^2$	···
		0.256	8.448	15–2000	COMP	$(7.9 \pm 3.0) \times 10^{-3}$	-1.11 ± 0.08	2.5×10^2	···
010427	67452.969	0	0.256	15–3000	COMP	$(2.7 \pm 2.1) \times 10^{-2}$	-0.37 ± 0.16	$(8.3 \pm 2.3) \times 10^2$	···
010616	23724.080	0	0.064	15–1000	COMP	1.2 ± 0.7	0.29 ± 0.16	$(8.1 \pm 0.8) \times 10^1$	···
		0.064	0.128	15–1000	COMP	$(8.9 \pm 12.4) \times 10^{-1}$	0.06 ± 0.44	$(4.5 \pm 1.2) \times 10^1$	···
010624	48929.130	0	0.256	15–1000	COMP	$(2.6 \pm 1.3) \times 10^{-1}$	-0.65 ± 0.15	$(9.8 \pm 1.5) \times 10^1$	···
010628a	4206.816	0	0.256	15–5000	GRB	$(1.5 \pm 0.2) \times 10^{-1}$	-0.49 ± 0.20	$(2.4 \pm 0.7) \times 10^2$	-2.24 ± 0.20
		0.256	8.448	15–3000	COMP	$(7.9 \pm 4.4) \times 10^{-3}$	-1.15 ± 0.12	$(1.3 \pm 0.6) \times 10^3$	···
011024	74609.296	0	0.256	15–1000	COMP	$(7.4 \pm 5.9) \times 10^{-2}$	-1.42 ± 0.21	$(5.1 \pm 3.5) \times 10^2$	···
		0.256	8.448	15–500	PL	$(2.9 \pm 3.8) \times 10^{-3}$	-2.25 ± 0.33	···	···
011101	34754.534	0	0.256	15–3000	COMP	$(5.2 \pm 4.7) \times 10^{-2}$	-0.65 ± 0.19	$(6.3 \pm 1.9) \times 10^2$	···
020117	45909.324	0	0.256	15–1000	COMP	$(2.0 \pm 1.9) \times 10^{-1}$	-0.73 ± 0.29	$(9.5 \pm 3.2) \times 10^1$	···
020306	68280.713	0	0.128	15–6000	COMP	$(4.9 \pm 3.8) \times 10^{-2}$	-0.47 ± 0.15	$(1.1 \pm 0.3) \times 10^3$	···
020326	39182.941	0	0.064	15–1000	COMP	$(1.0 \pm 2.1) \times 10^{-1}$	0.28 ± 0.47	$(1.8 \pm 0.7) \times 10^2$	···
020504	55835.141	0	0.256	15–5000	GRB	$(1.3 \pm 0.1) \times 10^{-1}$	-1.03 ± 0.10	$(1.1 \pm 0.4) \times 10^3$	-2.16 ± 0.39
		0.256	8.448	15–2000	PL	$(1.3 \pm 0.0) \times 10^{-2}$	-1.50 ± 0.30	···	···
020525a	16014.630	0	0.128	15–2000	COMP	$(2.3 \pm 2.6) \times 10^{-2}$	-0.63 ± 0.23	$(1.2 \pm 0.7) \times 10^3$	···
020602b	63030.315	0	0.256	15–1000	COMP	$(3.0 \pm 2.9) \times 10^{-2}$	-0.97 ± 0.23	$(6.0 \pm 3.7) \times 10^2$	···
020715a	54866.135	0	0.128	15–2000	COMP	$(7.2 \pm 6.0) \times 10^{-2}$	-0.56 ± 0.20	$(3.2 \pm 0.9) \times 10^2$	···
020731a	1635.905	0	0.128	15–2000	GRB	$(1.5 \pm 0.1) \times 10^{-1}$	-0.56 ± 0.14	$(3.9 \pm 0.8) \times 10^2$	-3.67 ± 3.78
020731b	50231.739	0	0.128	15–1000	COMP	$(3.9 \pm 9.8) \times 10^{-2}$	-0.40 ± 0.63	$(2.2 \pm 1.8) \times 10^2$	···
020828	20737.981	0	0.256	15–3000	COMP	$(3.0 \pm 1.5) \times 10^{-2}$	-0.98 ± 0.11	$(1.6 \pm 0.7) \times 10^3$	···

[1]in designations of section 3

[2]The spectrum of this GRB, accumulated in the time interval 0-0.256 s, was fitted by the sum of COMP and PL models. The parameters of these models are given in two lines (for COMP and PL model respectively)

Table 3. GRBs with afterglow: Fluences and Peak Fluxes

Burst name	Figure number	T_0, s UT	Energy interval, keV	Time interval for Fluence, s	Fluence, ergs cm^{-2}	Time interval for Peak Flux, s	Peak Flux photons $cm^{-2}s^{-1}$	Peak Flux ergs $cm^{-2}s^{-1}$
951014a	11	13108.167	15–5000	-0.088–2.048	2.9×10^{-5}	0.232–0.280	1.5×10^{2}	7.3×10^{-5}
	13		15–3000	2.048–50.176	8.2×10^{-6}	6.144–10.240	1.7	3.1×10^{-7}
980605	66	51131.976	15–3000	-0.016–0.140	1.4×10^{-6}	-0.008–0.000	1.3×10^{2}	5.1×10^{-5}
	67		15–1000	0.512–70.144	3.6×10^{-6}	16.896–33.280	4.3×10^{-1}	7.6×10^{-8}
980706a	71	57586.277	15–8000	-0.056–0.528	3.9×10^{-5}	0.092–0.108	1.9×10^{2}	1.5×10^{-4}
	72		15–1000	0.768–50.176	3.3×10^{-6}	2.816–21.504	3.0×10^{-1}	8.0×10^{-8}
981107	78	781.395	15–8000	-0.008–0.784	1.1×10^{-4}	0.340–0.348	3.3×10^{2}	5.2×10^{-4}
	79		15–1000	0.768–90.880	6.3×10^{-6}	0.768–13.312	6.3×10^{-1}	1.6×10^{-7}
990313	90	33712.652	15–2500	-0.024–0.396	1.5×10^{-6}	-0.004–0.012	9.9×10^{1}	2.0×10^{-5}
	91		15–1000	0.768–123.648	3.1×10^{-6}	0.768–61.696	4.0×10^{-1}	3.1×10^{-8}
990327	92	22911.102	15–4000	-0.060–0.116	7.0×10^{-6}	0.012–0.020	1.8×10^{2}	1.5×10^{-4}
	93		15–1000	0.768–70.400	1.2×10^{-5}	5.376–8.448	4.5	1.1×10^{-6}
990516	97	86065.136	15–8000	-0.014–0.432	2.4×10^{-5}	0.252–0.256	2.6×10^{2}	2.6×10^{-4}
	99		15–1000	1.024–75.776	8.3×10^{-6}	10.240–24.576	1.6	2.3×10^{-7}
990712a	101	27915.510	15–4000	-0.080–0.656	2.0×10^{-5}	0.296–0.312	6.1×10^{1}	5.4×10^{-5}
	102		15–1000	1.024–87.296	6.9×10^{-6}	27.648–36.096	2.5	1.9×10^{-7}
000218	115	58744.596	15–6000	-0.176–1.296	3.4×10^{-5}	0.104–0.136	9.8×10^{1}	9.2×10^{-5}
	116		15–1000	1.280–63.232	2.7×10^{-5}	5.120–6.144	1.2×10^{1}	2.7×10^{-6}
000701b	126	25961.013	15–2500	-0.176–1.296	1.1×10^{-5}	-0.016–0.016	3.3×10^{1}	2.5×10^{-5}
	127		15–1000	1.280–5.376	8.3×10^{-7}	2.816–3.840	1.9	3.2×10^{-7}
000727	129	70955.931	15–2500	-0.042–1.040	1.1×10^{-5}	0.046–0.056	3.9×10^{2}	5.5×10^{-5}
	131		15–1000	6.704–8.272	9.8×10^{-6}	6.832–6.960	3.0×10^{2}	2.0×10^{-5}

Table 4. GRBs with early afterglow: Spectral parameters

Burst name	T_0	Time interval Start	Time interval Stop	Energy interval	Model[1]	α	E_0	β
	s UT	s	s	keV			keV	
951014a	13108.167	0	0.256	15–5000	GRB	-0.17 ± 0.13	$(2.1 \pm 0.3) \times 10^{2}$	-2.1 ± 0.1
		0.512	7.936	15–3000	GRB	-1.36 ± 0.12	$(4.5 \pm 1.8) \times 10^{2}$	-2.2 ± 0.1
980605	51131.976	0	0.064	15–5000	COMP	-0.74 ± 0.25	$(1.0 \pm 0.8) \times 10^{3}$	···
		0.512	70.144	15–1000	COMP	-1.04 ± 0.40	$(2.3 \pm 1.8) \times 10^{2}$	···
980706a	57586.277	0	0.256	15–6000	COMP	-0.75 ± 0.03	$(1.3 \pm 0.1) \times 10^{3}$	···
		0.768	50.176	15–1000	COMP	-0.94 ± 0.45	$(3.6 \pm 3.3) \times 10^{2}$	···
981107	781.395	0	0.128	15–8000	COMP	-0.08 ± 0.16	$(8.0 \pm 1.3) \times 10^{2}$	···
		0.768	90.88	15–1000	PL	-1.44 ± 0.13	···	···
990313	33712.652	0	0.128	15–2000	GRB	-1.08 ± 0.18	$(2.0 \pm 0.9) \times 10^{2}$	-2.4 ± 0.4
		0.768	123.648	15–1000	PL	-2.03 ± 0.17	···	···
990327	22911.102	0	0.064	15–5000	COMP	-0.86 ± 0.11	$(2.1 \pm 0.8) \times 10^{3}$	···
		0.768	70.4	15–1000	COMP	-1.07 ± 0.20	$(3.3 \pm 1.2) \times 10^{2}$	···
990516	86065.136	0	0.064	15–5000	COMP	-1.26 ± 0.16	$(1.9 \pm 2.4) \times 10^{3}$	···
		1.024	75.776	15–1000	PL	-1.81 ± 0.09	···	···
990712a	27915.510	0	0.256	15–5000	COMP	-0.20 ± 0.13	$(6.1 \pm 1.0) \times 10^{2}$	···
		1.024	96.768	15–1000	PL	-2.31 ± 0.14	···	···
000218	58744.596	0	0.256	15–6000	COMP	-0.43 ± 0.05	$(9.0 \pm 0.8) \times 10^{2}$	···
		1.28	70.144	15–1000	PL	-1.58 ± 0.30	···	···
000701b	25961.013	0	0.256	15–3000	COMP	-0.35 ± 0.17	$(7.2 \pm 1.9) \times 10^{2}$	···
		1.28	5.376	15–1000	COMP	-1.44 ± 0.30	$(5.6 \pm 3.7) \times 10^{2}$	···
000727	70955.931	0	0.128	15–1000	COMP	-0.55 ± 0.14	$(1.0 \pm 0.1) \times 10^{2}$	···
		0.768	8.704	15–2500	PL	-2.50 ± 0.04	···	···

[1] in designations of section 3

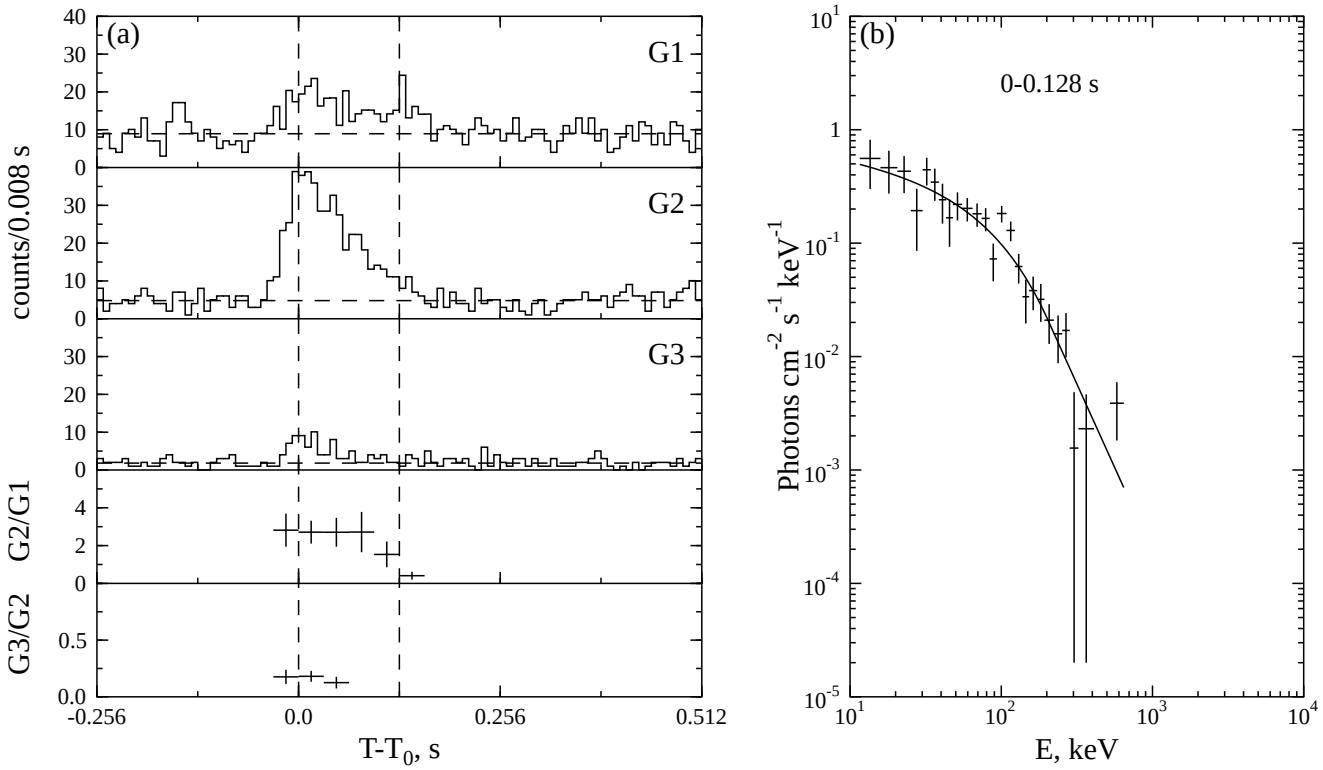

Fig. 1.— GRB 950210. T_0=8424.148 s UT.

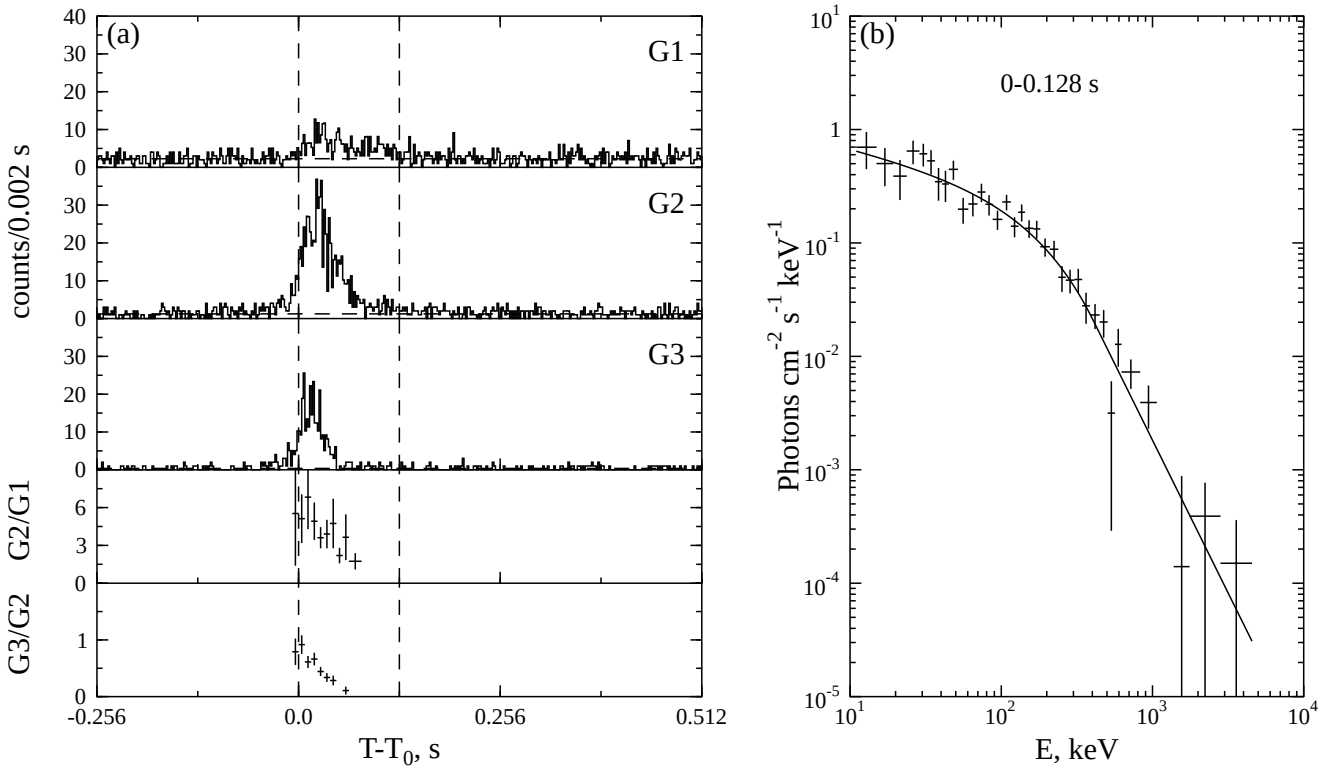

Fig. 2.— GRB 950211a. T_0=8697.749 s UT.

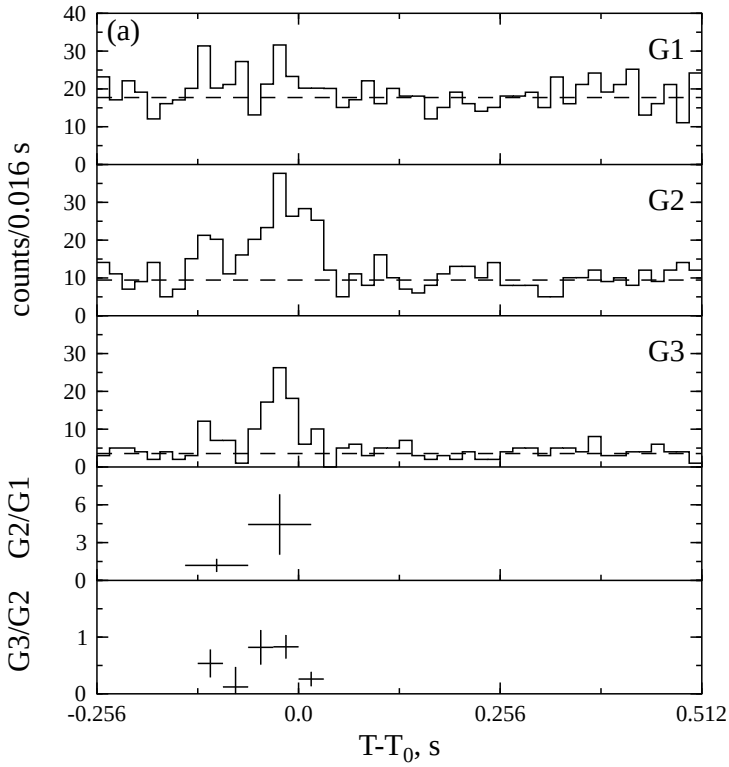

Fig. 3.— GRB 950414. T_0=40882.798 s UT.

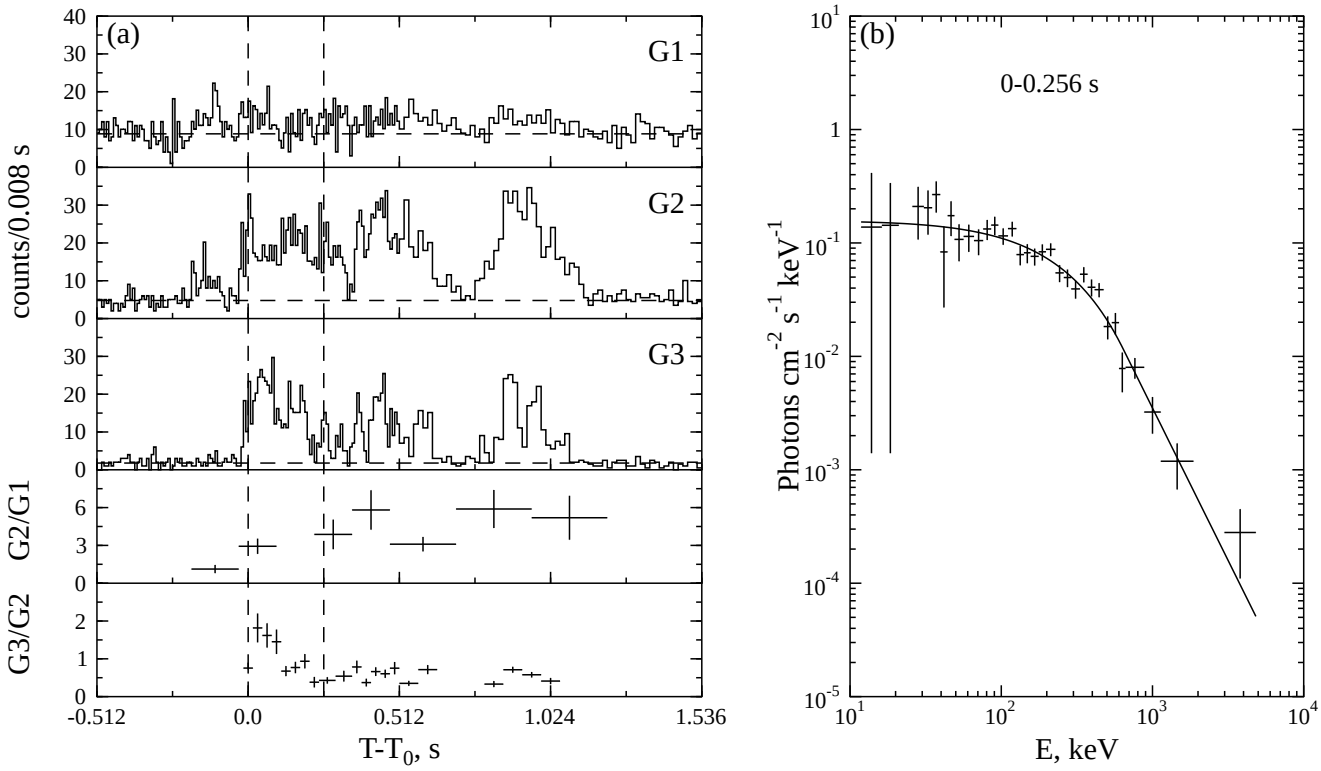

Fig. 4.— GRB 950419a. T_0=8628.860 s UT.

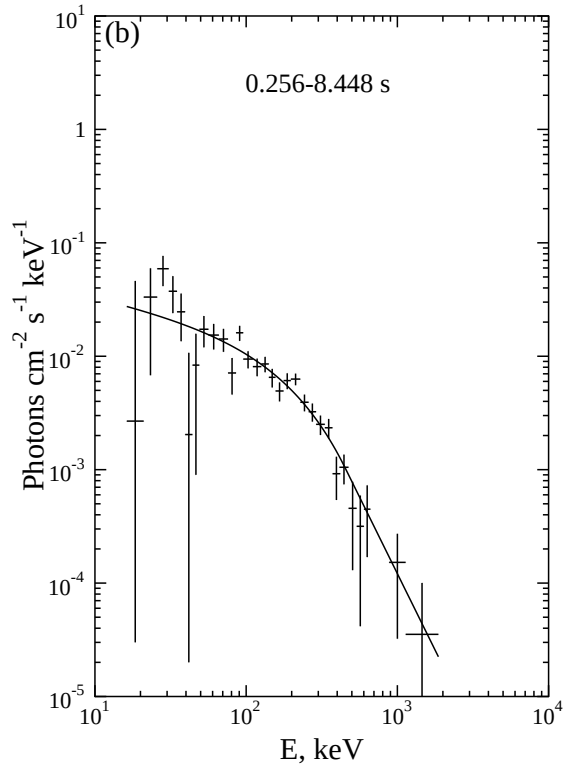

Fig. 5.— Energy spectrum of the GRB 950419a. T_0=8628.860 s UT (continued from Fig. 4).

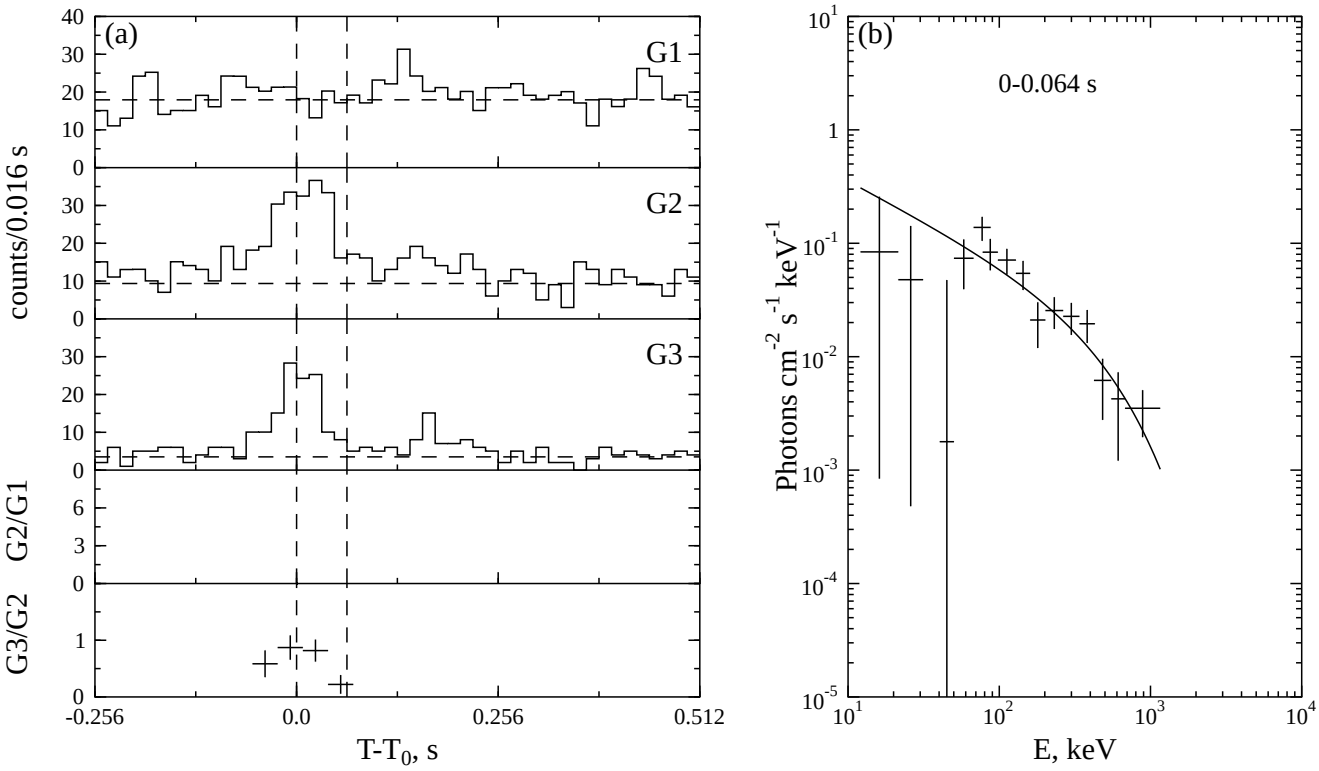

Fig. 6.— GRB 950520. T_0=83271.404 s UT.

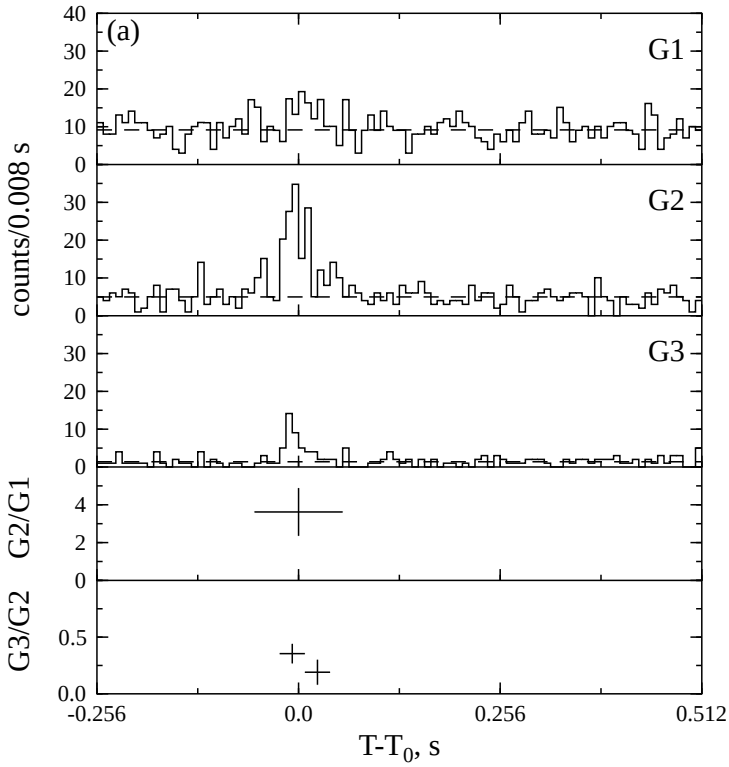

Fig. 7.— GRB 950610b. T_0=19096.034 s UT.

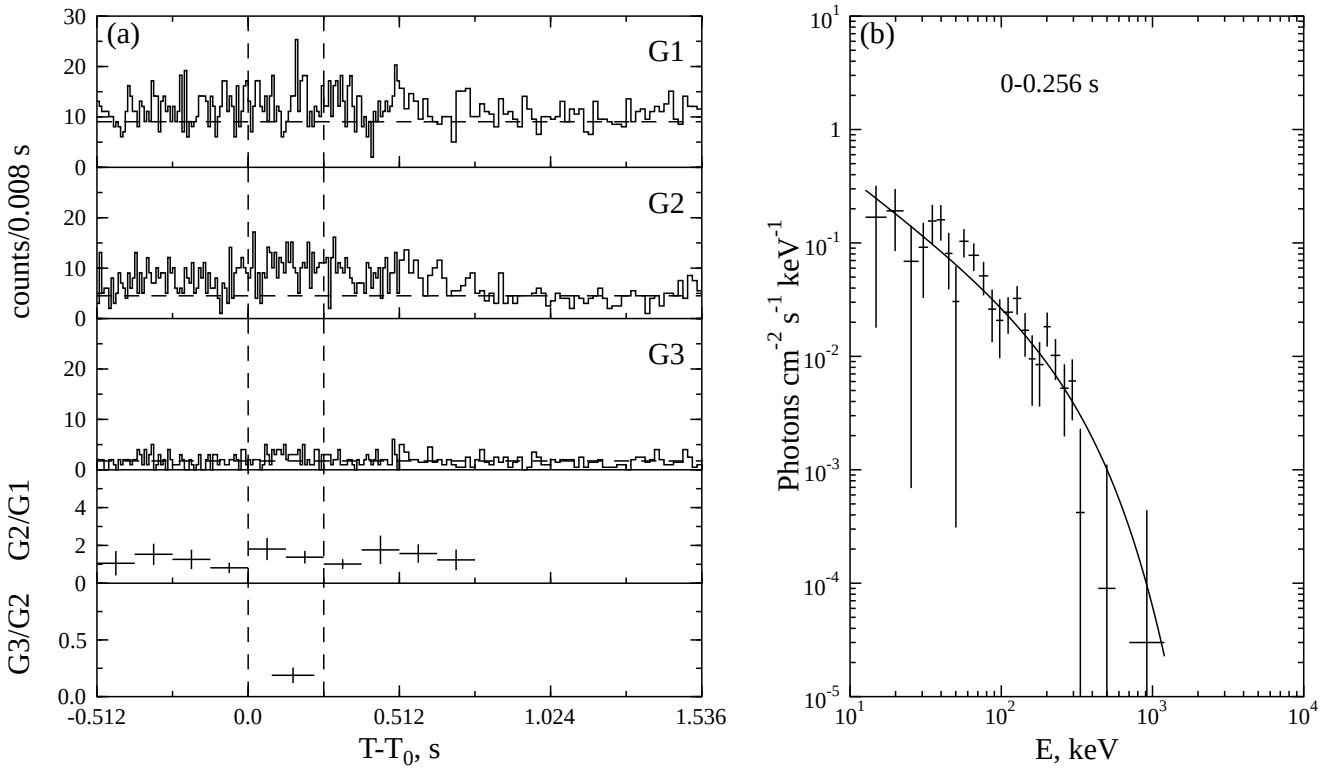

Fig. 8.— GRB 950726. T_0=51579.299 s UT.

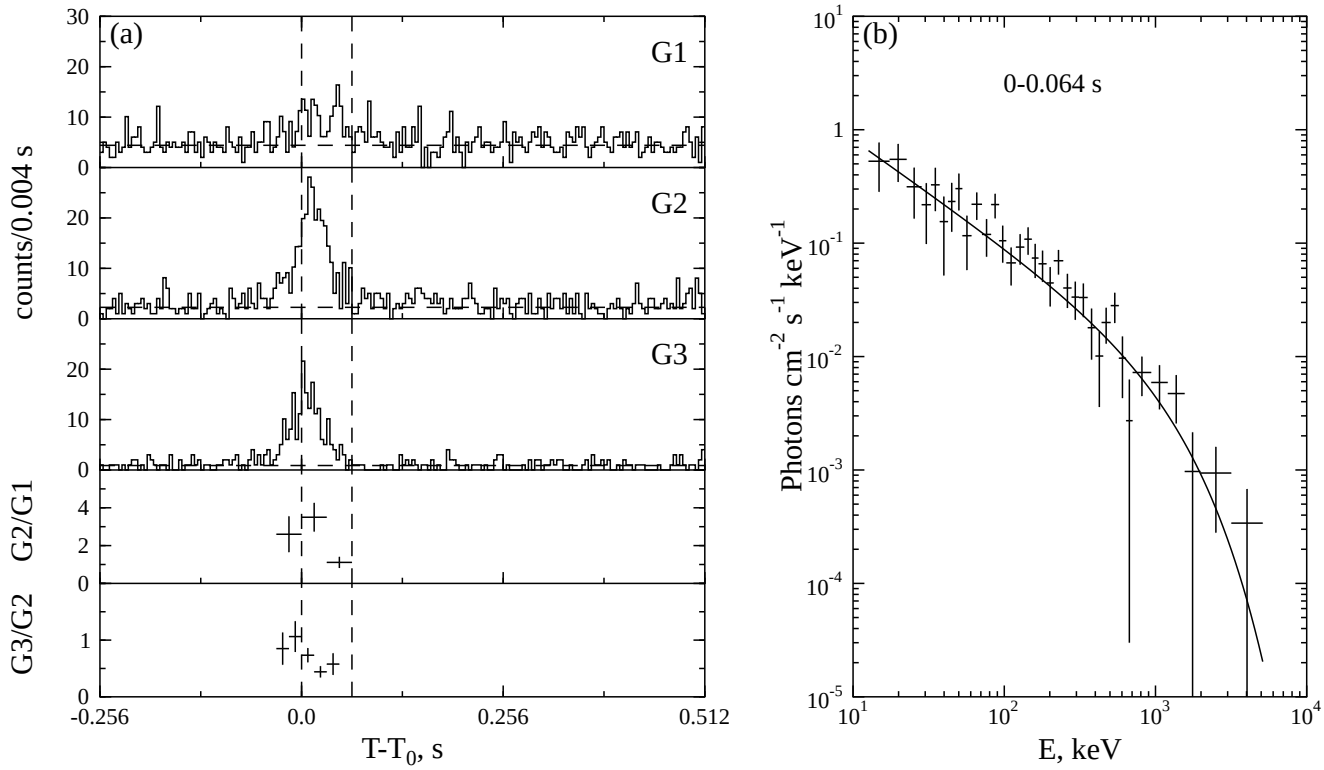

Fig. 9.— GRB 950805b. T_0=13454.144 s UT.

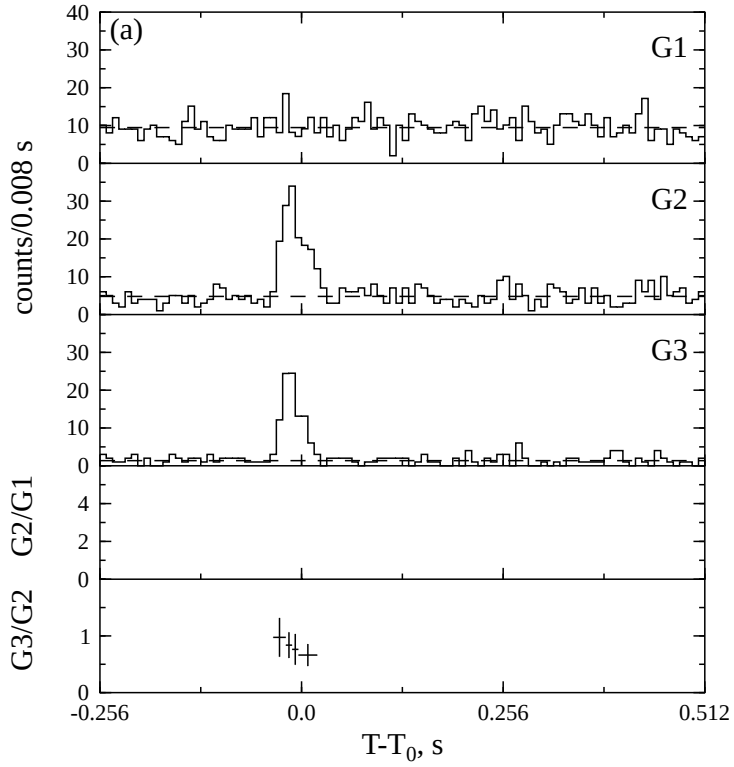

Fig. 10.— GRB 951013. T_0=57097.299 s UT.

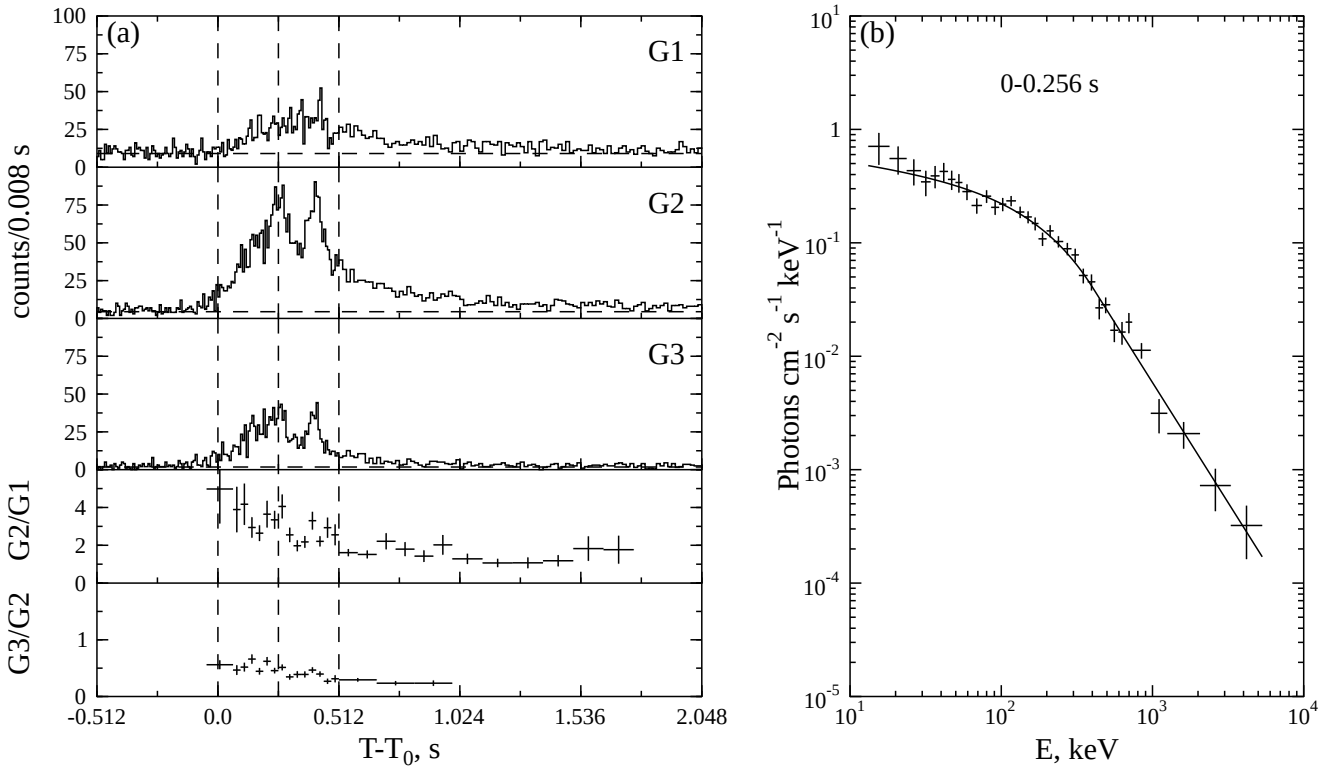

Fig. 11.— GRB 951014a. T_0=13108.167 s UT.

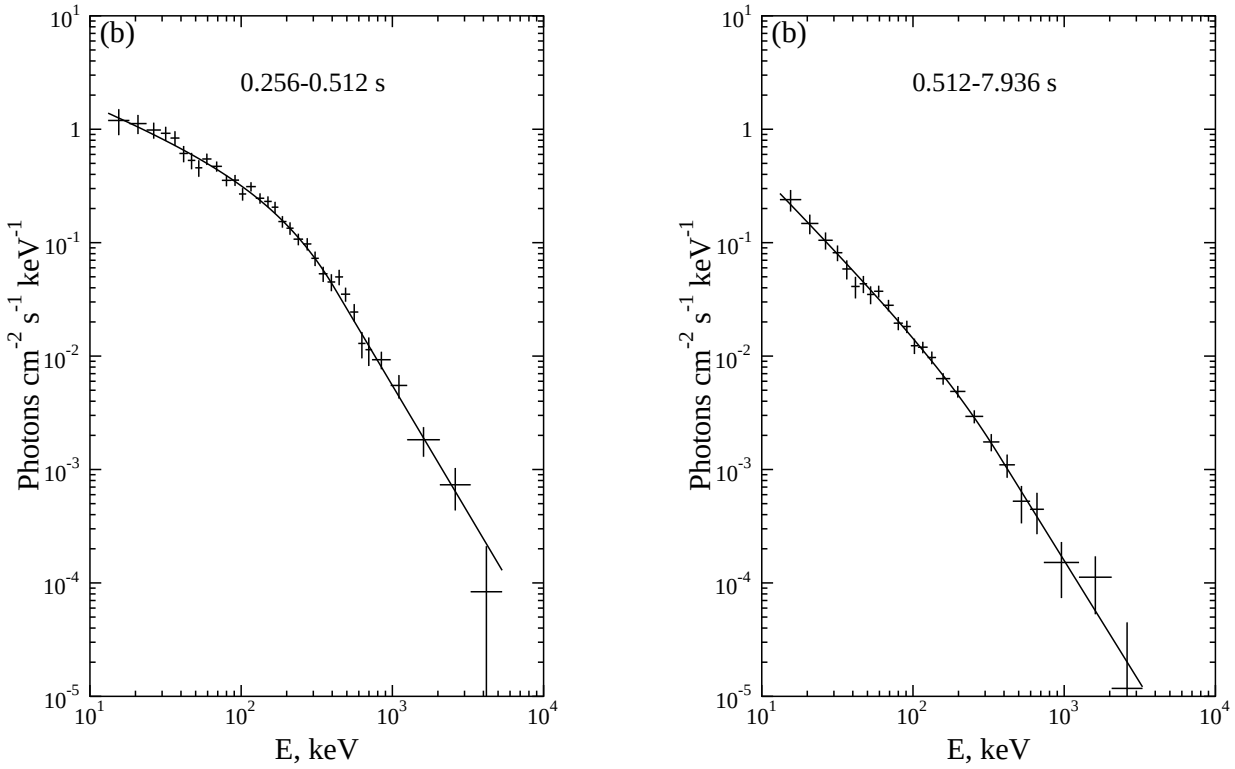

Fig. 12.— GRB 951014a. T_0=13108.167 s UT (continued from Fig. 11).

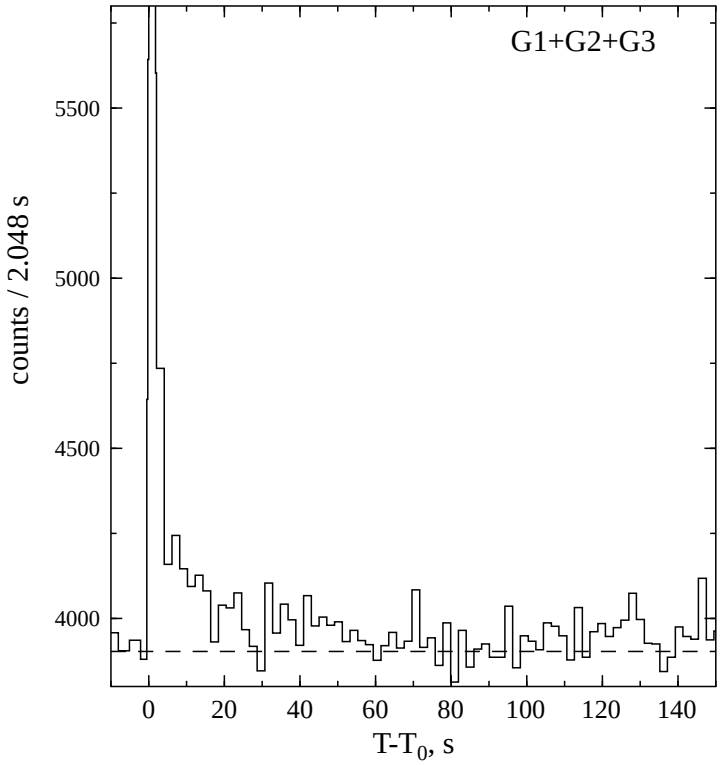

Fig. 13.— GRB 951014a. T_0=13108.167 s UT (continued from Fig. 11).

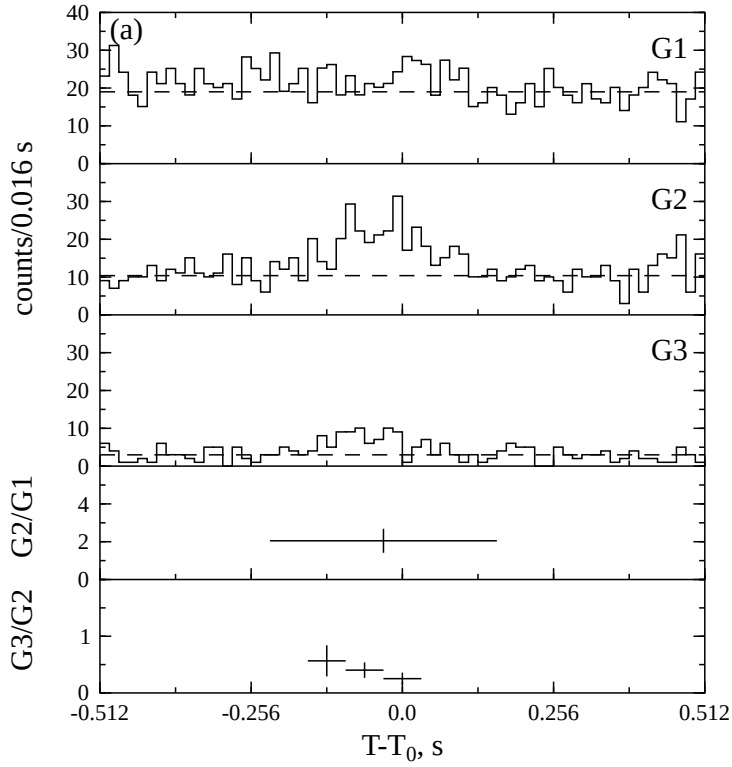

Fig. 14.— GRB 960312. T_0=35074.697 s UT.

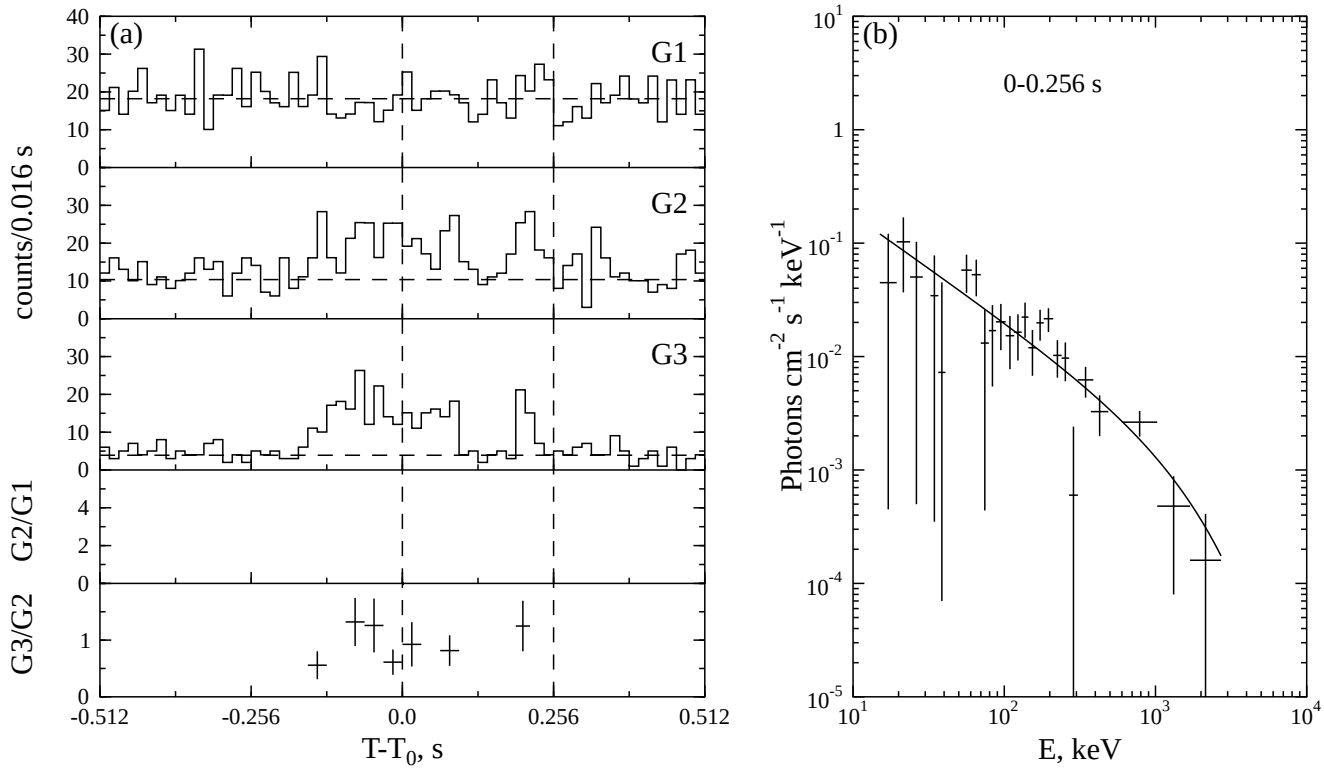

Fig. 15.— GRB 960319. T_0=51992.828 s UT.

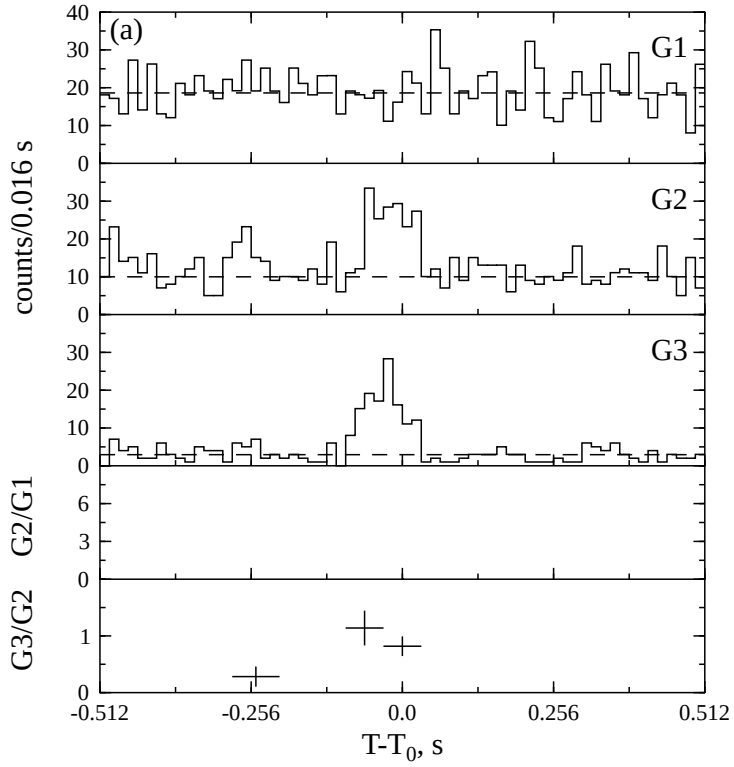

Fig. 16.— GRB 960420. T_0=16844.809 s UT.

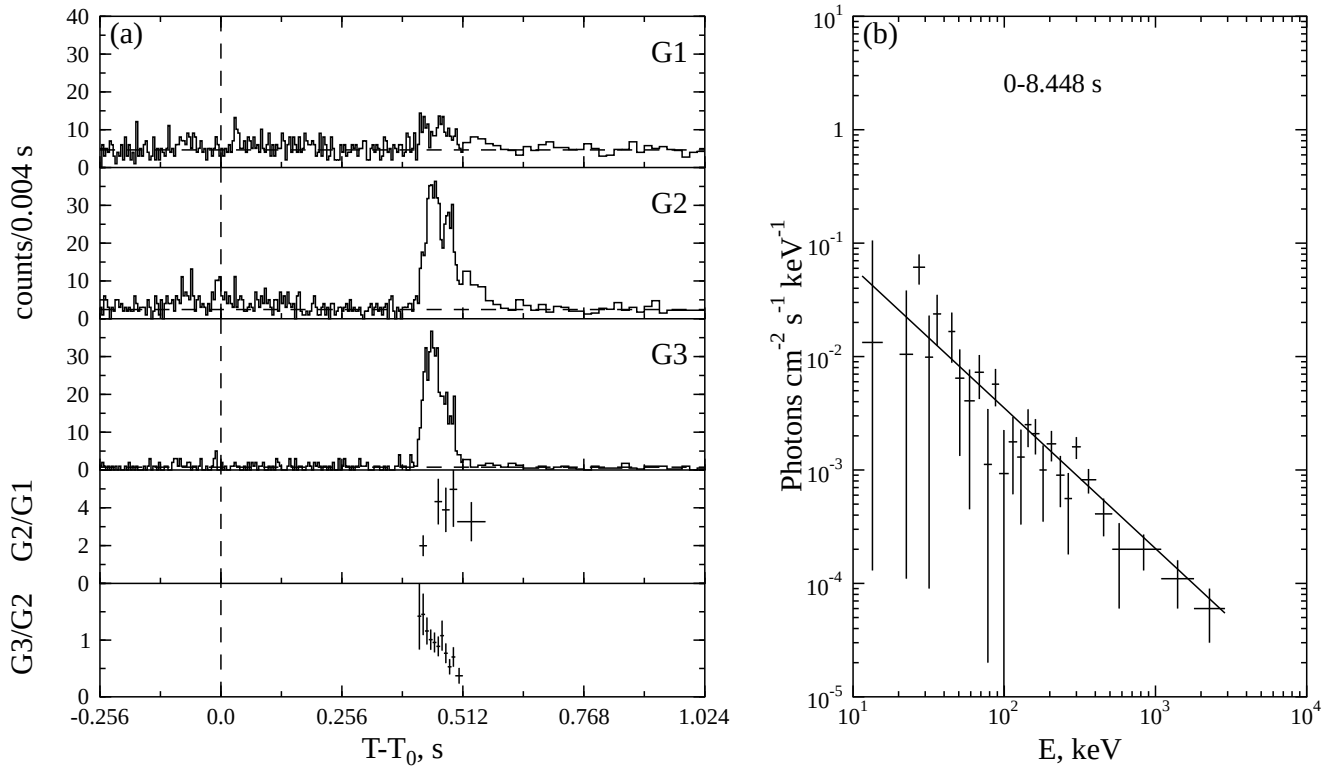

Fig. 17.— GRB 960519. T_0=14766.283 s UT.

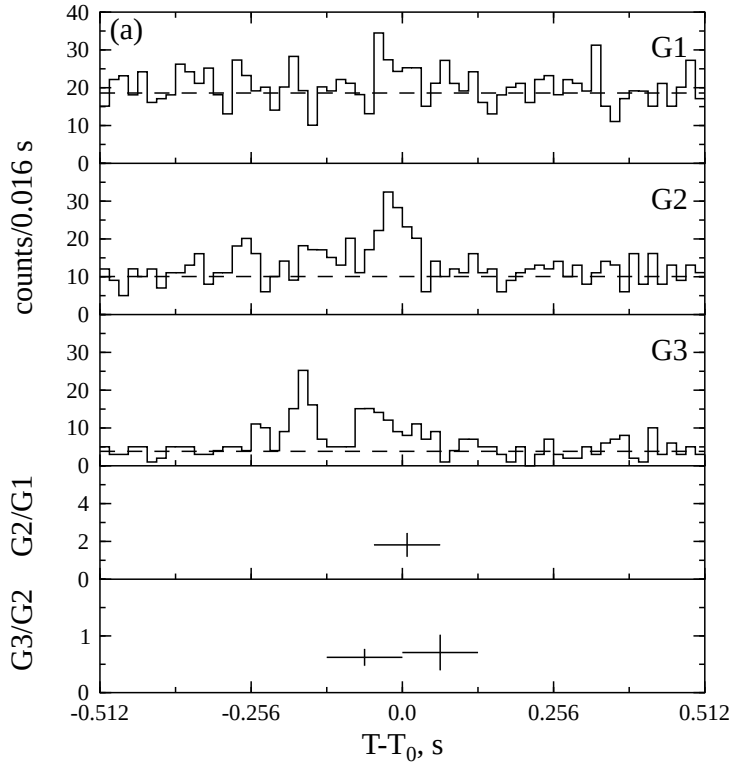

Fig. 18.— GRB 960602. T_0=42664.032 s UT.

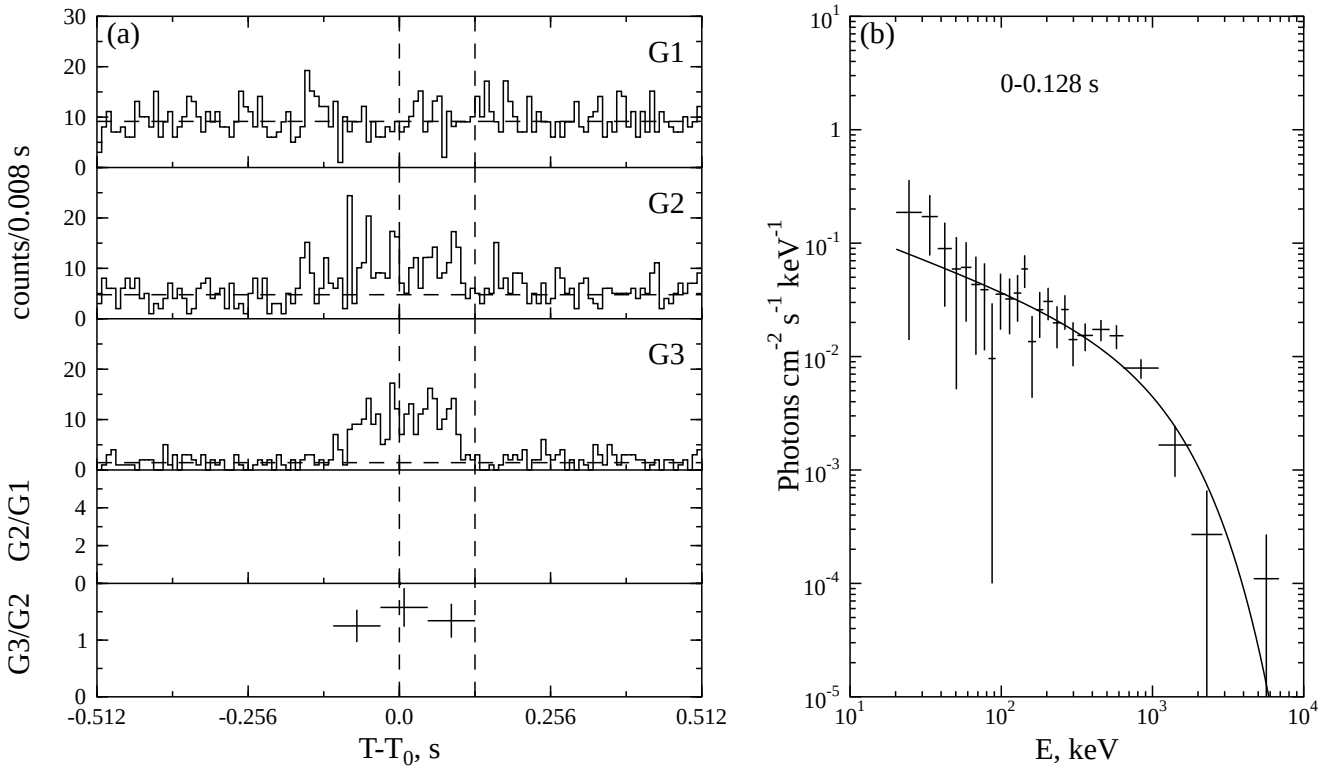

Fig. 19.— GRB 960610. T_0=84502.254 s UT.

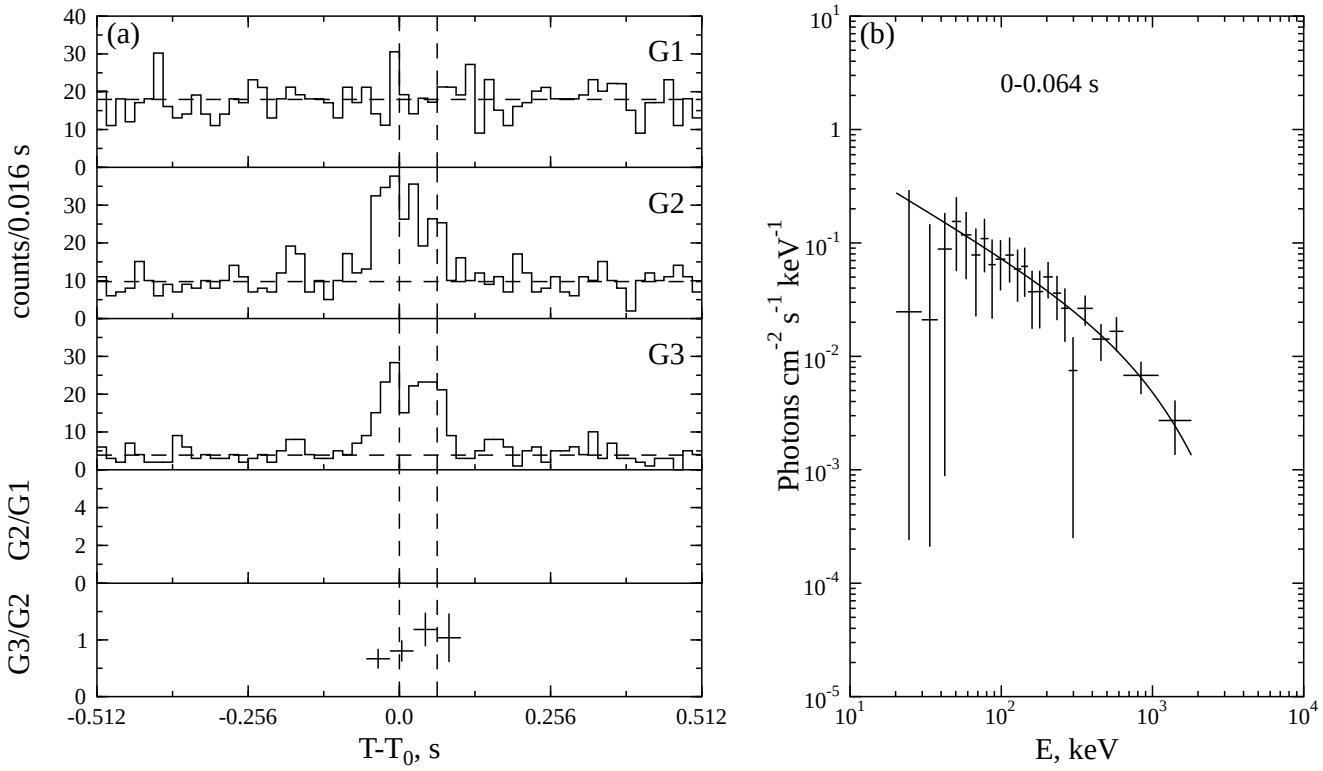

Fig. 20.— GRB 960614. T_0=67654.516 s UT.

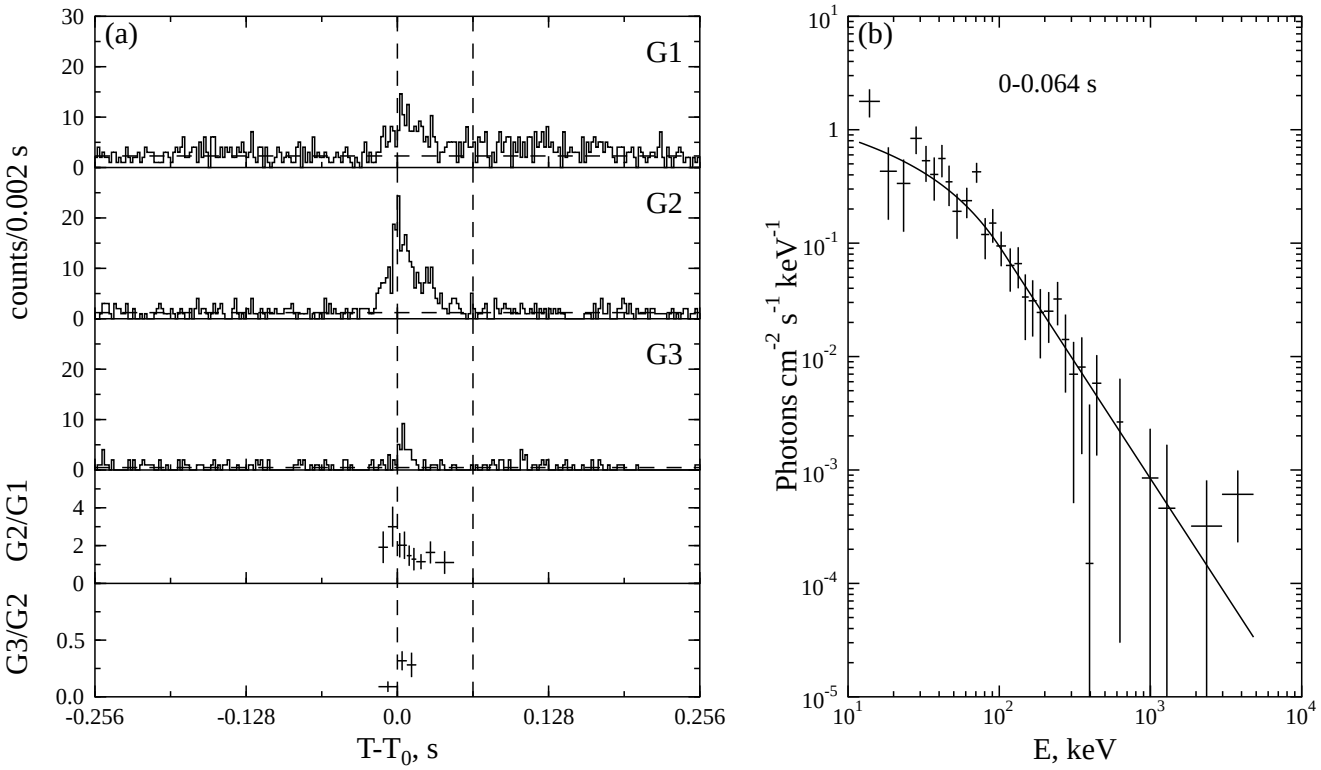

Fig. 21.— GRB 960803. T_0=67525.033 s UT.

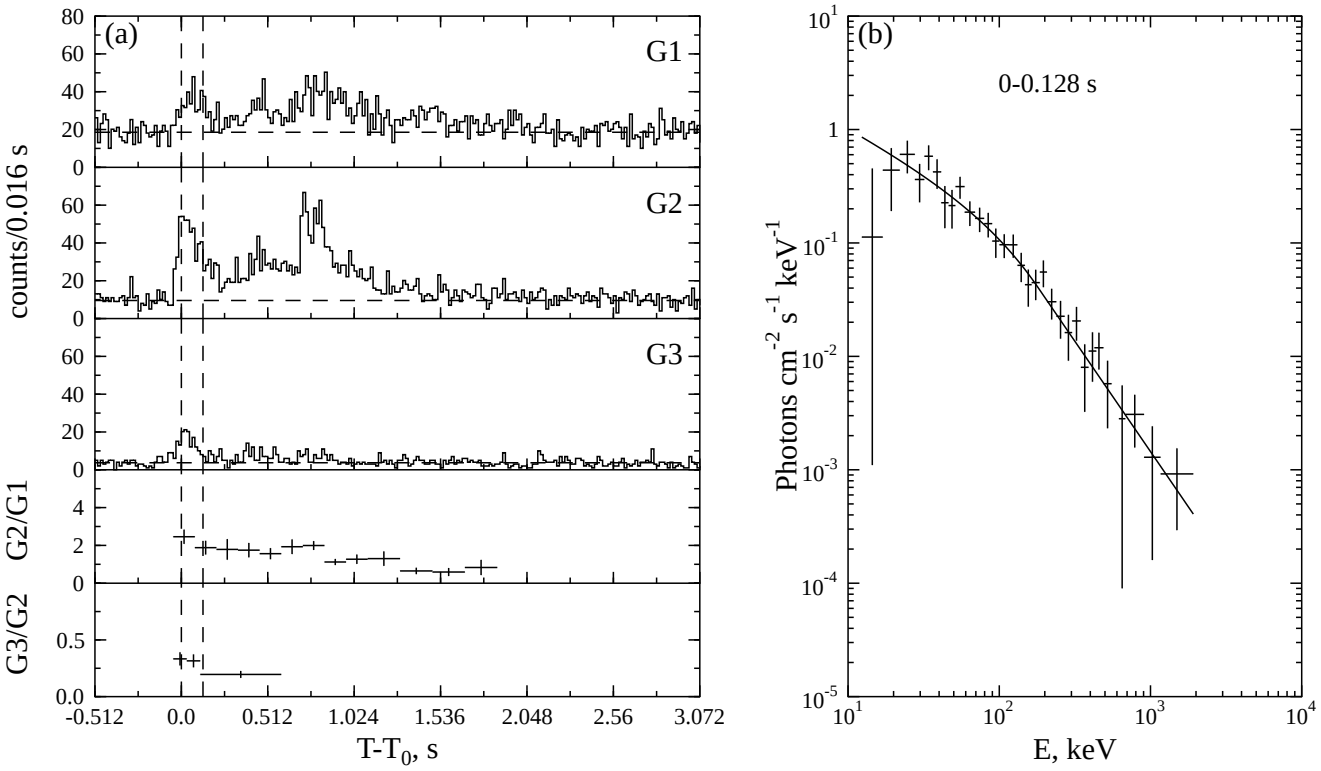

Fig. 22.— GRB 960902. T_0=58097.128 s UT.

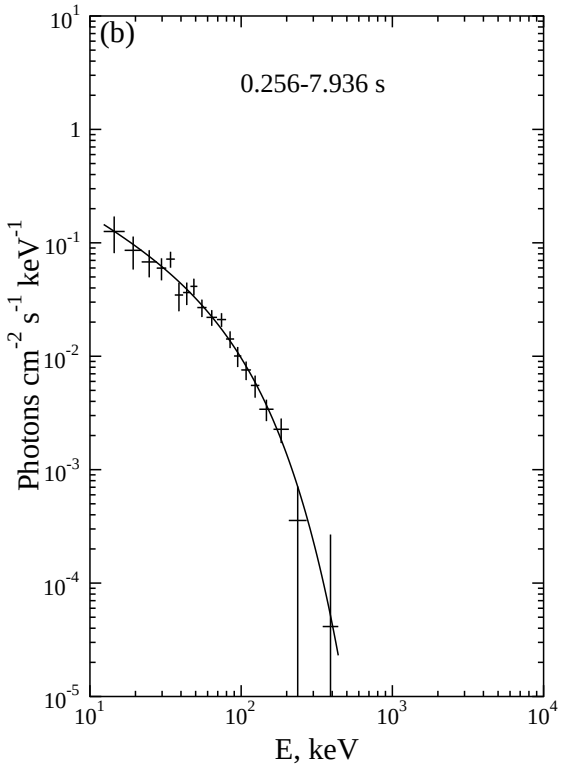

Fig. 23.— GRB 960902. T_0=58097.128 s UT (continued from Fig. 22).

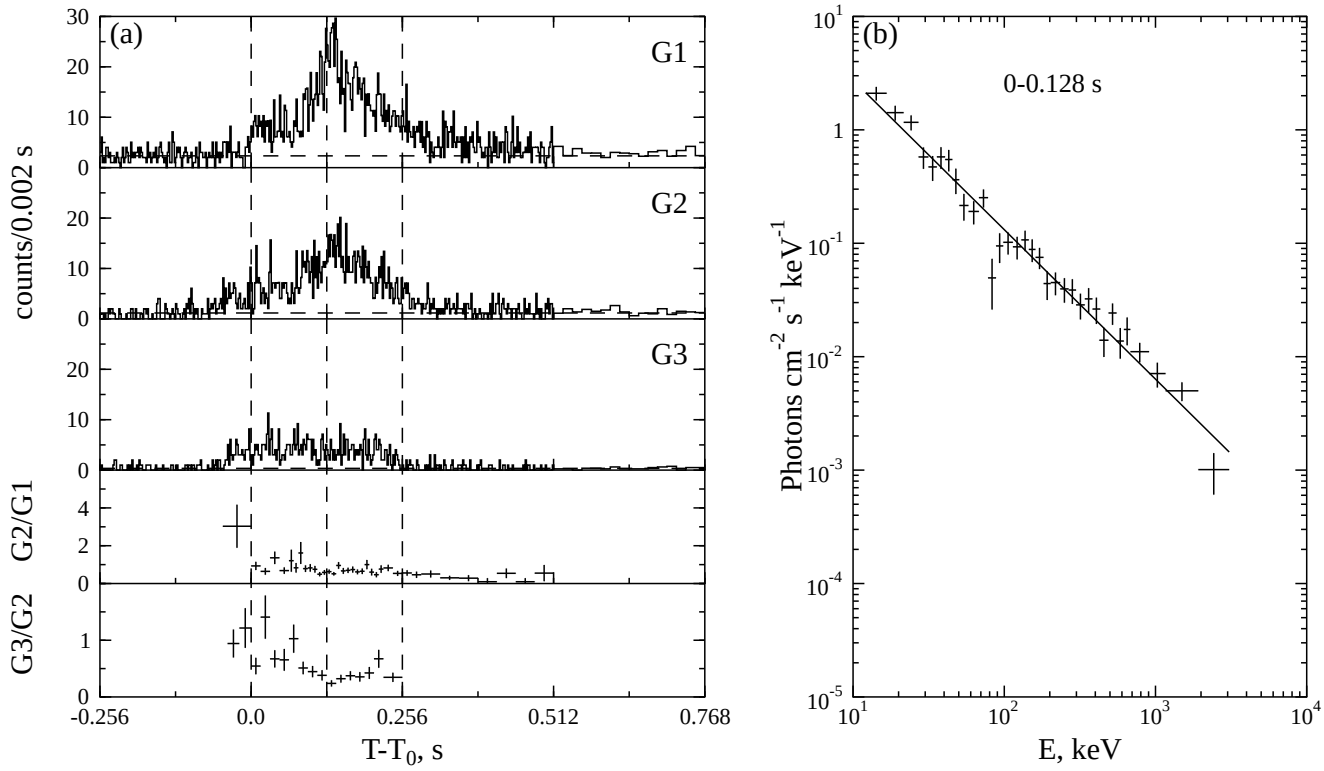

Fig. 24.— GRB 960908. T_0=25028.442 s UT.

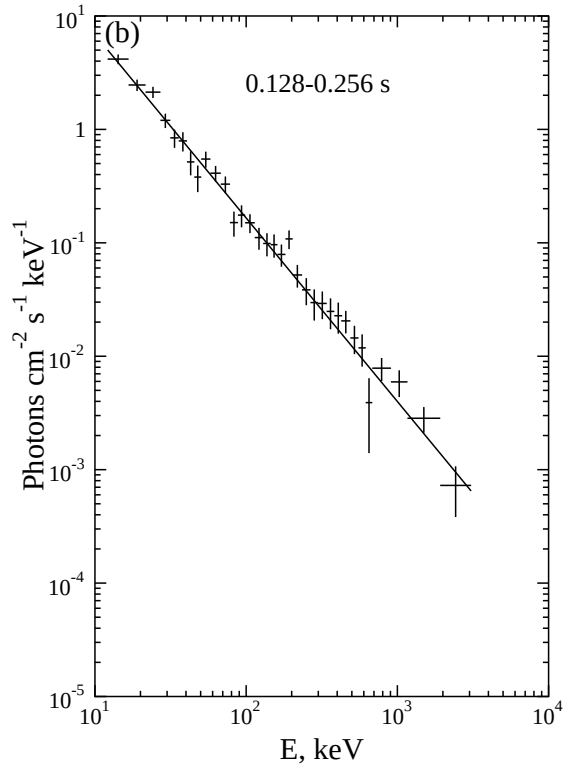

Fig. 25.— GRB 960908. T_0=25028.442 s UT (continued from Fig. 24).

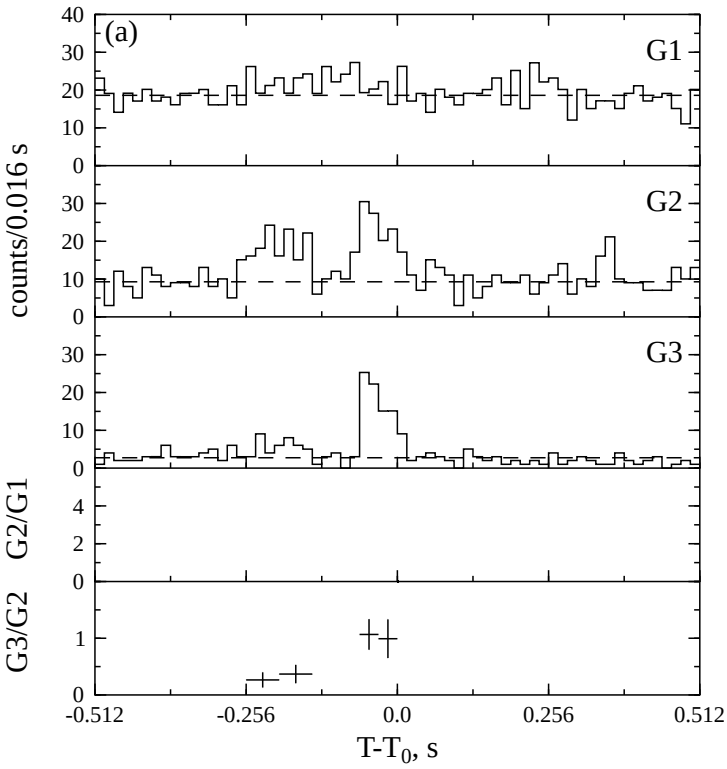

Fig. 26.— GRB 961113. T_0=80522.580 s UT.

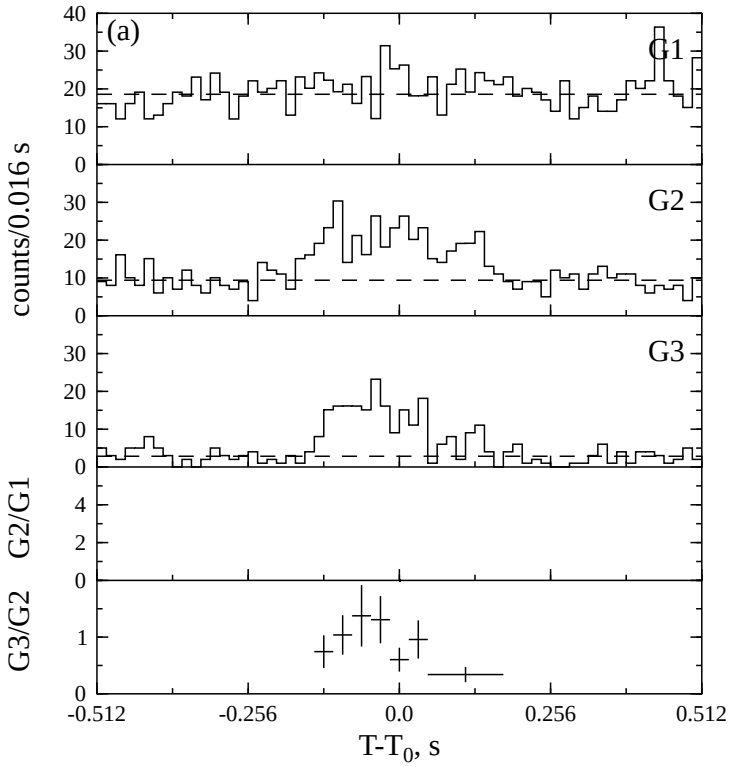

Fig. 27.— GRB 961123. T_0=59317.593 s UT.

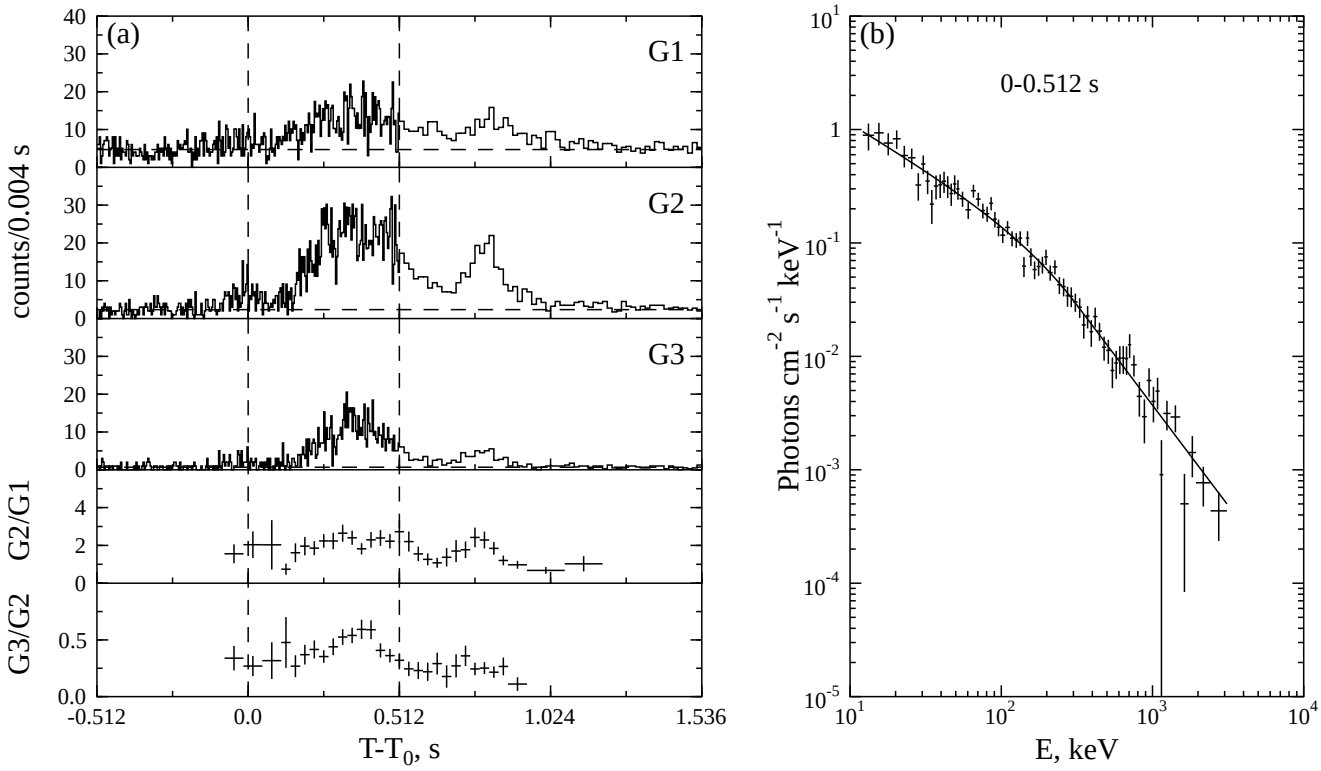

Fig. 28.— GRB 961212. T_0=14870.487 s UT.

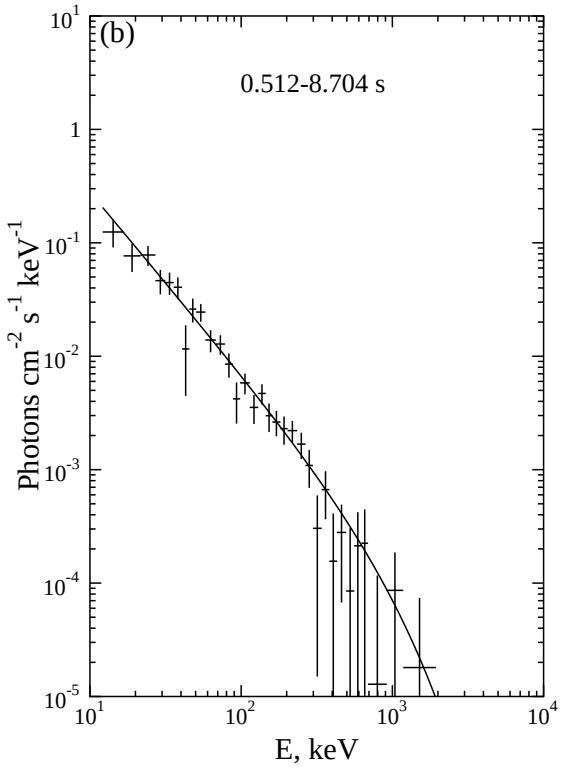

Fig. 29.— Energy spectrum of the GRB 961212. T_0=14870.487 s UT (continued from Fig. 28).

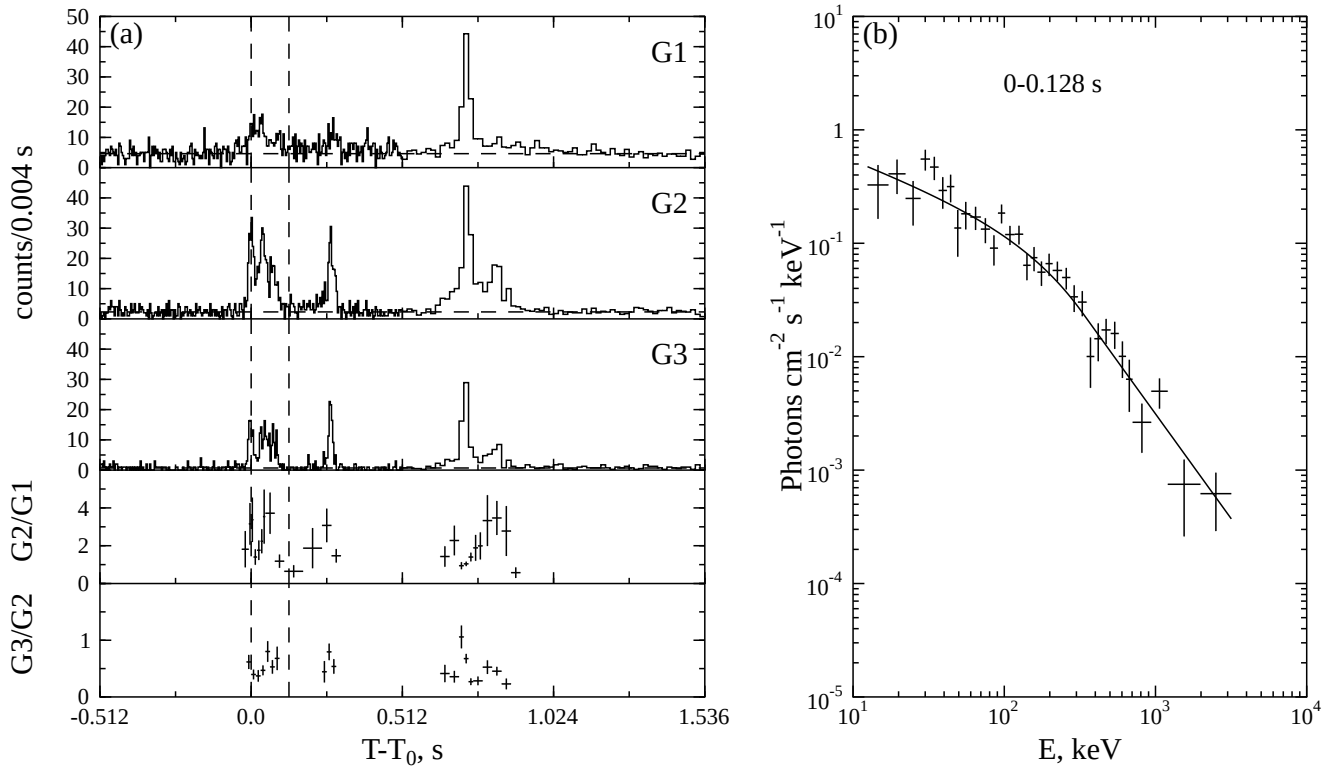

Fig. 30.— GRB 970222. T_0=86006.565 s UT.

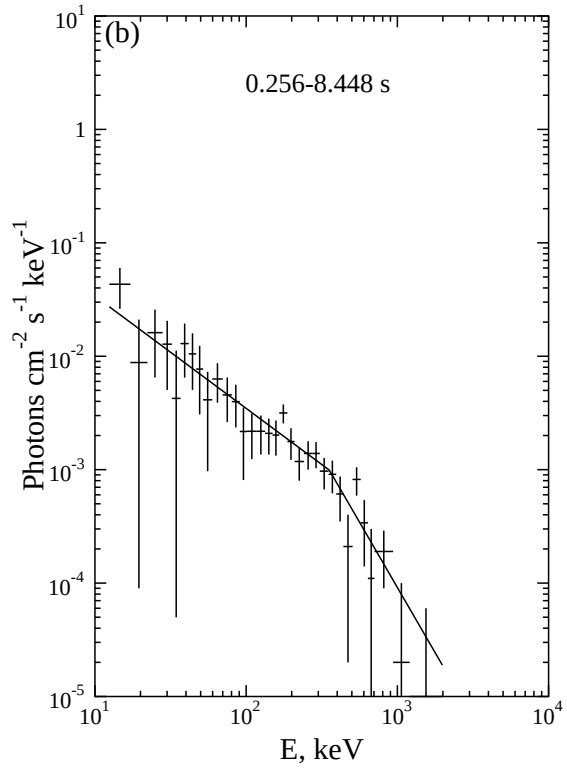

Fig. 31.— Energy spectrum of the GRB 970222. T_0=86006.565 s UT (continued from Fig. 30).

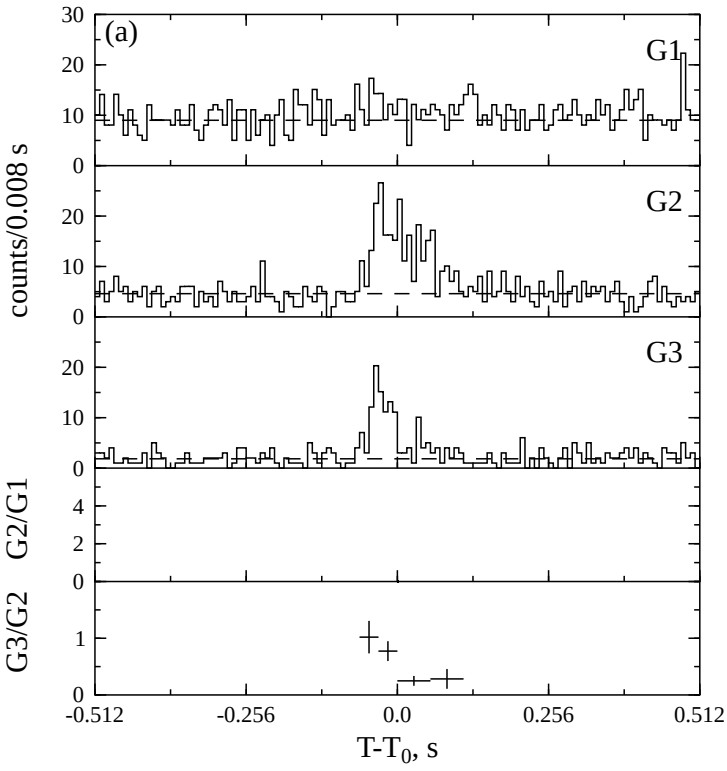

Fig. 32.— GRB 970315b. T_0=30064.853 s UT.

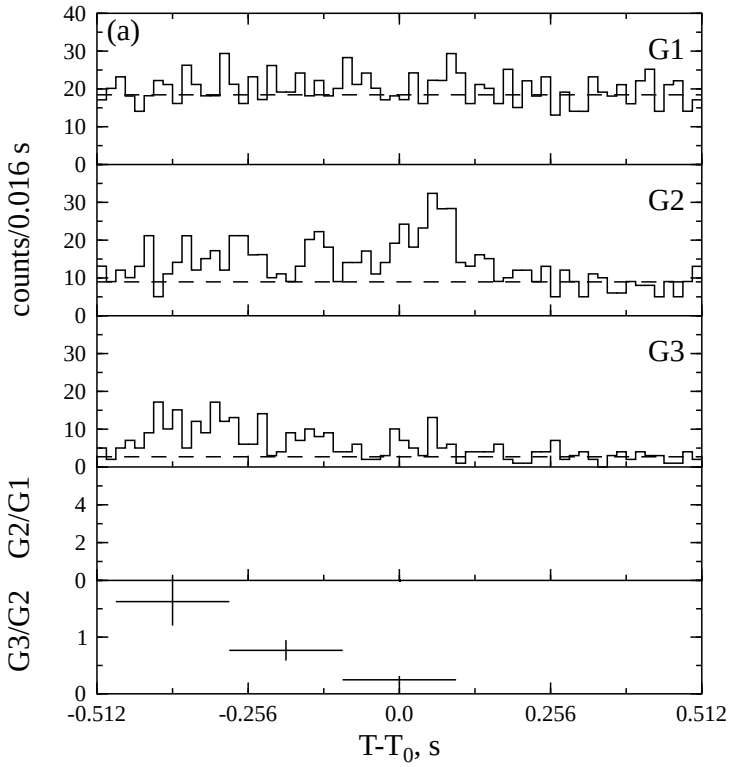

Fig. 33.— GRB 970330. T_0=43988.805 s UT.

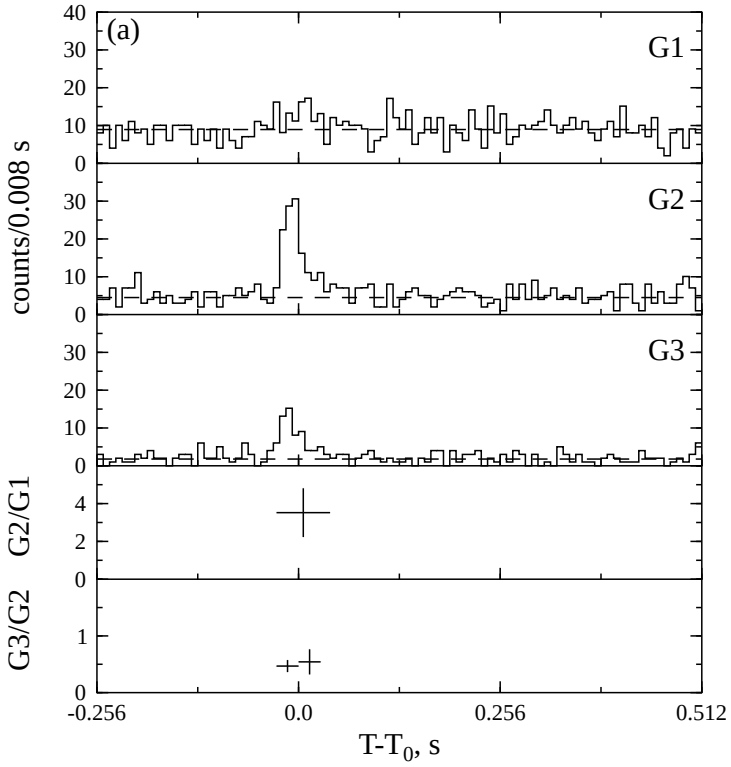

Fig. 34.— GRB 970427. T_0=45723.327 s UT.

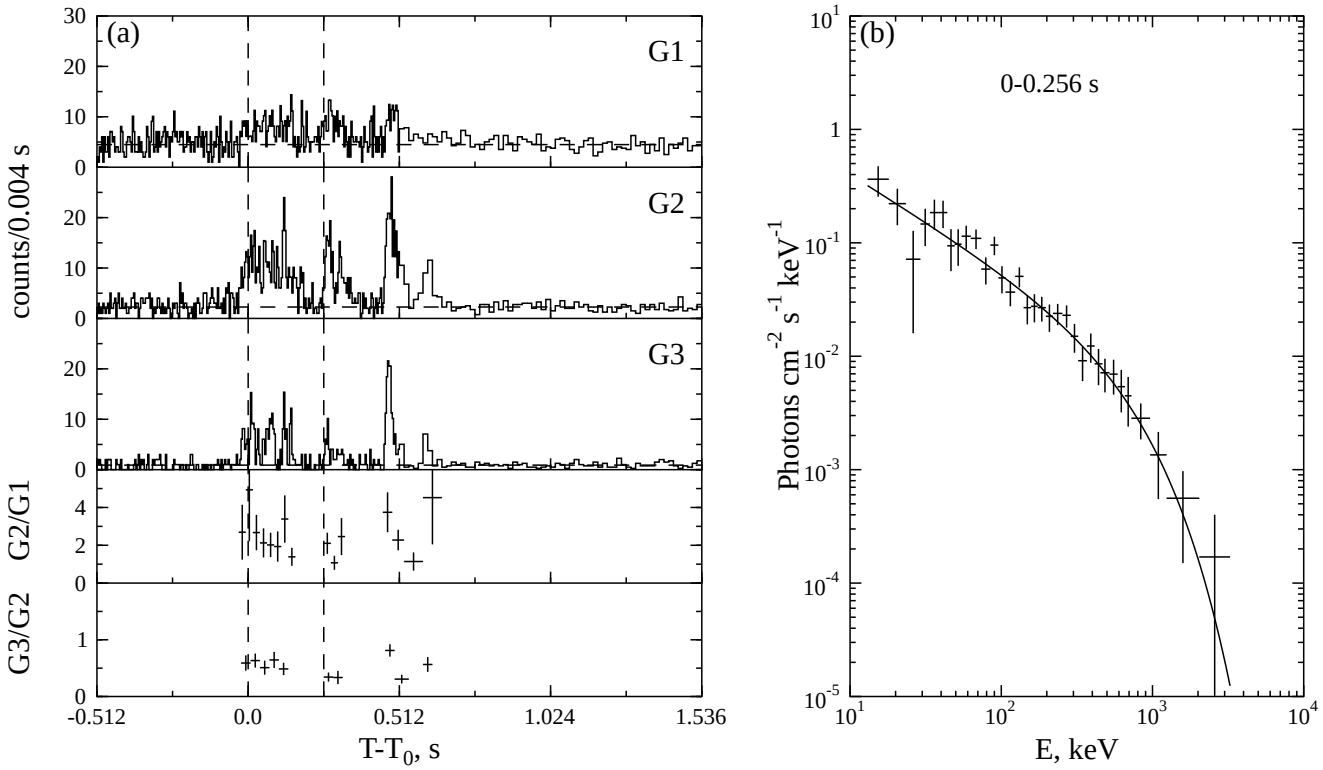

Fig. 35.— GRB 970428. T_0=13365.268 s UT.

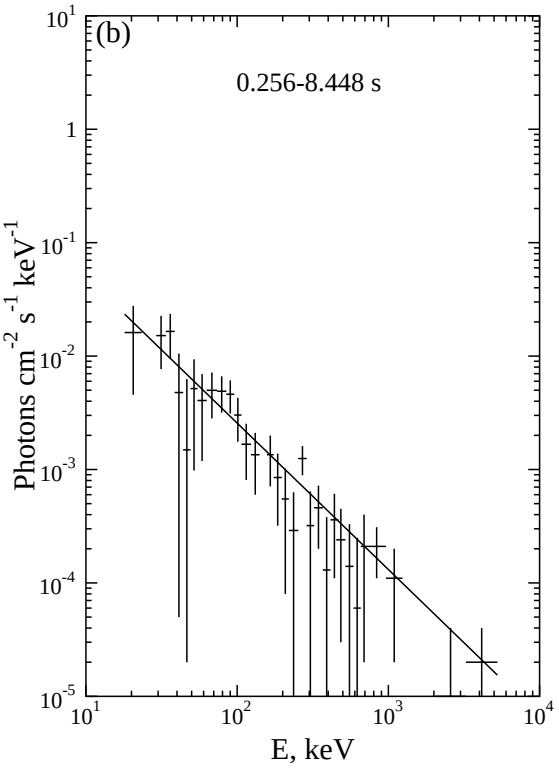

Fig. 36.— Energy spectrum of the GRB 970428. T_0=13365.268 s UT (continued from Fig. 35).

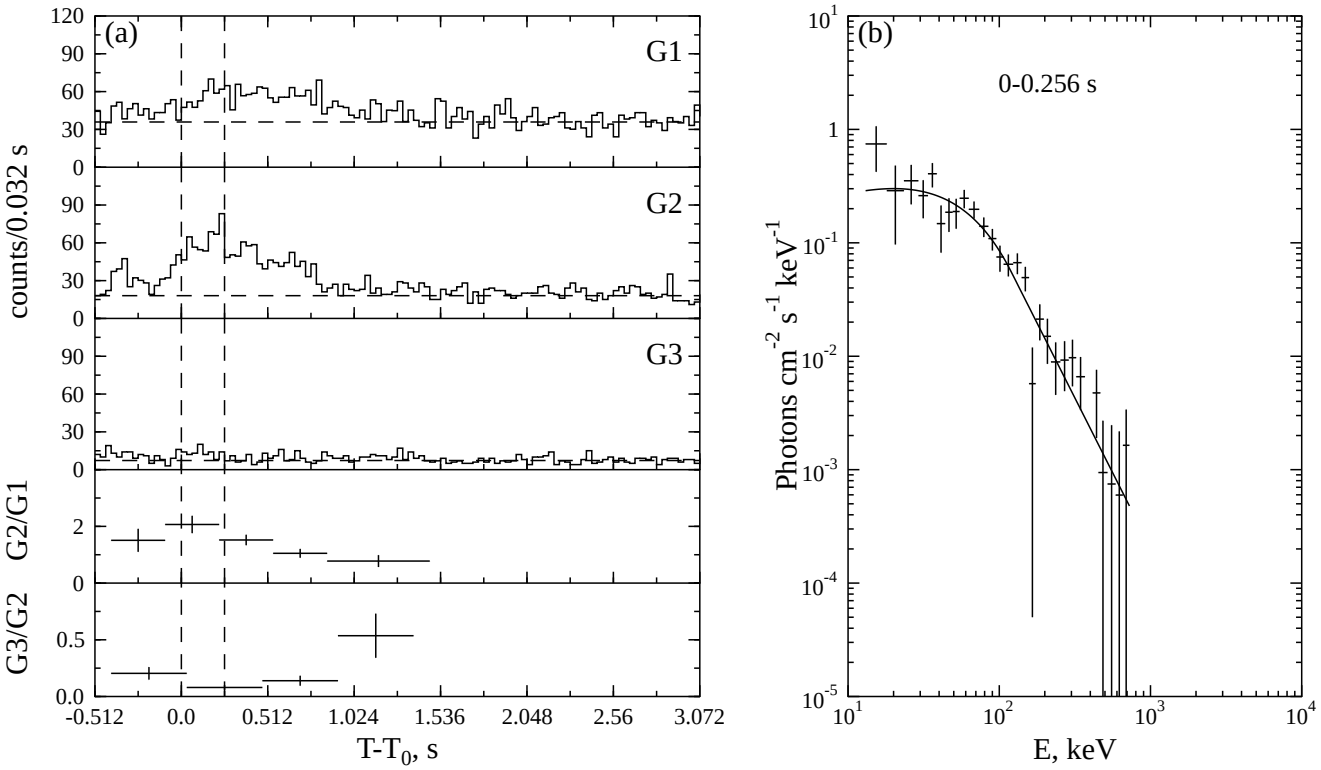

Fig. 37.— GRB 970506. T_0=56603.264 s UT.

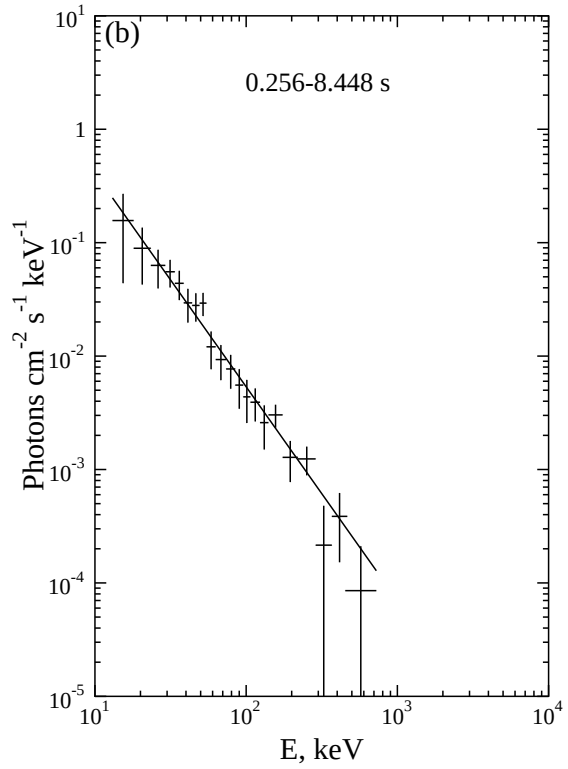

Fig. 38.— GRB 970506. T_0=56603.264 s UT (continued from Fig. 37).

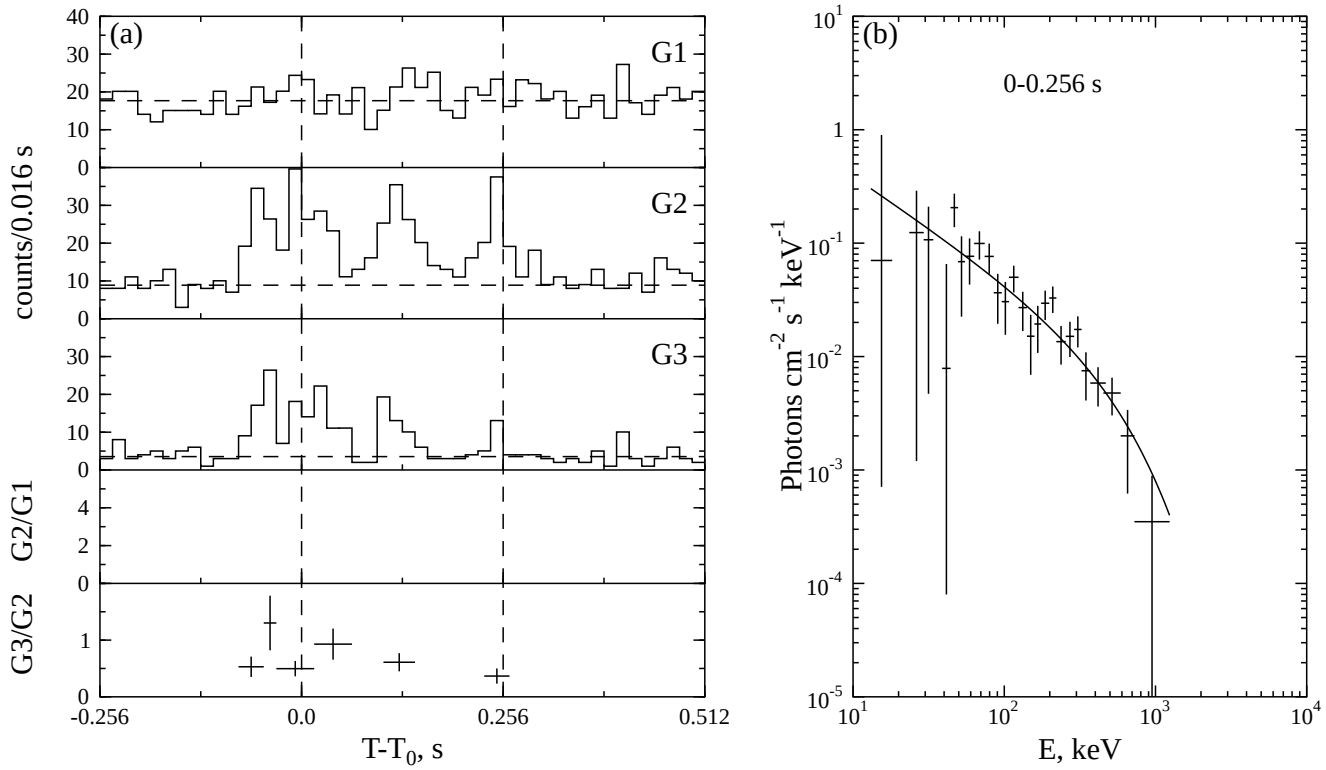

Fig. 39.— GRB 970521. T_0=49991.214 s UT.

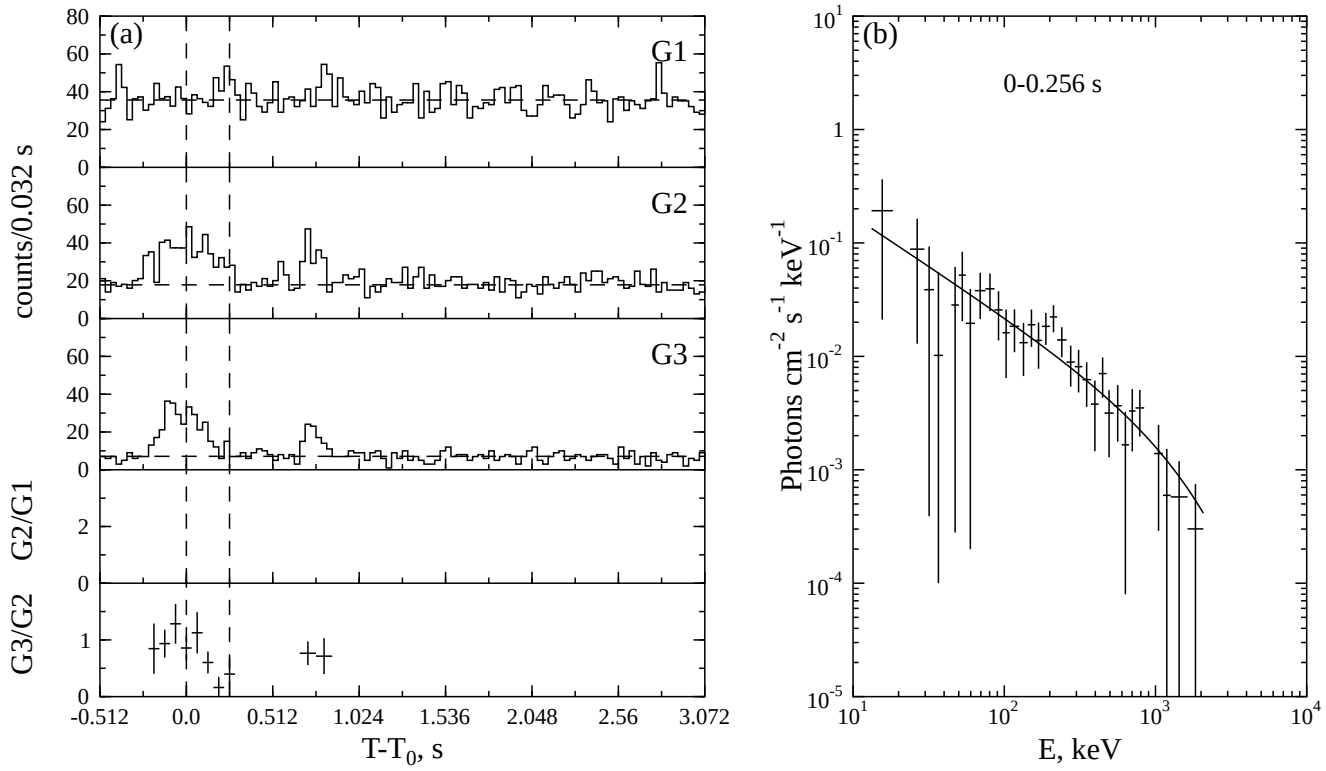

Fig. 40.— GRB 970608. T_0=49032.954 s UT.

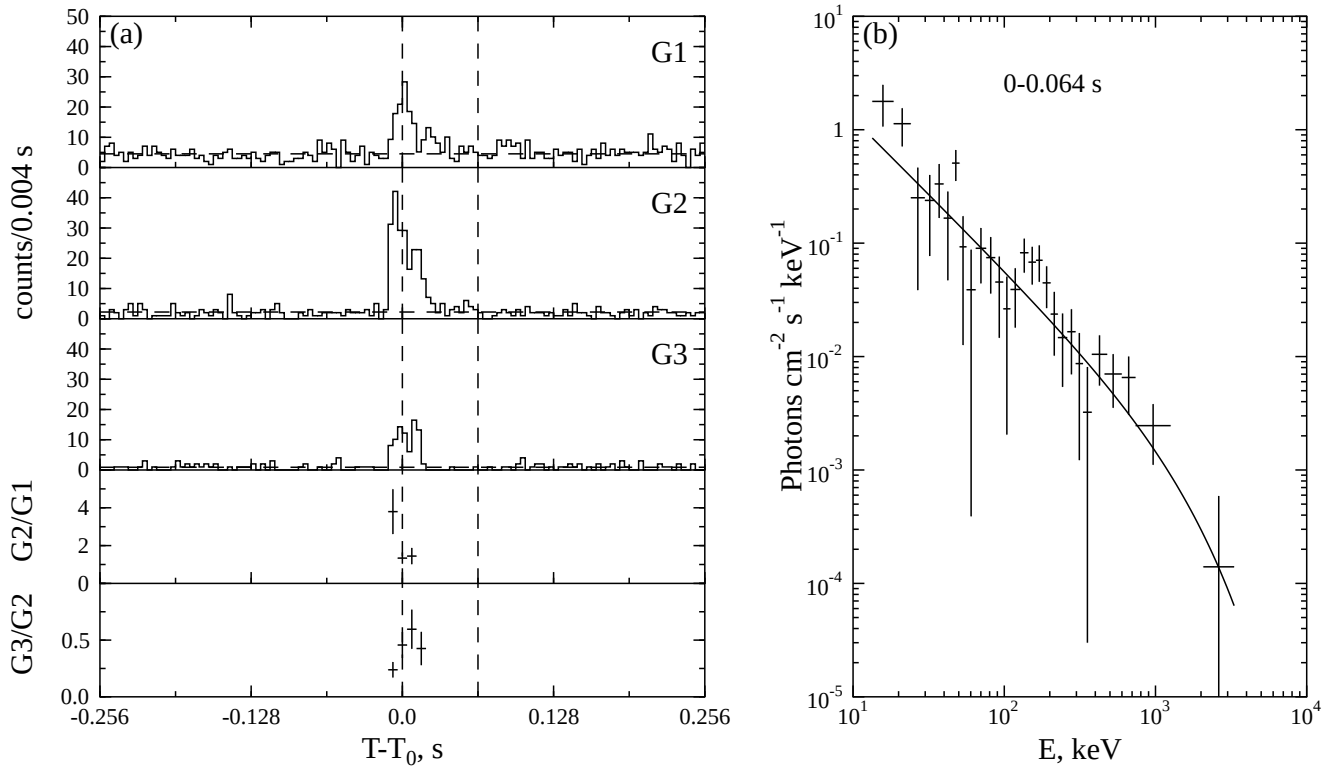

Fig. 41.— GRB 970625a. T_0=23681.548 s UT.

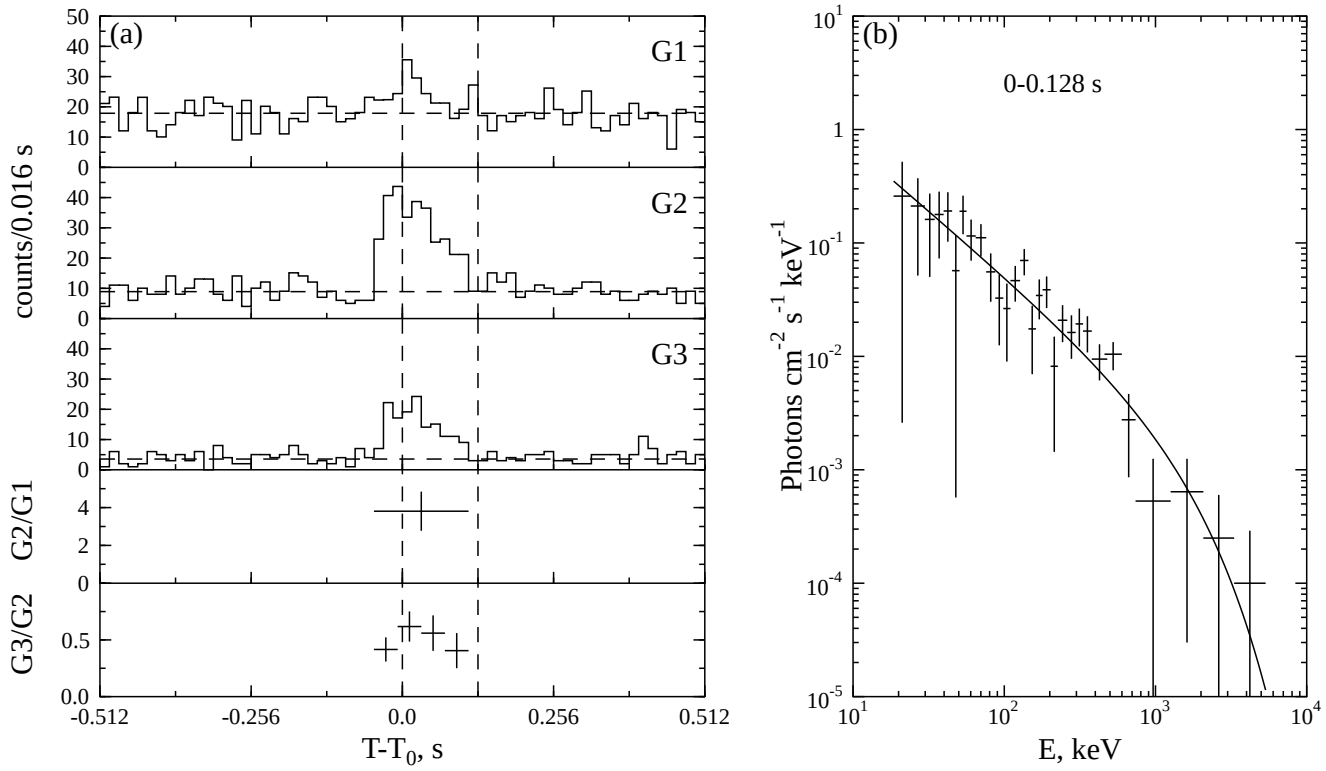

Fig. 42.— GRB 970626. T_0=6239.033 s UT.

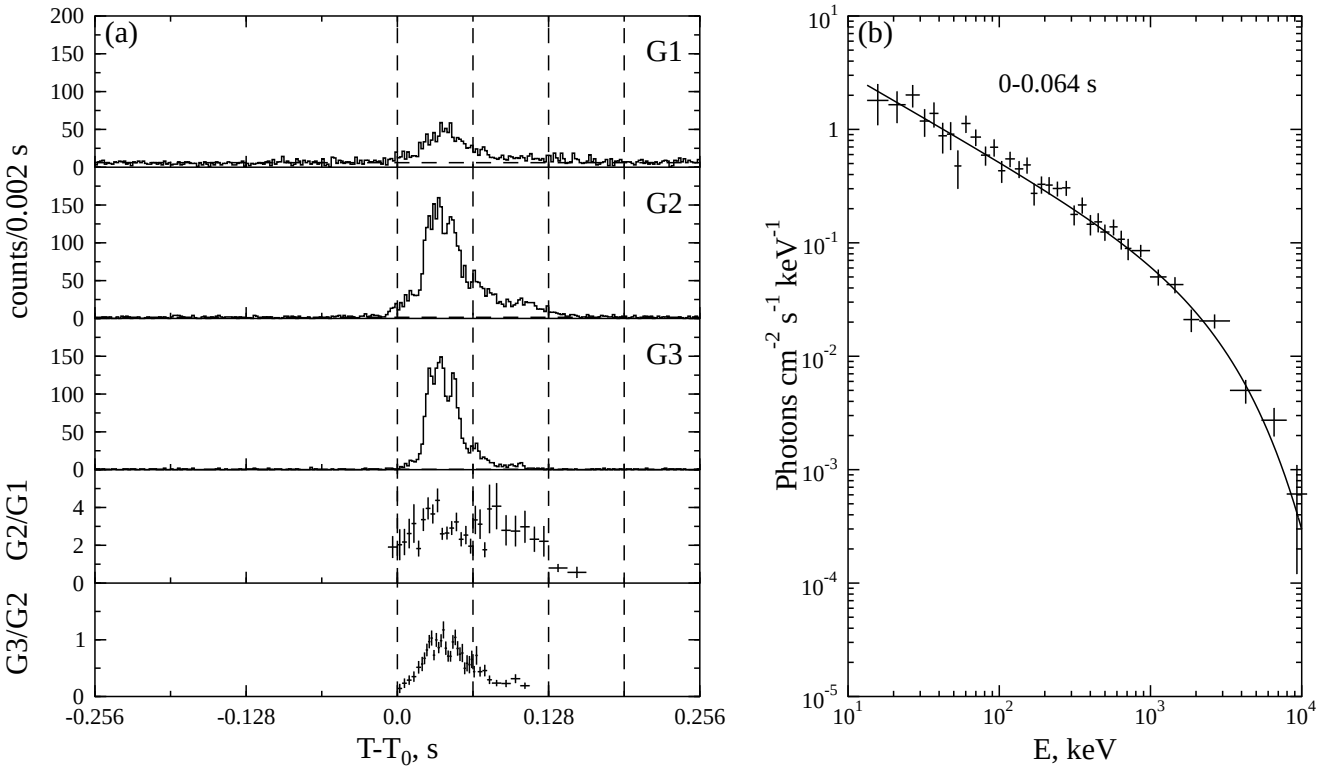

Fig. 43.— GRB 970704. T_0=4097.025 s UT.

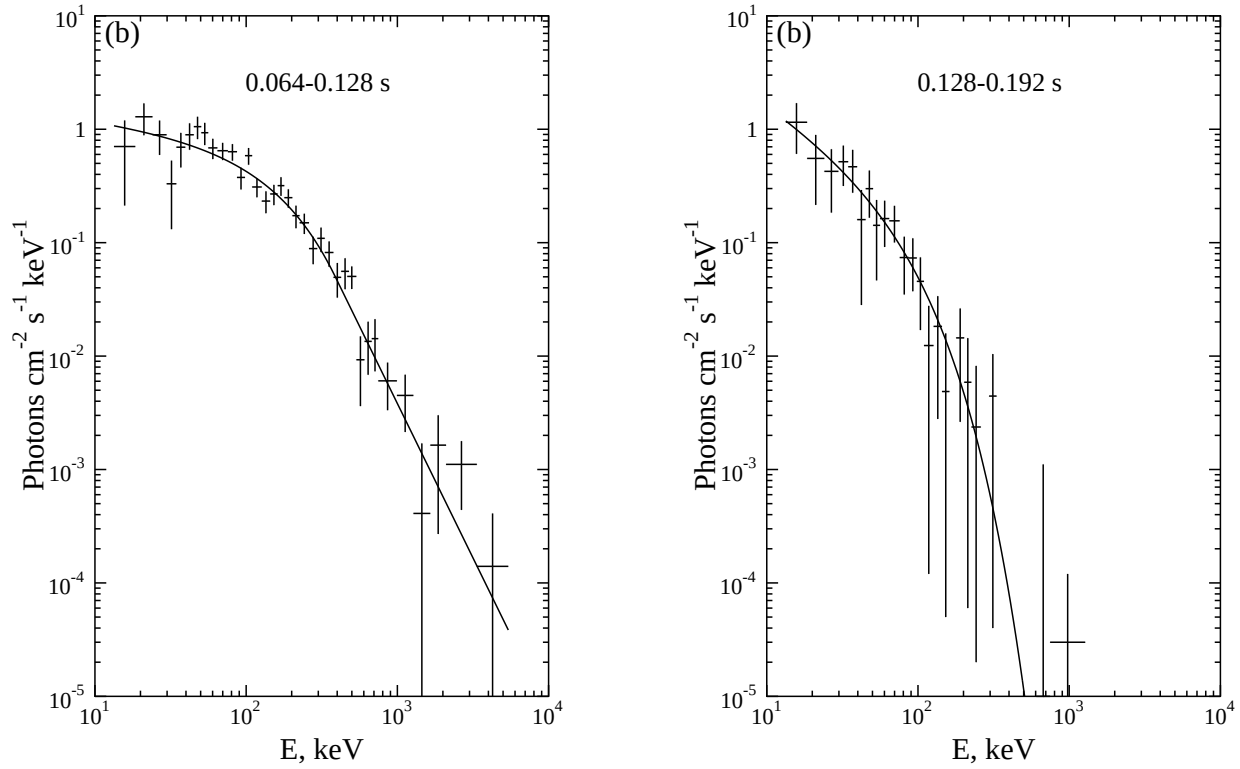

Fig. 44.— Energy spectra of the GRB 970704. T_0=4097.025 s UT (continued from Fig. 43).

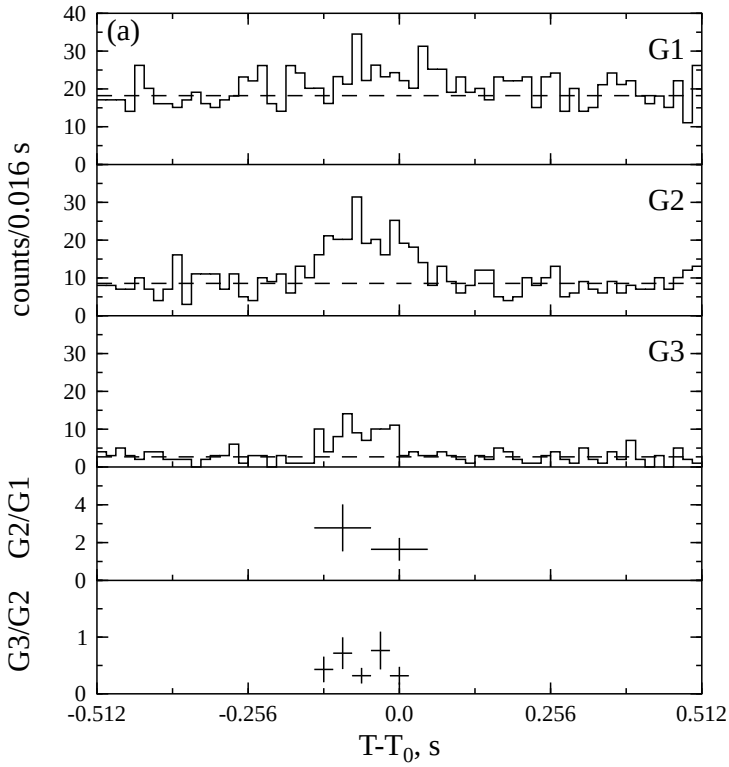

Fig. 45.— GRB 970803. T_0=66535.704 s UT.

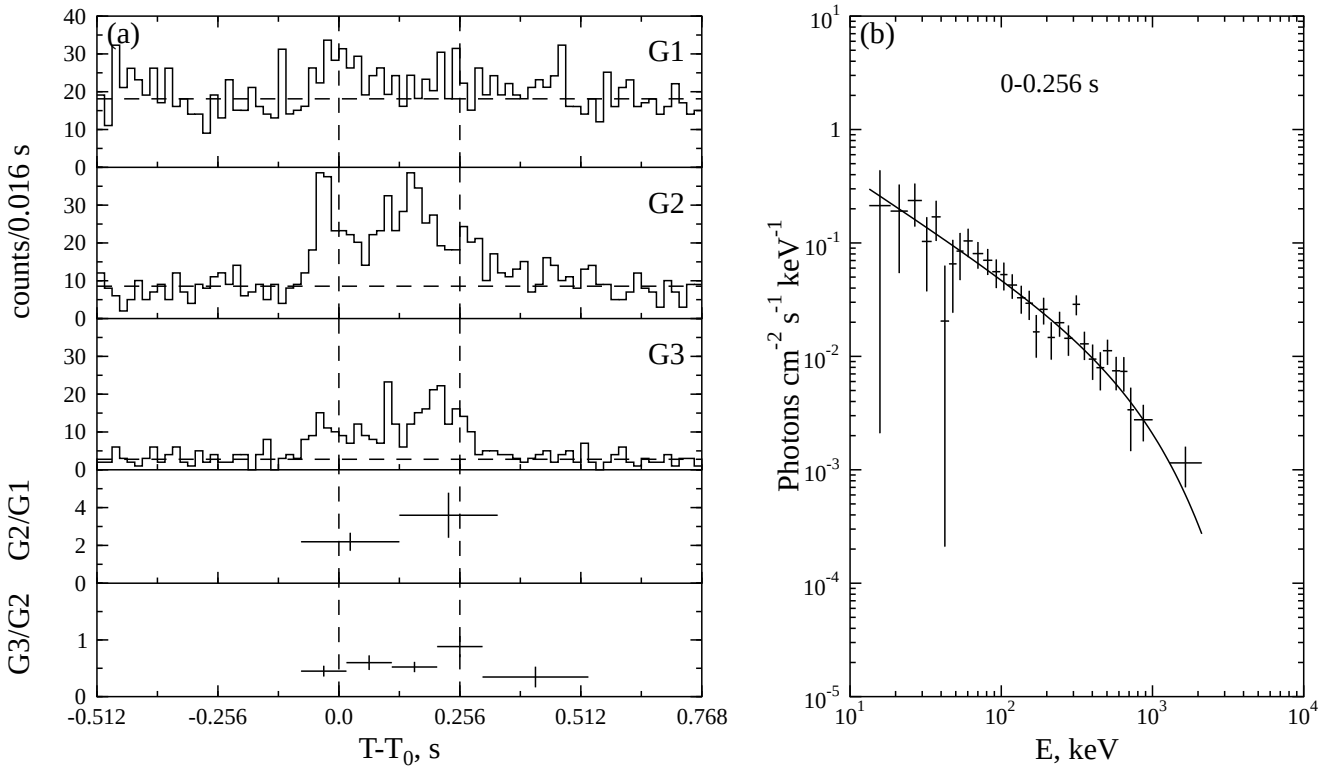

Fig. 46.— GRB 970902a. T_0=27561.329 s UT.

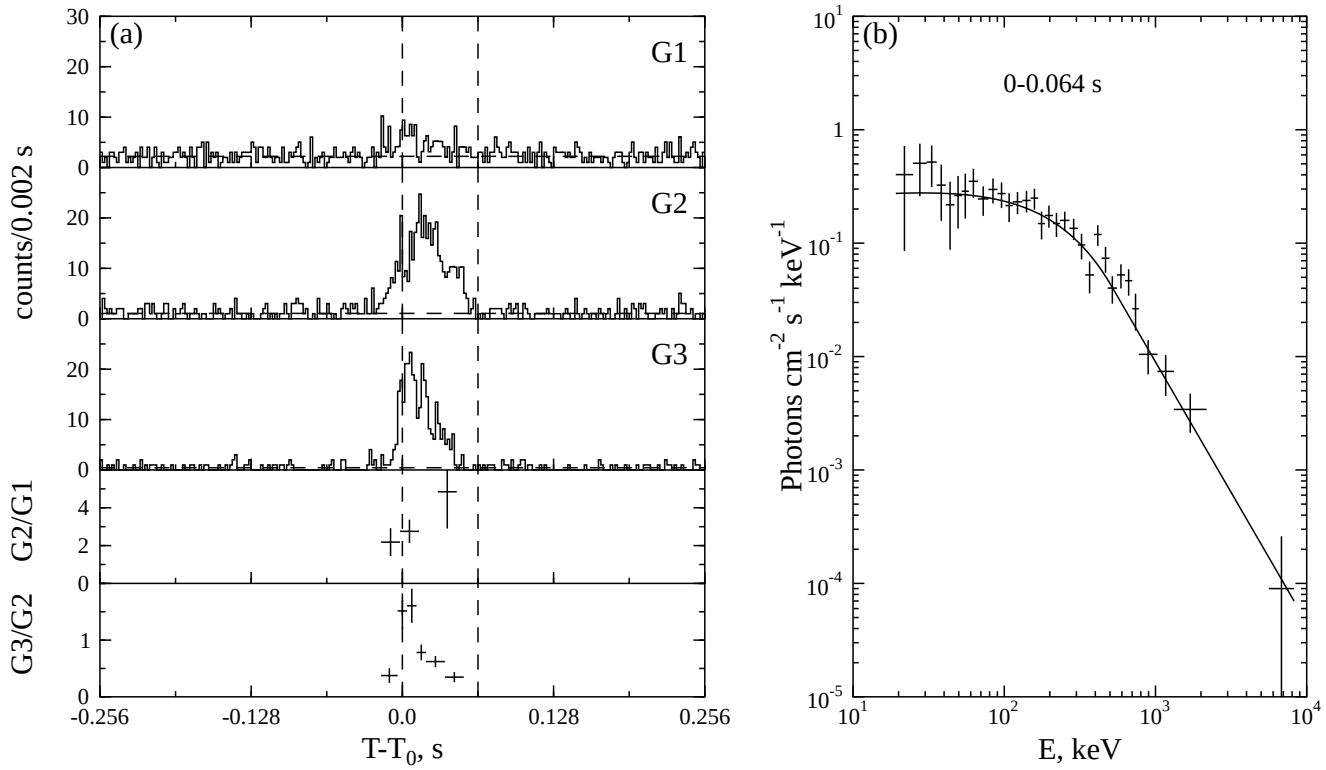

Fig. 47.— GRB 970921. T_0=83828.200 s UT.

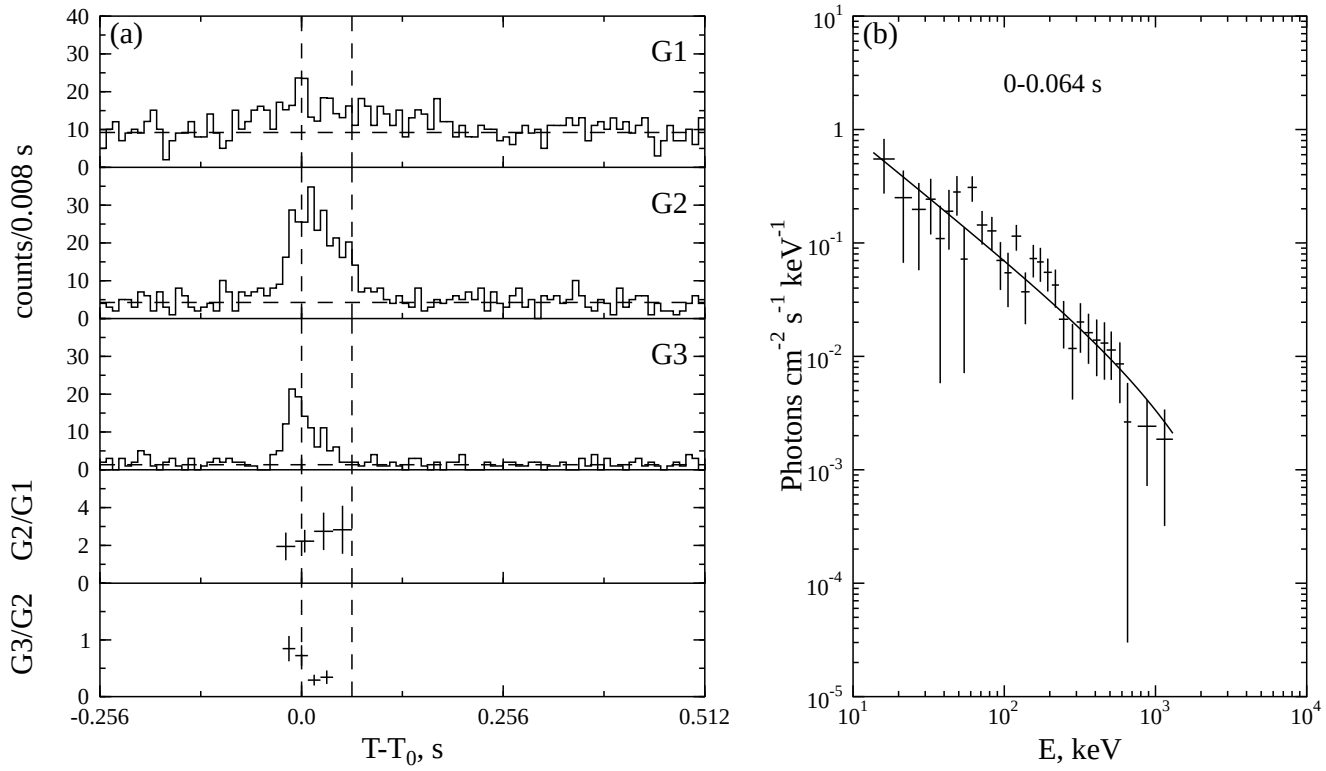

Fig. 48.— GRB 971015. T_0=30459.796 s UT.

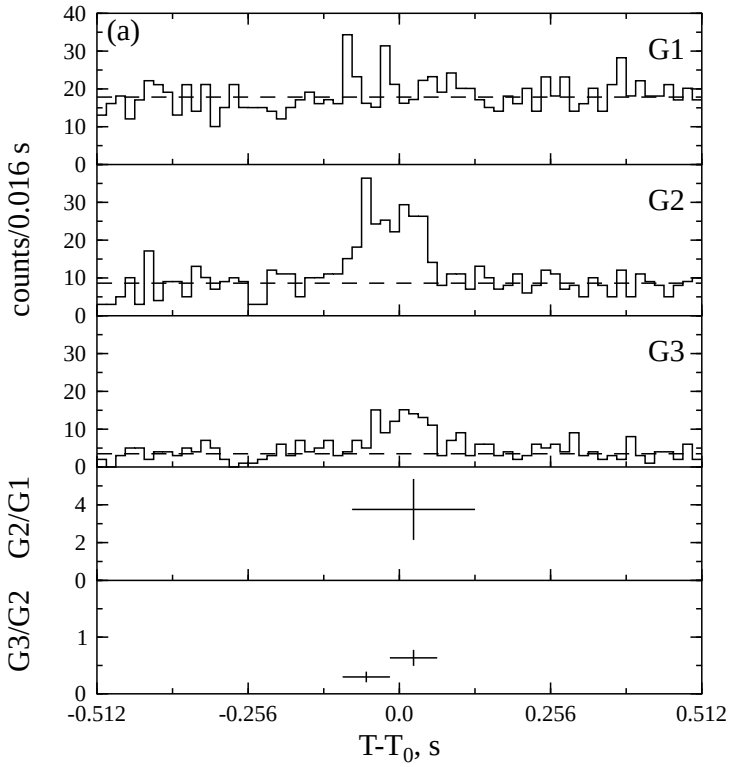

Fig. 49.— GRB 971031. T_0=23420.942 s UT.

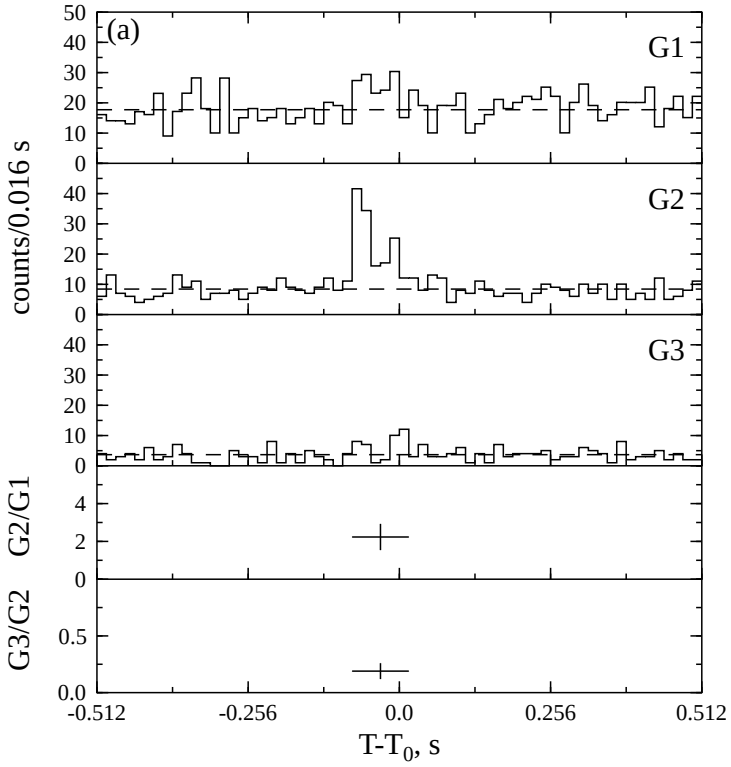

Fig. 50.— GRB 971118. T_0=29008.529 s UT.

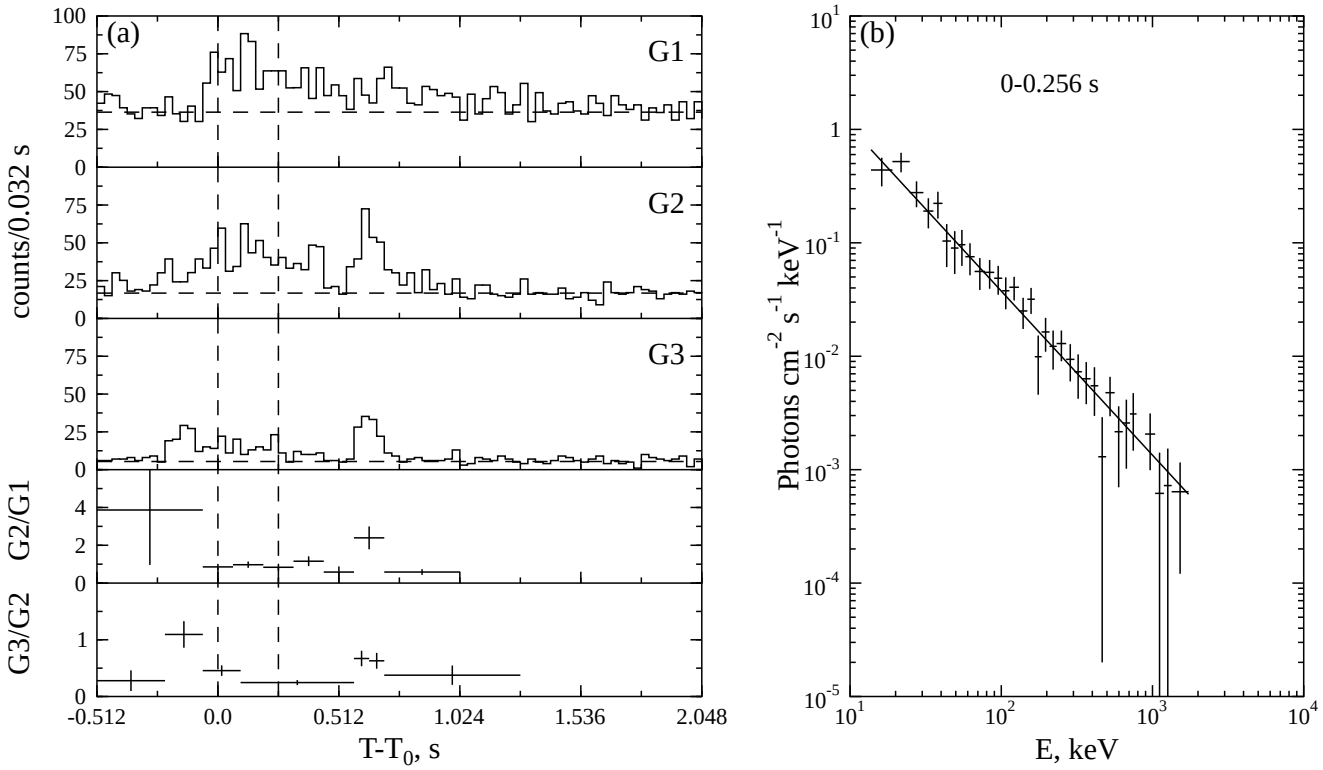

Fig. 51.— GRB 971218b. T_0=52503.029 s UT.

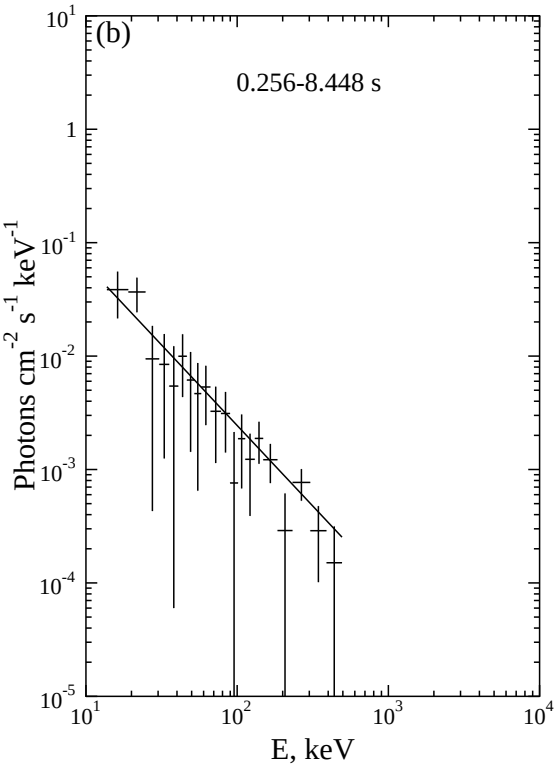

Fig. 52.— GRB 971218b. T_0=52503.029 s UT (continued from Fig. 51).

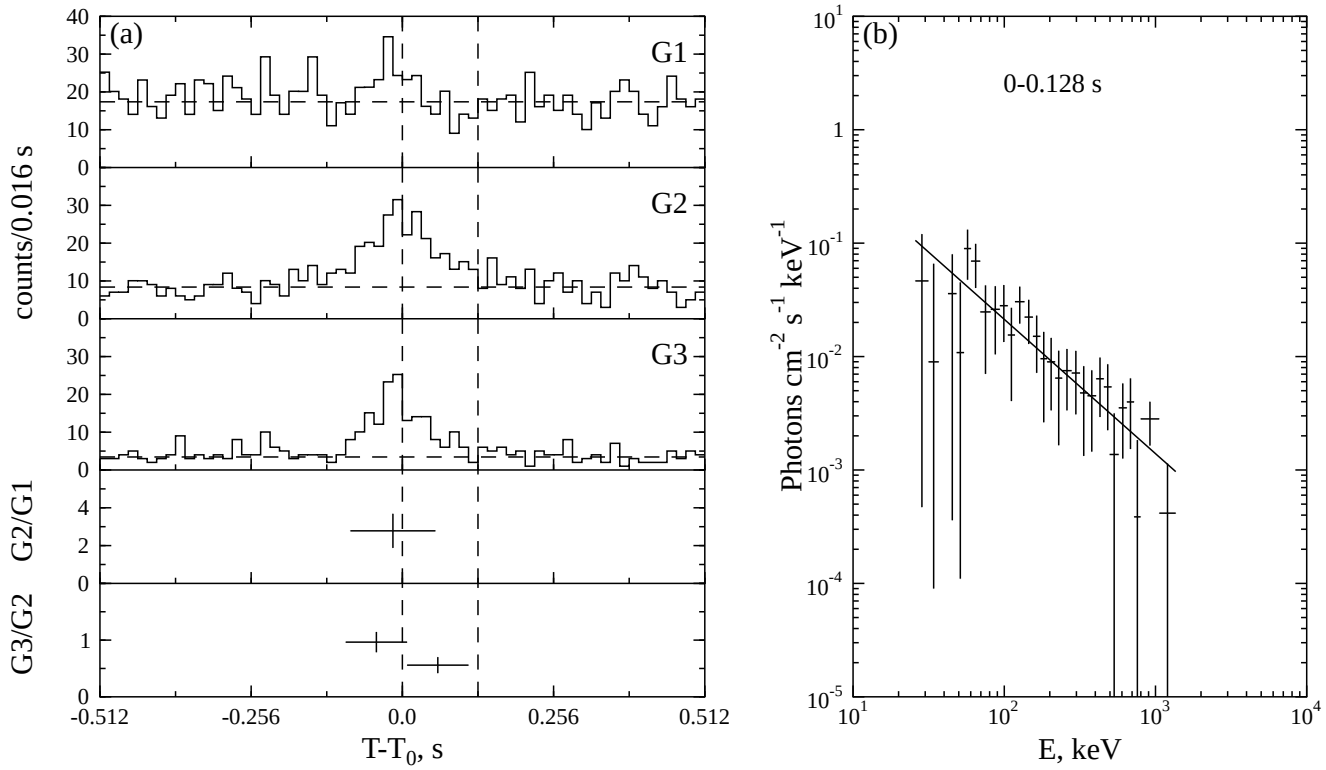

Fig. 53.— GRB 971230. T_0=83750.187 s UT.

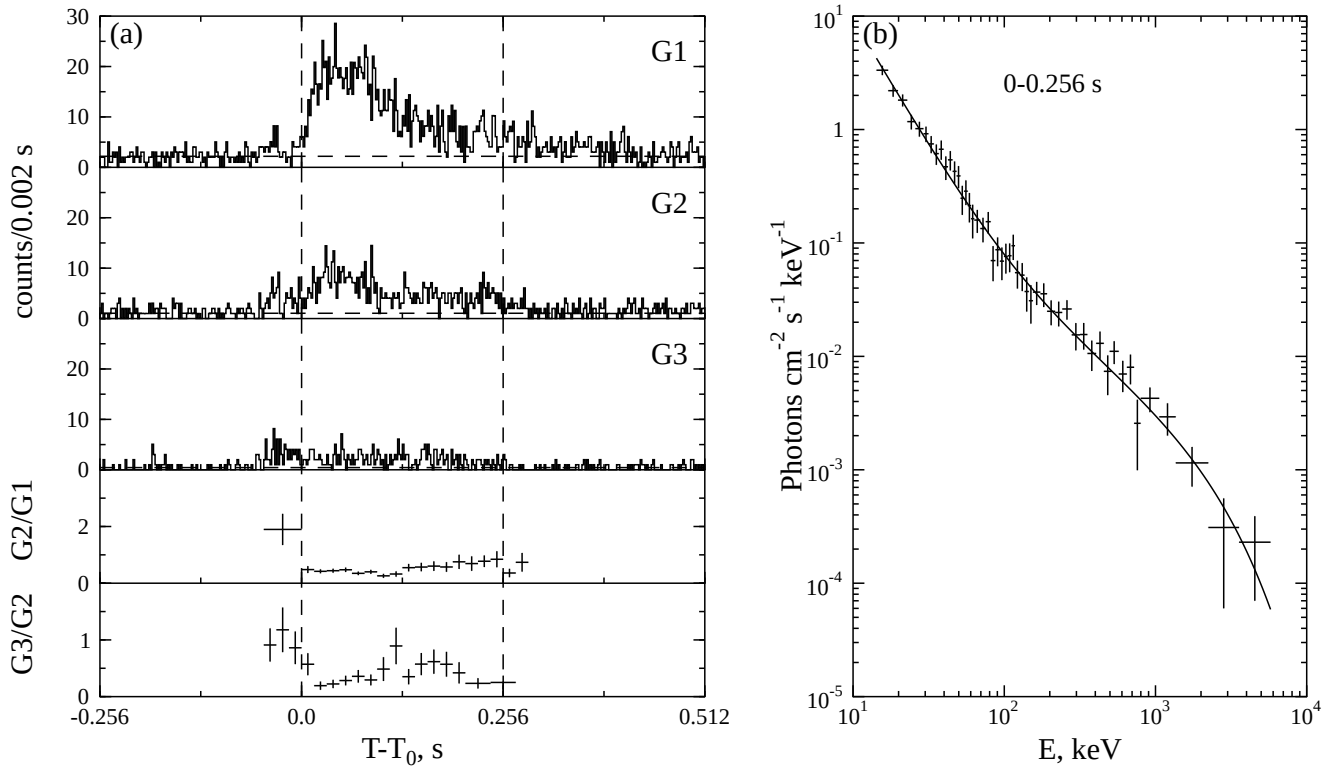

Fig. 54.— GRB 980205. T_0=19785.239 s UT.

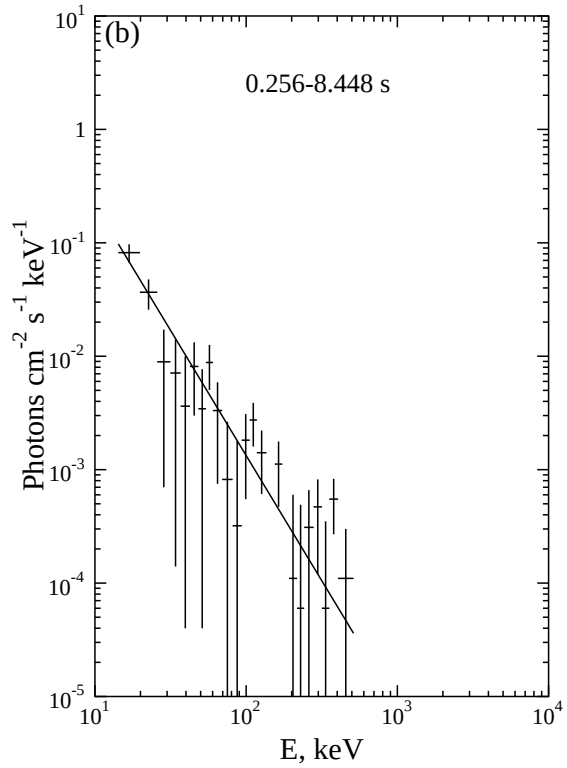

Fig. 55.— Energy spectrum of the GRB 980205. T_0=19785.239 s UT (continued from Fig. 54).

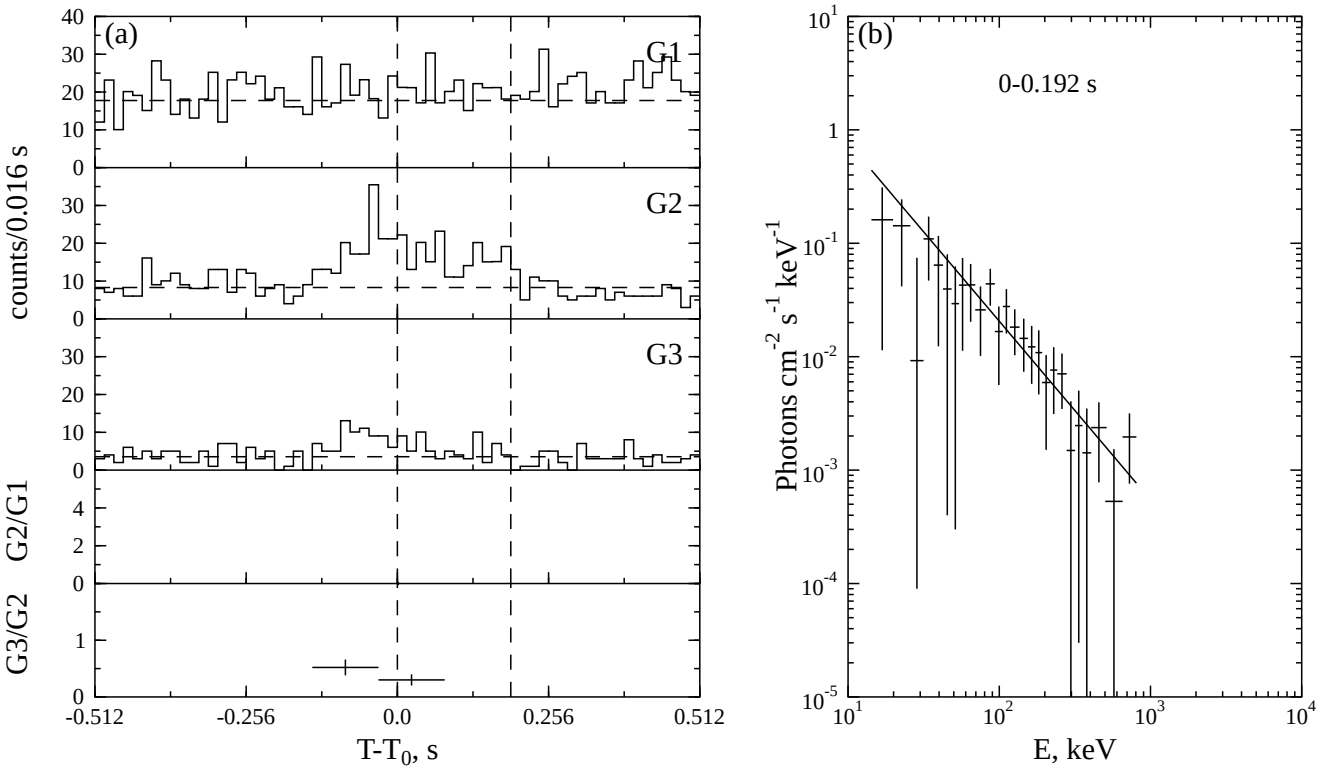

Fig. 56.— GRB 980218b. T_0=54768.157 s UT.

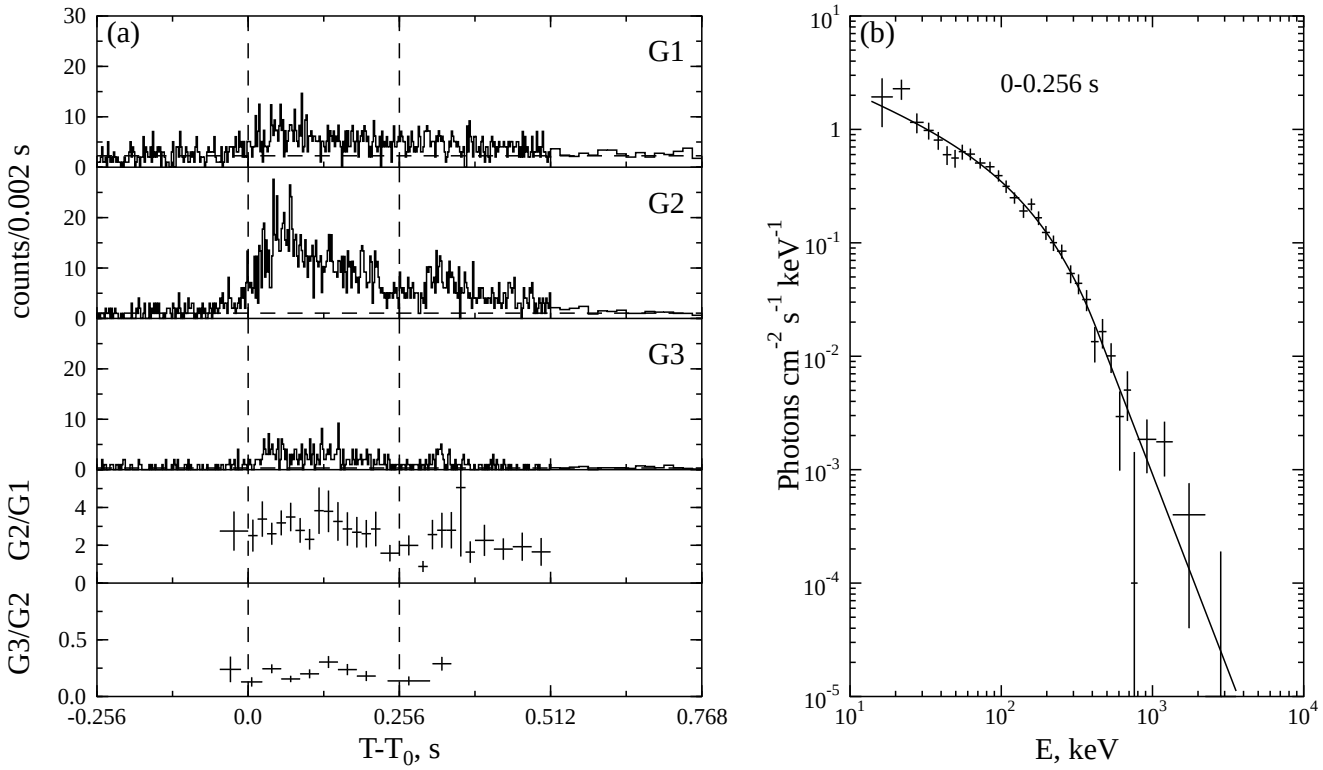

Fig. 57.— GRB 980228a. T_0=24244.602 s UT.

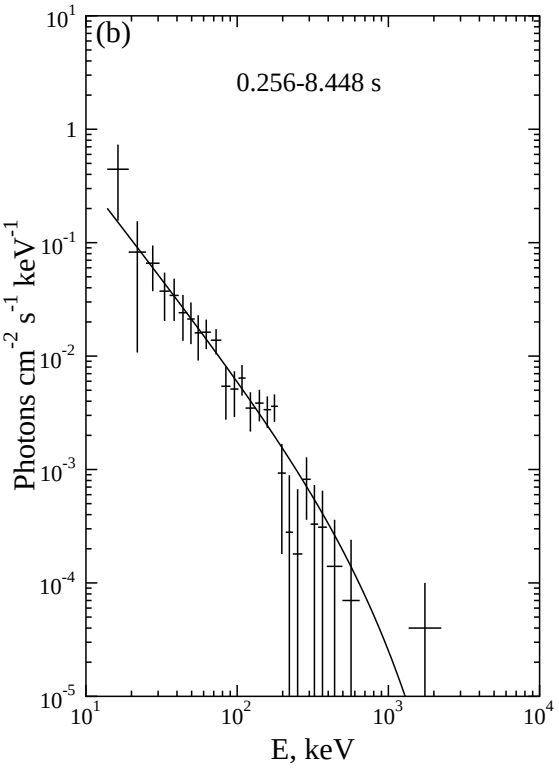

Fig. 58.— Energy spectrum of the GRB 980228a. T_0=24244.602 s UT (continued from Fig. 57).

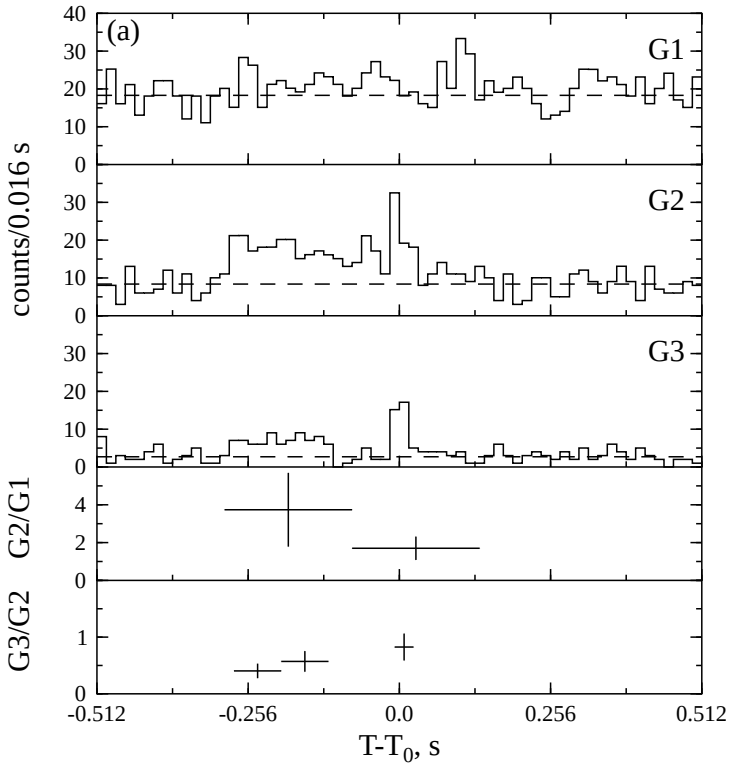

Fig. 59.— GRB 980302b. T_0=29955.993 s UT.

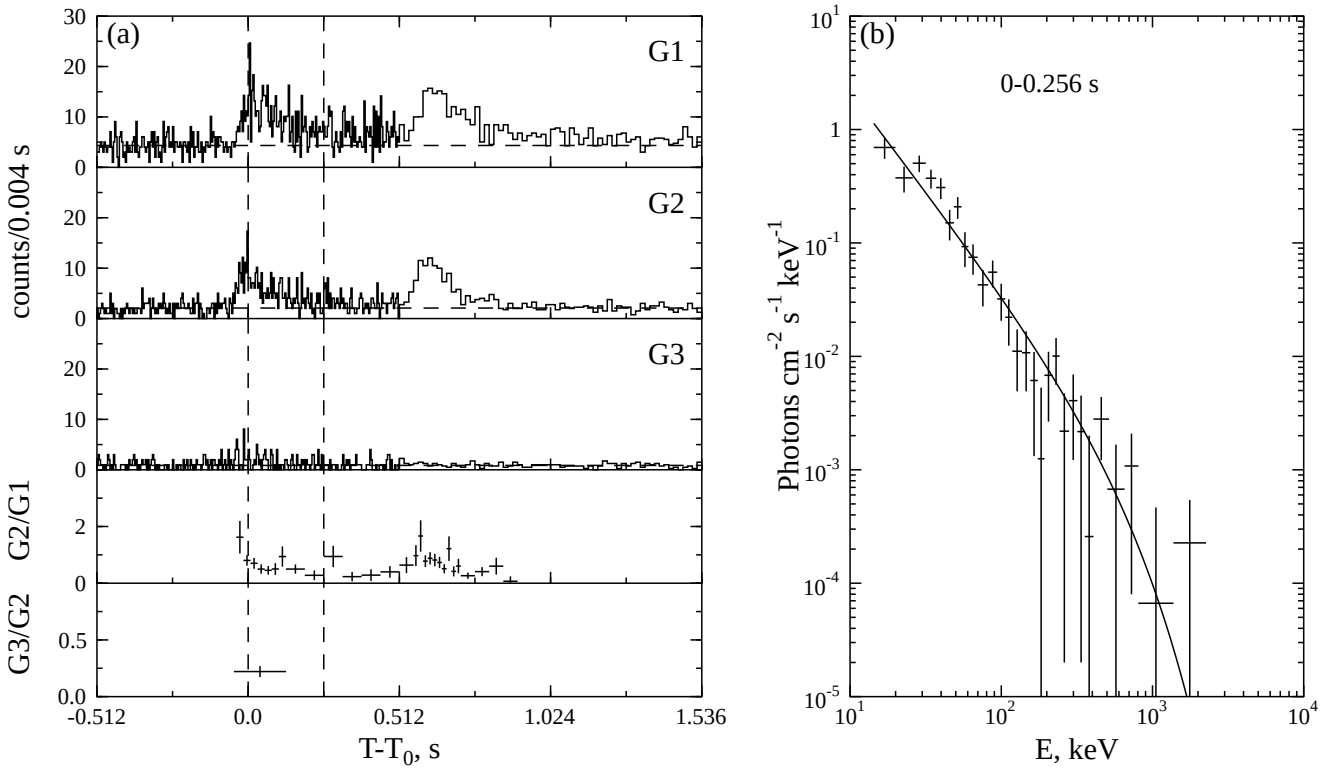

Fig. 60.— GRB 980310a. T_0=50261.054 s UT.

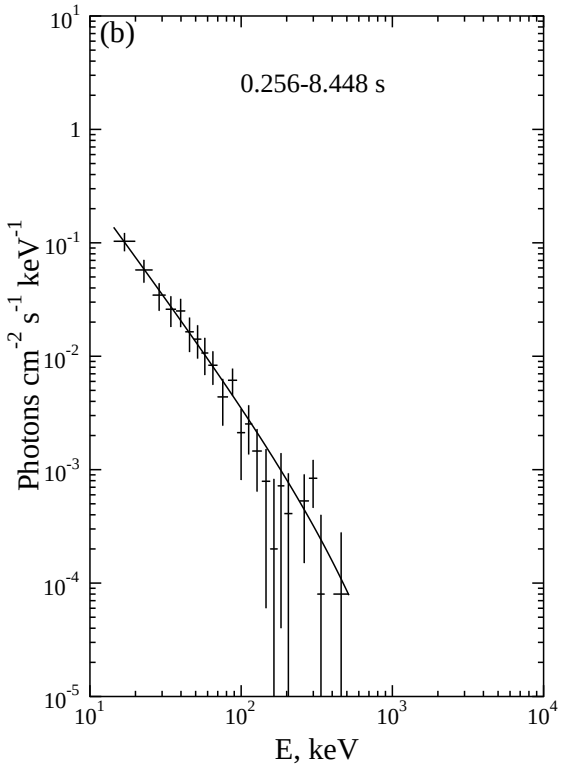

Fig. 61.— Energy spectrum of the GRB 980310a. T_0=50261.054 s UT (continued from Fig. 60).

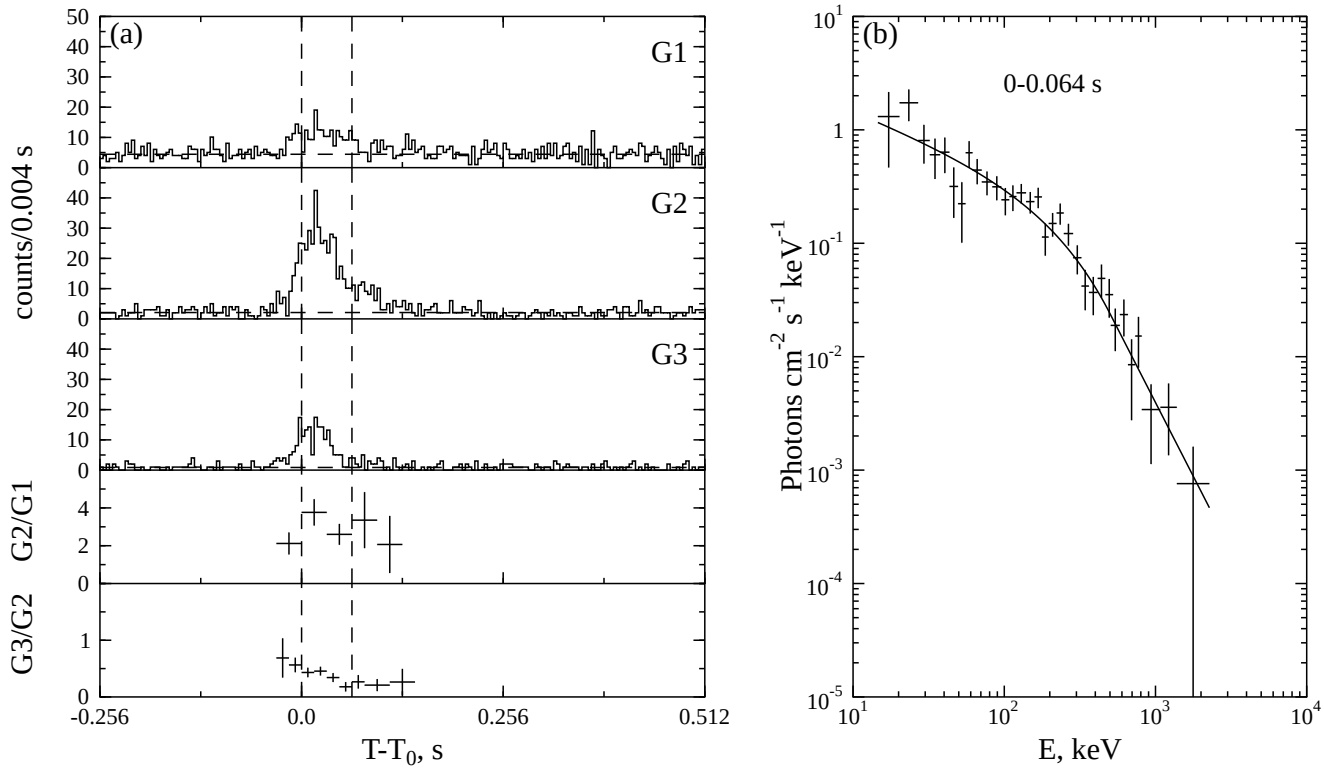

Fig. 62.— GRB 980330a. T_0=96.711 s UT.

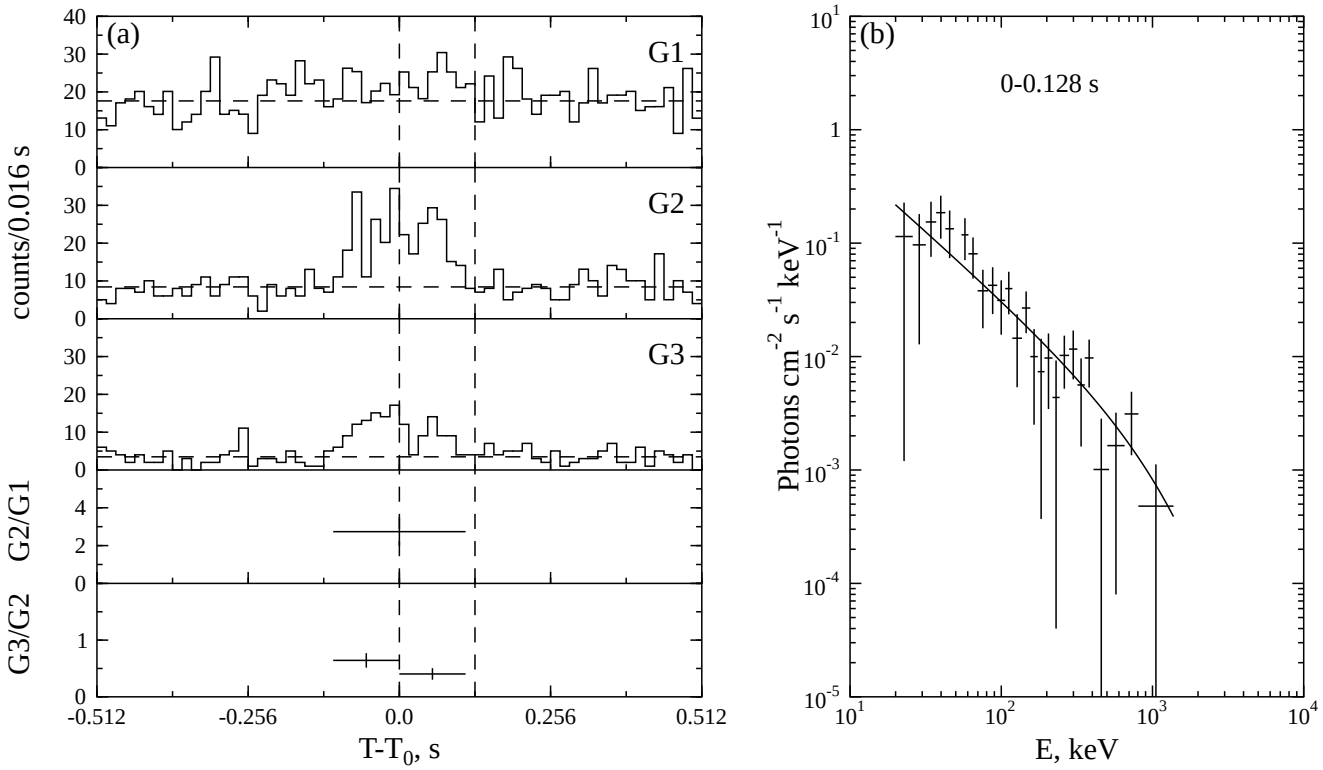

Fig. 63.— GRB 980331. T_0=61078.449 s UT.

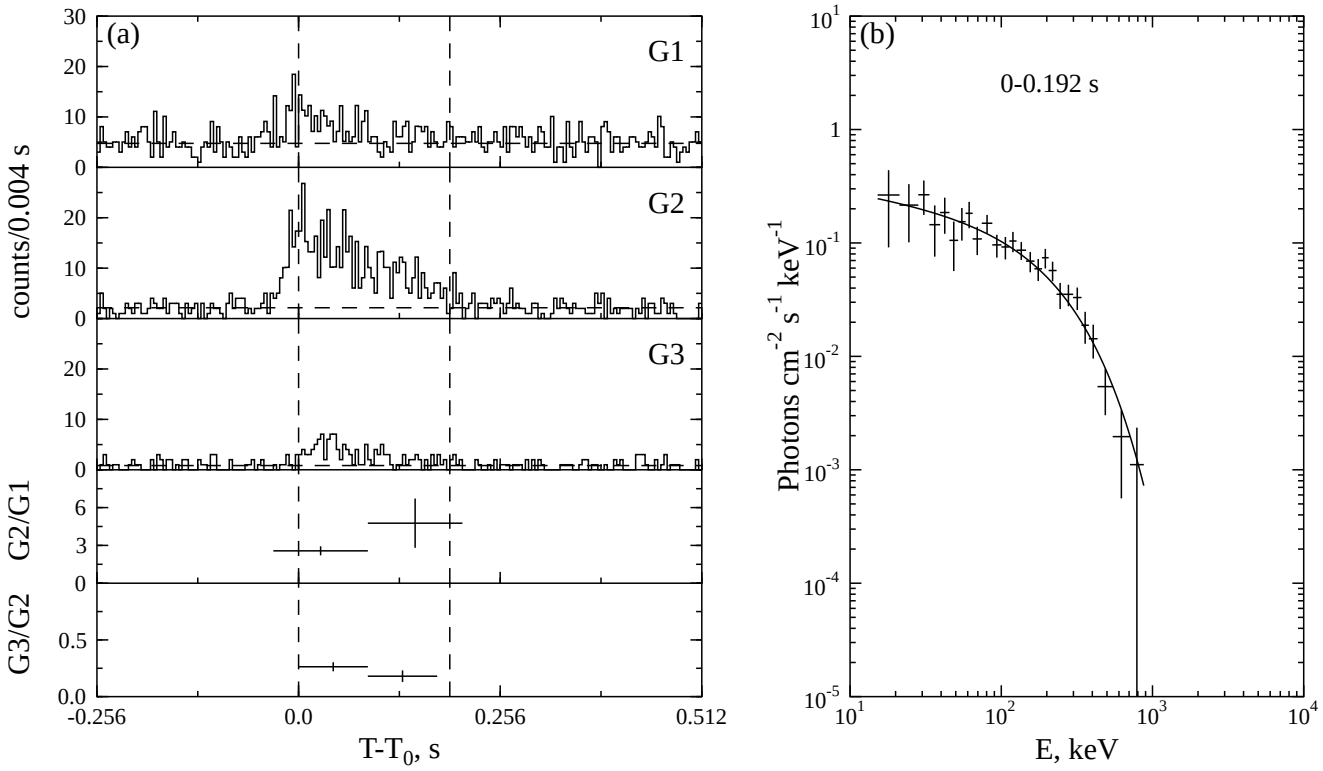

Fig. 64.— GRB 980429. T_0=20492.079 s UT.

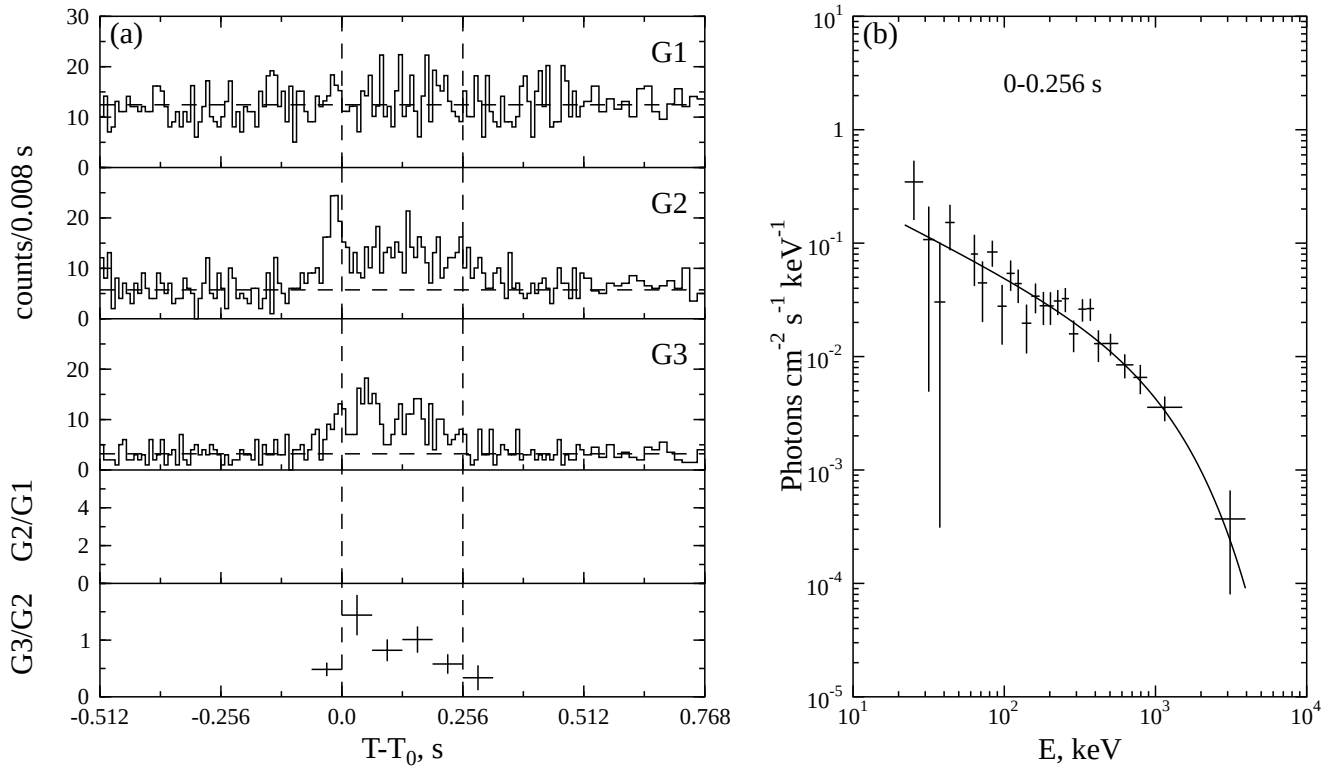

Fig. 65.— GRB 980430. T_0=59702.214 s UT.

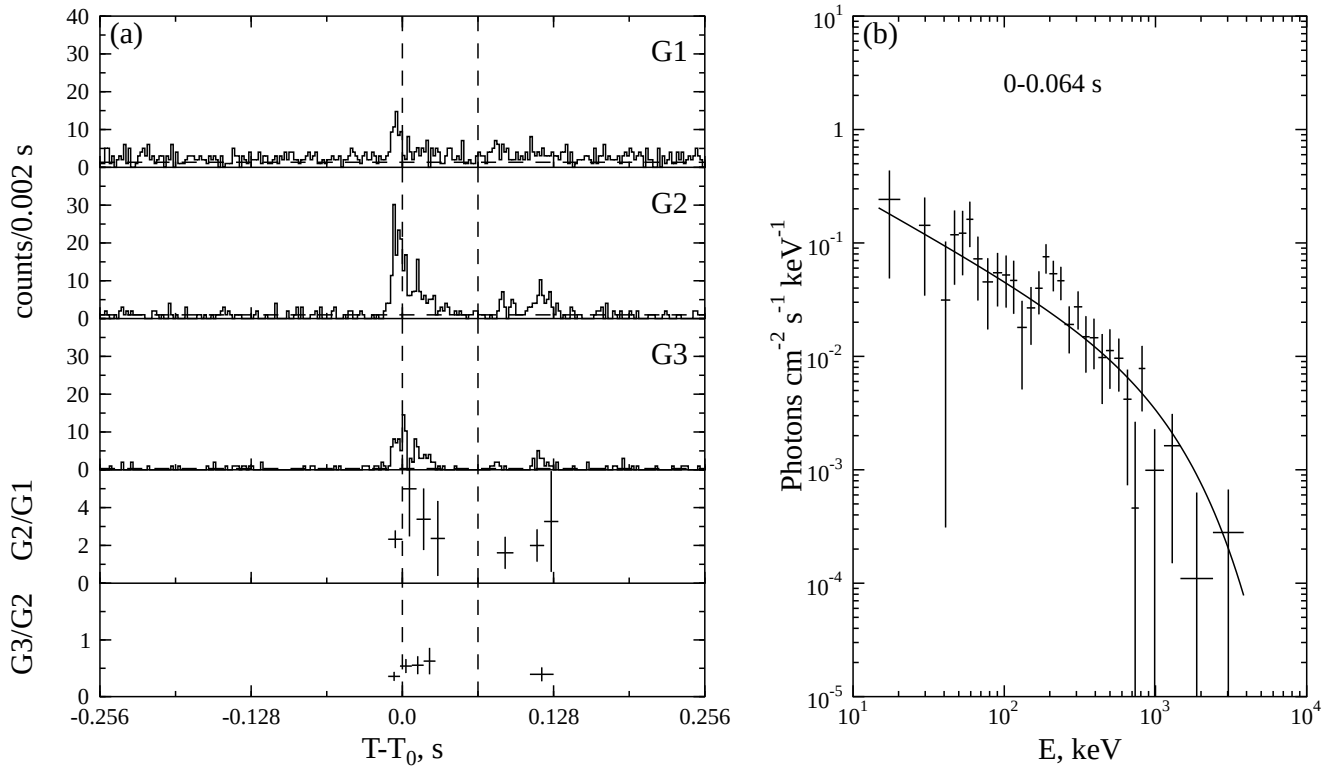

Fig. 66.— GRB 980605. T_0=51131.976 s UT.

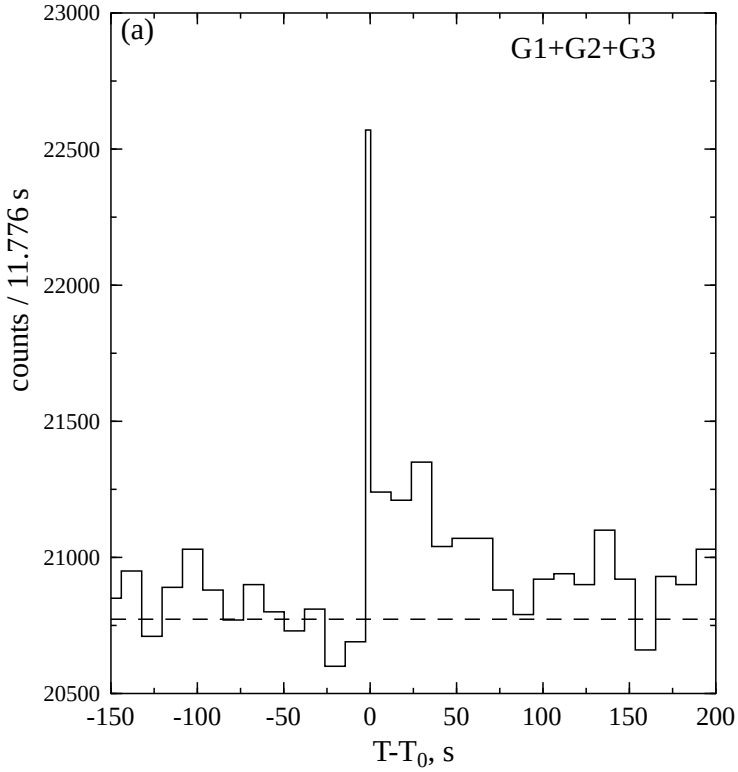

Fig. 67.— GRB 980605. T_0=51131.976 s UT (continued from Fig. 66).

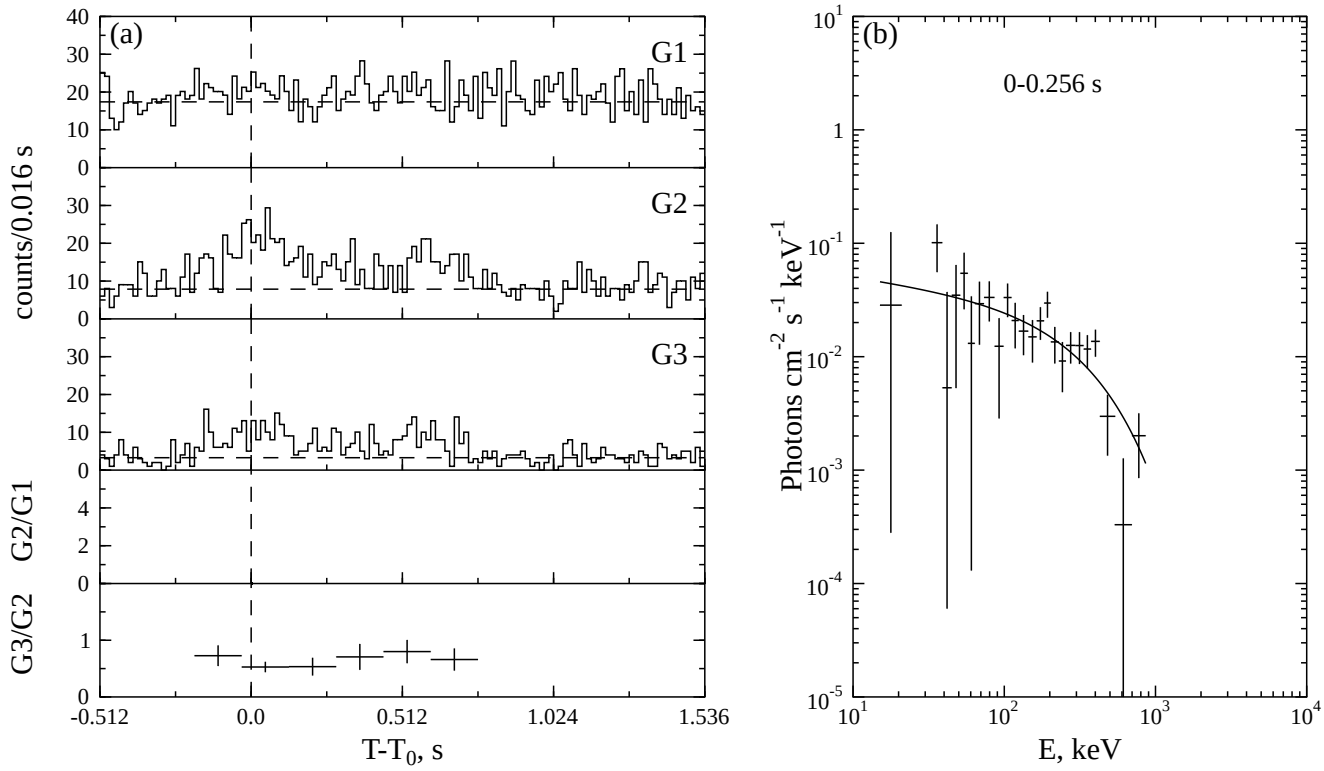

Fig. 68.— GRB 980610a. T_0=71546.850 s UT.

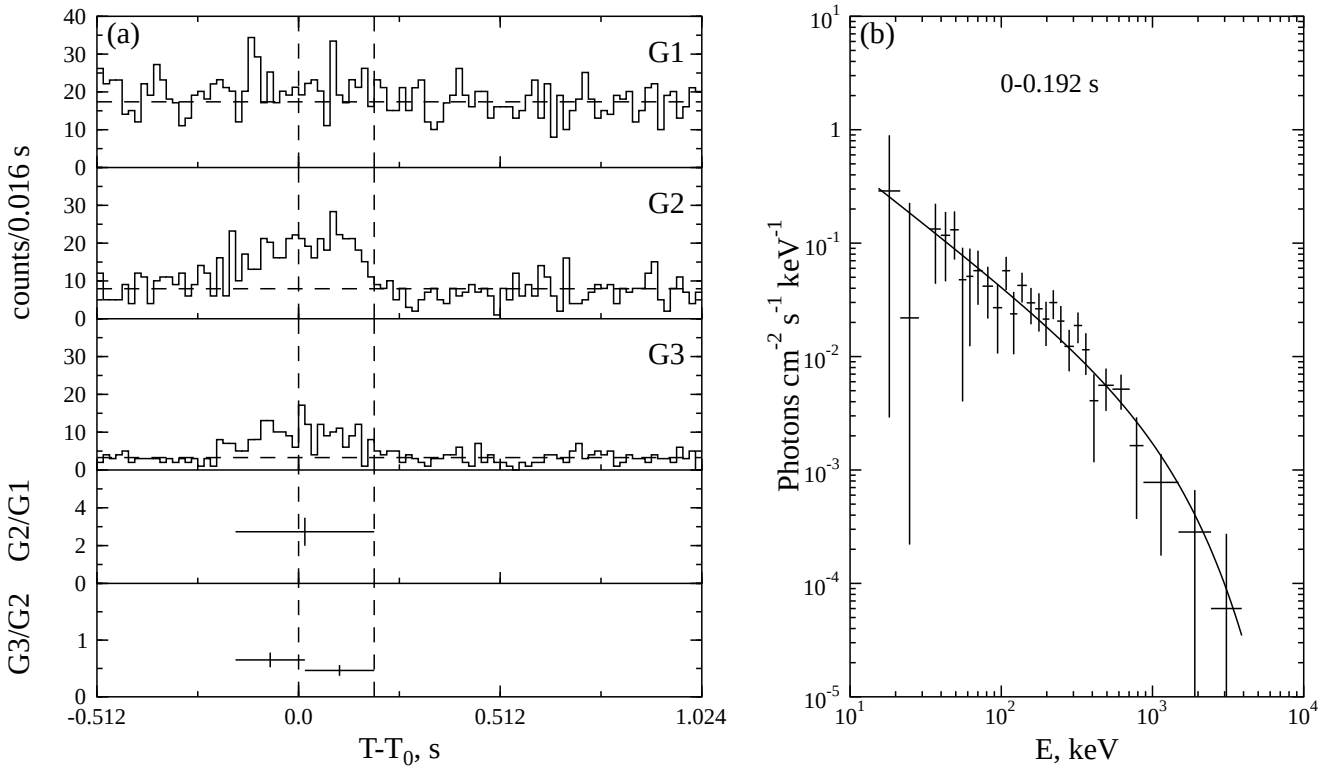

Fig. 69.— GRB 980610b. T_0=86195.164 s UT.

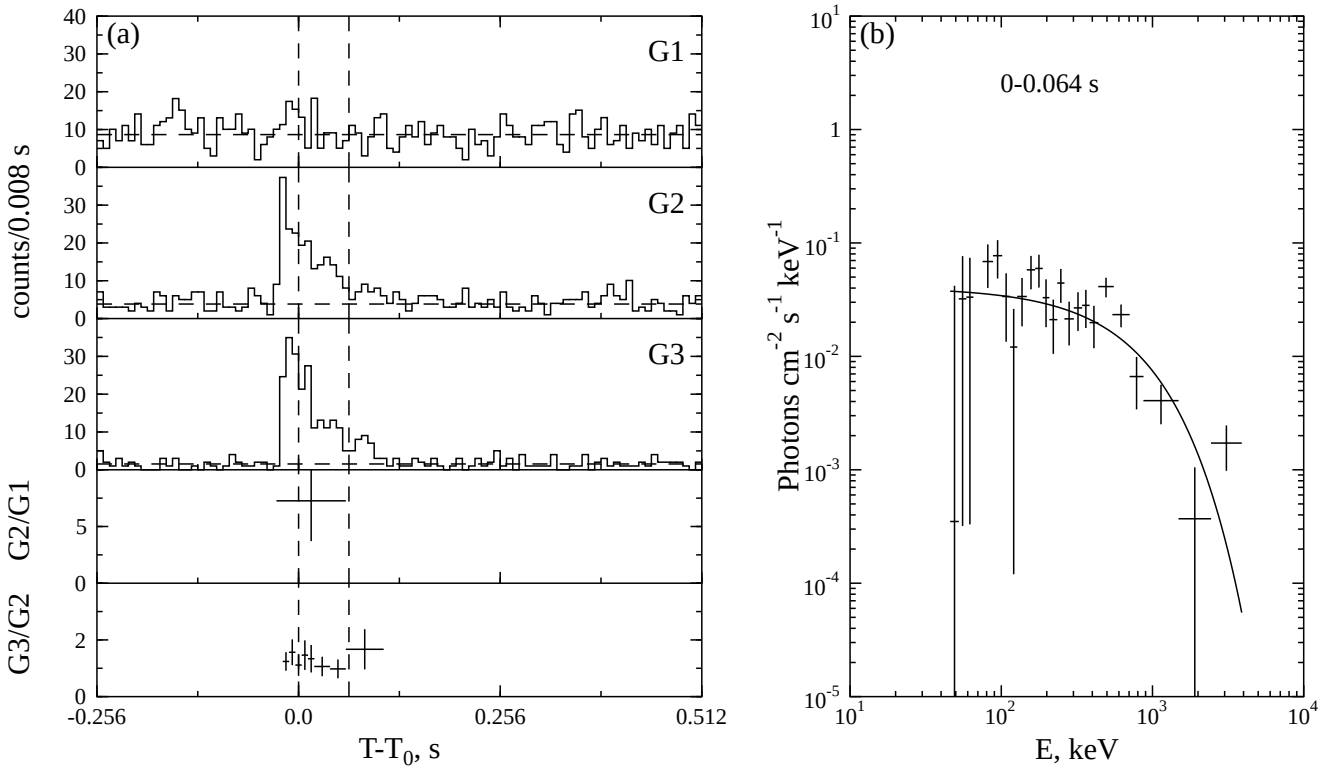

Fig. 70.— GRB 980619. T_0=47530.372 s UT.

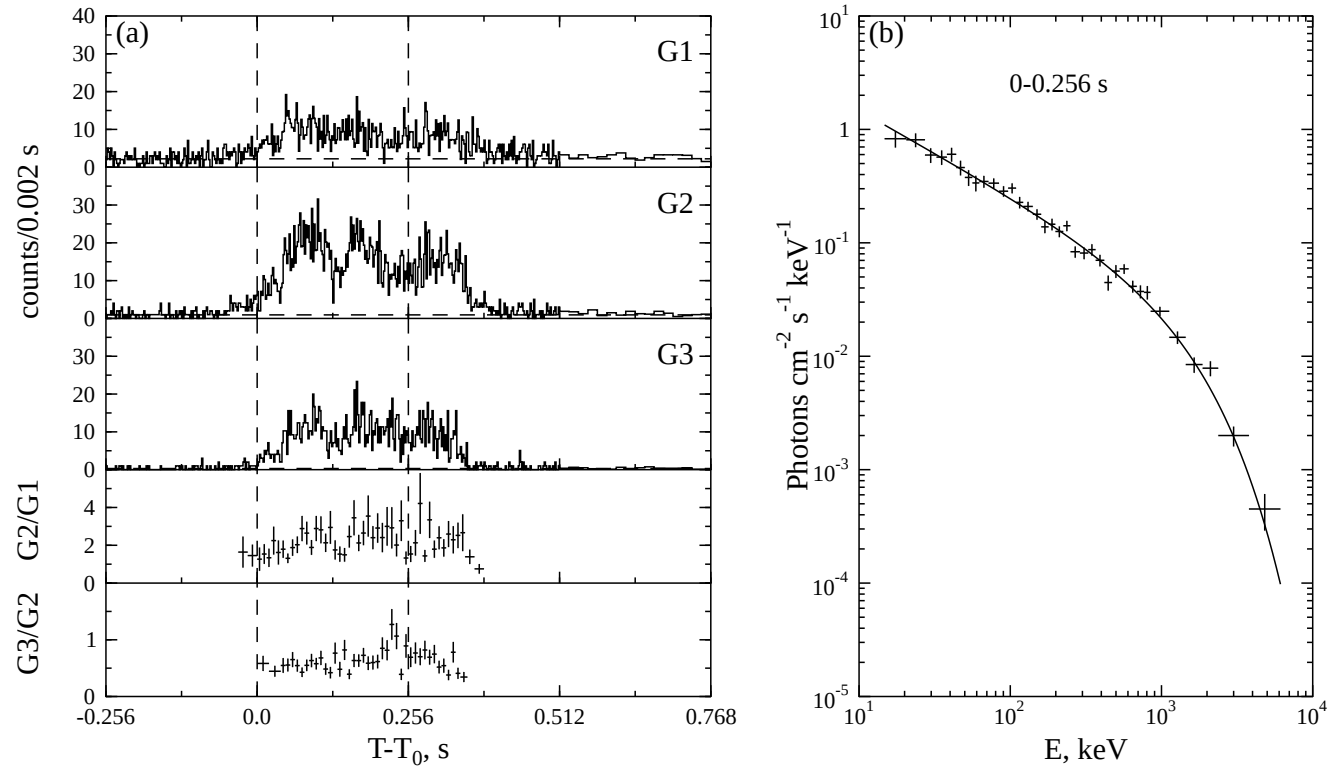

Fig. 71.— GRB 980706a. T_0=57586.277 s UT.

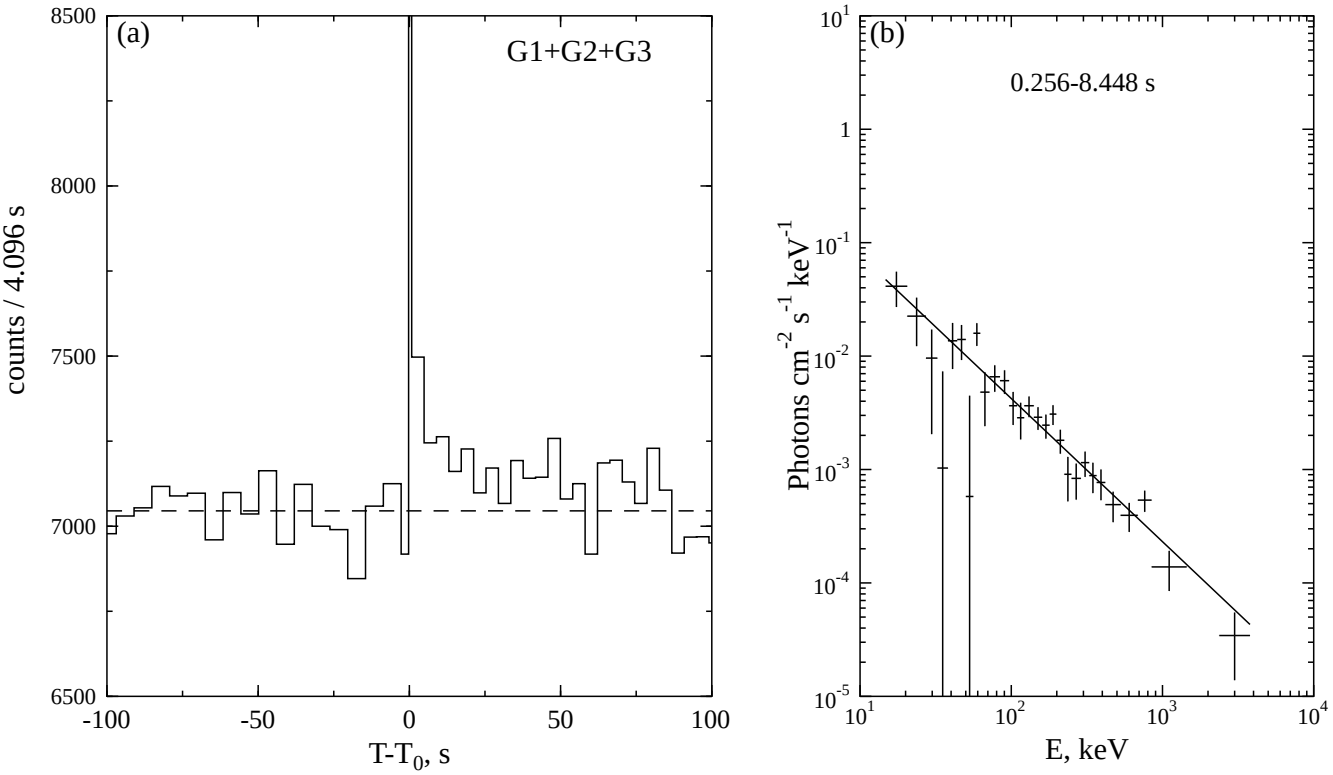

Fig. 72.— GRB 980706a. T_0=57586.277 s UT (continued from Fig. 71).

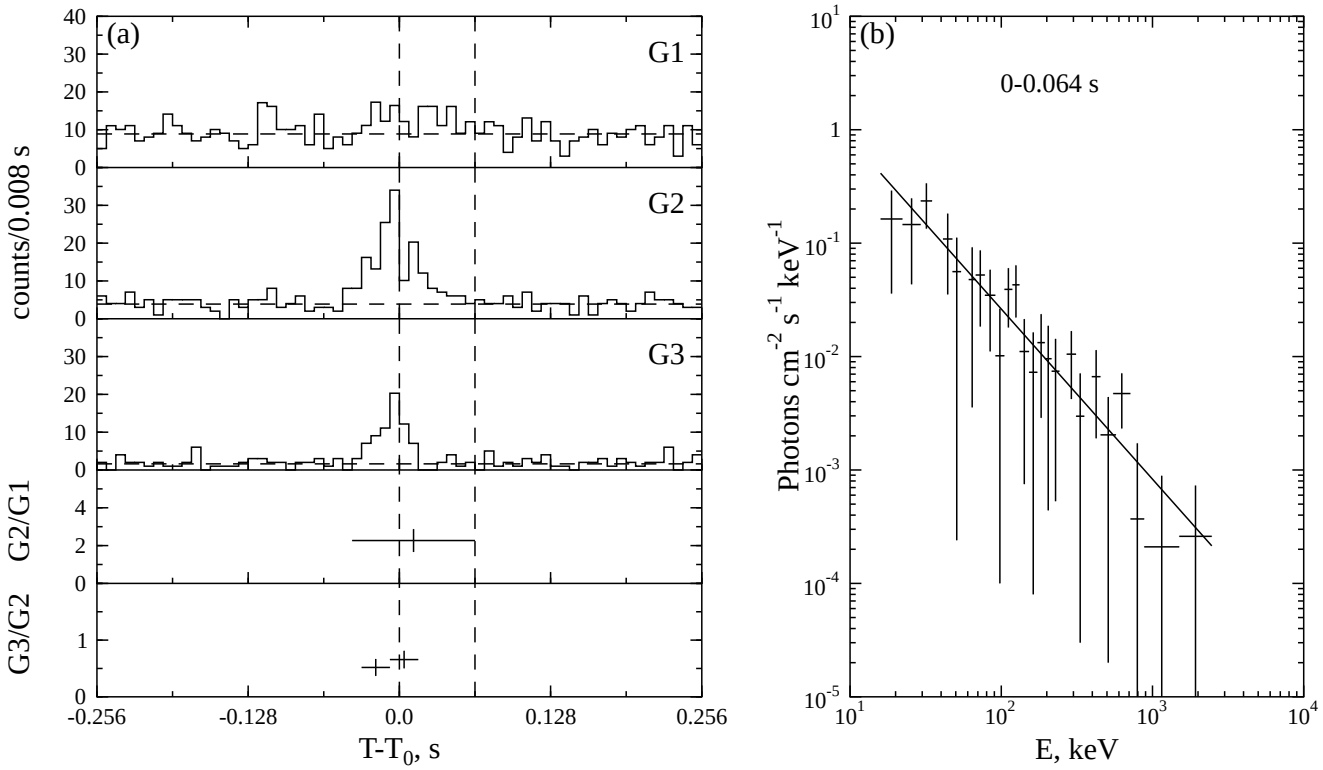

Fig. 73.— GRB 980904. T_0=31349.014 s UT.

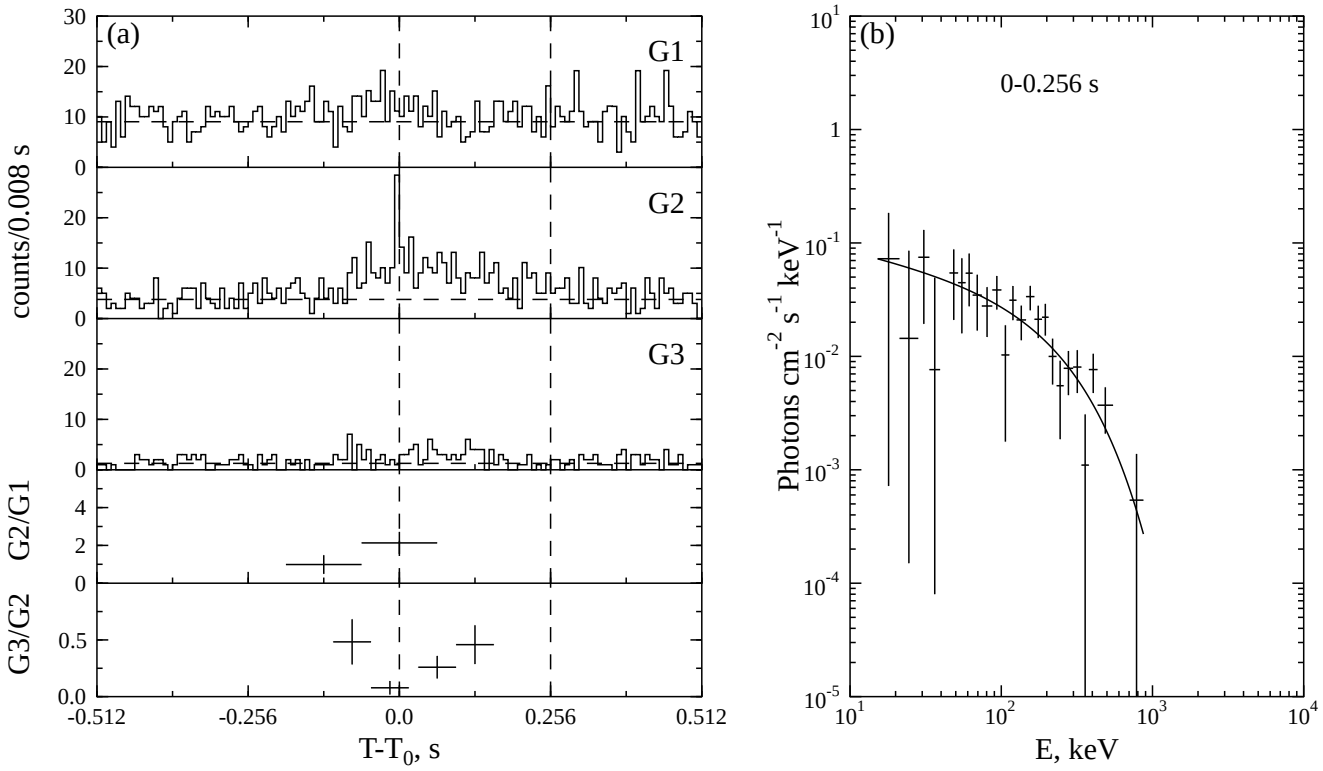

Fig. 74.— GRB 980908. T_0=82263.835 s UT.

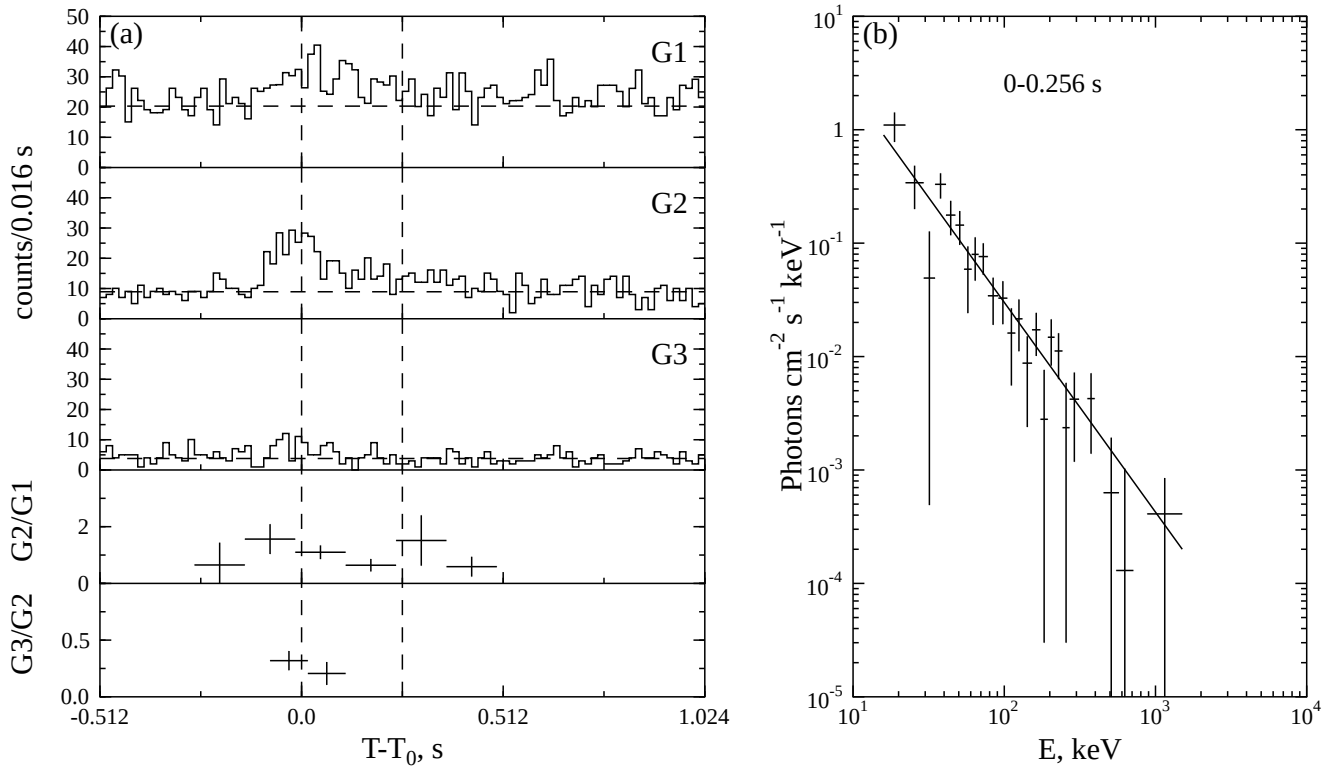

Fig. 75.— GRB 980925a. T_0=17571.284 s UT.

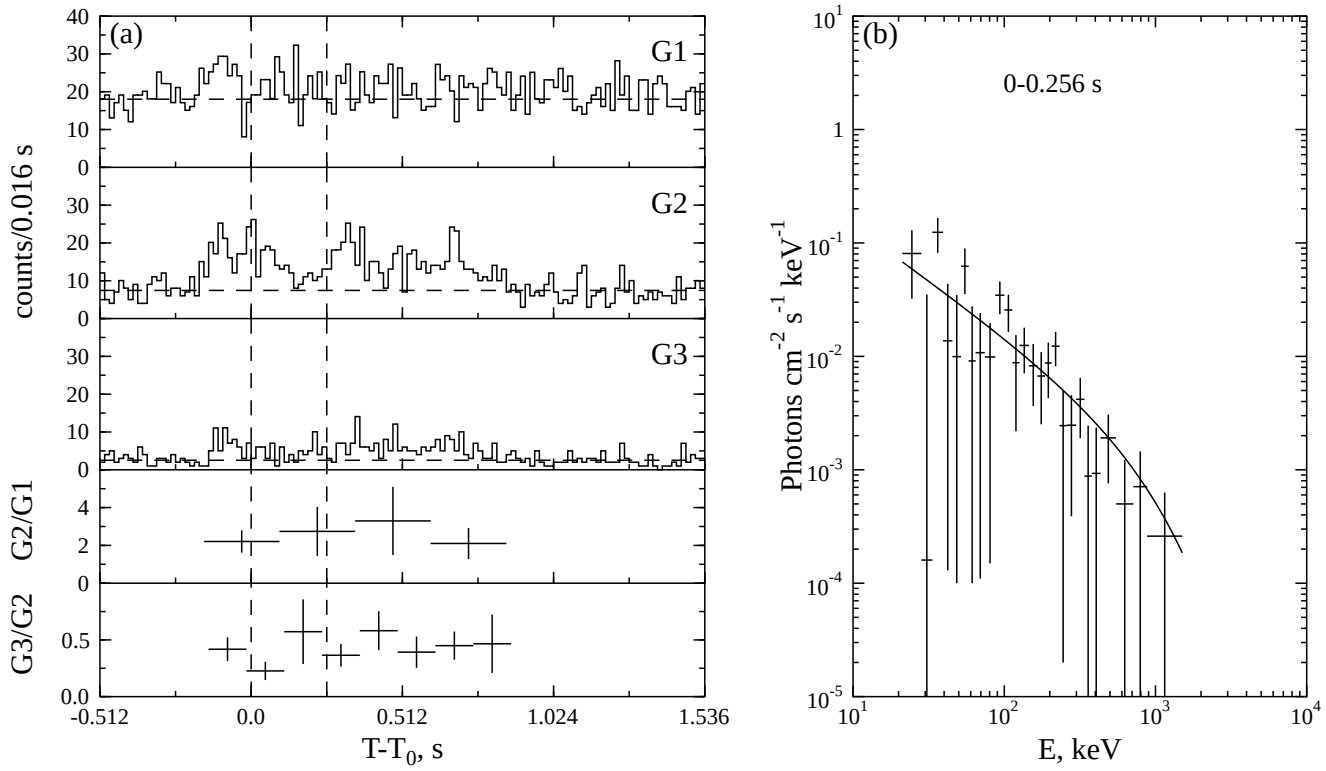

Fig. 76.— GRB 981005. T_0=64826.466 s UT.

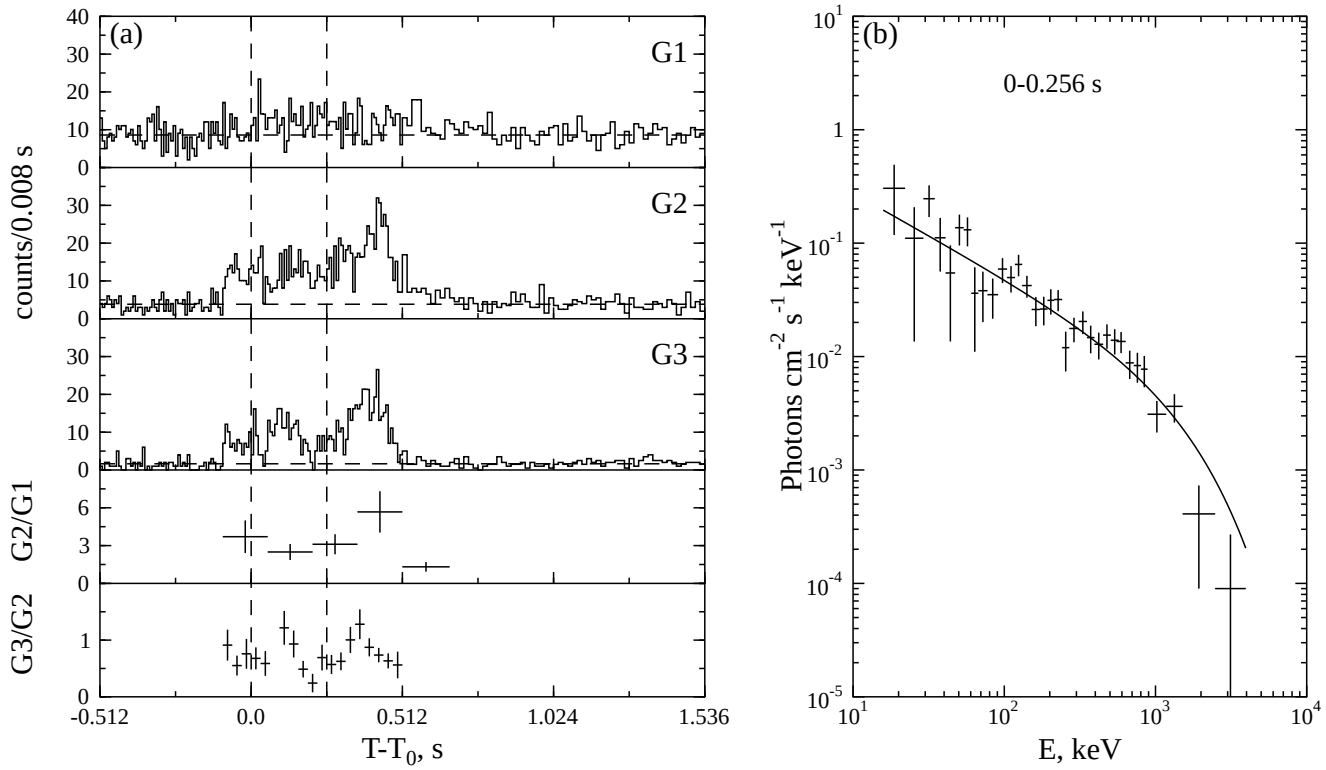

Fig. 77.— GRB 981102. T_0=28554.533 s UT.

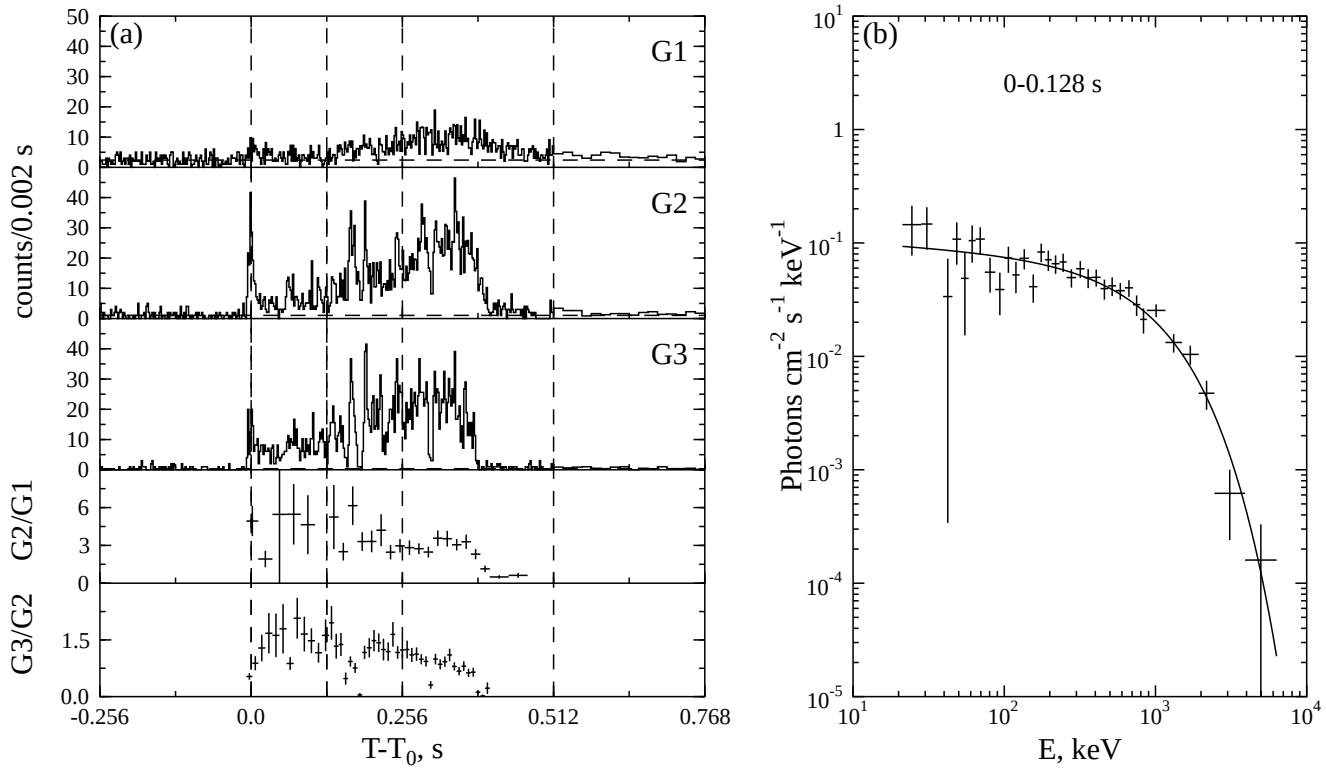

Fig. 78.— GRB 981107. T_0=781.395 s UT.

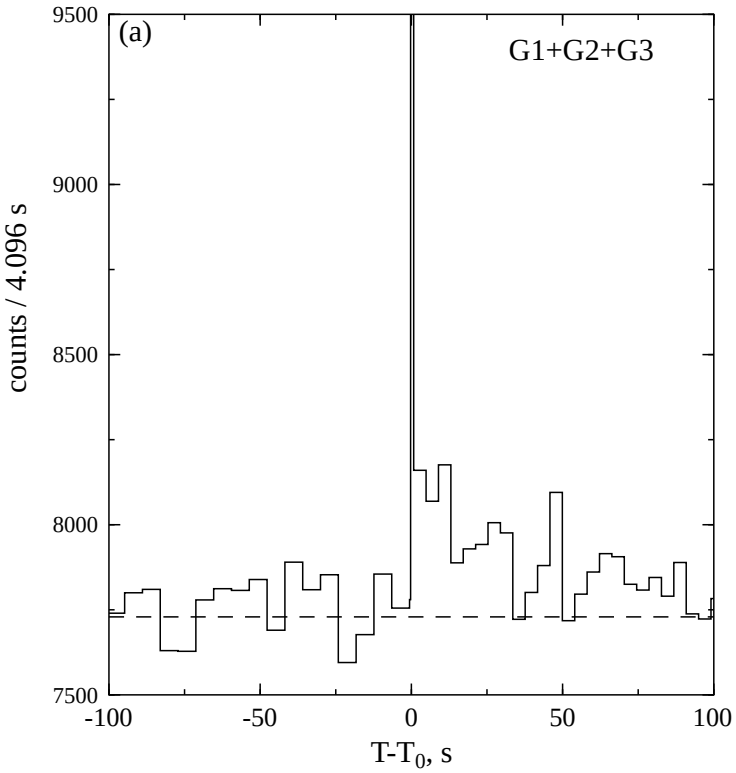

Fig. 79.— GRB 981107. T_0=781.395 s UT (continued from Fig. 78).

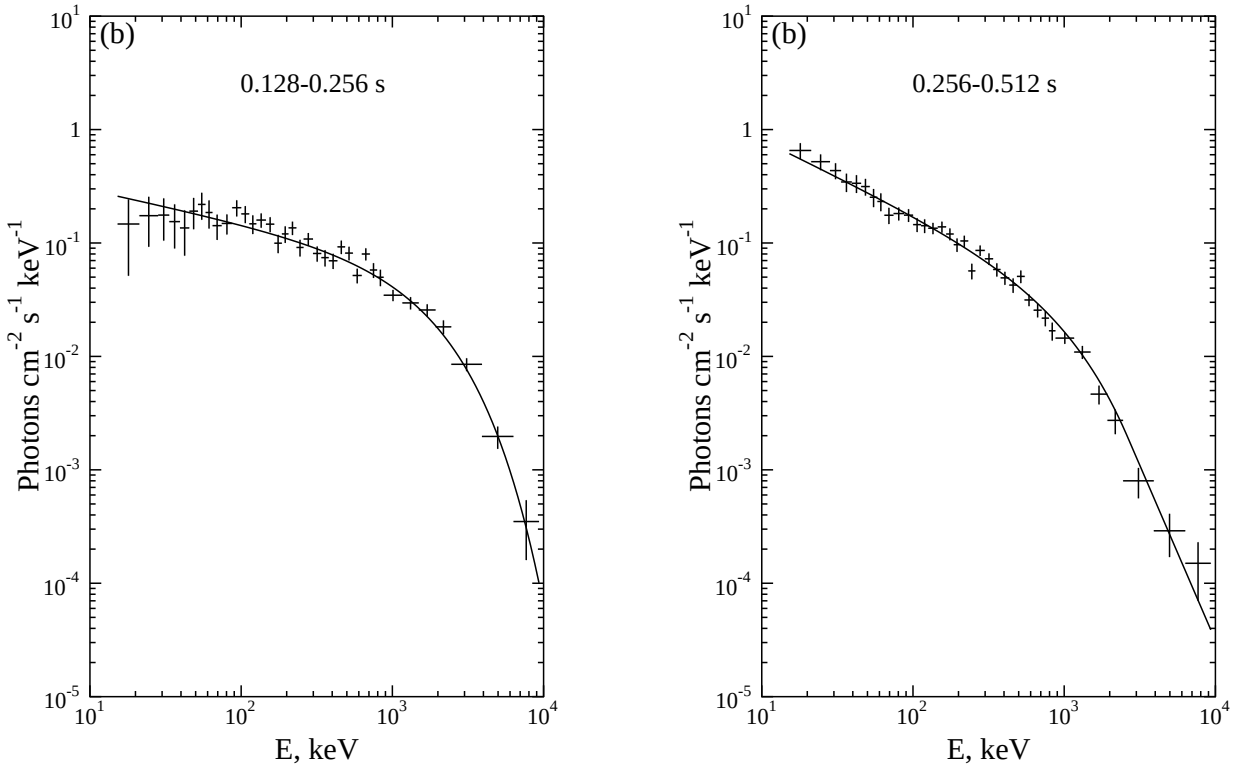

Fig. 80.— Energy spectra of the GRB 981107. T_0=781.395 s UT (continued from Fig. 78).

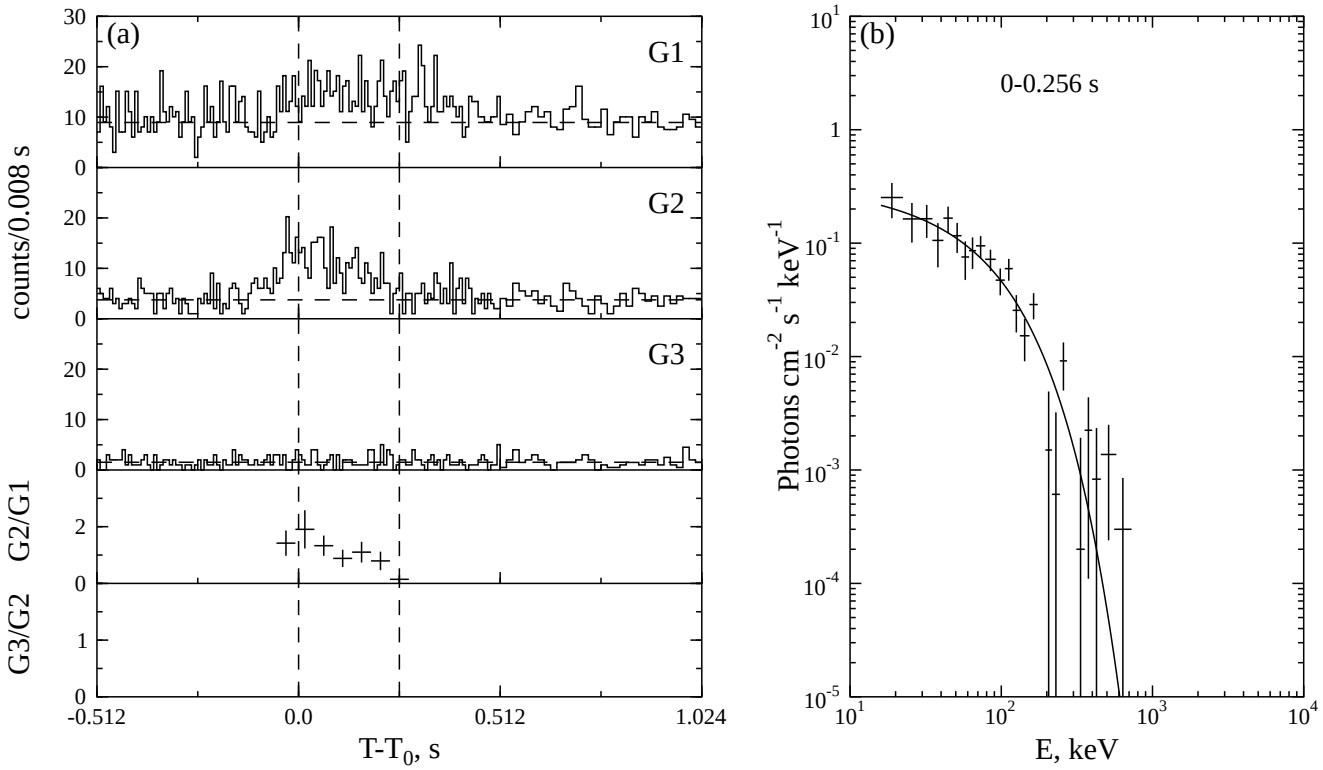

Fig. 81.— GRB 981218. T_0=62134.933 s UT.

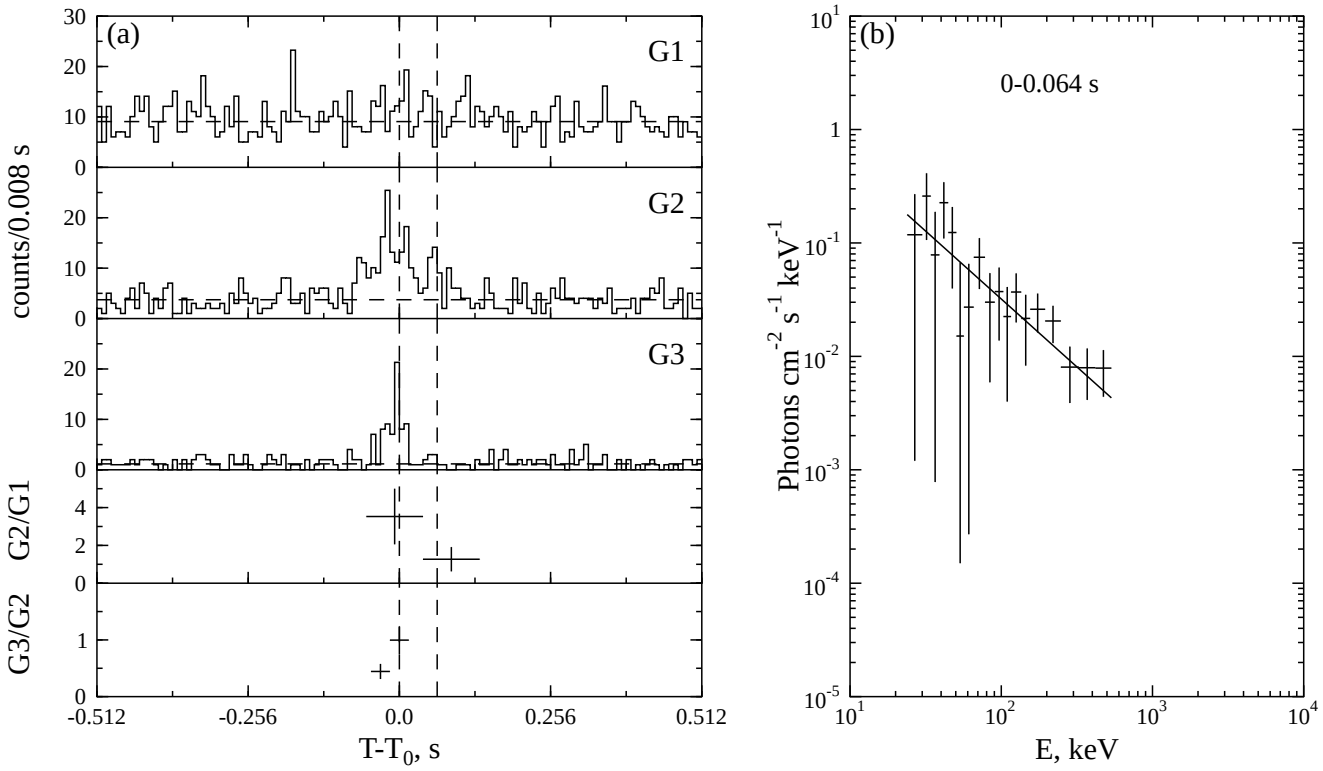

Fig. 82.— GRB 981221. T_0=9057.150 s UT.

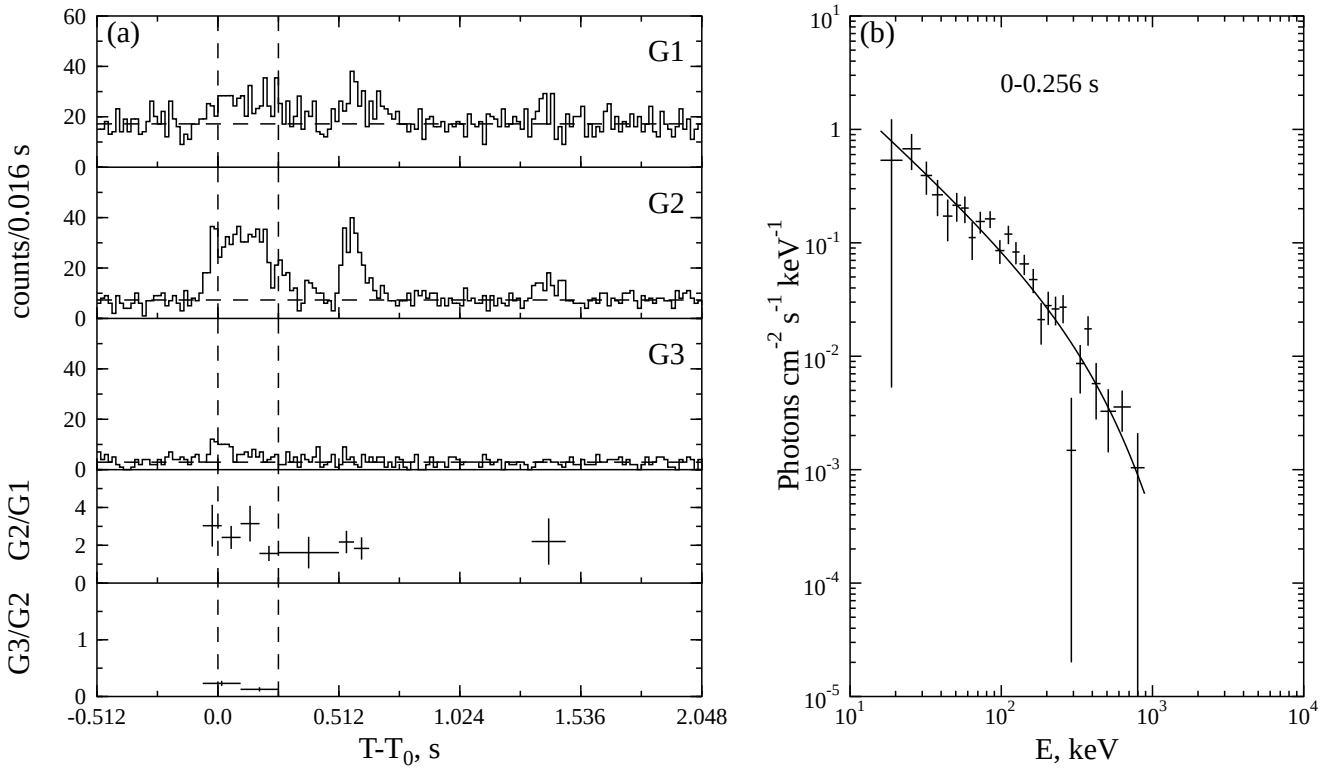

Fig. 83.— GRB 981226. T_0=38822.991 s UT.

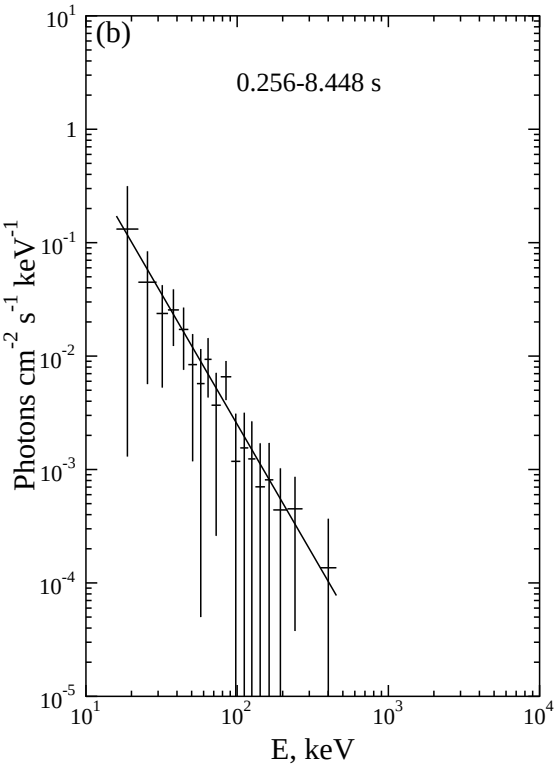

Fig. 84.— GRB 981226. T_0=38822.991 s UT (continued from Fig. 83).

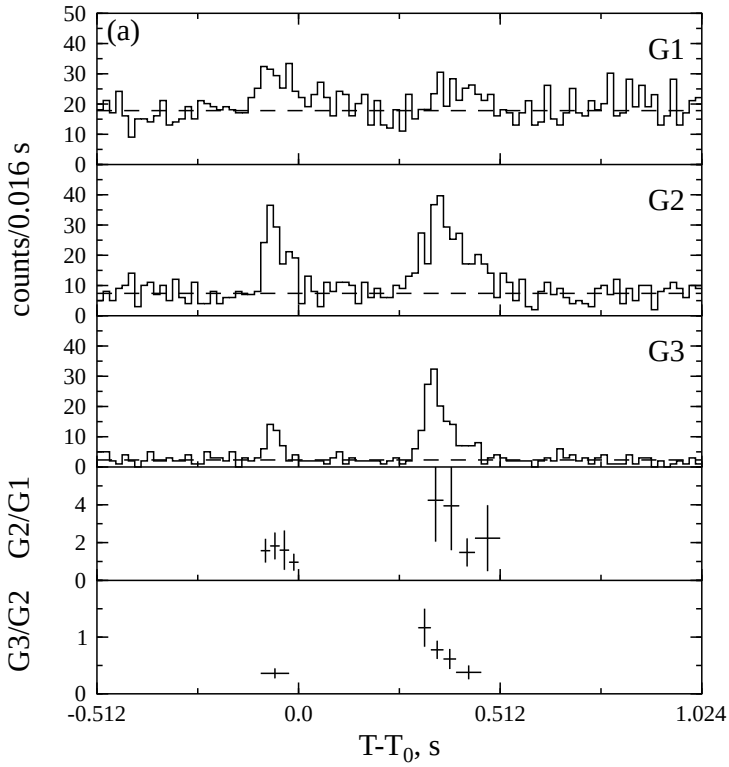

Fig. 85.— GRB 990105. T_0=31789.507 s UT.

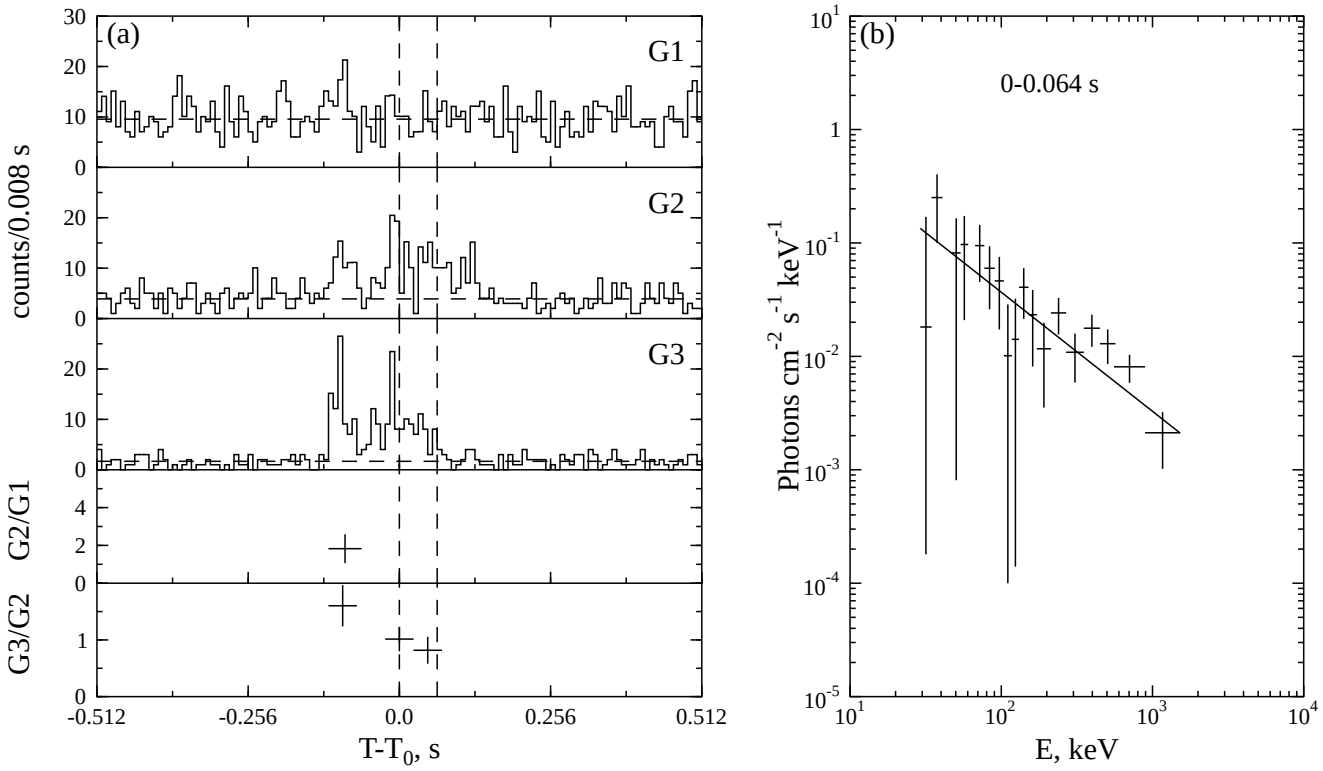

Fig. 86.— GRB 990126. T_0=51844.333 s UT.

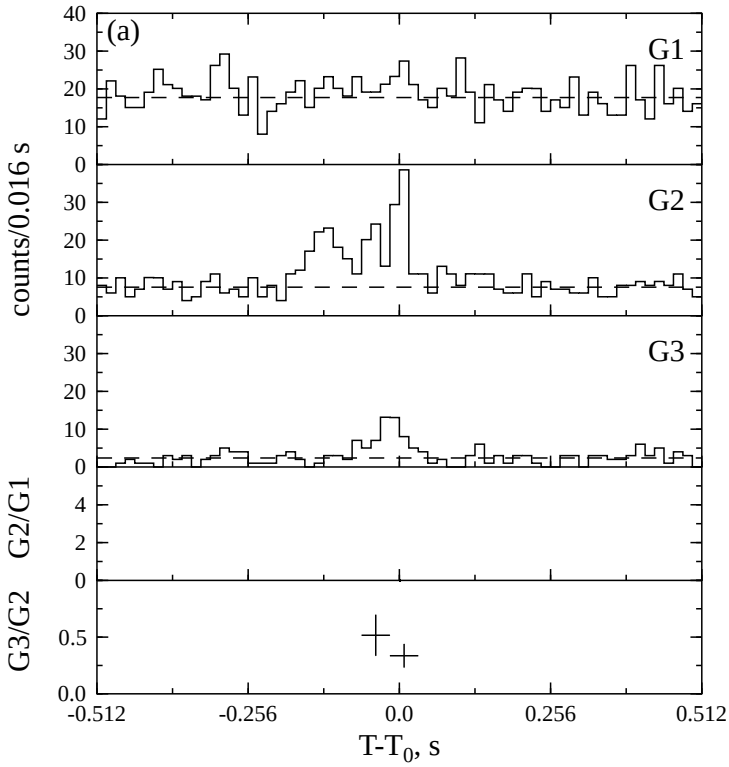

Fig. 87.— GRB 990206c. T_0=57061.328 s UT.

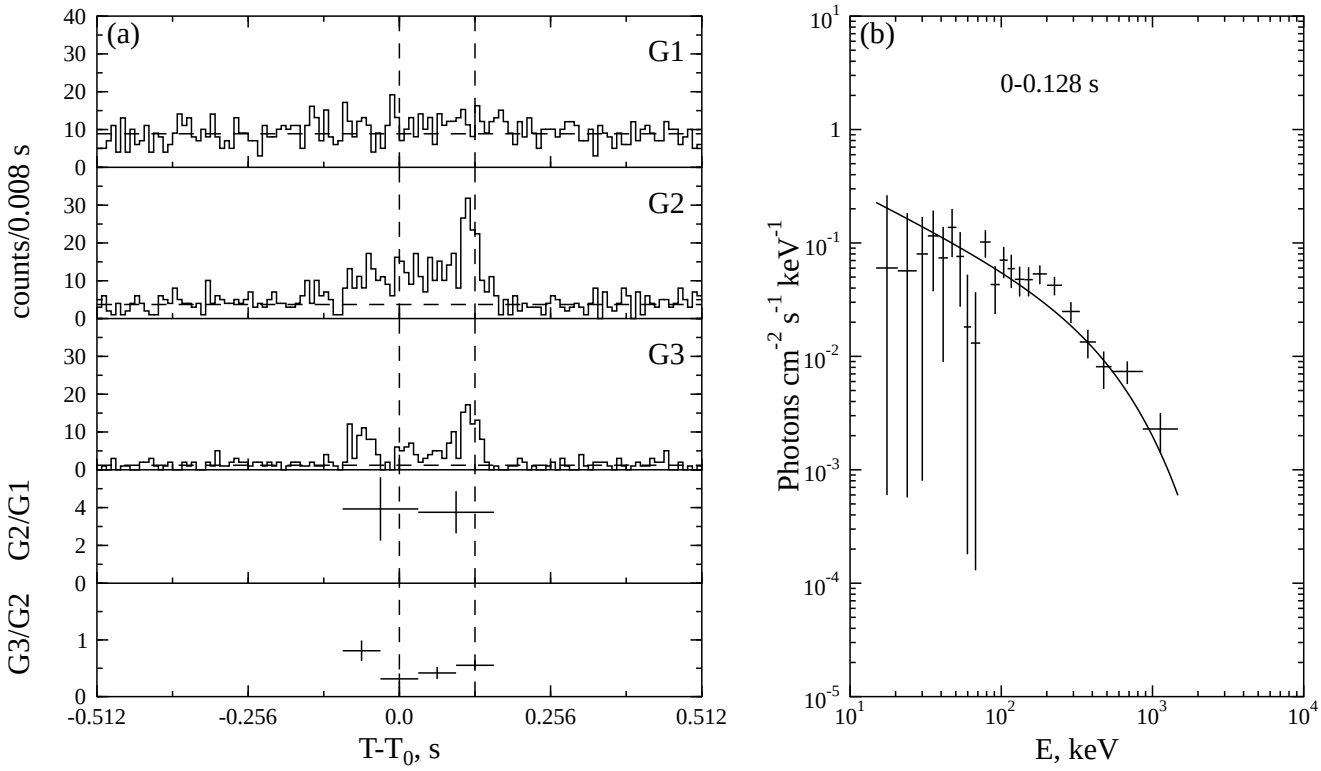

Fig. 88.— GRB 990207. T_0=69675.009 s UT.

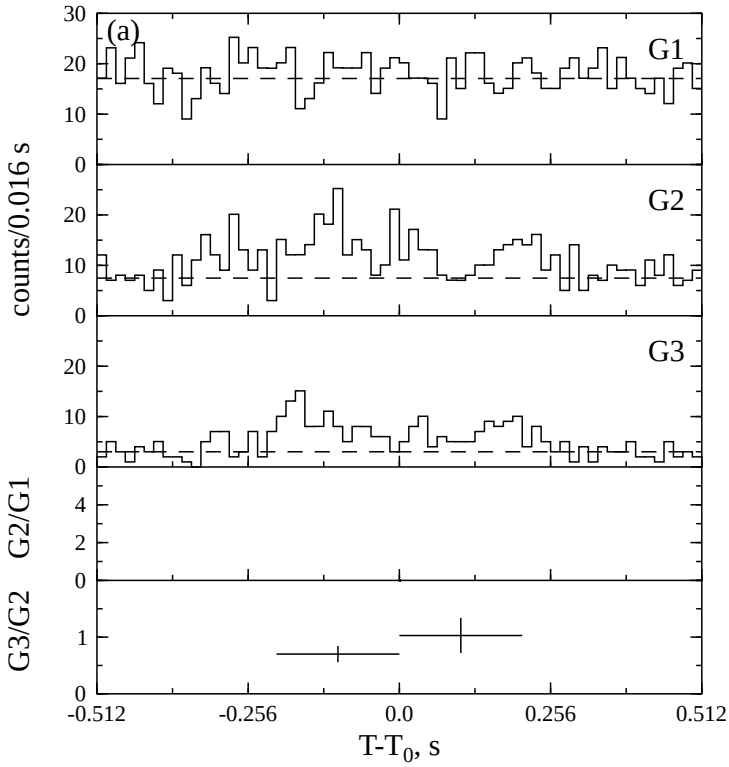

Fig. 89.— GRB 990208. T_0=15166.066 s UT.

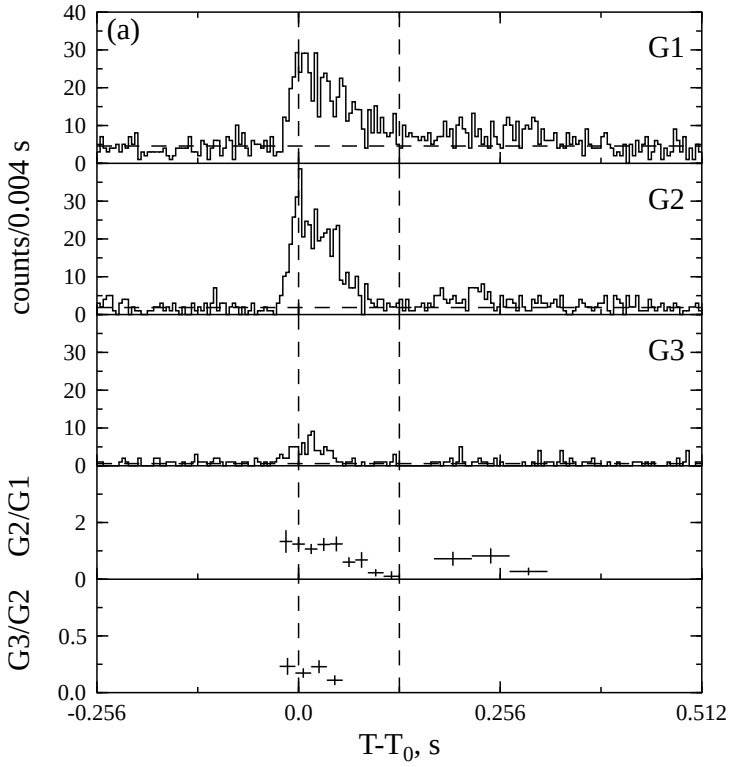

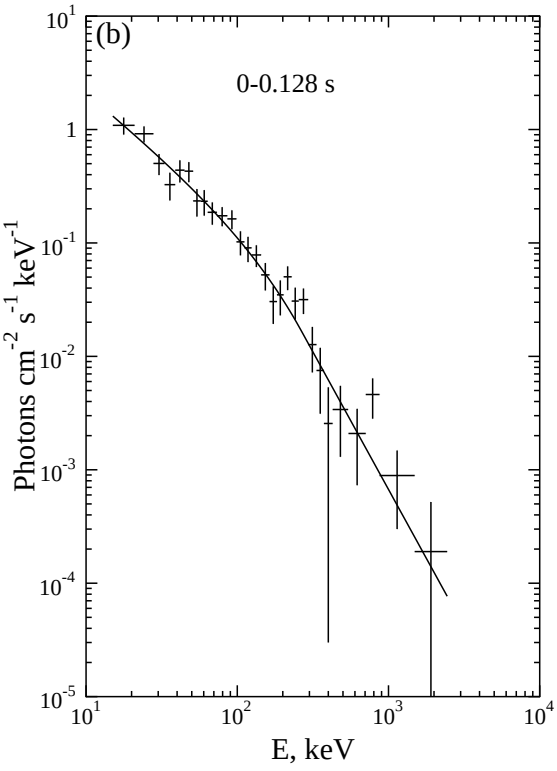

Fig. 90.— GRB 990313. T_0=33712.652 s UT.

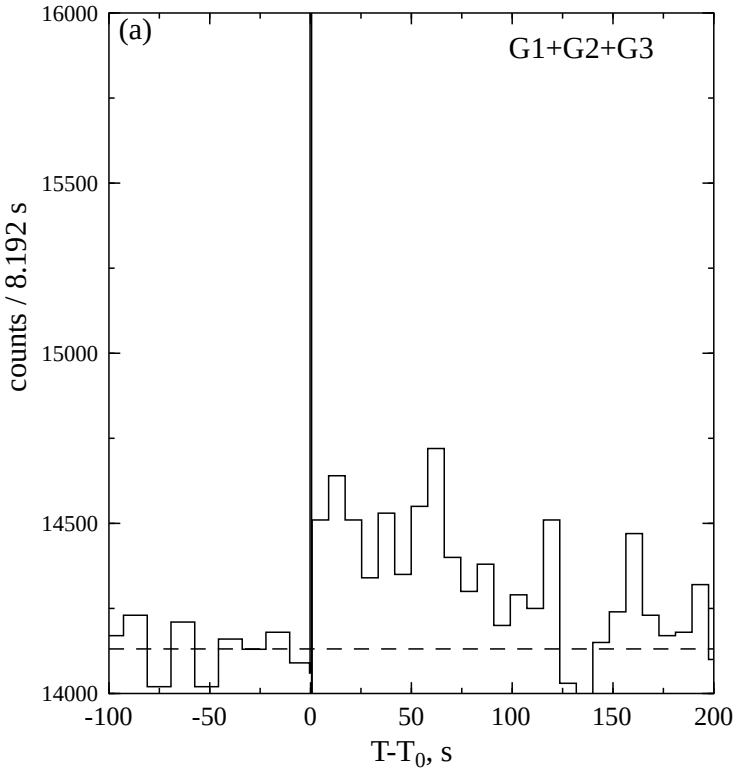

Fig. 91.— GRB 990313. T_0=33712.652 s UT (continued from Fig. 90).

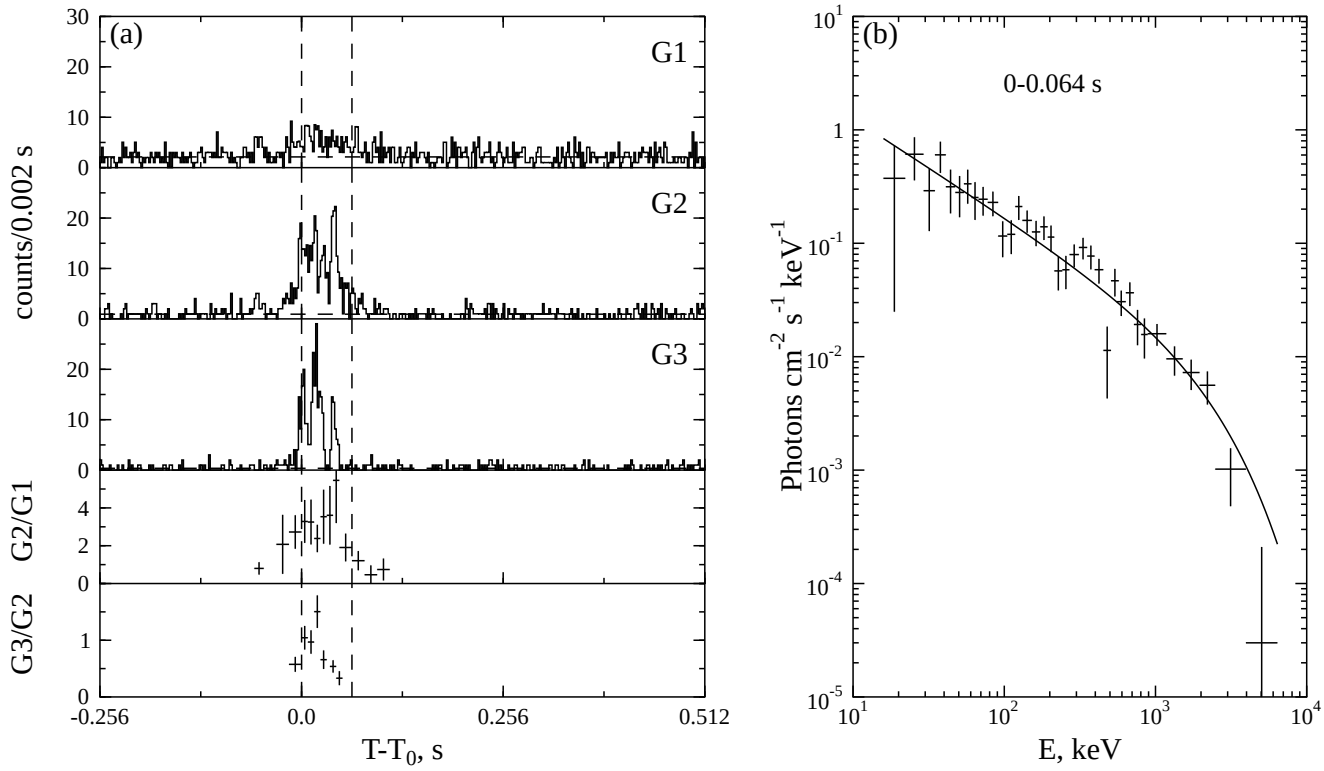

Fig. 92.— GRB 990327. T_0=22911.102 s UT.

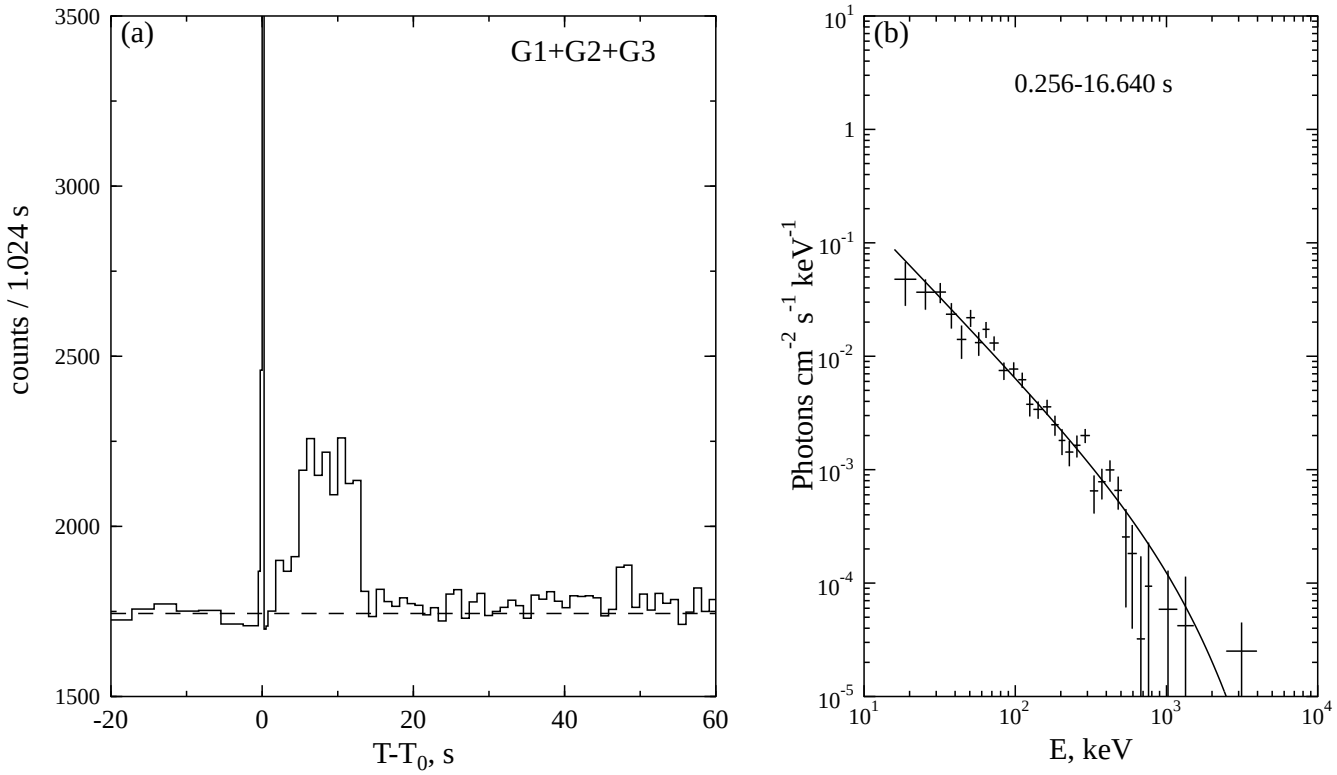

Fig. 93.— GRB 990327. T_0=22911.102 s UT (continued from Fig. 92).

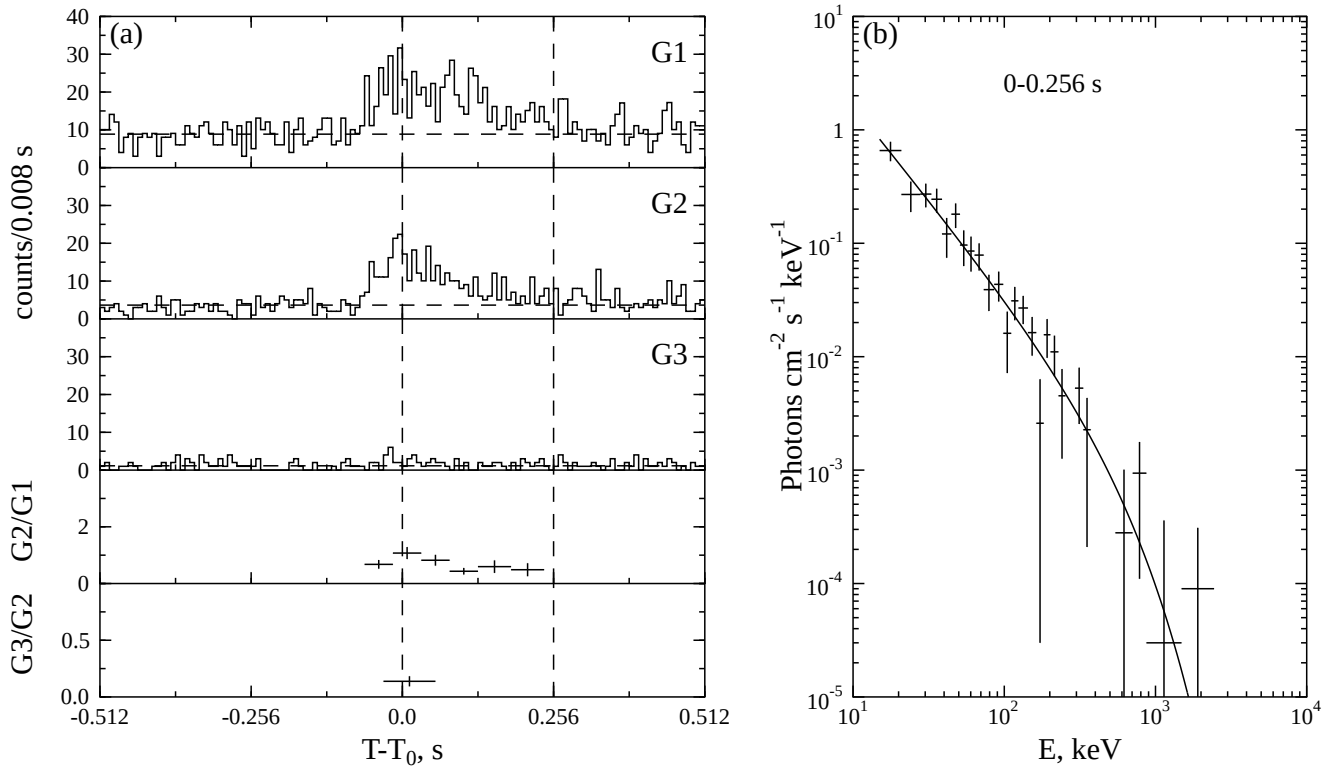

Fig. 94.— GRB 990405b. T_0=30059.858 s UT.

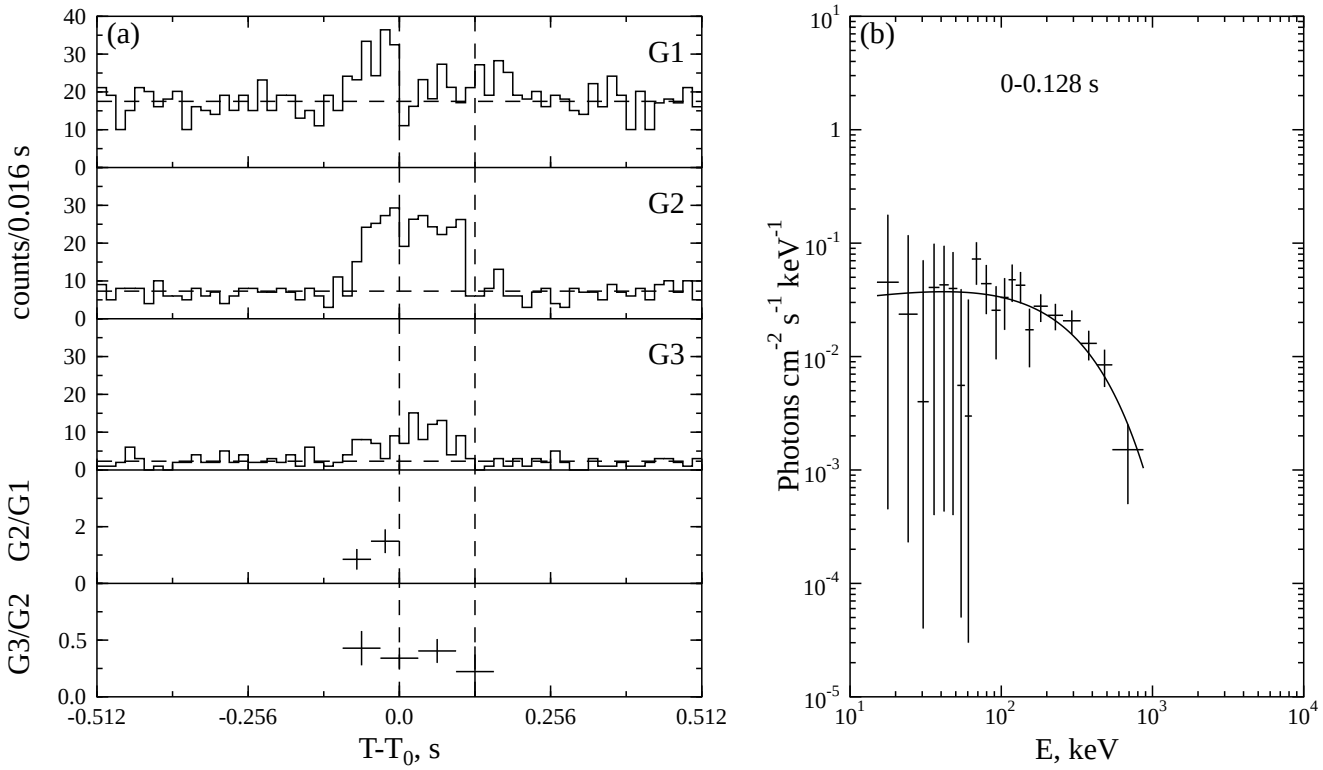

Fig. 95.— GRB 990415. T_0=2297.309 s UT.

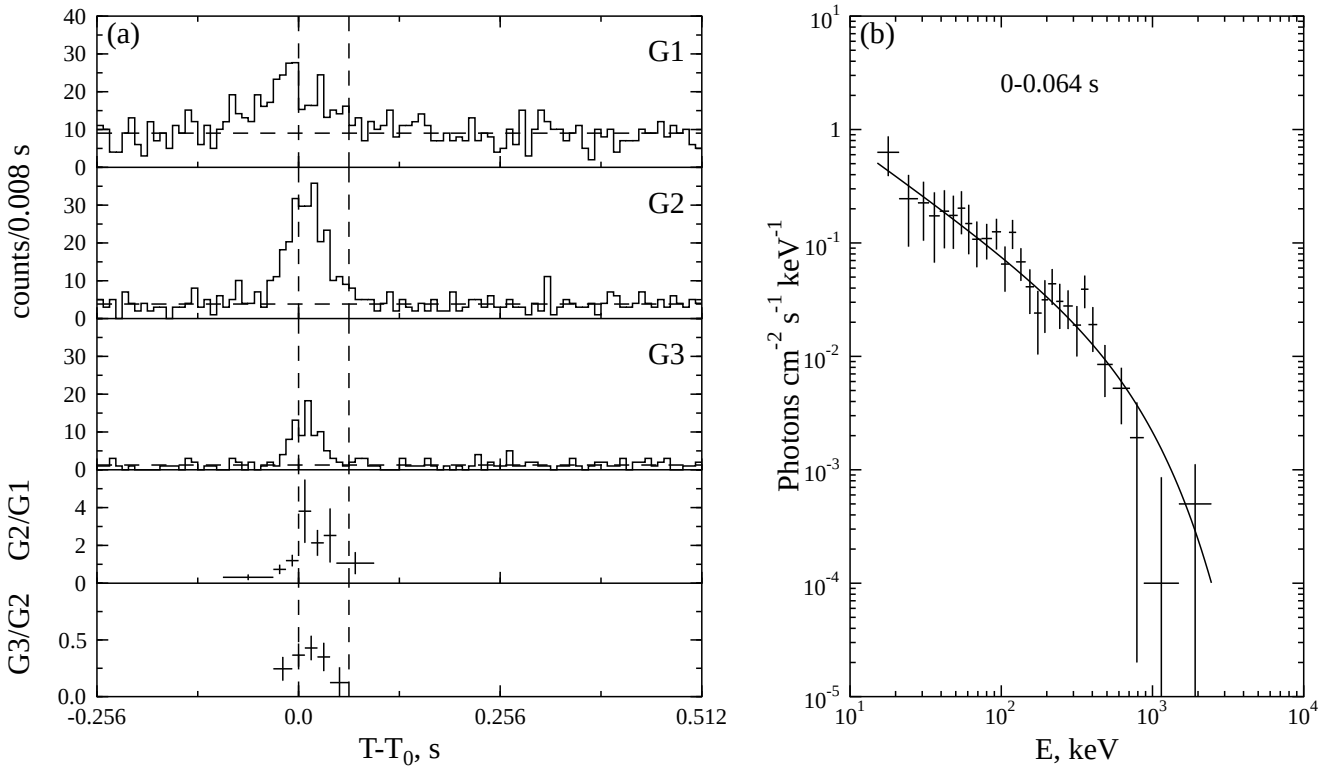

Fig. 96.— GRB 990504. T_0=67586.484 s UT.

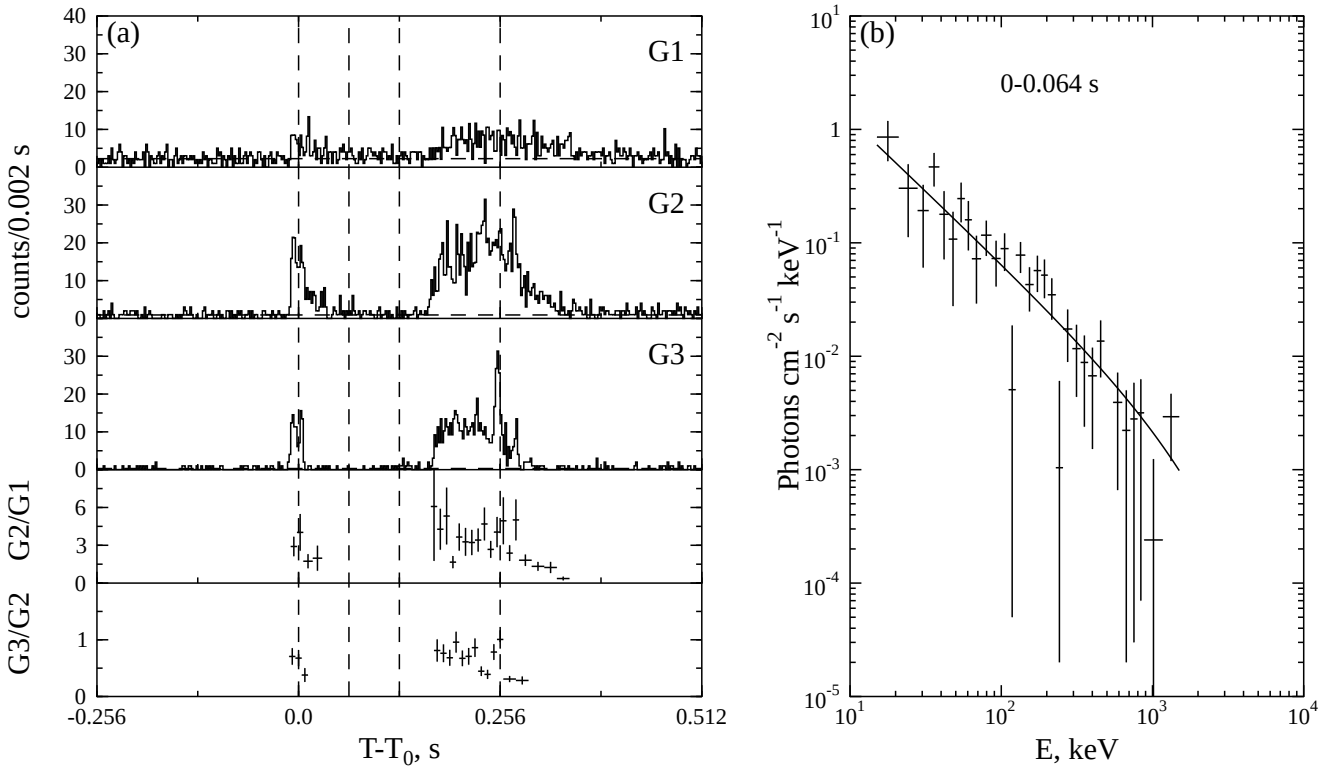

Fig. 97.— GRB 990516. T_0=86065.136 s UT.

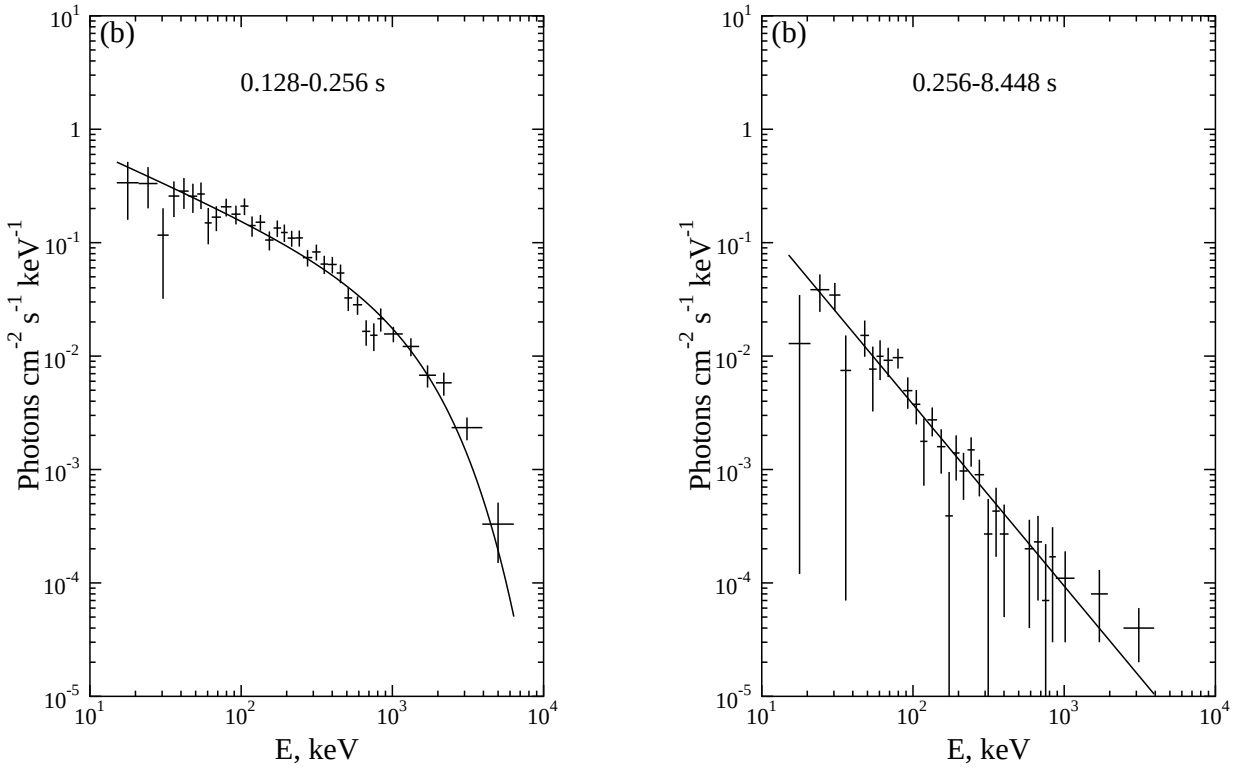

Fig. 98.— Energy spectra of the GRB 990516. T_0=86065.136 s UT (continued from Fig. 97).

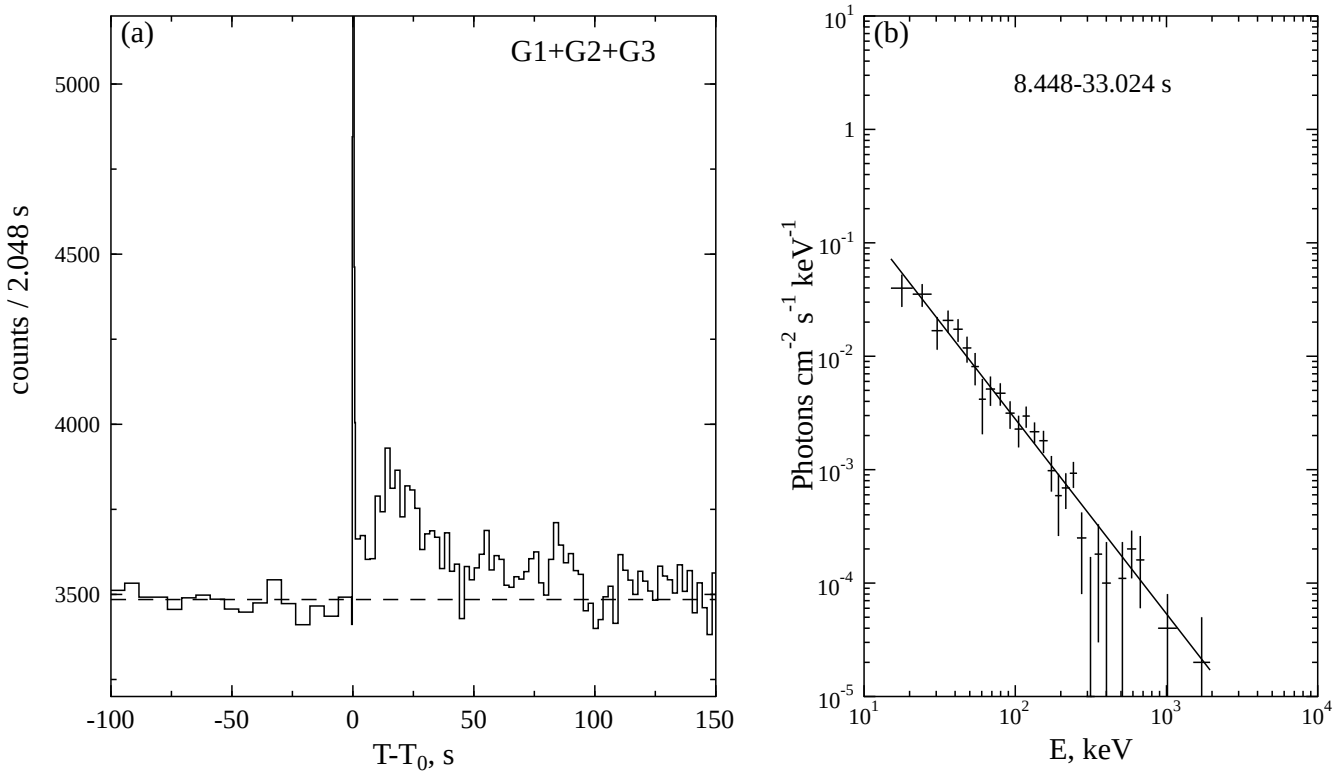

Fig. 99.— GRB 990516. T_0=86065.136 s UT (continued from Fig. 97, 98).

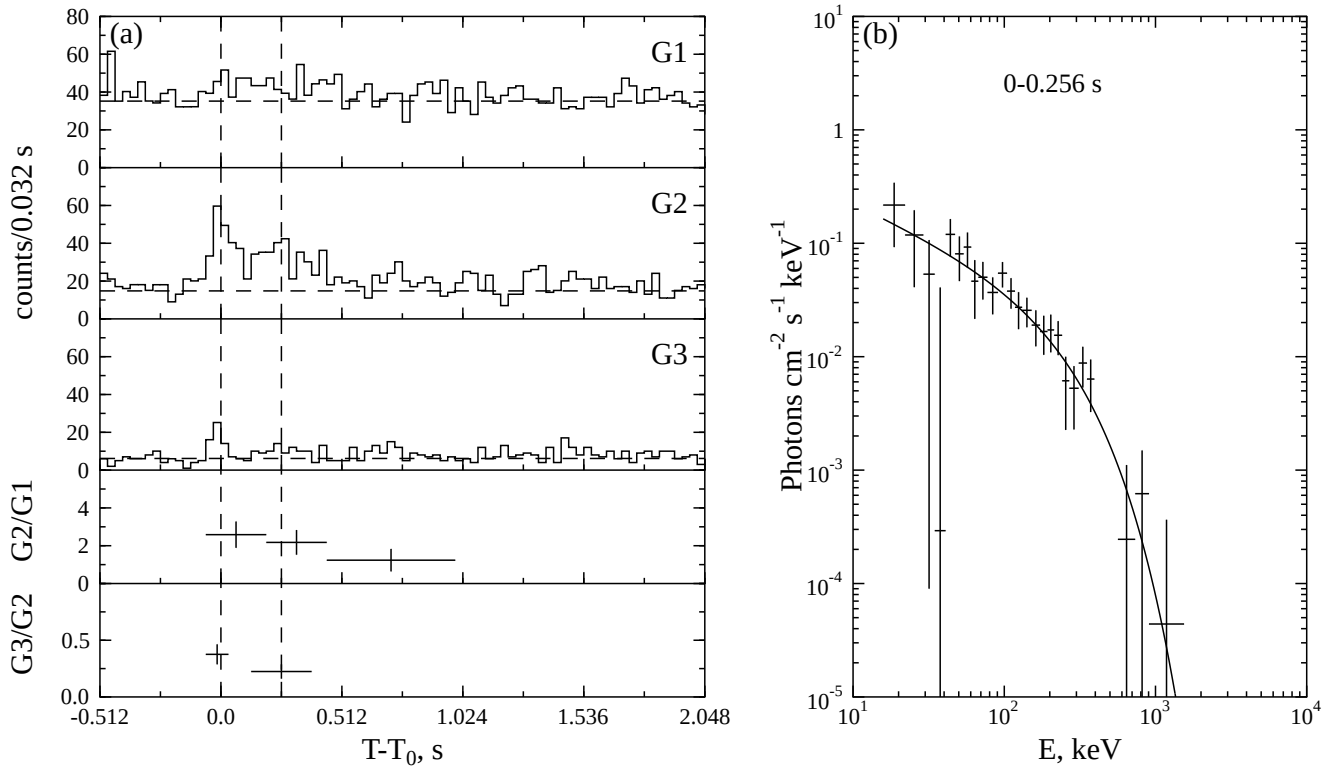

Fig. 100.— GRB 990619. T_0=46930.367 s UT.

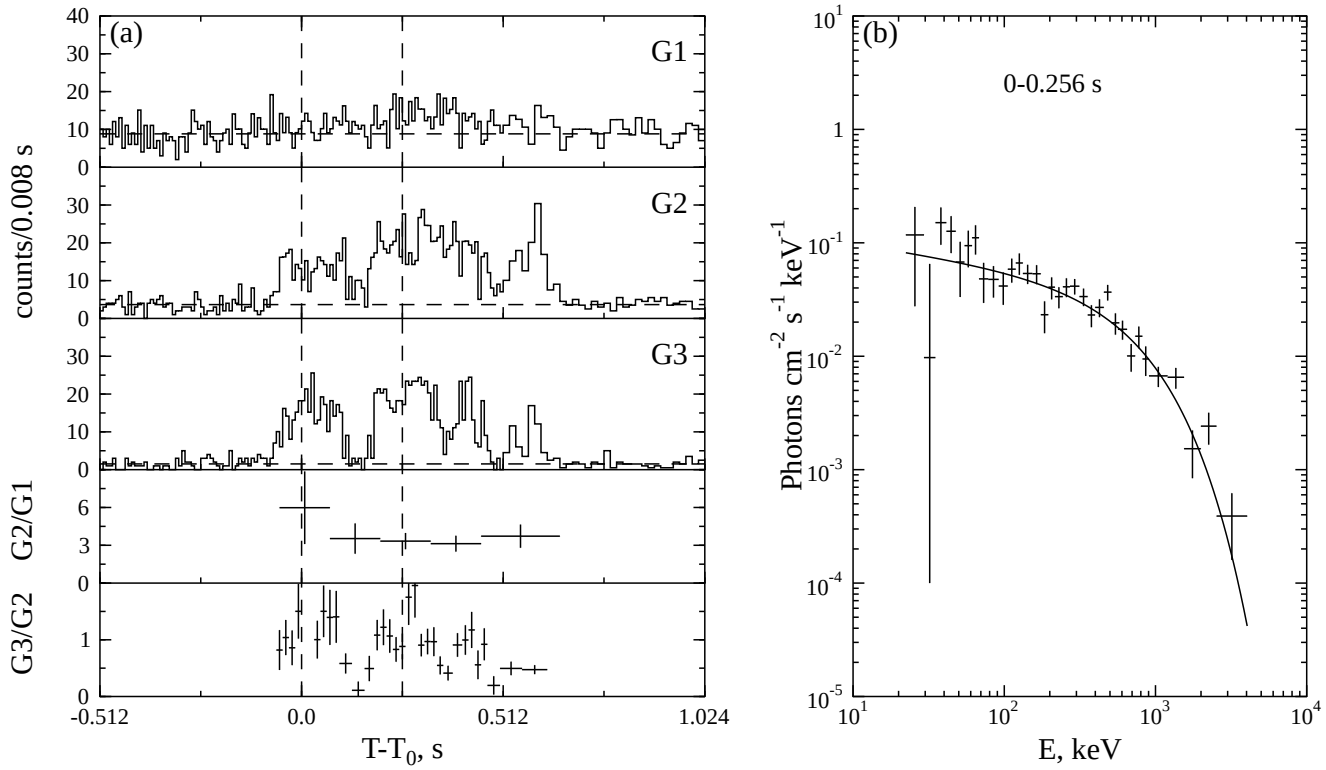

Fig. 101.— GRB 990712a. T_0=27915.510 s UT.

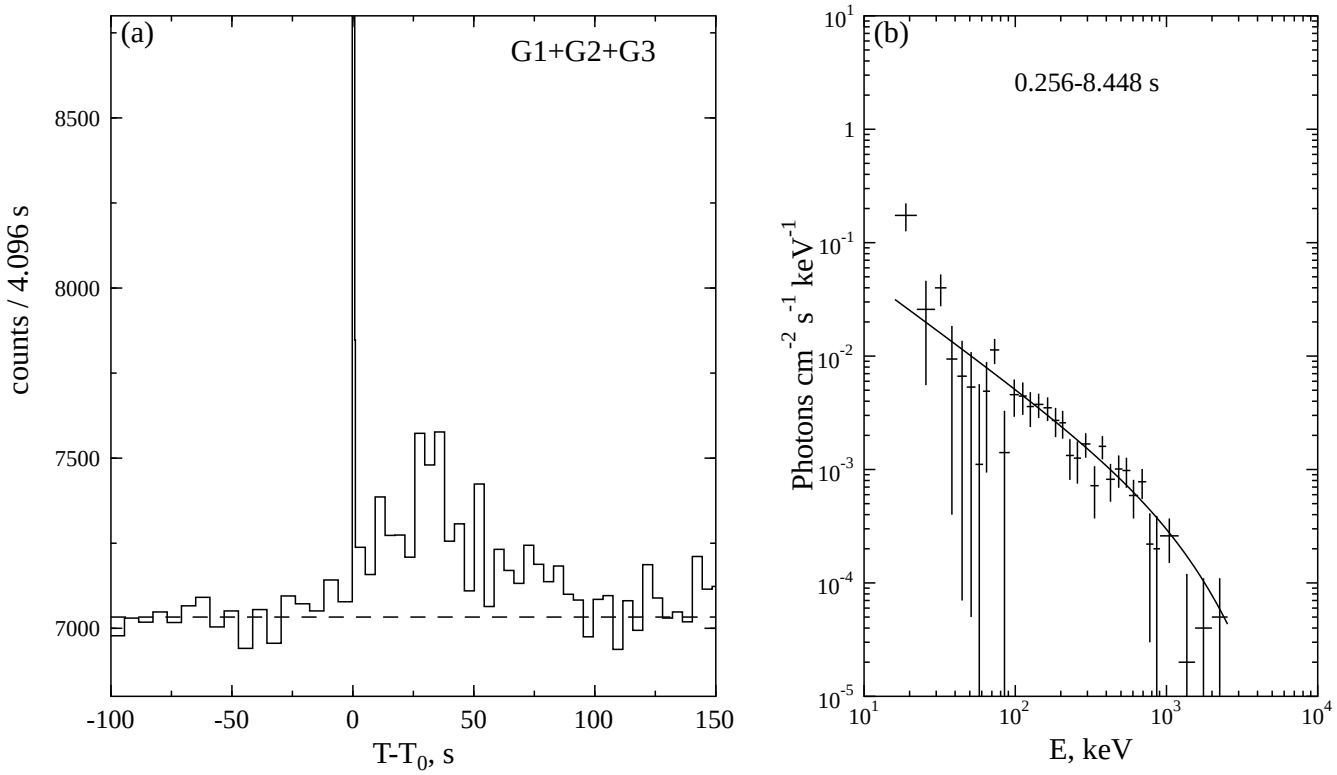

Fig. 102.— GRB 990712a. T_0=27915.510 s UT (continued from Fig. 101).

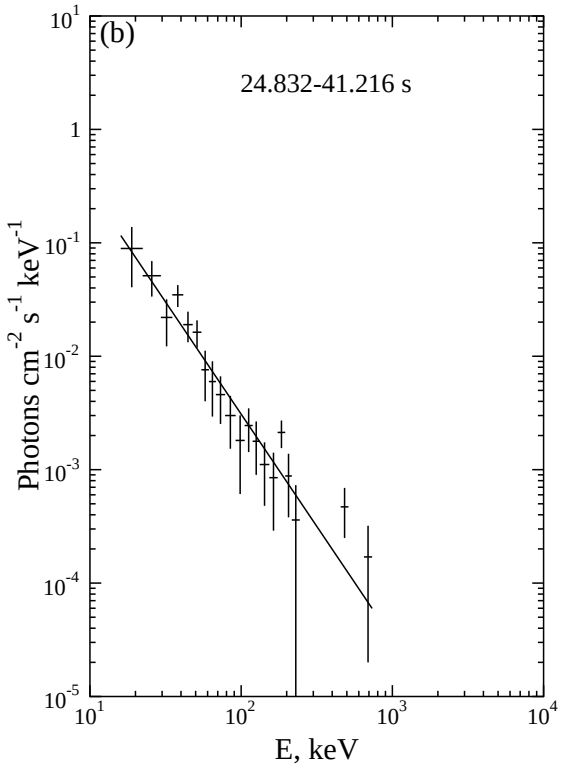

Fig. 103.— Energy spectrum of the GRB 990712a. T_0=27915.510 s UT (continued from Fig. 102).

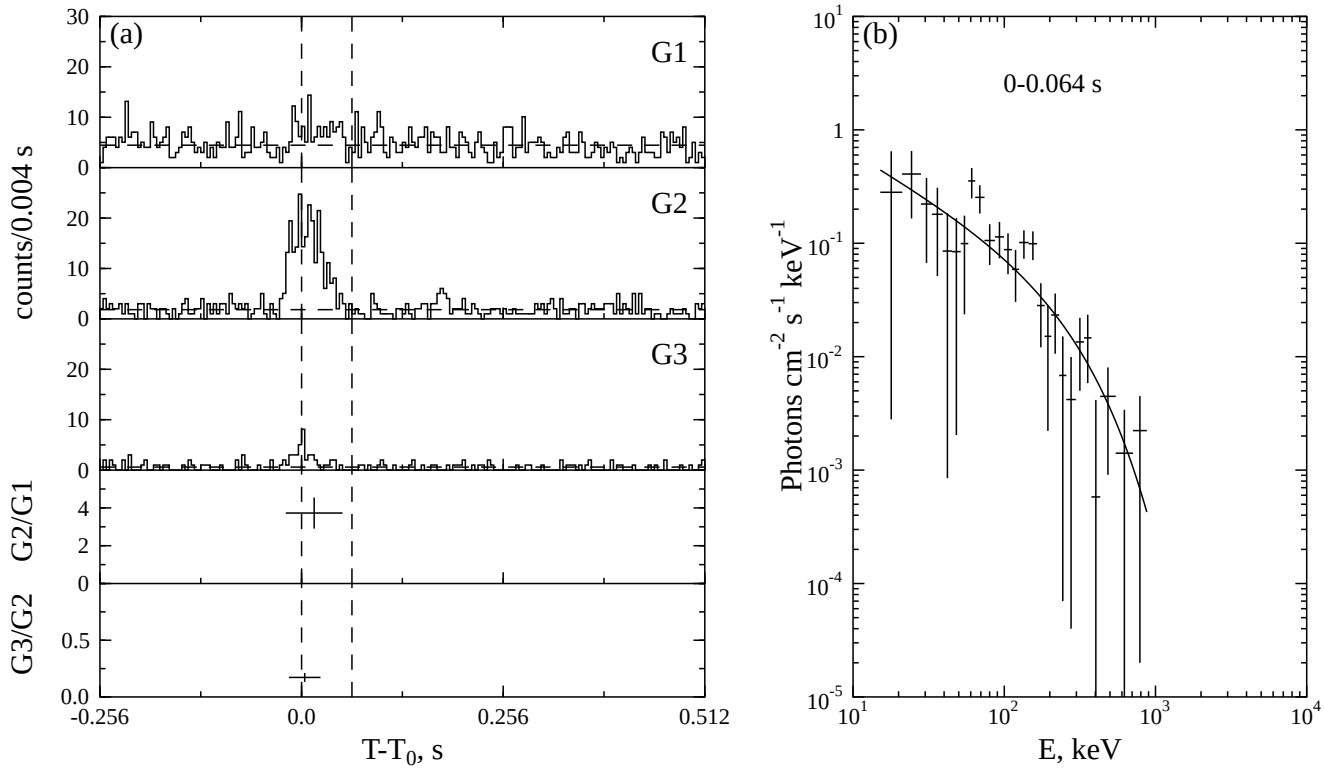

Fig. 104.— GRB 990719. T_0=61135.420 s UT.

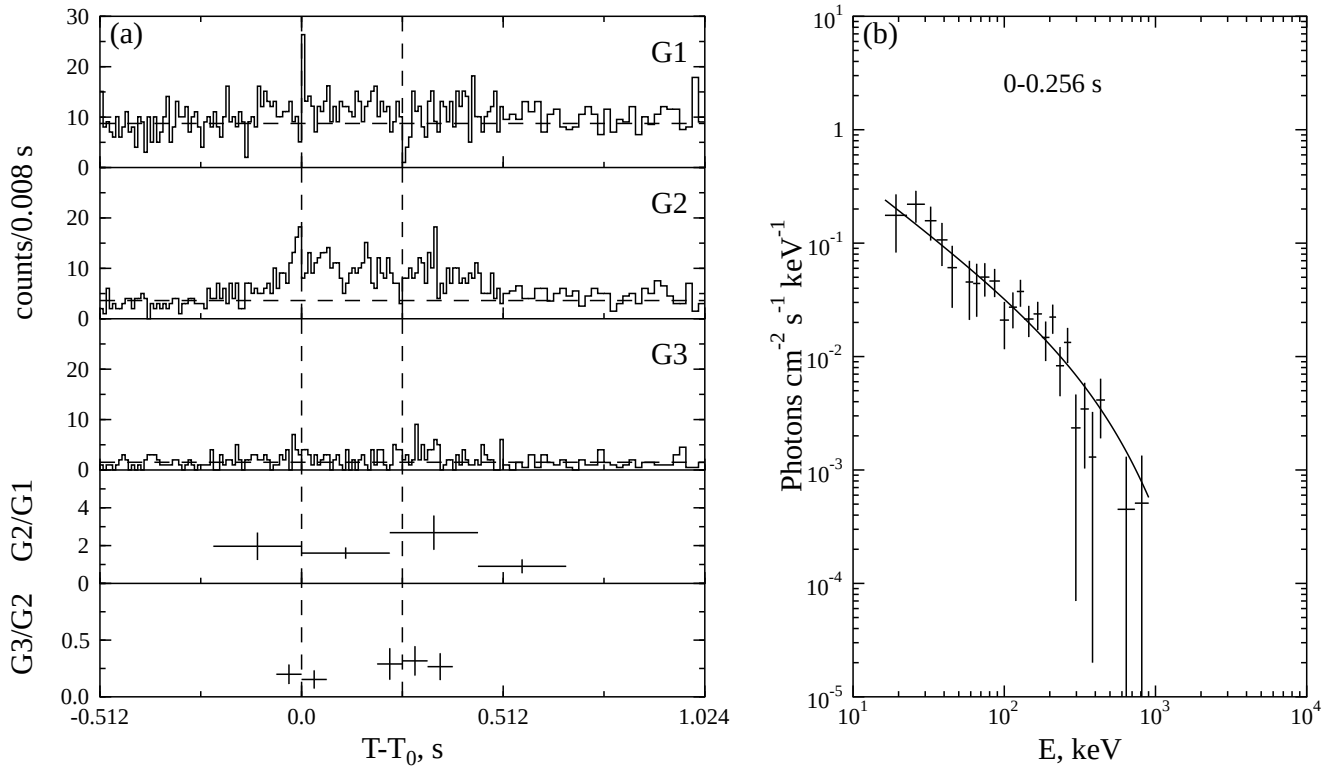

Fig. 105.— GRB 990720. T_0=75941.940 s UT.

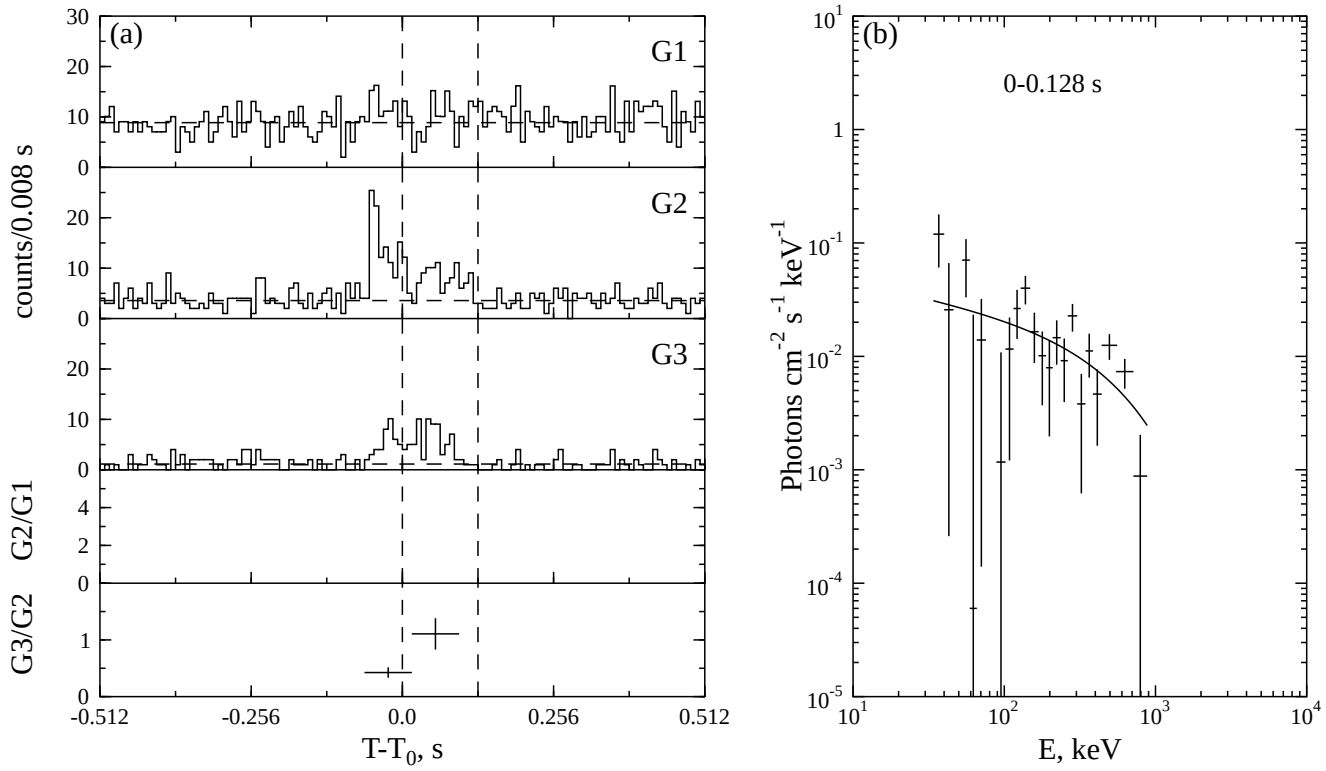

Fig. 106.— GRB 990806b. T_0=60168.676 s UT.

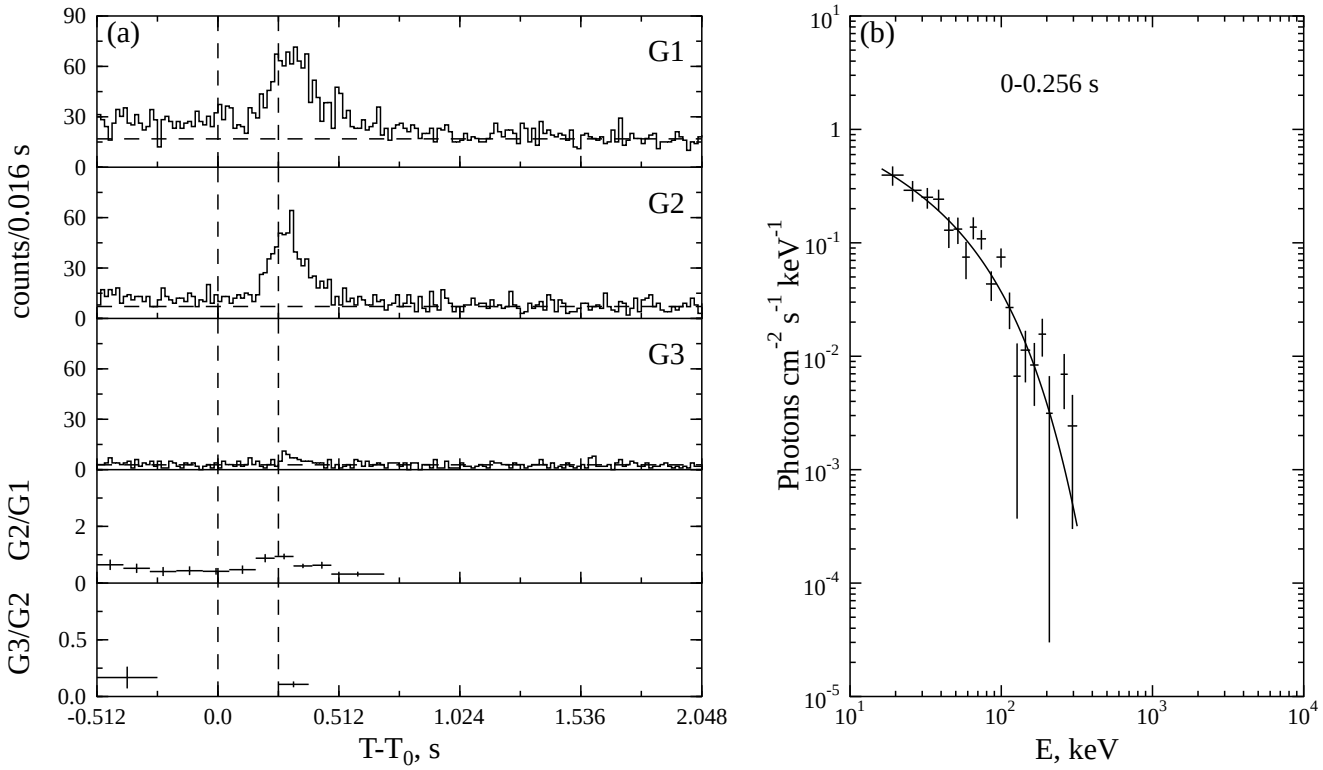

Fig. 107.— GRB 990828. T_0=70020.016 s UT.

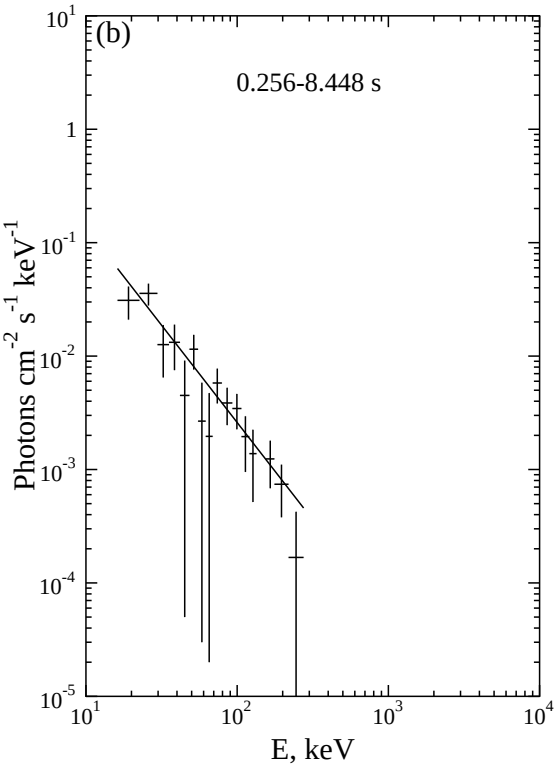

Fig. 108.— GRB 990828. T_0=70020.016 s UT (continued from Fig. 107).

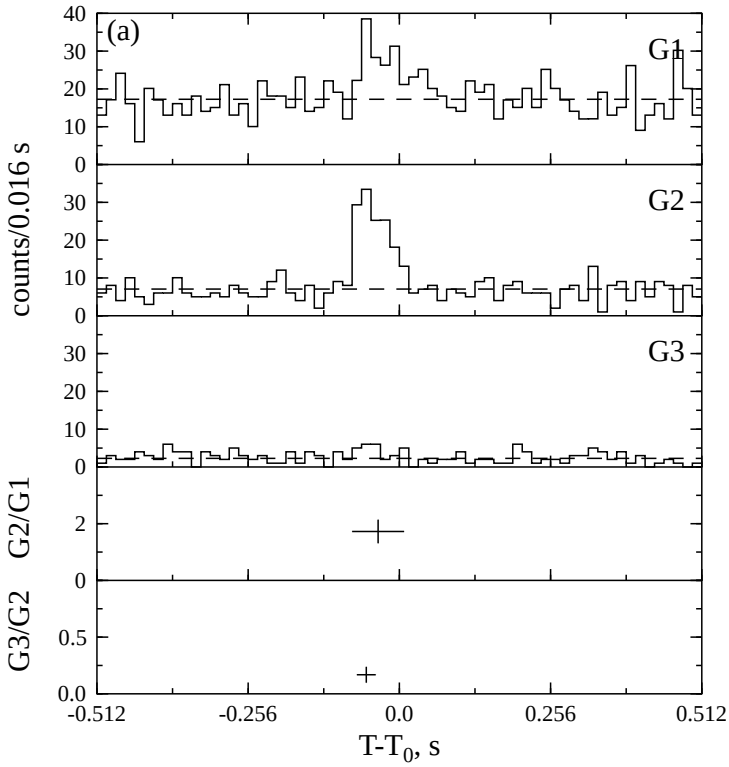

Fig. 109.— GRB 990831. T_0=41835.091 s UT.

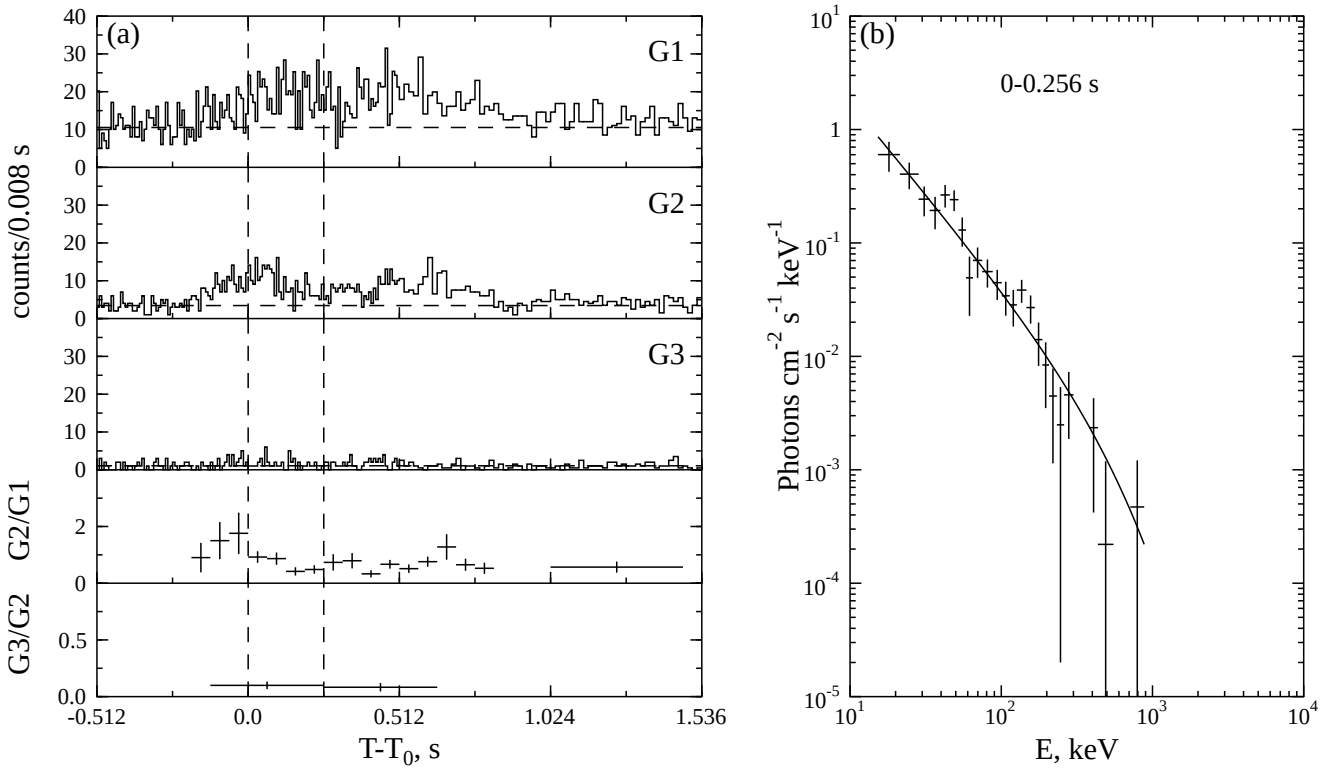

Fig. 110.— GRB 991001. T_0=4950.128 s UT.

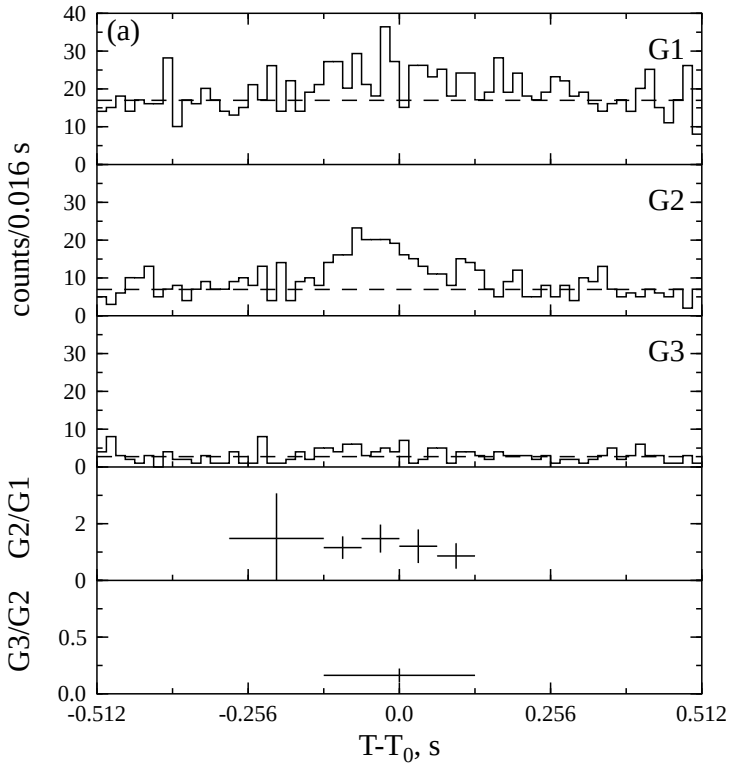

Fig. 111.— GRB 991002. T_0=82143.664 s UT.

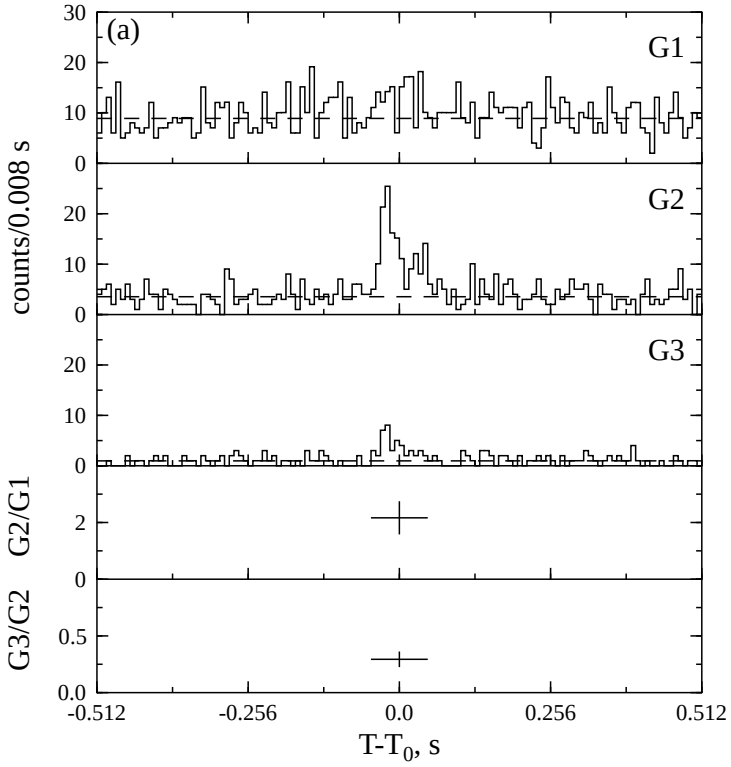

Fig. 112.— GRB 991226b. T_0=83339.767 s UT.

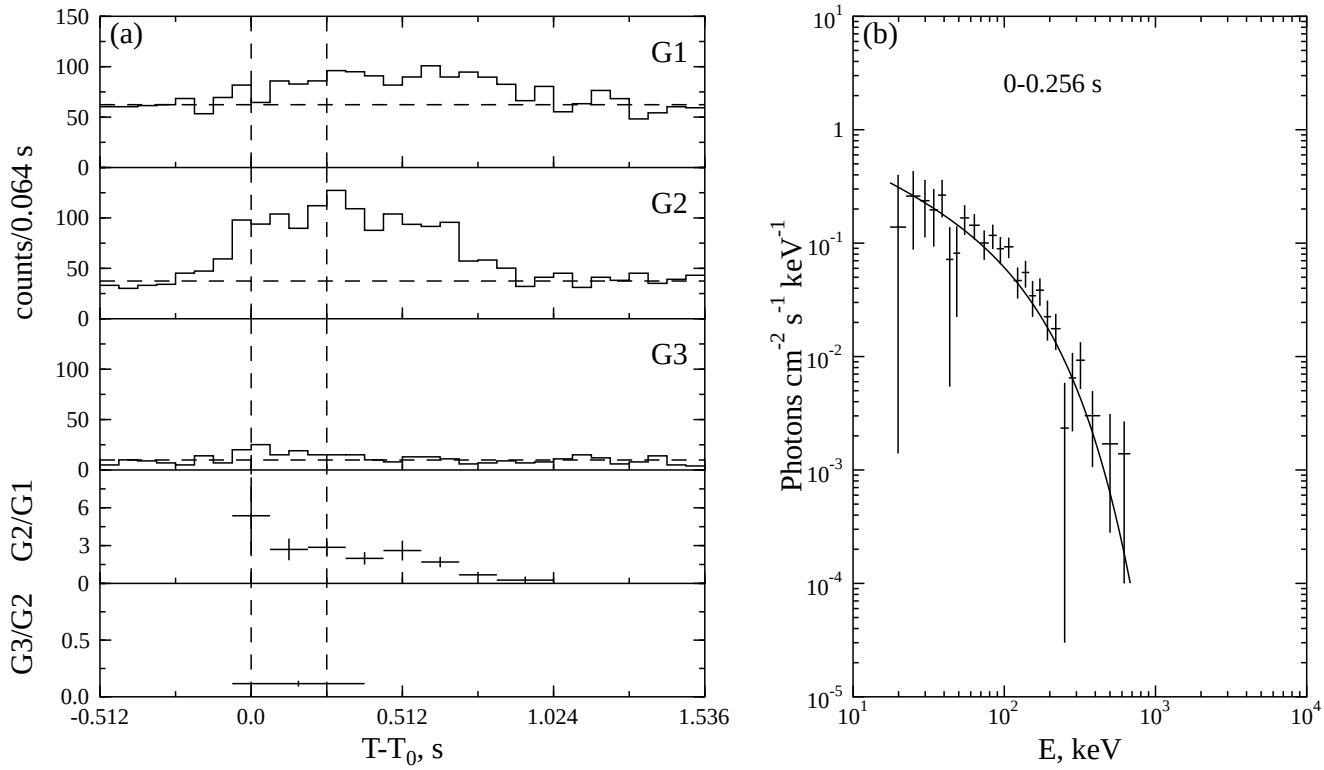

Fig. 113.— GRB 000108. T_0=60487.439 s UT.

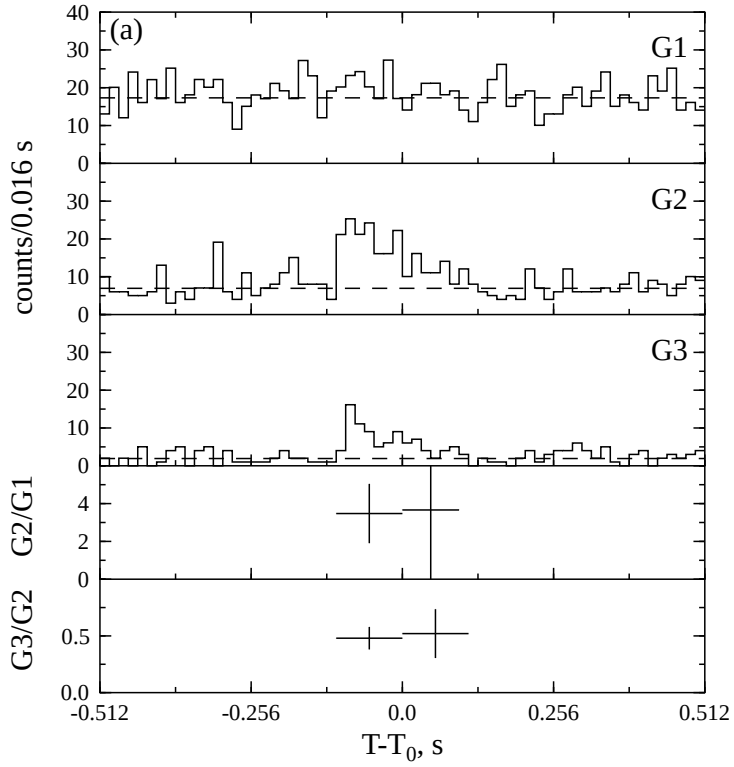

Fig. 114.— GRB 000212. T_0=61592.339 s UT.

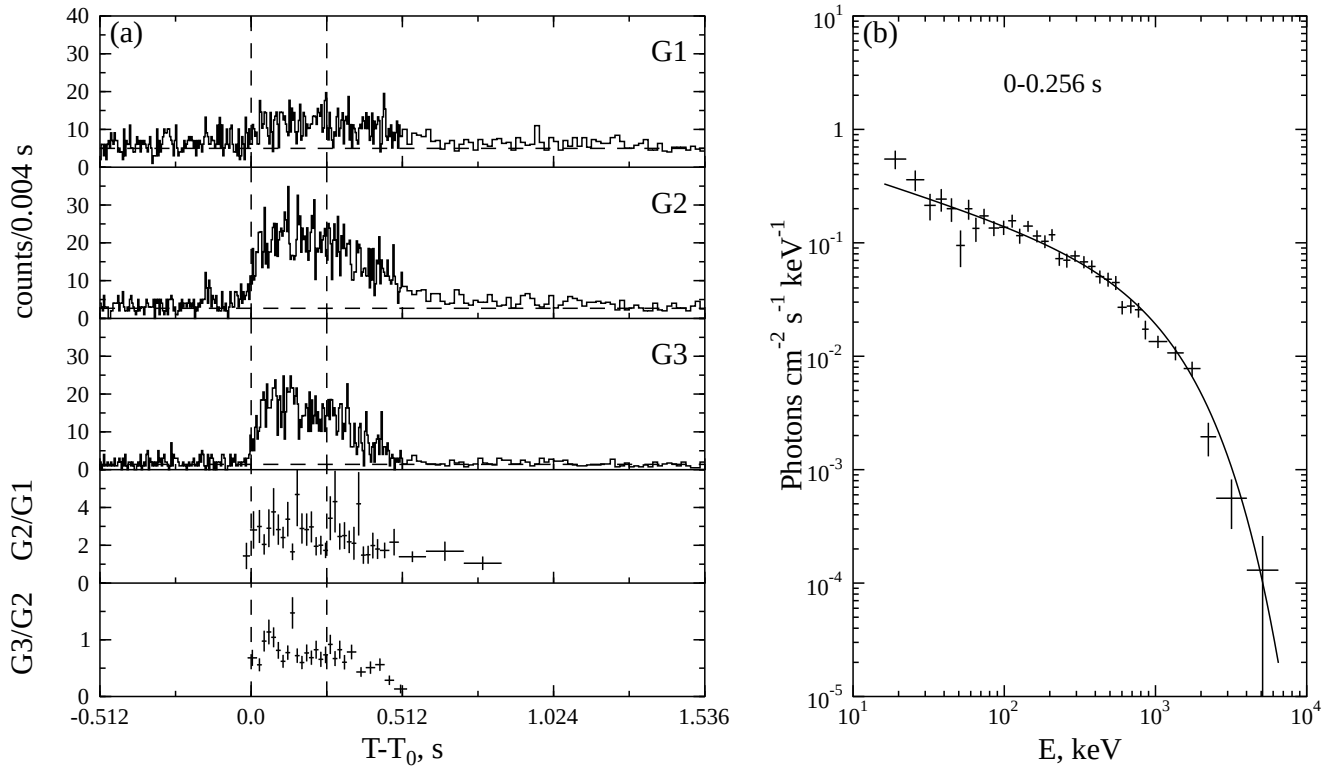

Fig. 115.— GRB 000218. T_0=58744.596 s UT.

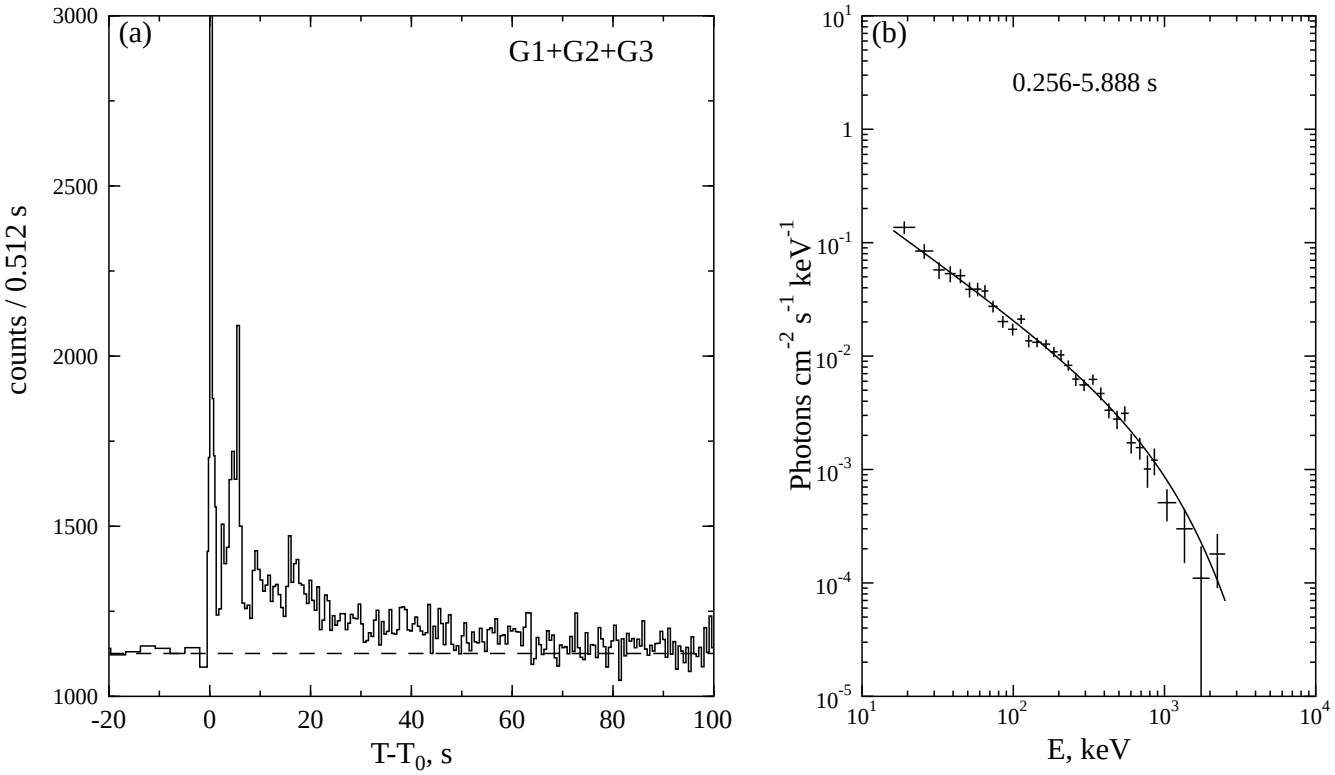

Fig. 116.— GRB 000218. T_0=58744.596 s UT (continued from Fig. 115).

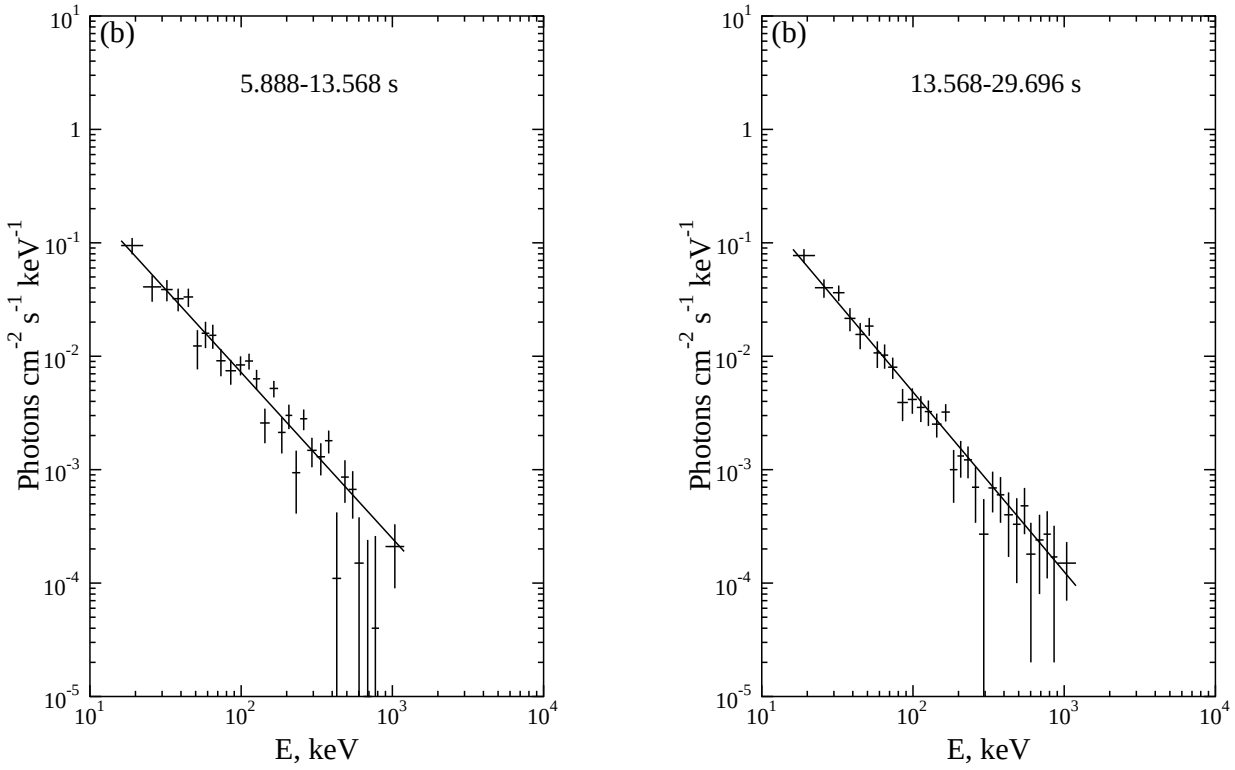

Fig. 117.— Energy spectra of the GRB 000218. T_0=58744.596 s UT (continued from Fig. 116).

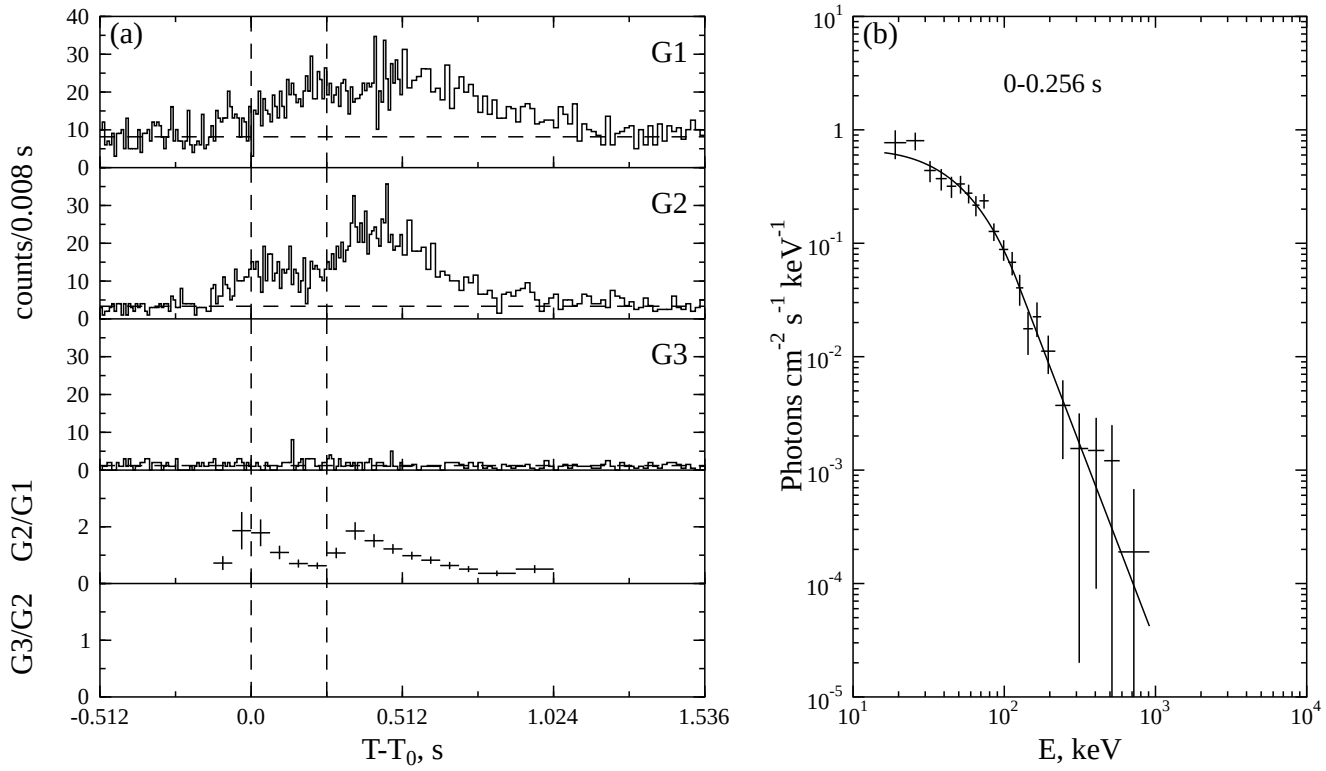

Fig. 118.— GRB 000326. T_0=19134.798 s UT.

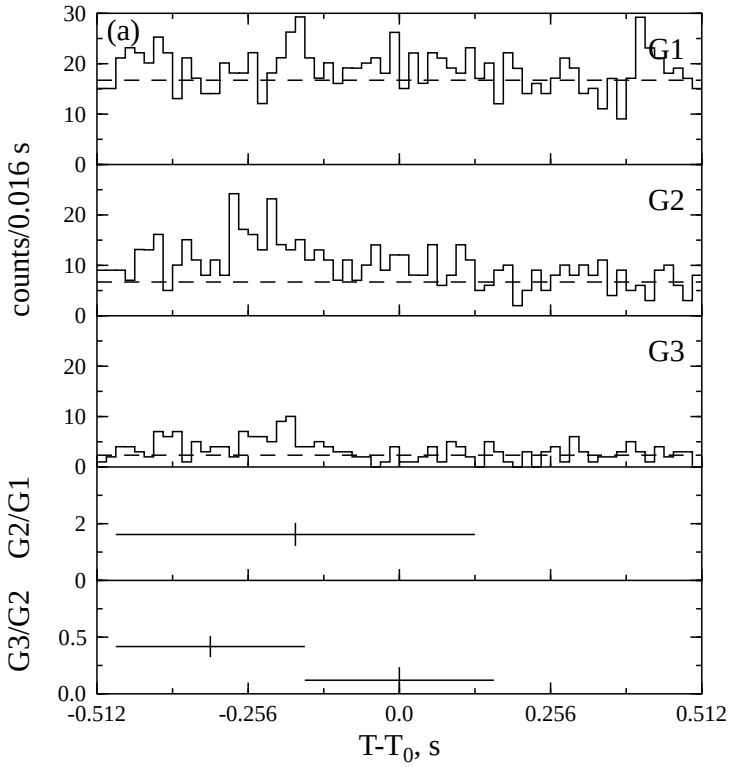

Fig. 119.— GRB 000412. T_0=42174.189 s UT.

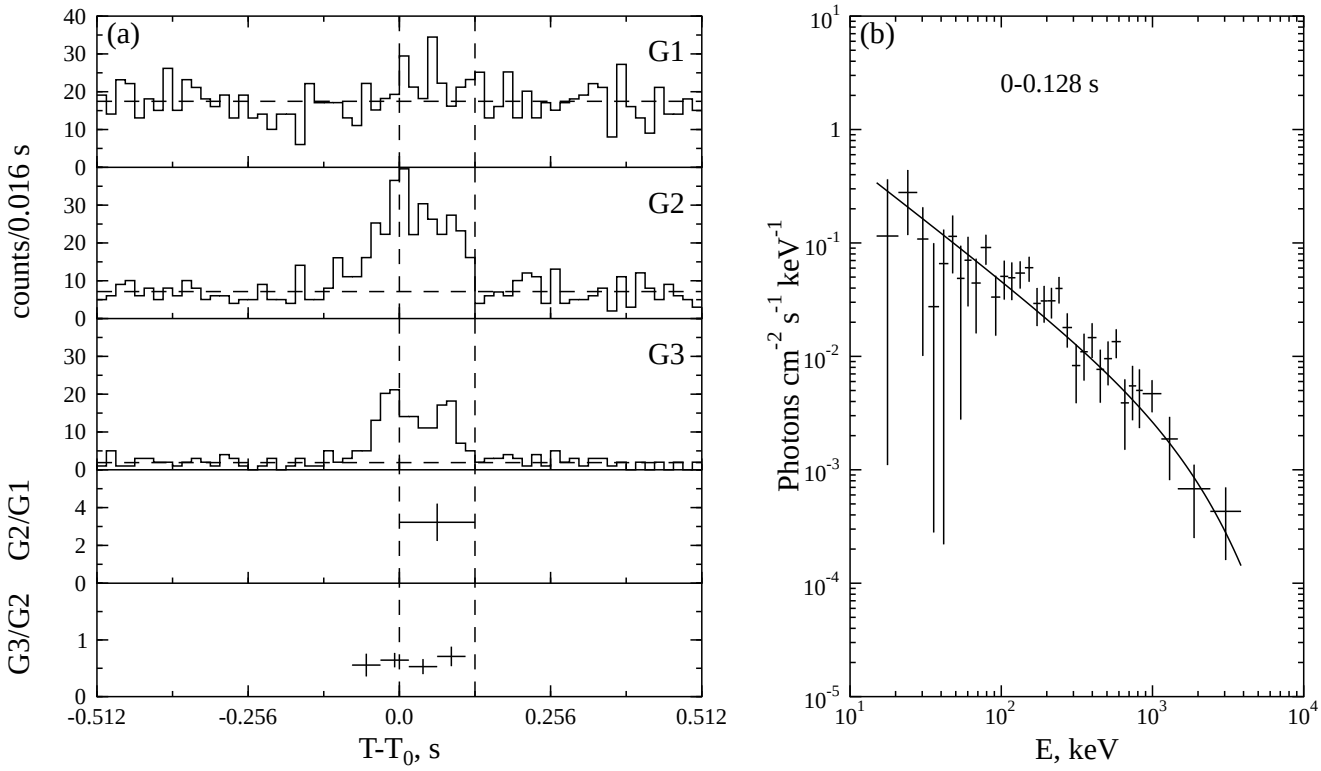

Fig. 120.— GRB 000420a. T_0=42271.144 s UT.

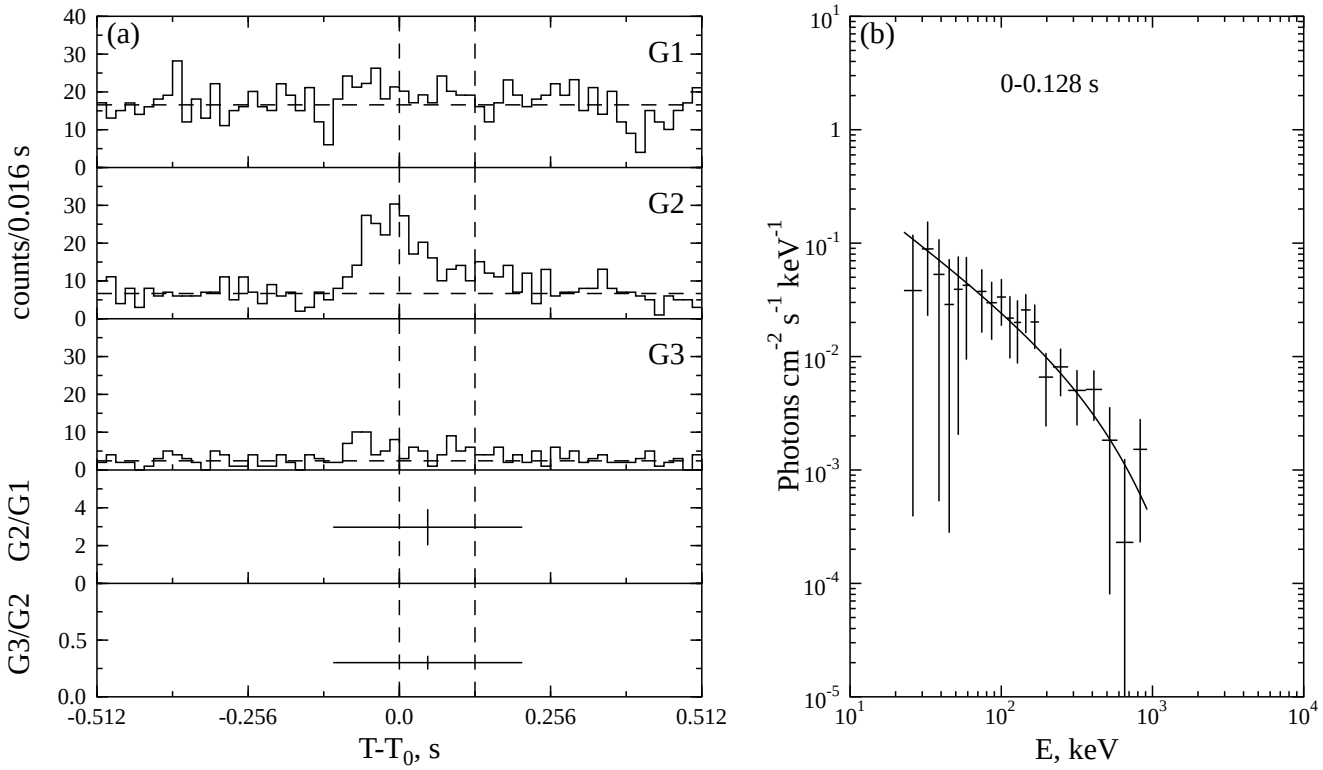

Fig. 121.— GRB 000513. T_0=40894.793 s UT.

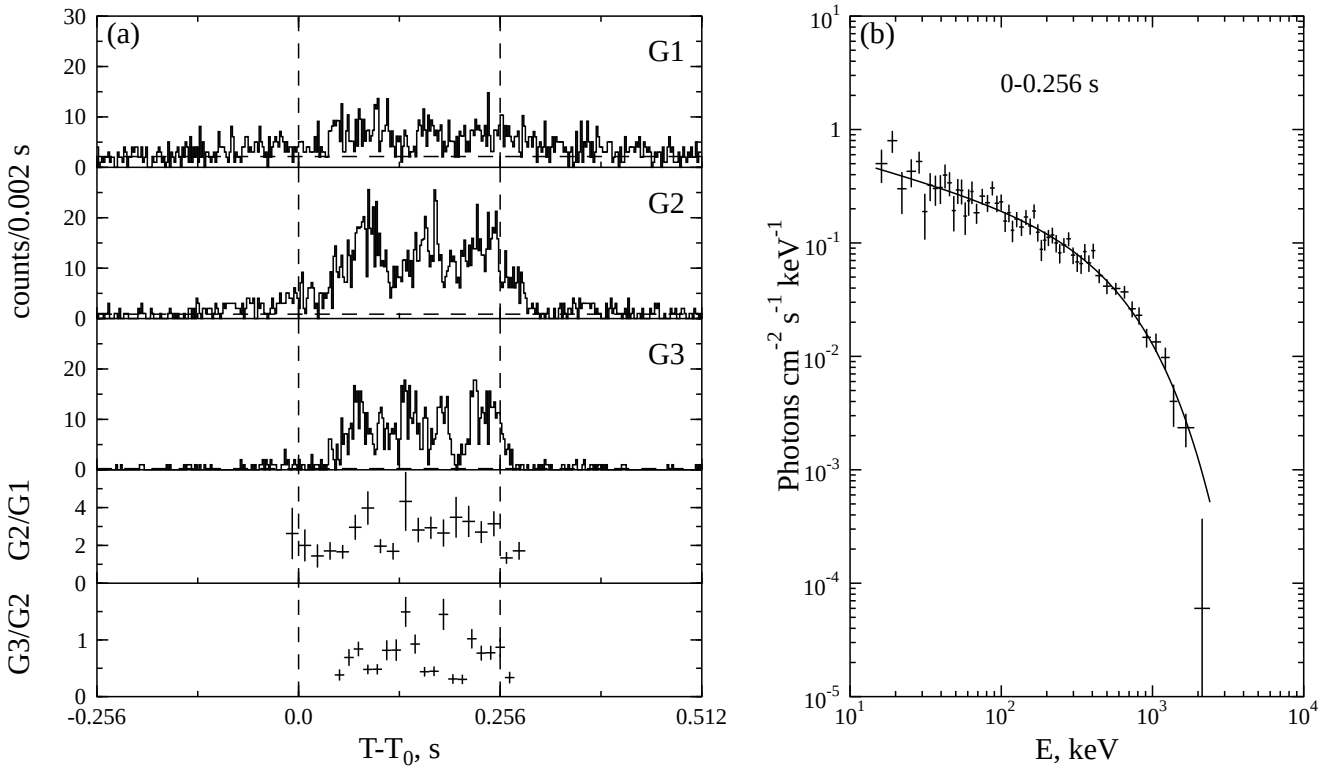

Fig. 122.— GRB 000526. T_0=84494.896 s UT.

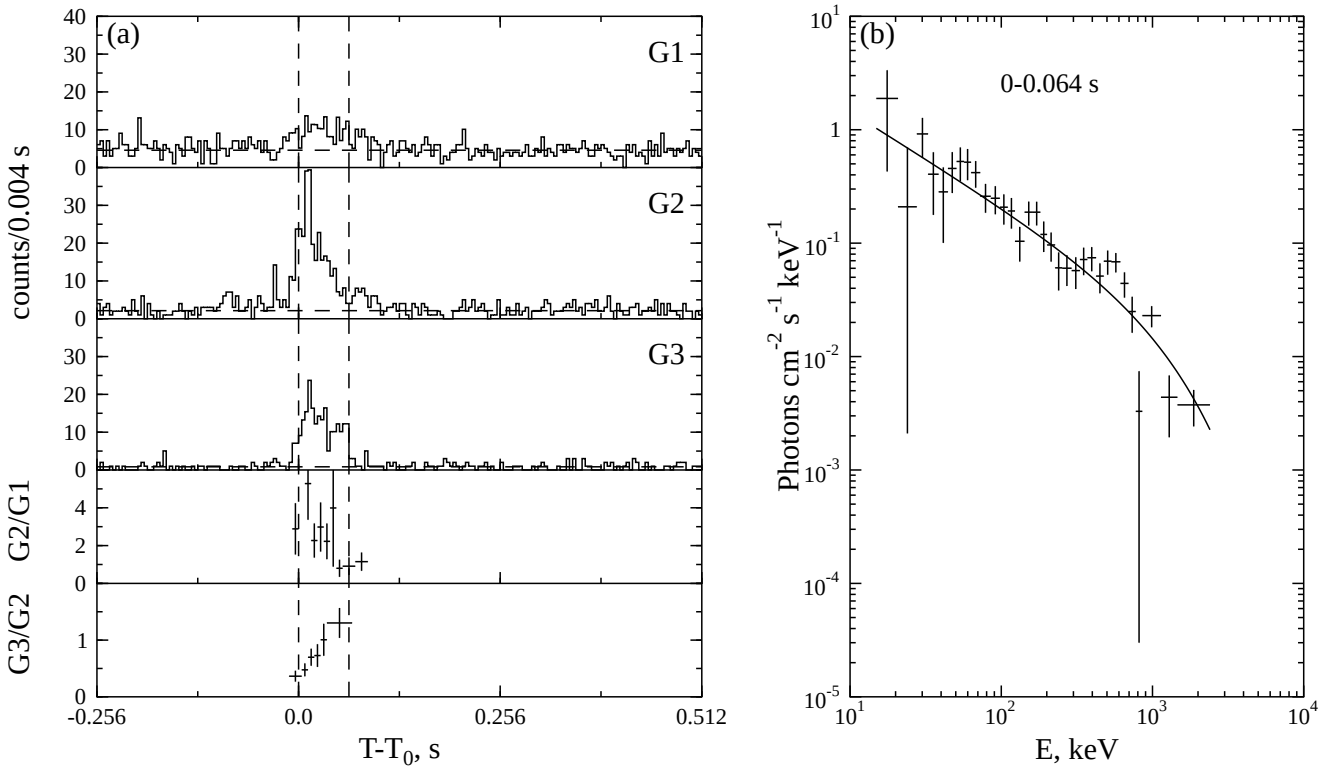

Fig. 123.— GRB 000607. T_0=8689.115 s UT.

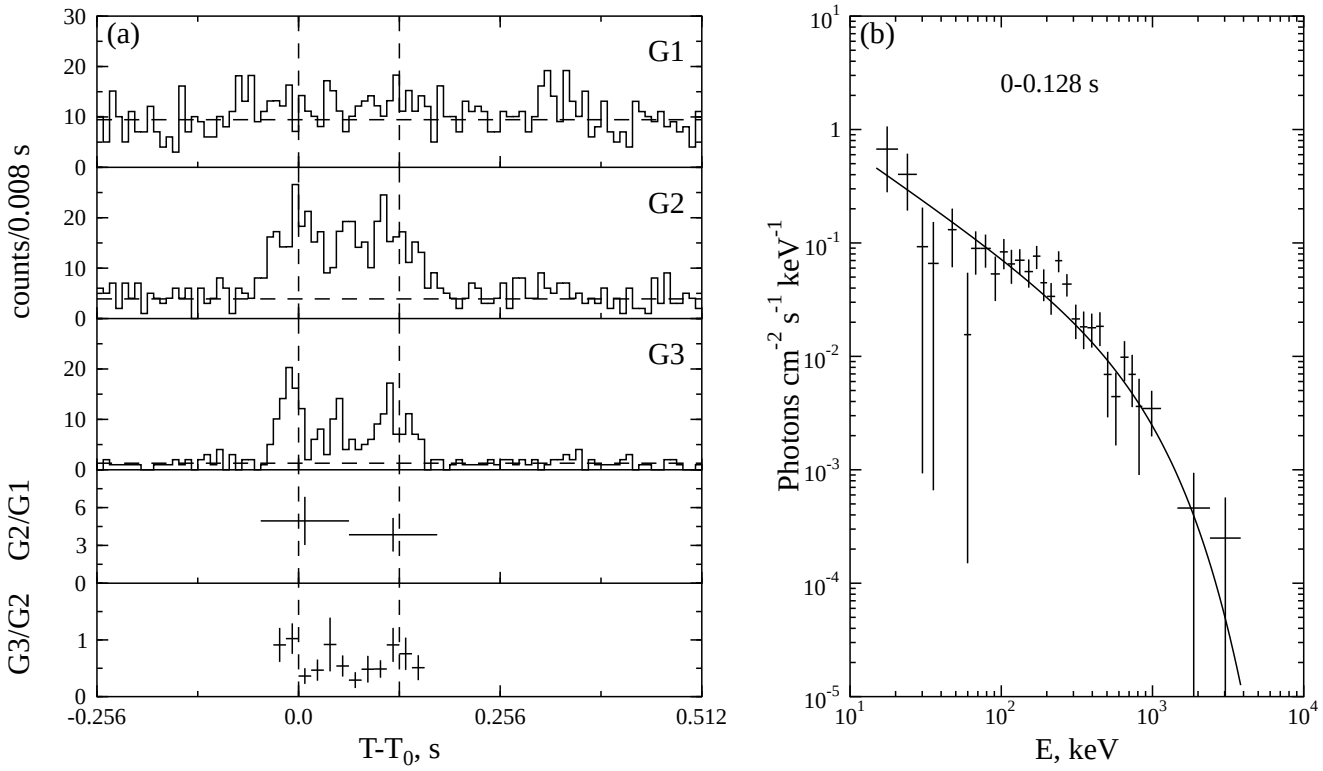

Fig. 124.— GRB 000608. T_0=70497.255 s UT.

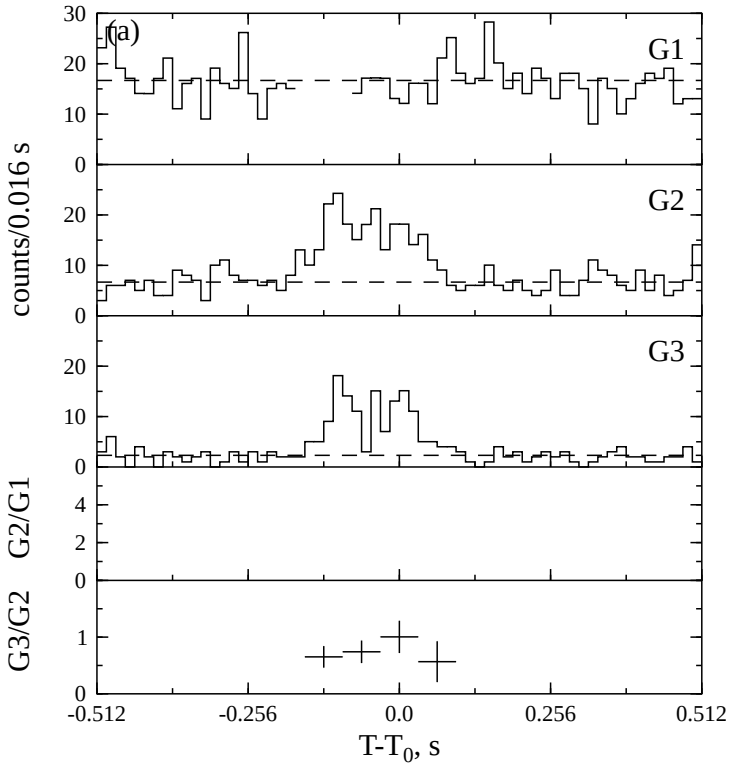

Fig. 125.— GRB 000623. T_0=3887.359 s UT.

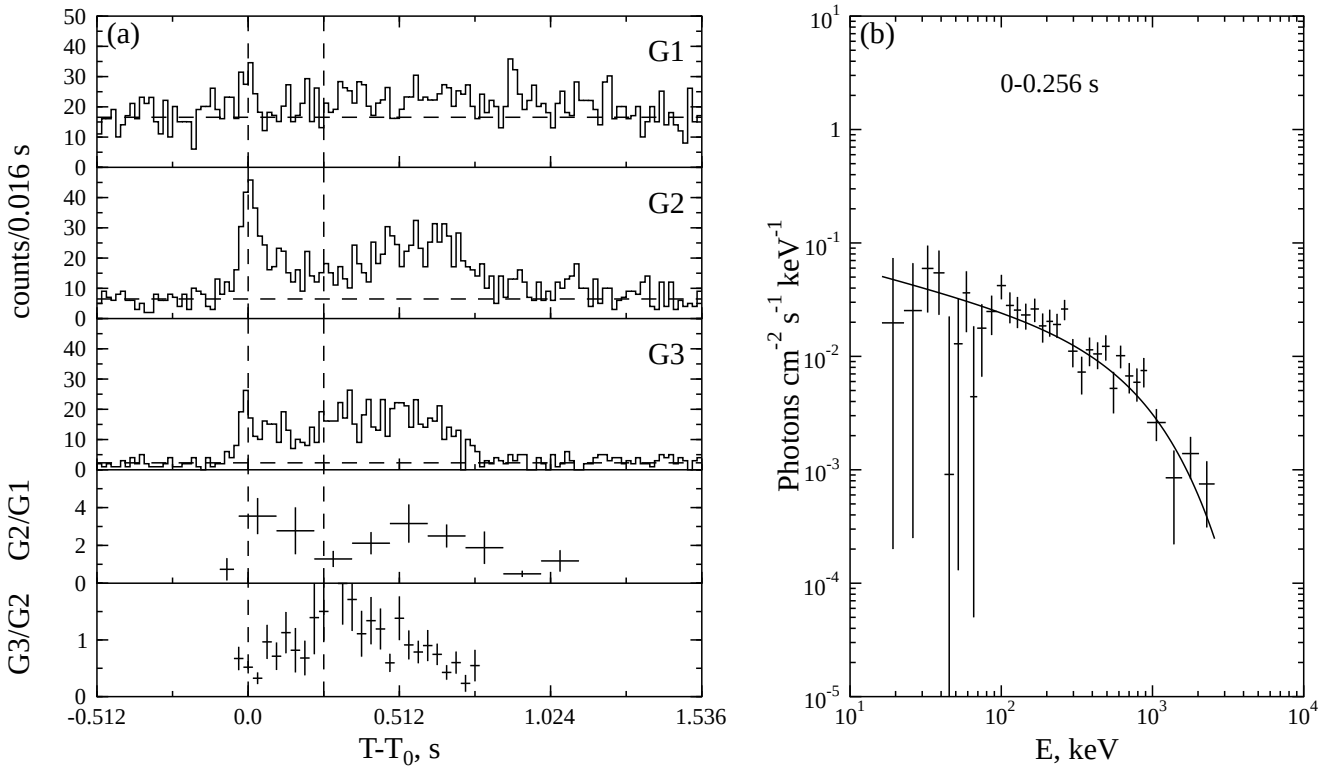

Fig. 126.— GRB 000701b. T_0=25961.013 s UT.

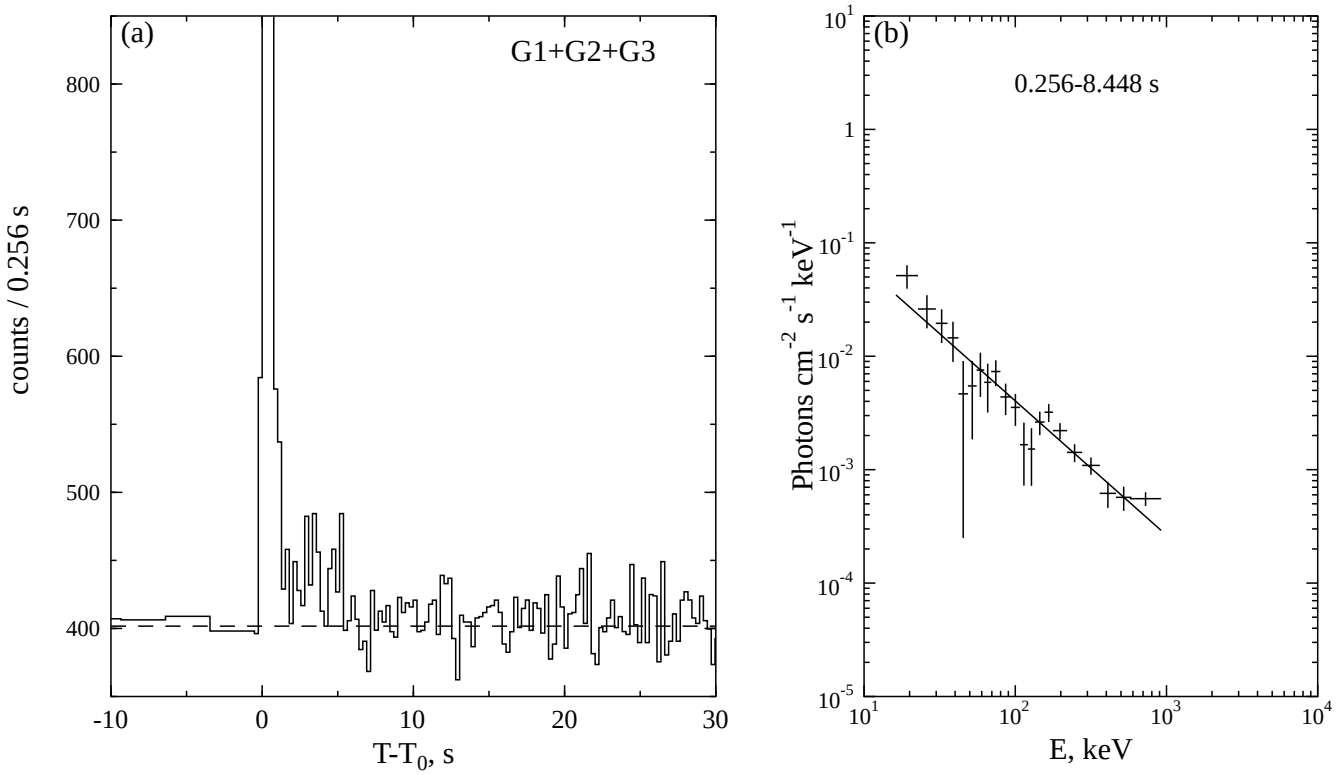

Fig. 127.— GRB 000701b. T_0=25961.013 s UT (continued from Fig. 126).

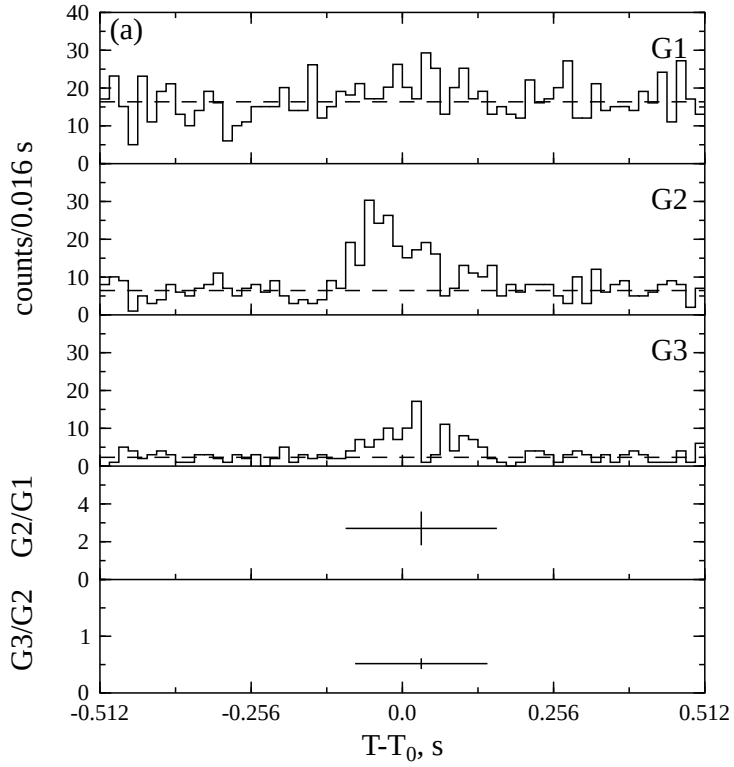

Fig. 128.— GRB 000707a. T_0=17372.072 s UT.

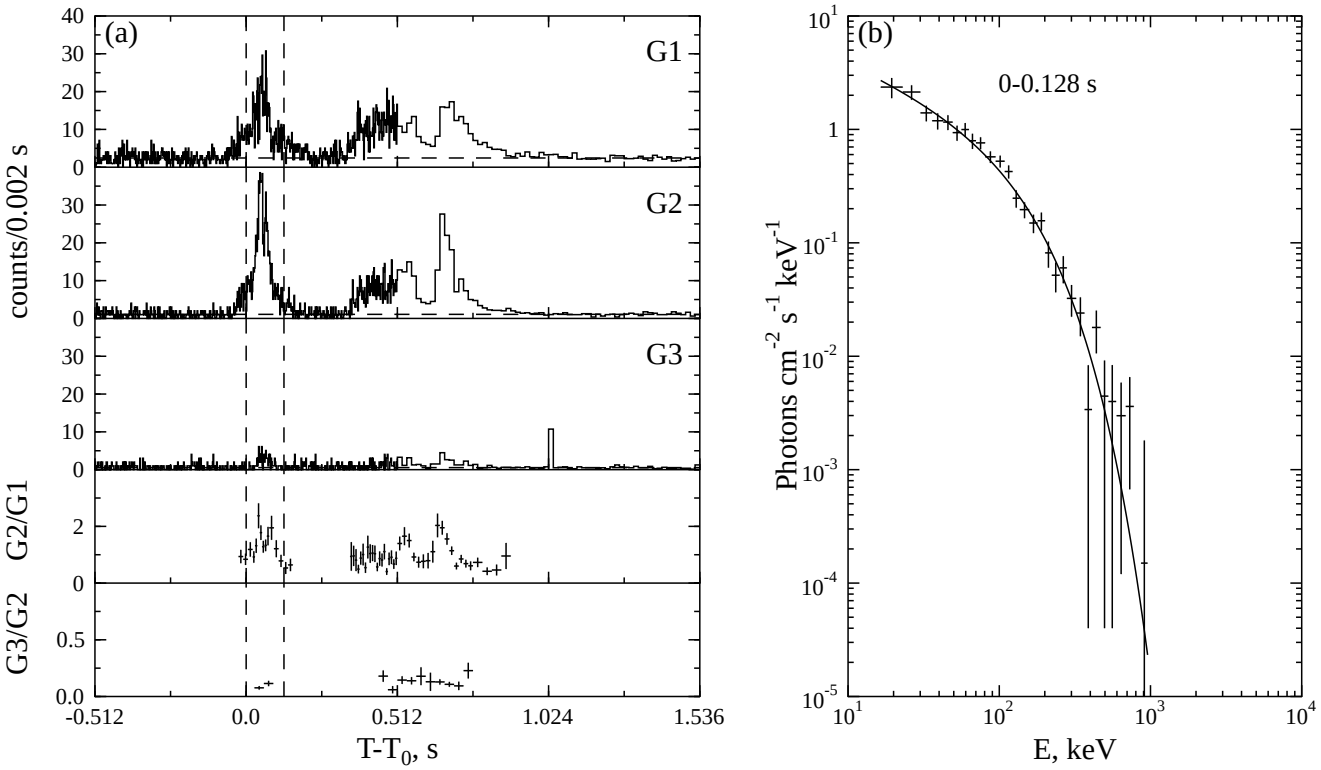

Fig. 129.— GRB 000727. T_0=70955.931 s UT.

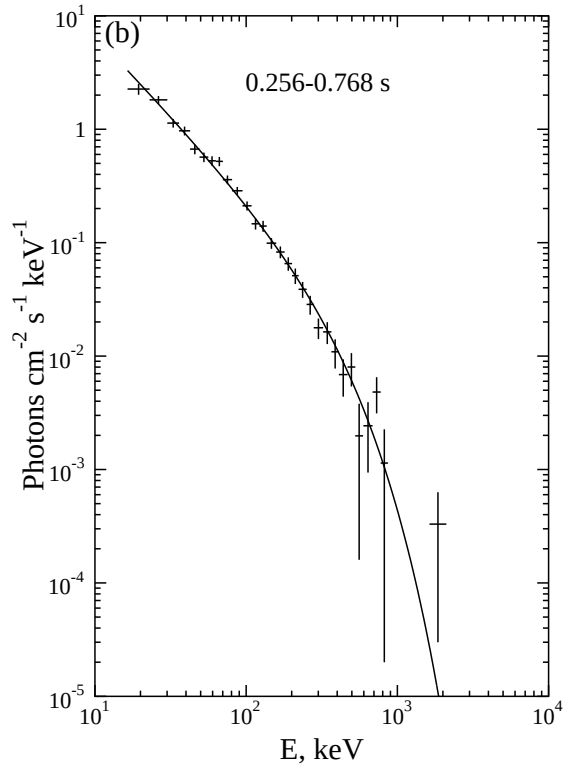

Fig. 130.— Energy spectrum of the GRB 000727. T_0=70955.931 s UT (continued from Fig. 129).

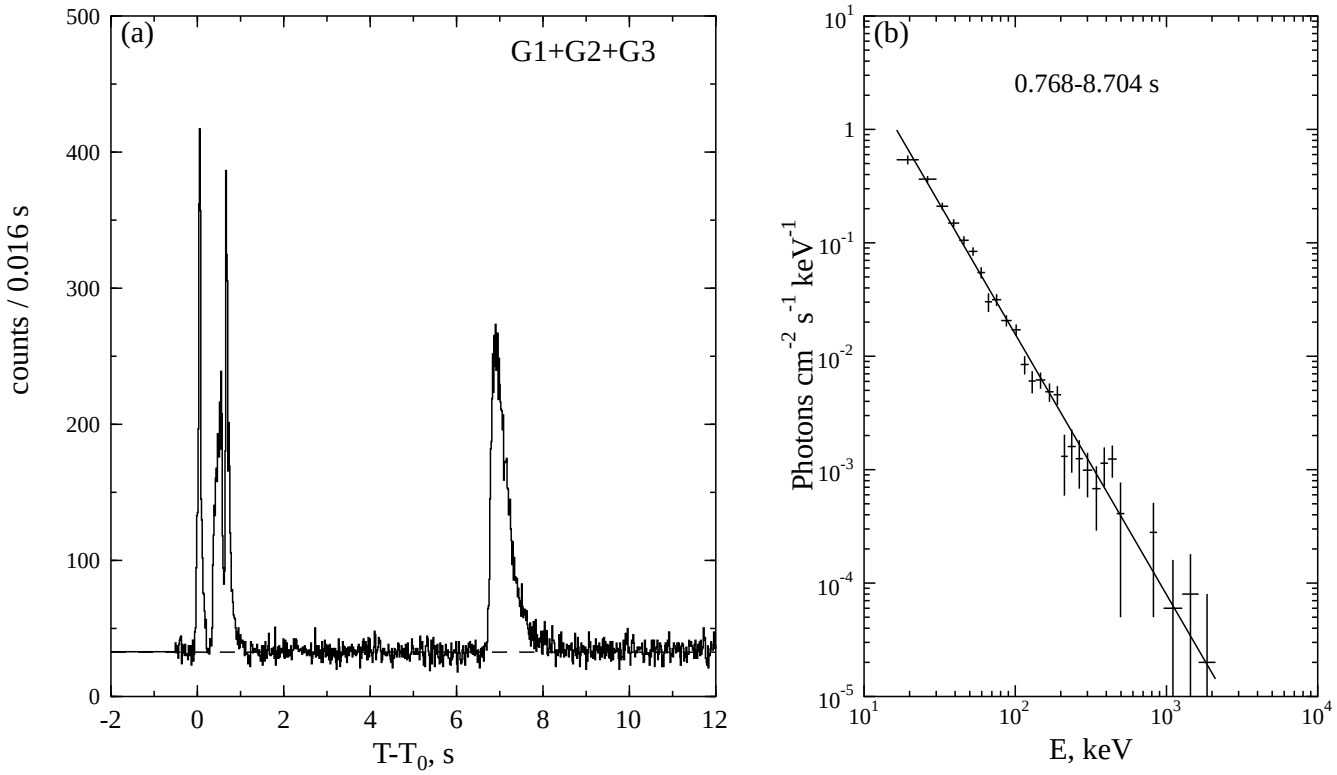

Fig. 131.— GRB 000727. T_0=70955.931 s UT (continued from Fig. 129, 130).

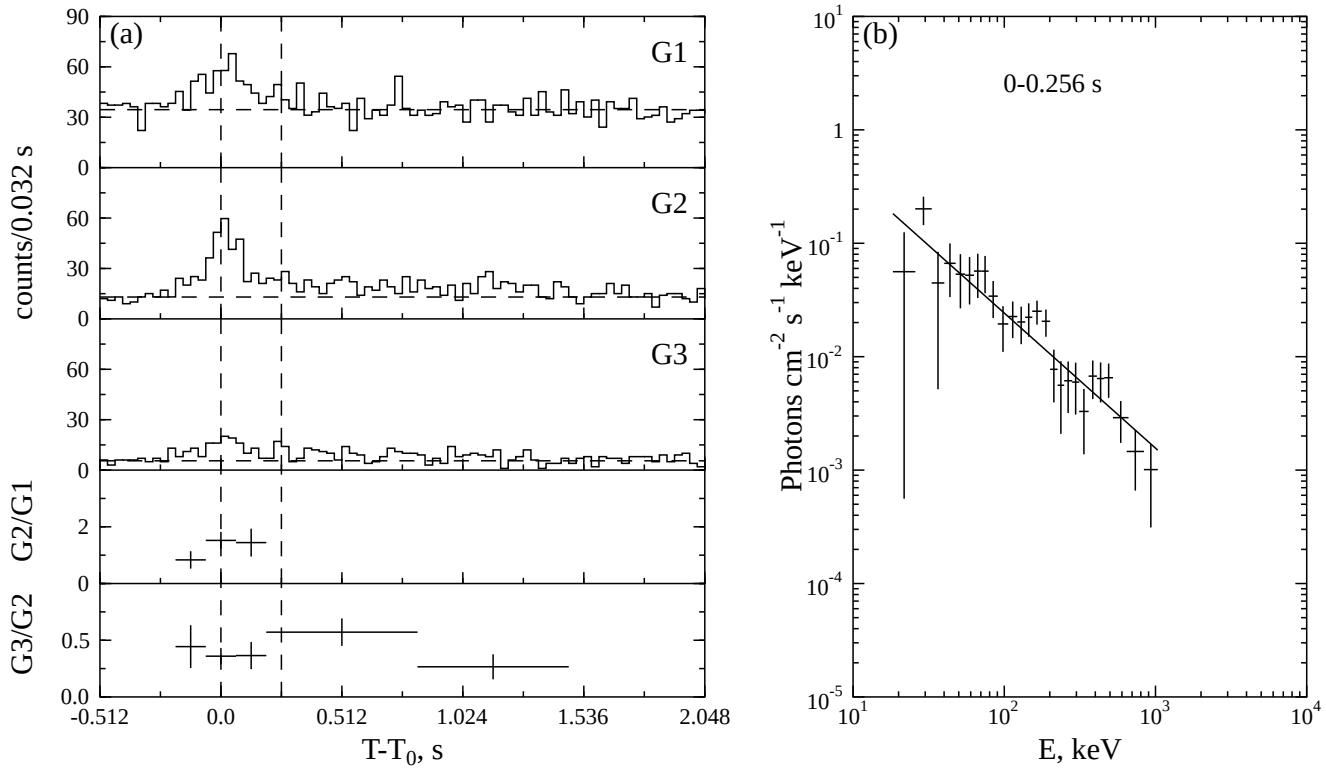

Fig. 132.— GRB 000818. T_0=72547.040 s UT.

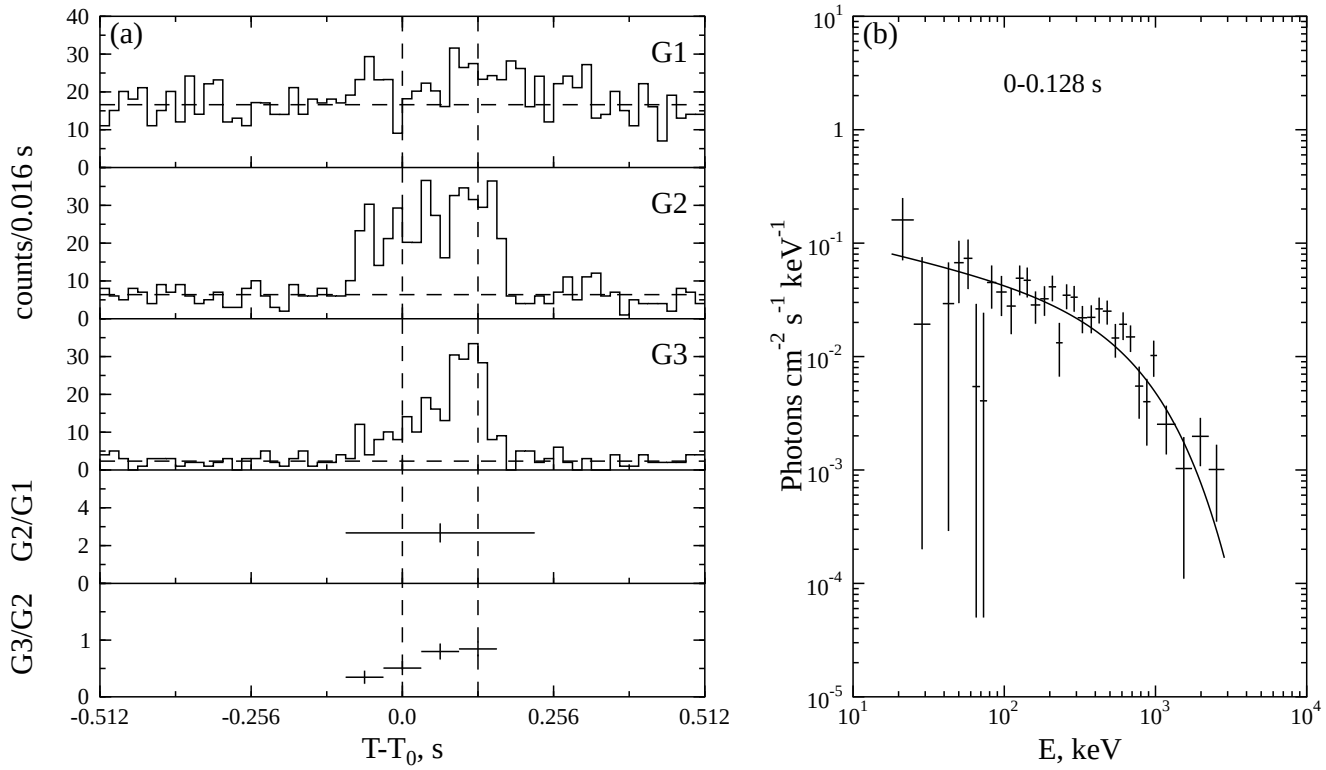

Fig. 133.— GRB 000928. T_0=6285.374 s UT.

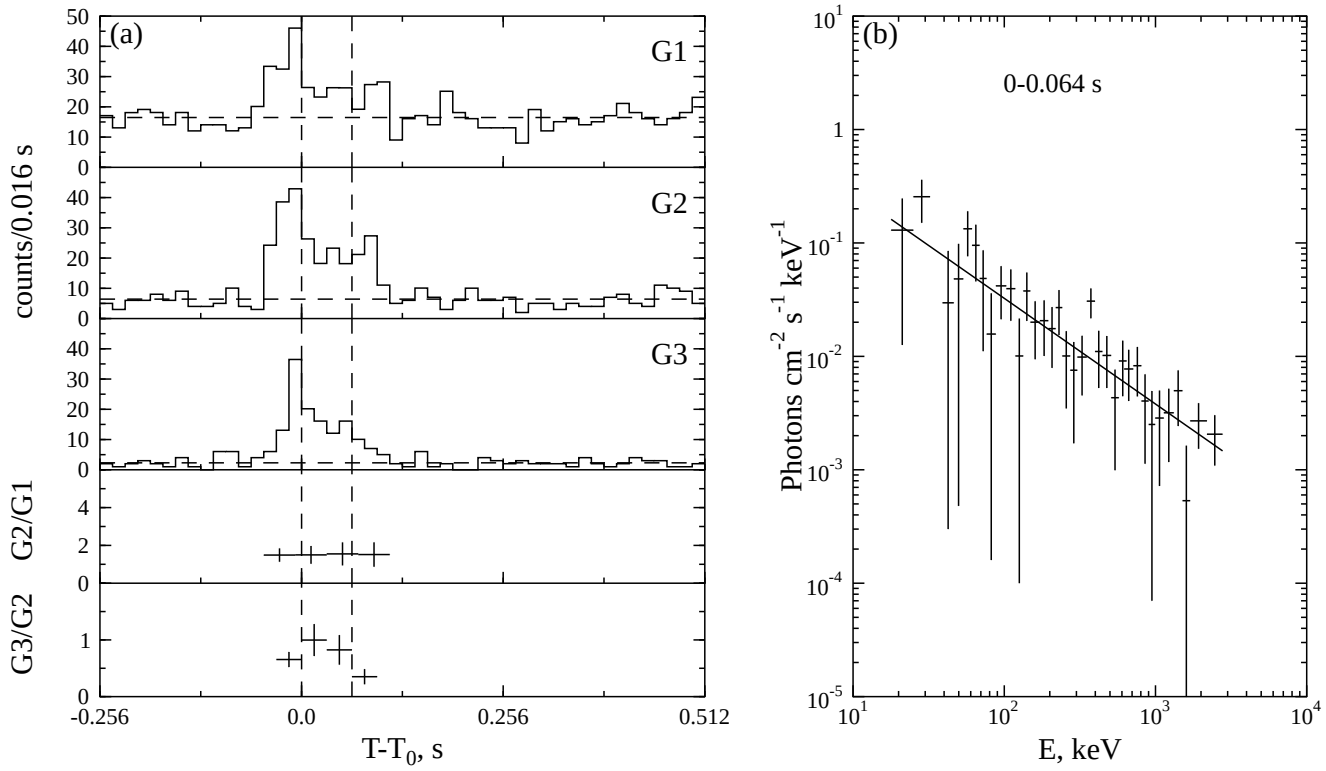

Fig. 134.— GRB 001022. T_0=20905.666 s UT.

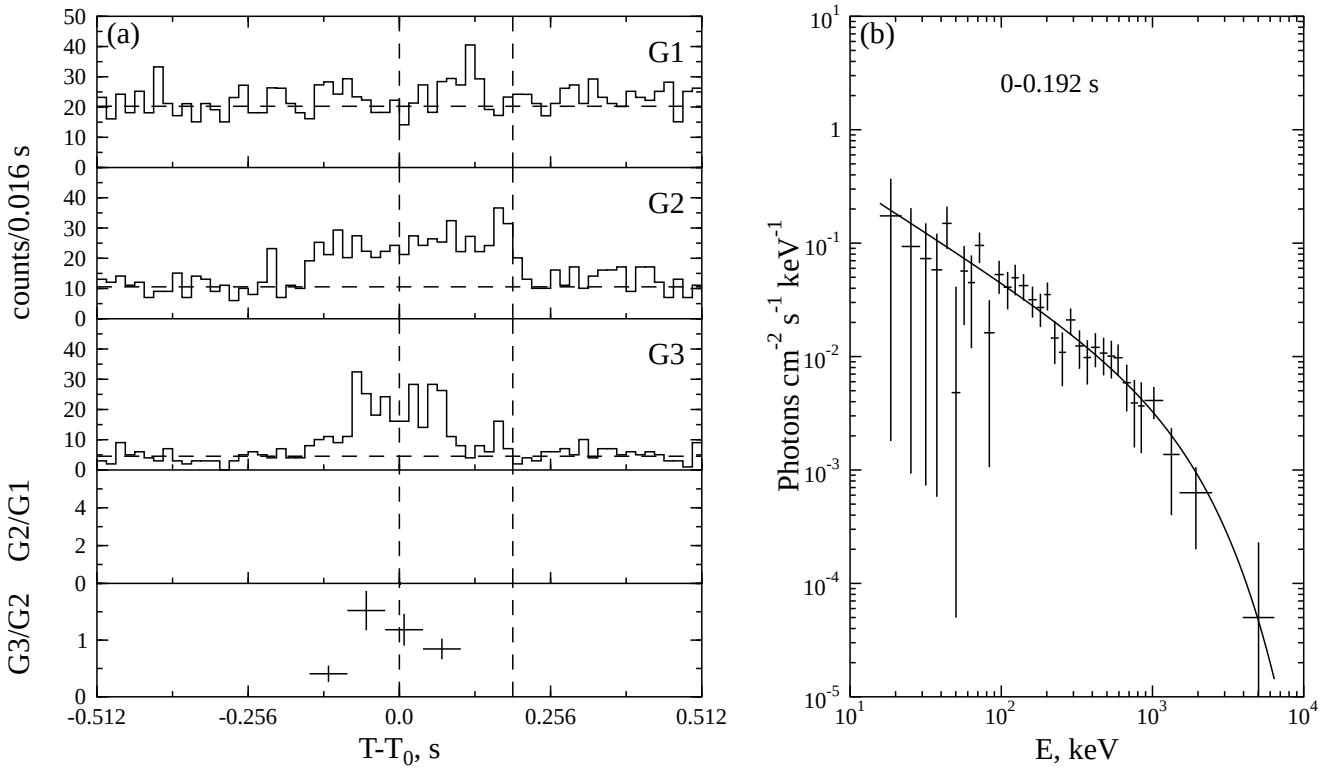

Fig. 135.— GRB 001025c. T_0=71369.963 s UT.

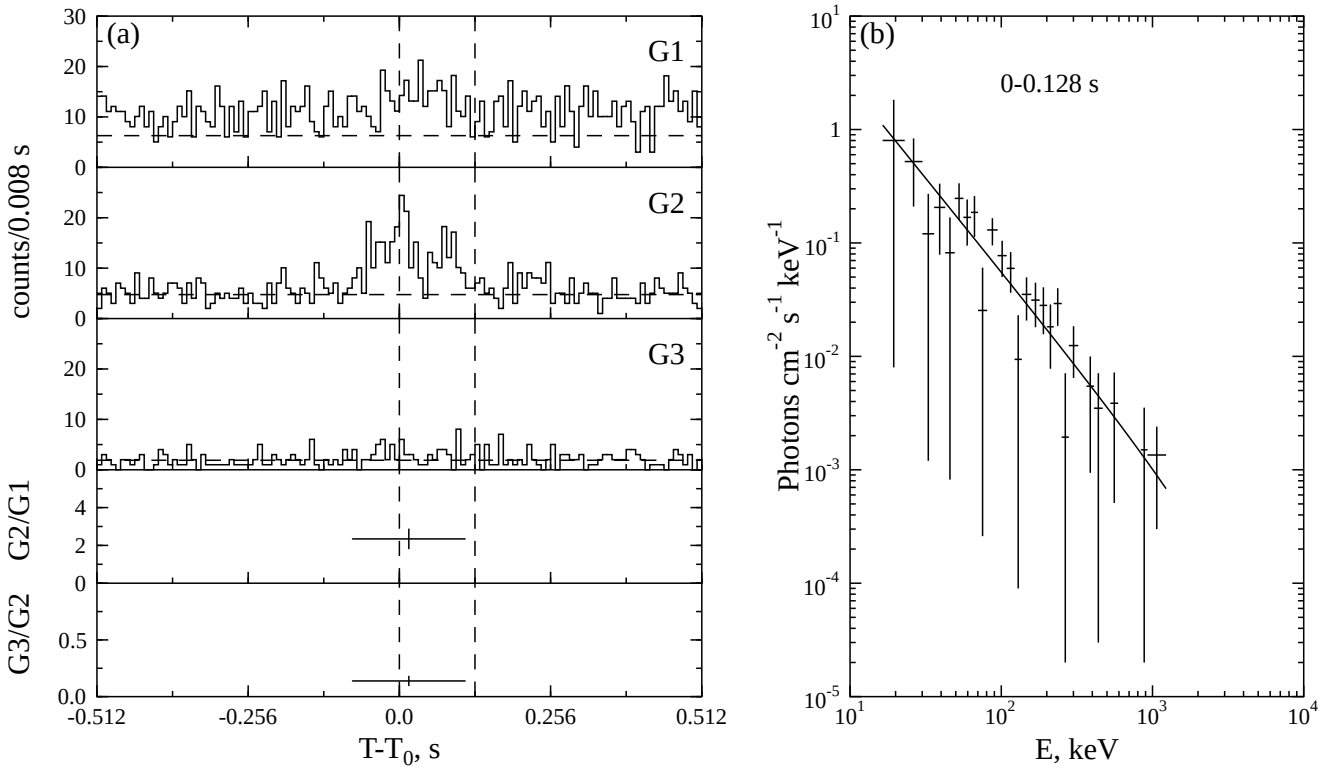

Fig. 136.— GRB 001204. T_0=28869.372 s UT.

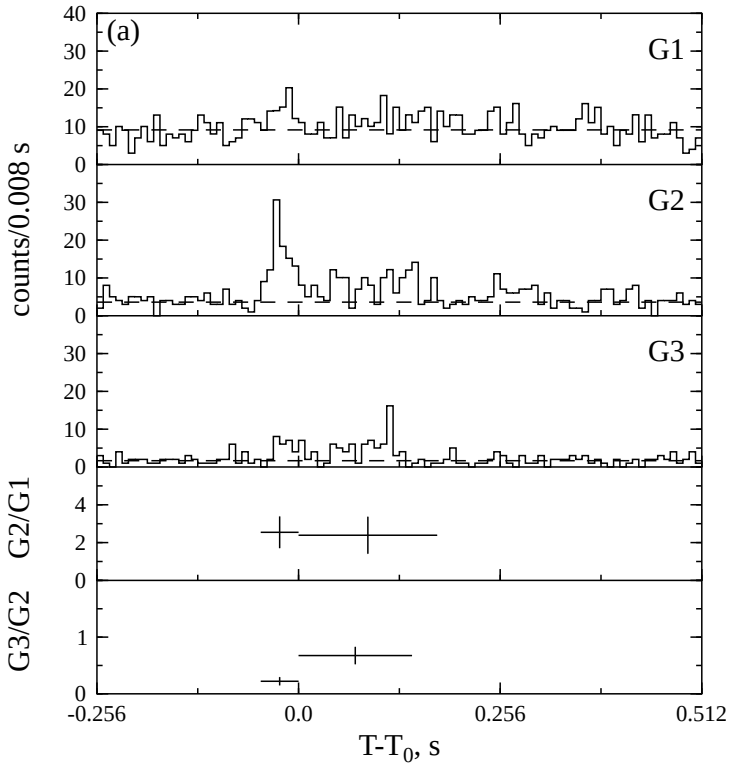

Fig. 137.— GRB 001207a. T_0=8815.958 s UT.

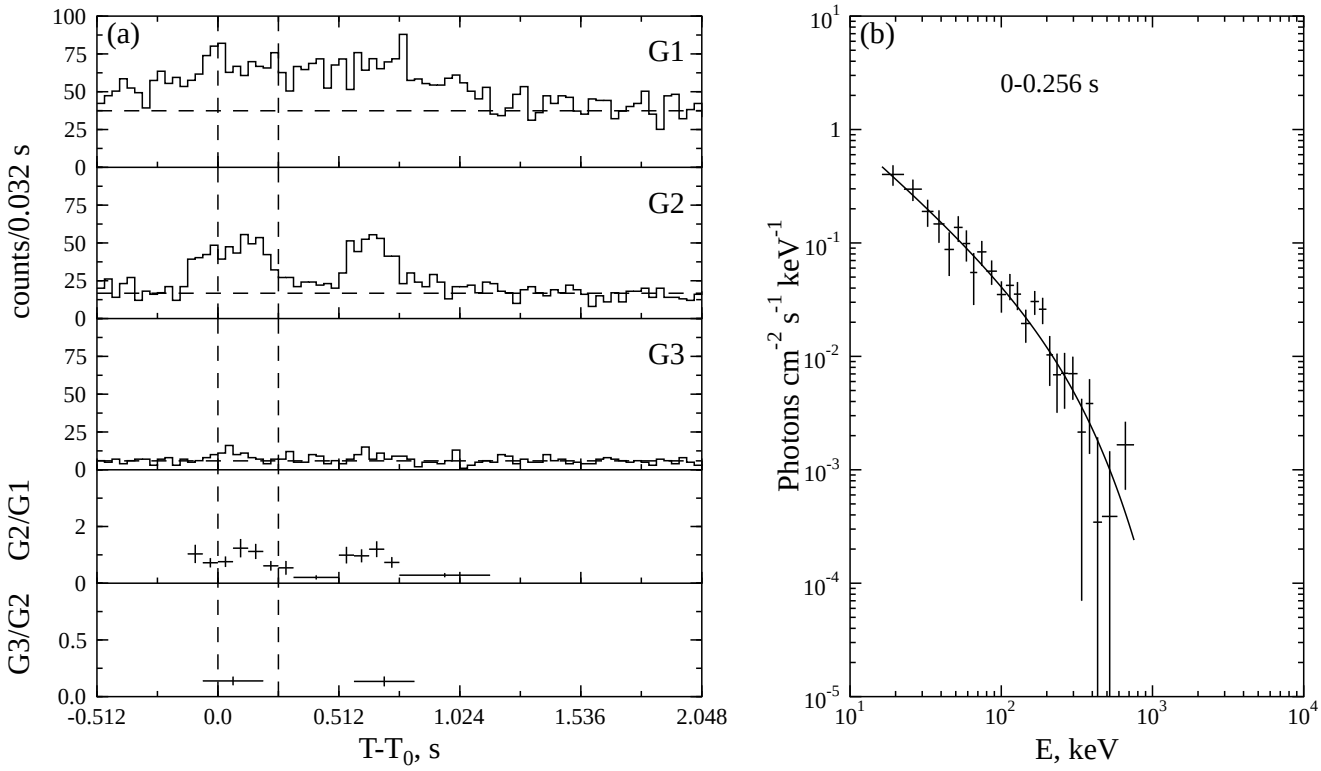

Fig. 138.— GRB 001207b. T_0=34185.588 s UT.

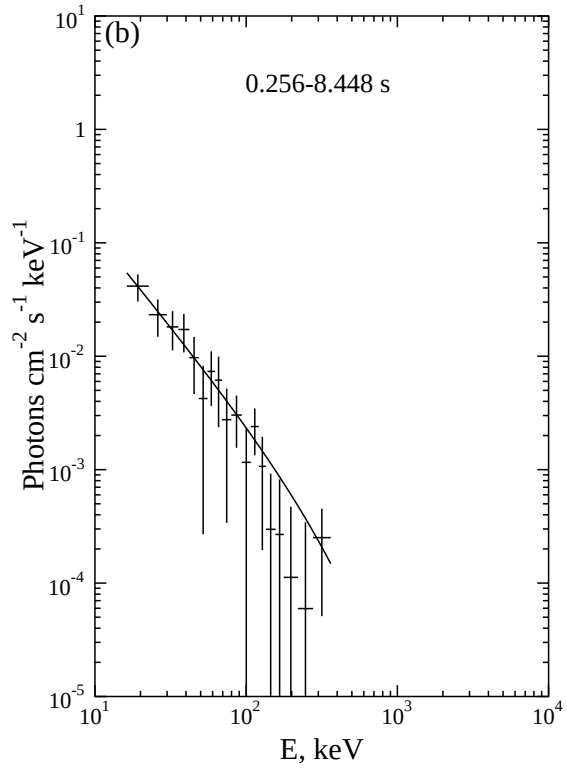

Fig. 139.— GRB 001207b. T_0=34185.588 s UT (continued from Fig. 138).

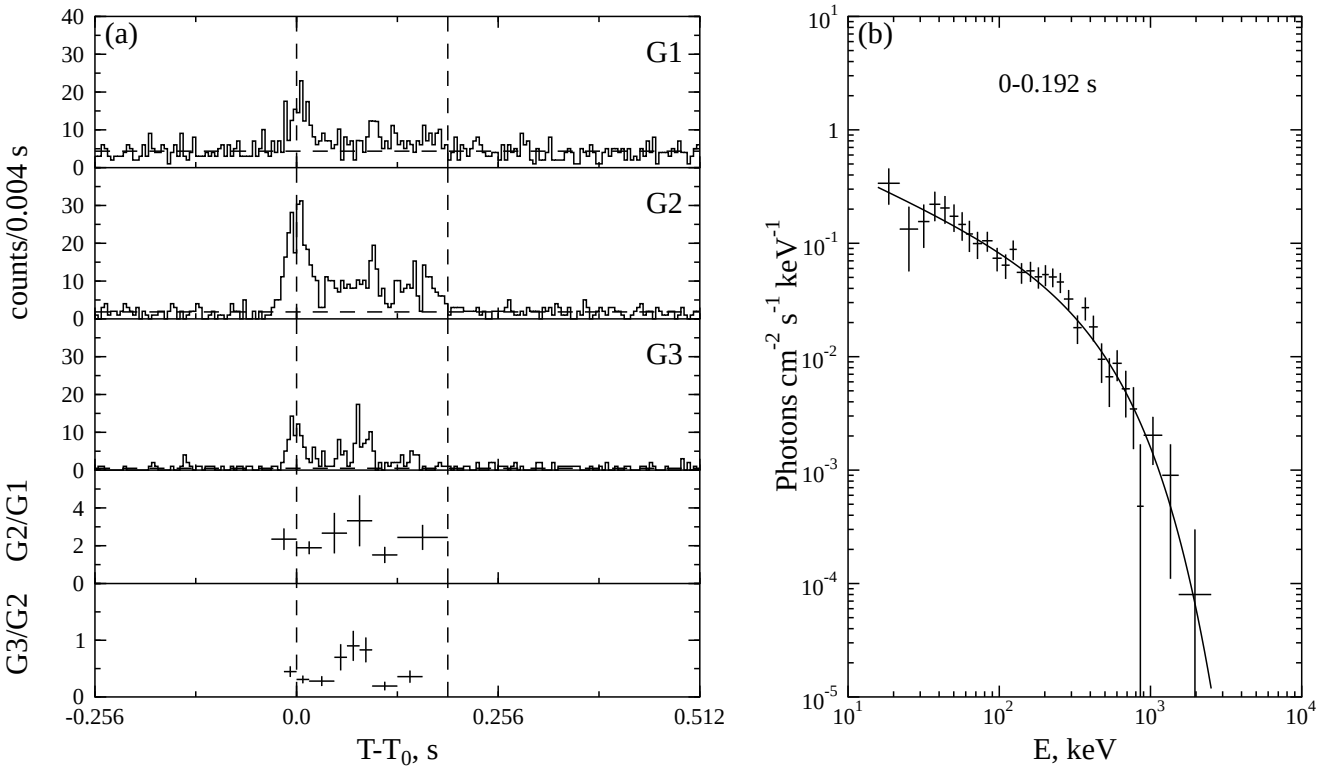

Fig. 140.— GRB 010119. T_0=37179.556 s UT.

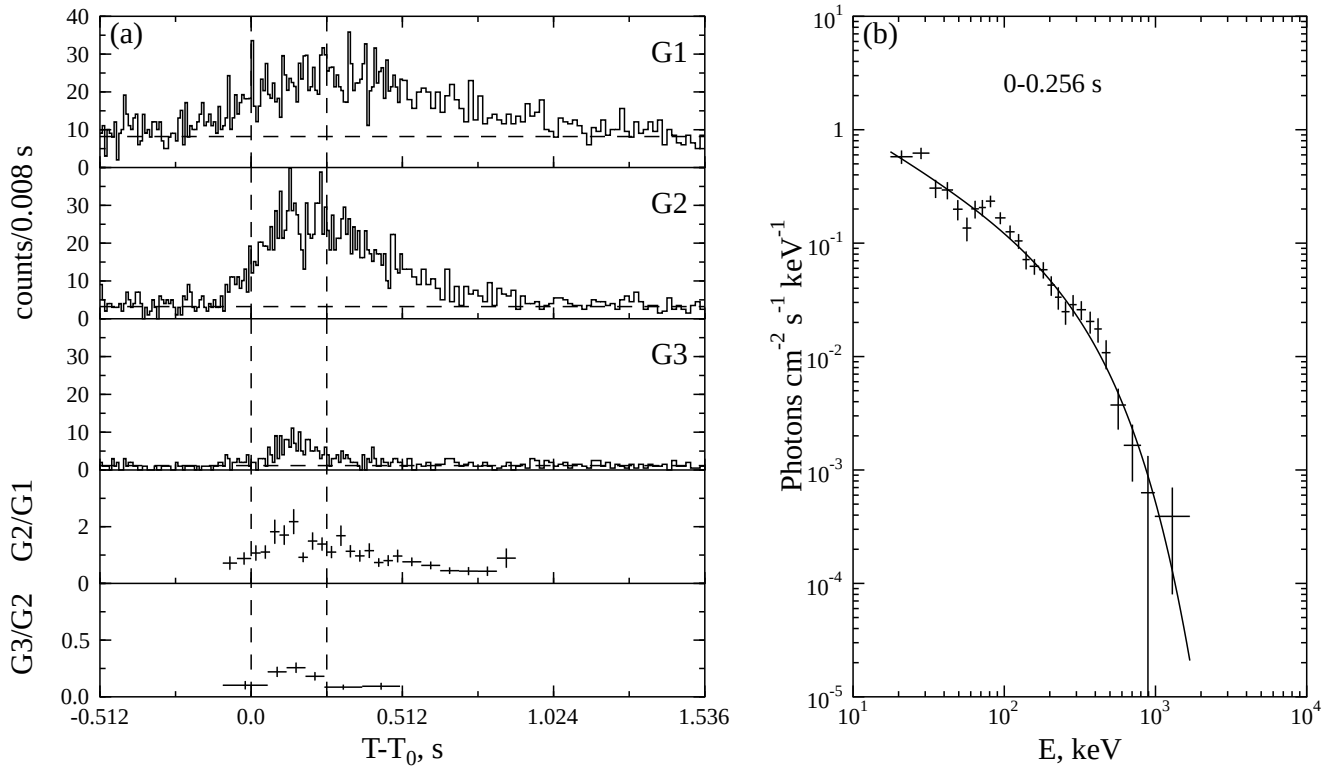

Fig. 141.— GRB 010308. T_0=56338.468 s UT.

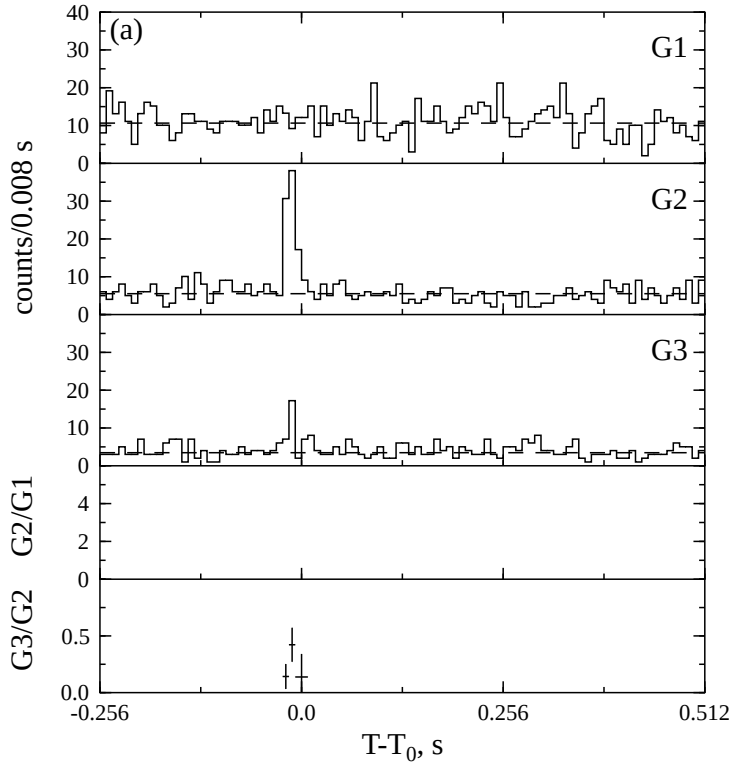

Fig. 142.— GRB 010420a. T_0=30786.674 s UT.

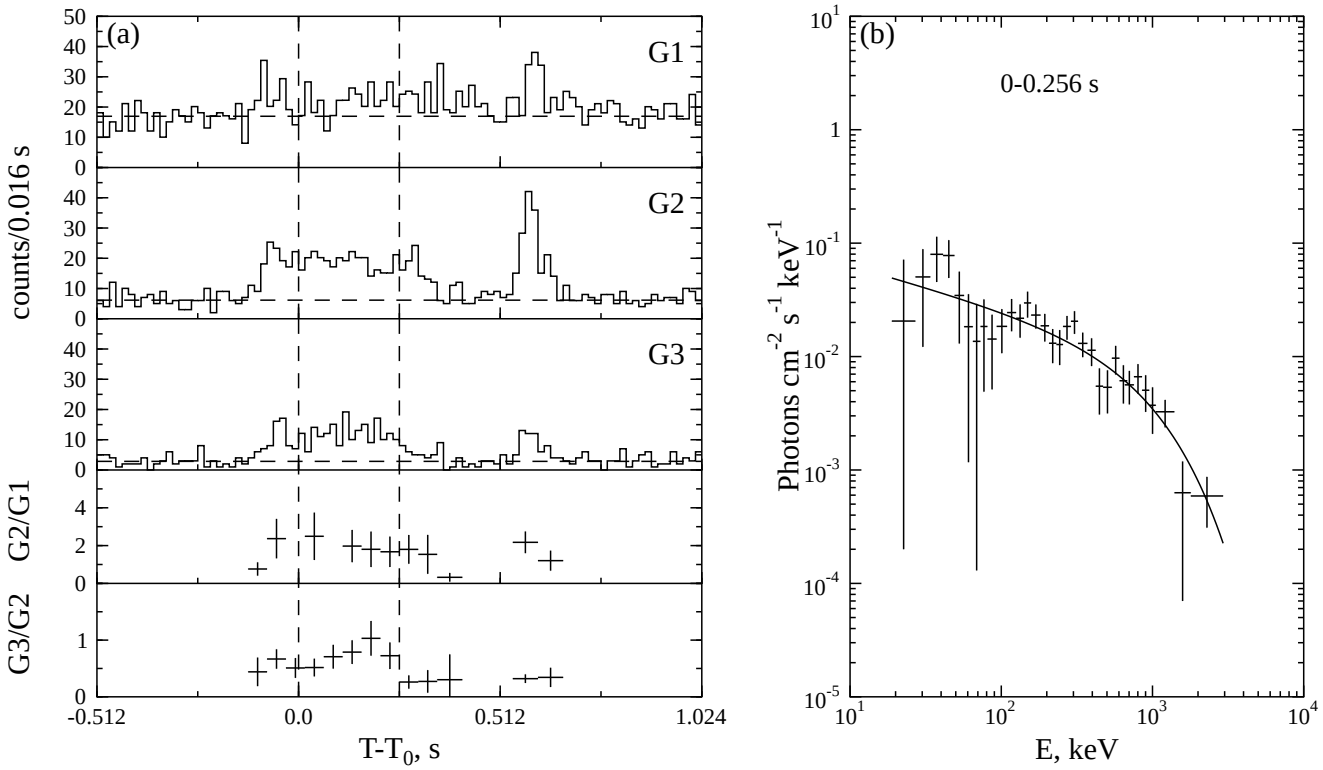

Fig. 143.— GRB 010427. T_0=67452.969 s UT.

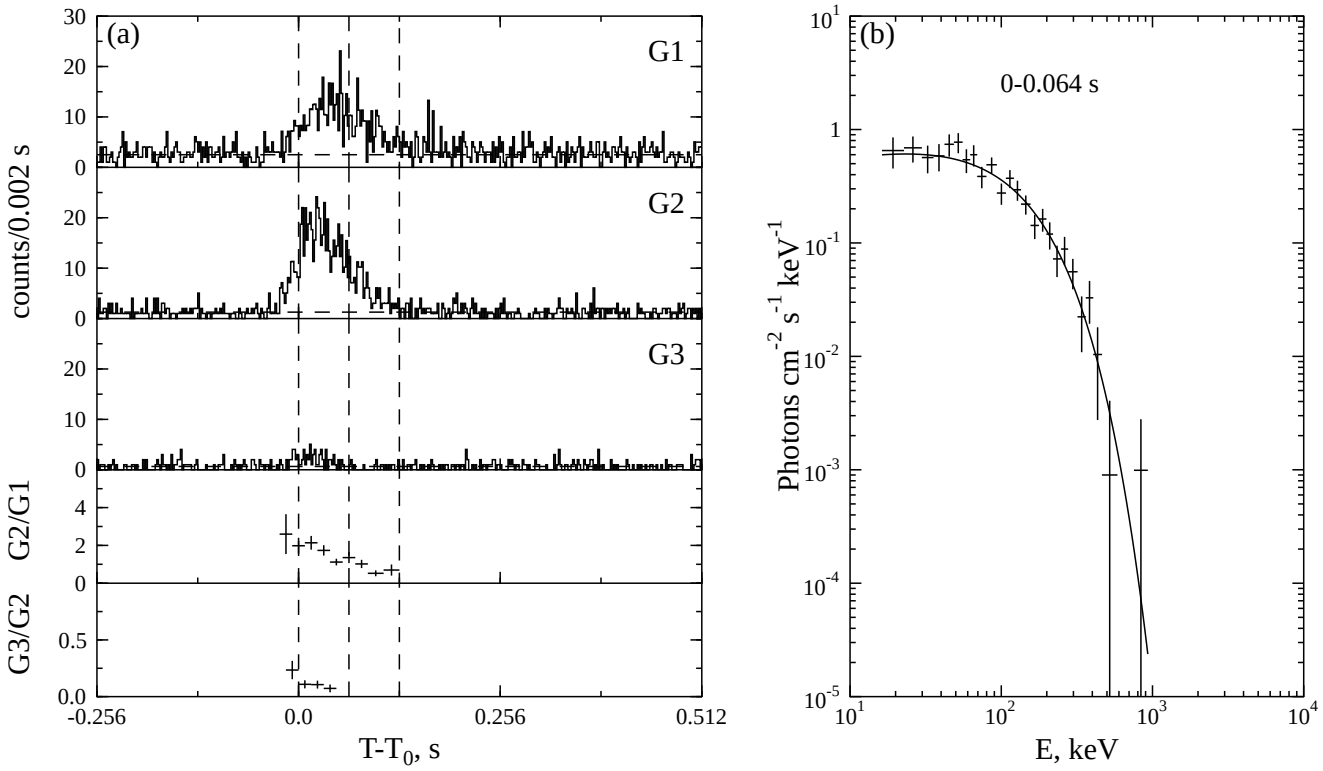

Fig. 144.— GRB 010616. T_0=23724.080 s UT.

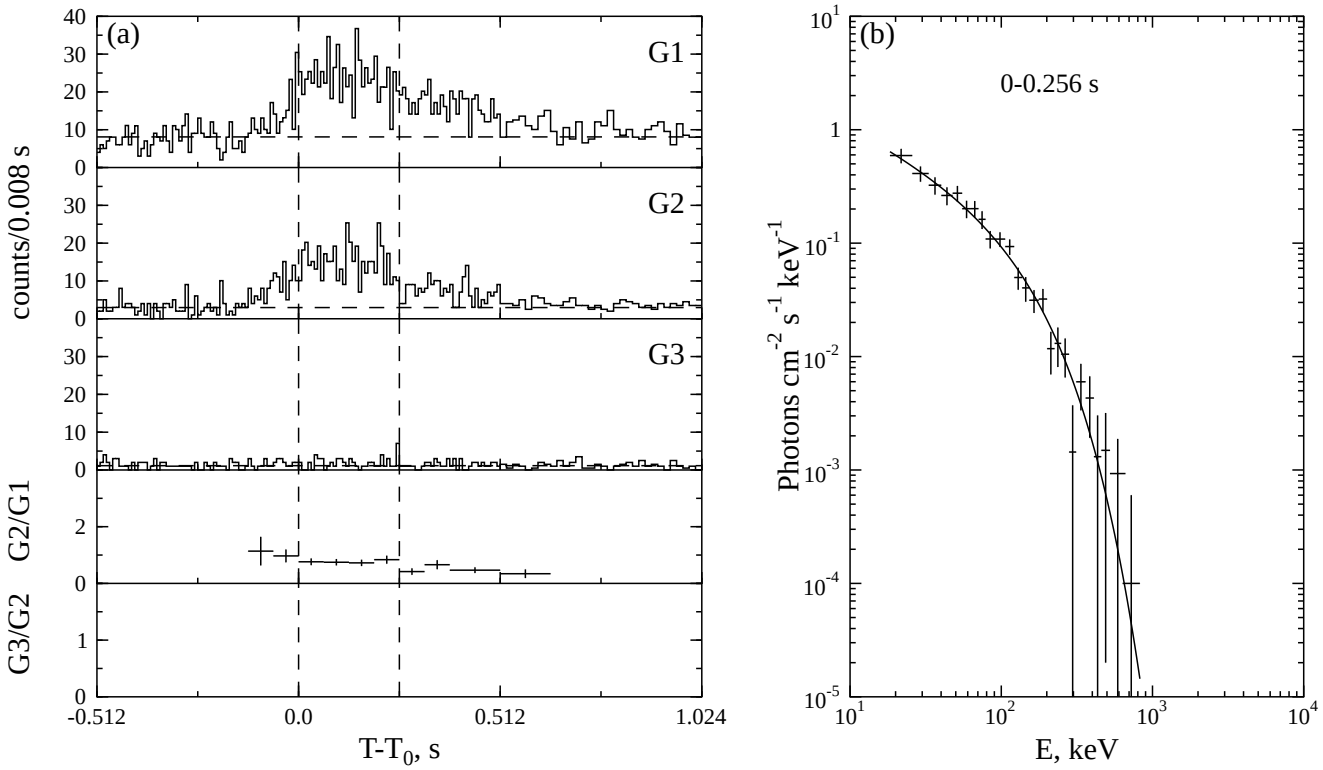

Fig. 145.— GRB 010624. T_0=48929.130 s UT.

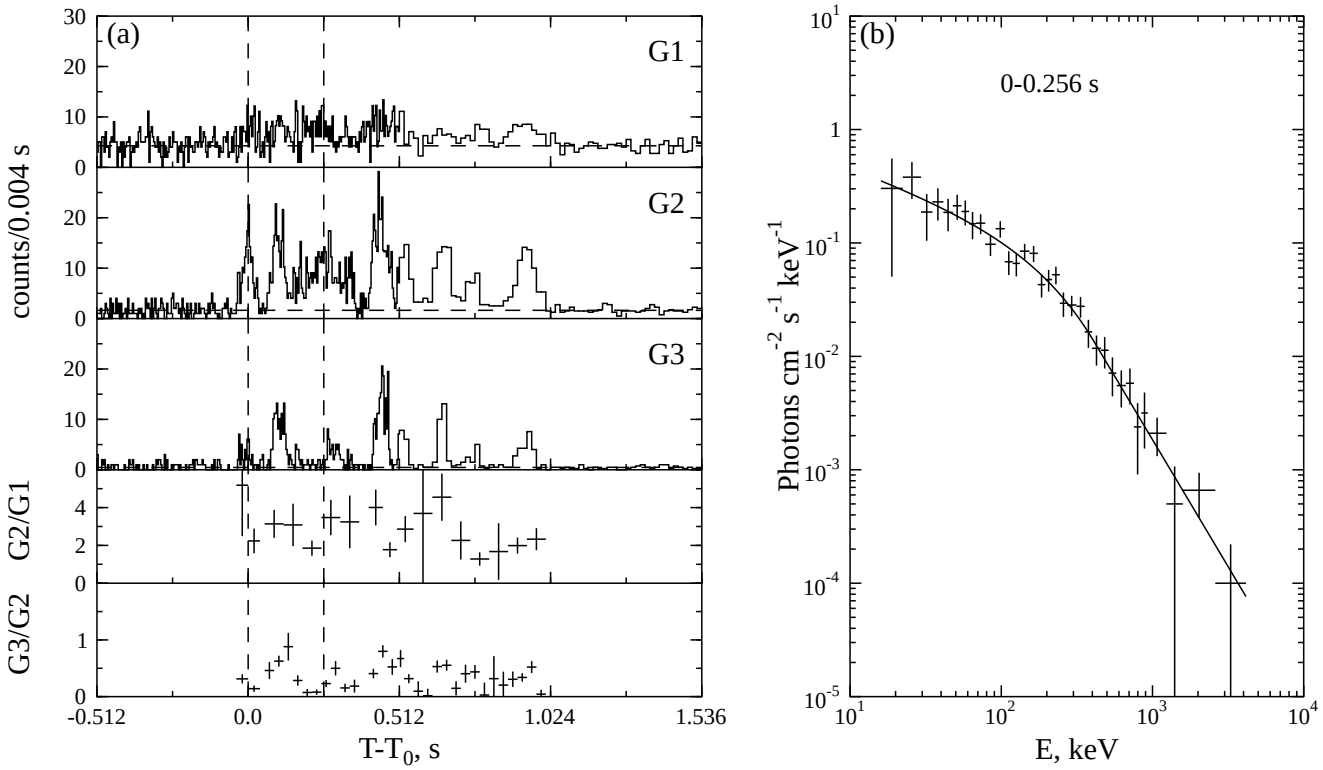

Fig. 146.— GRB 010628a. T_0=4206.816 s UT.

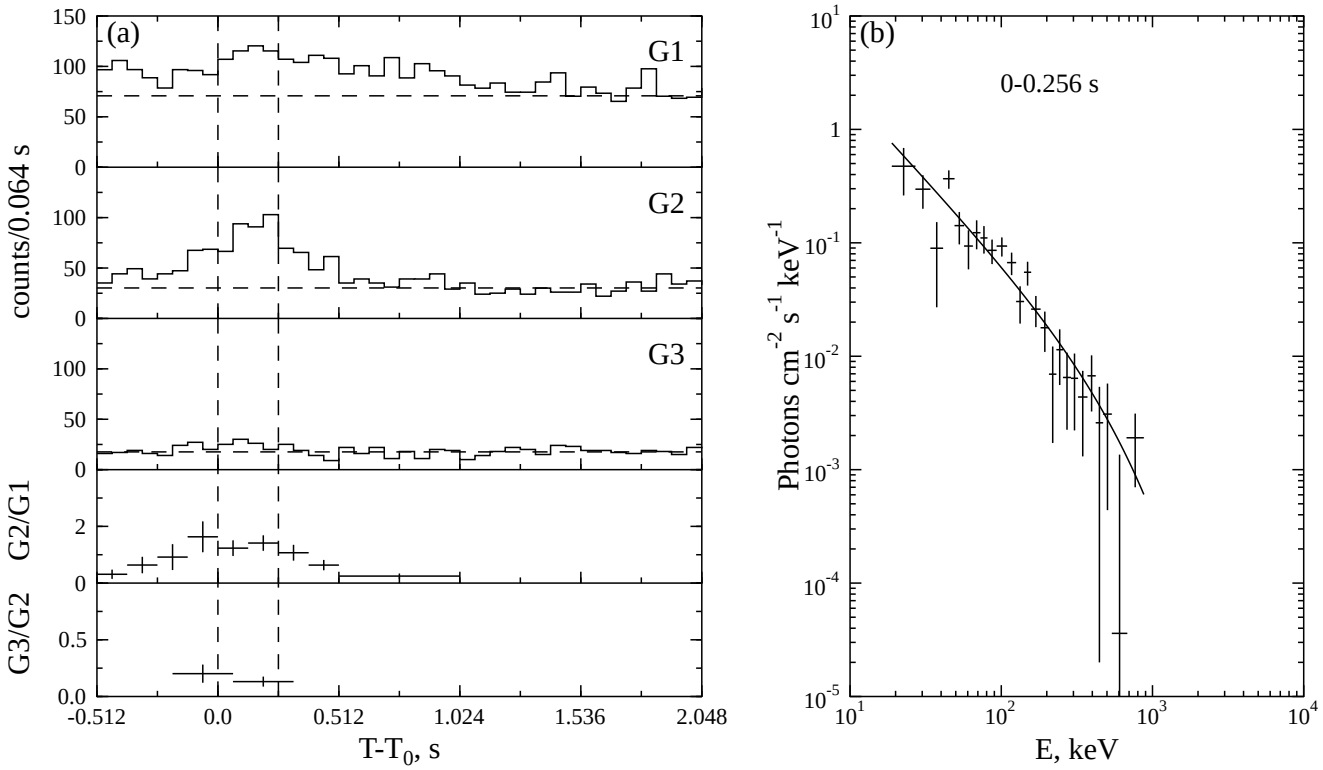

Fig. 147.— GRB 011024. T_0=74609.296 s UT.

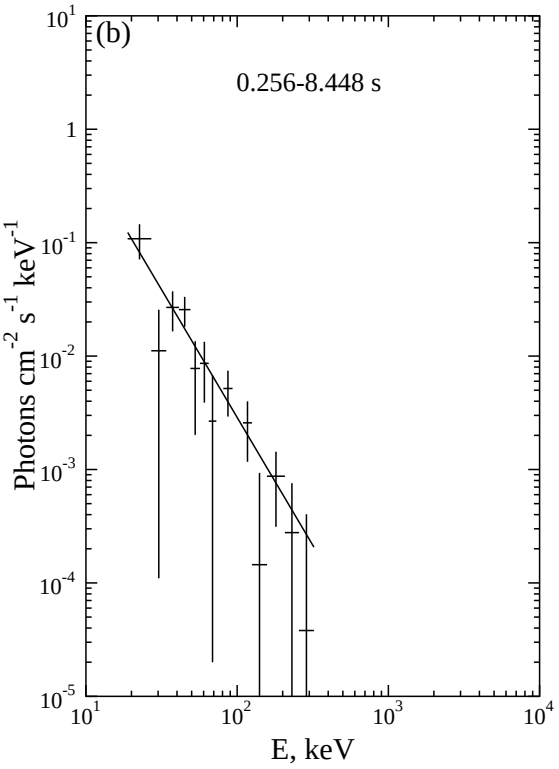

Fig. 148.— GRB 011024. T_0=74609.296 s UT (continued from Fig. 147).

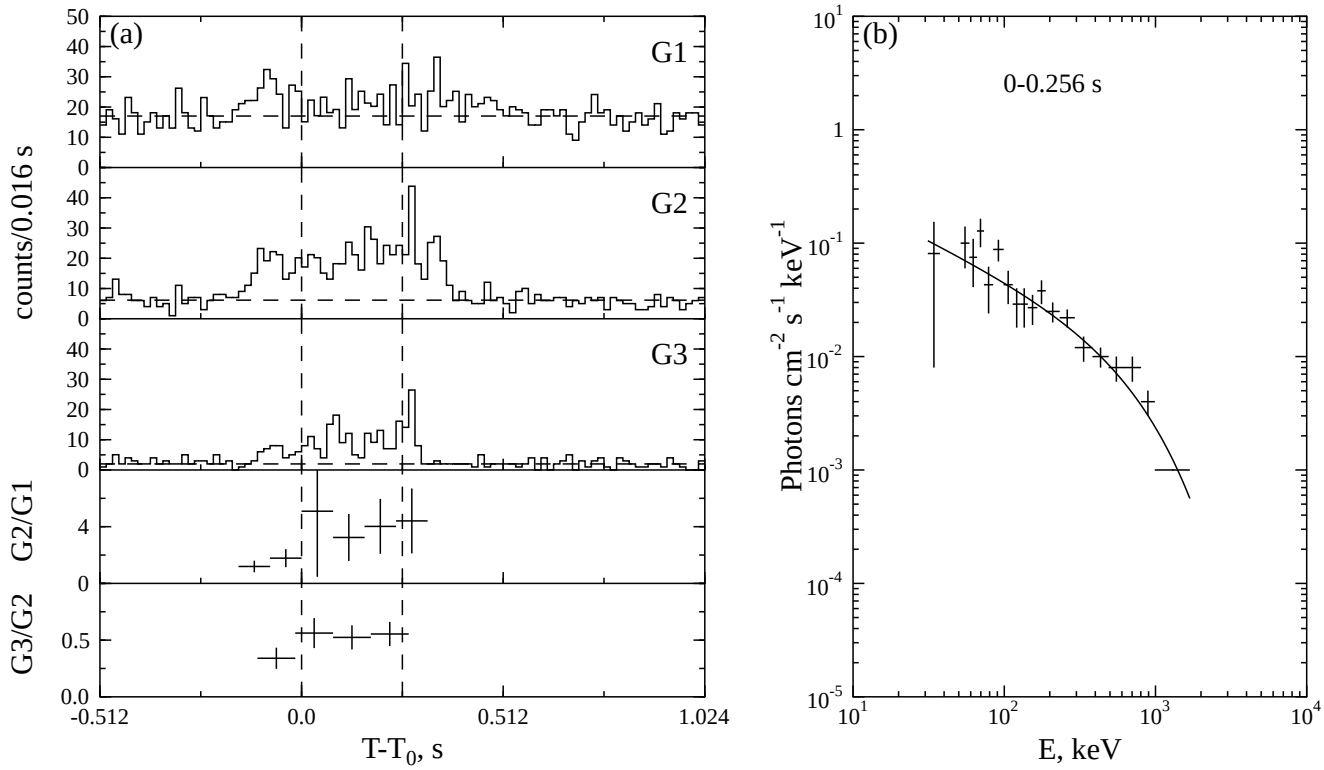

Fig. 149.— GRB 011101. T_0=34754.534 s UT.

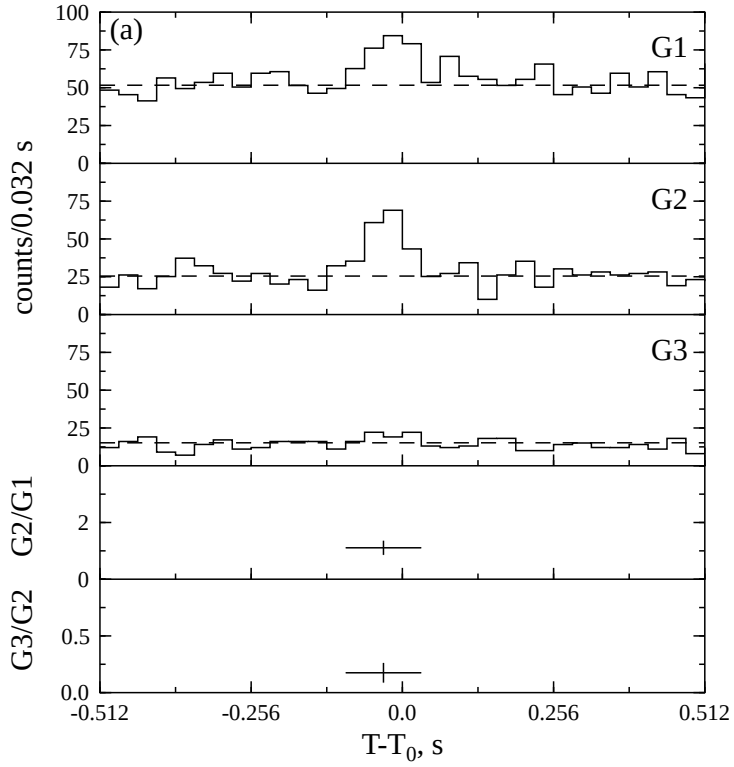

Fig. 150.— GRB 020116. T_0=67773.429 s UT.

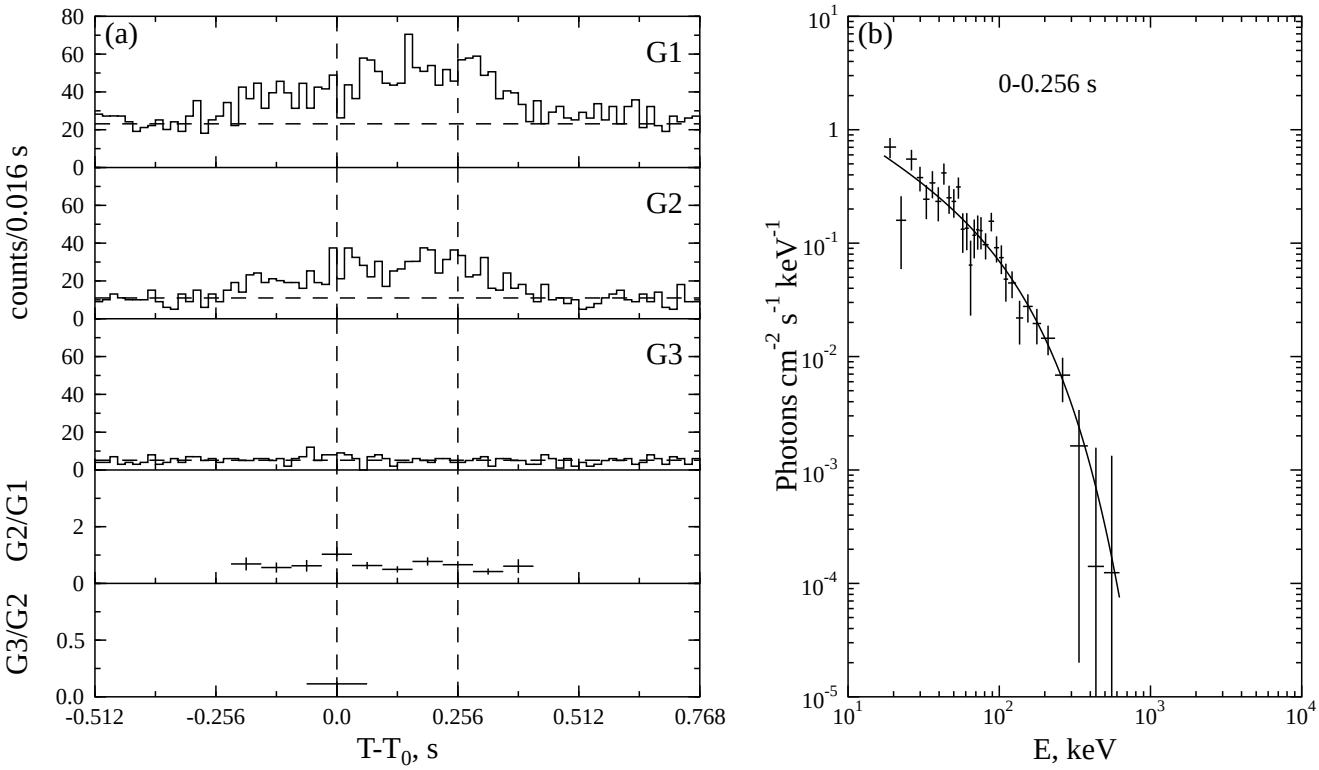

Fig. 151.— GRB 020117. T_0=45909.324 s UT.

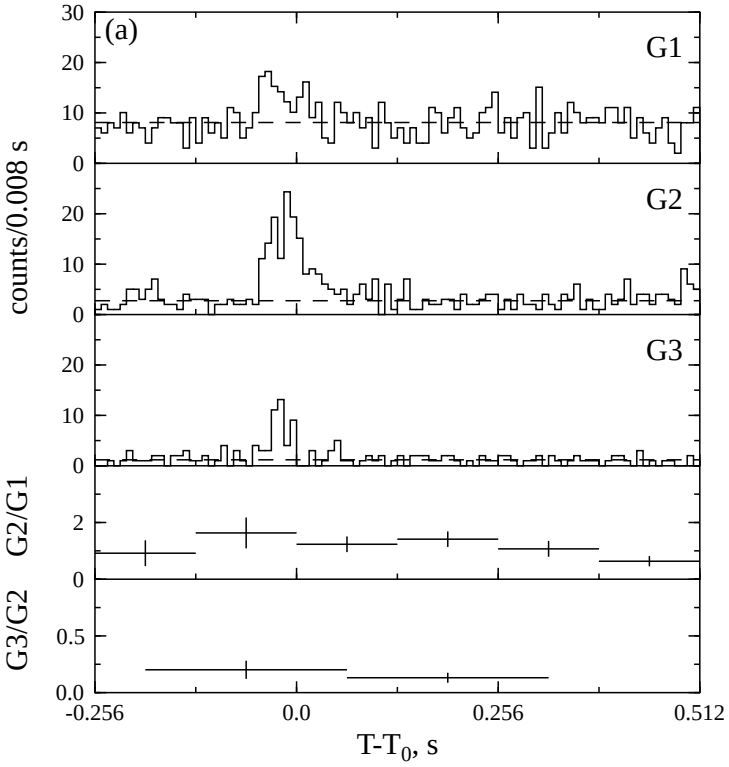

Fig. 152.— GRB 020218a. T_0=74609.296 s UT.

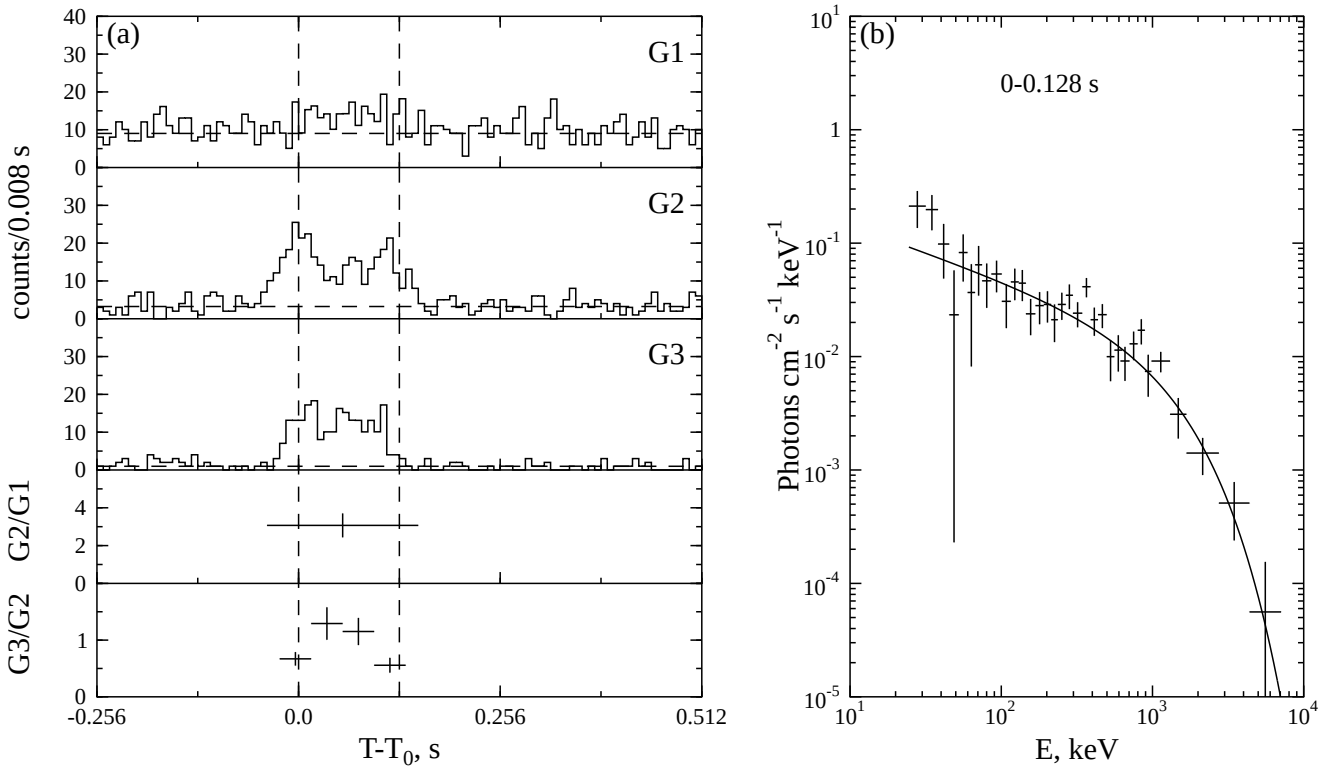

Fig. 153.— GRB 020306. T_0=68280.713 s UT.

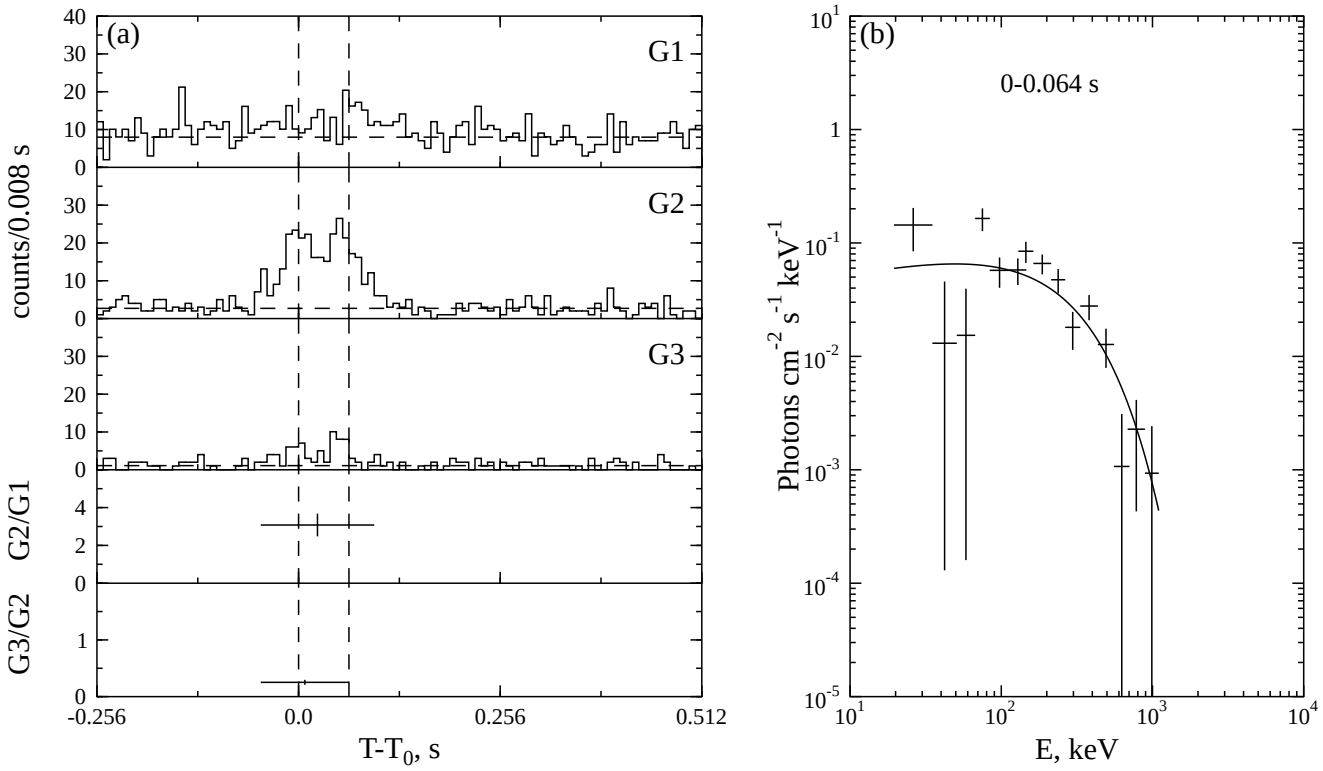

Fig. 154.— GRB 020326. T_0=39182.941 s UT.

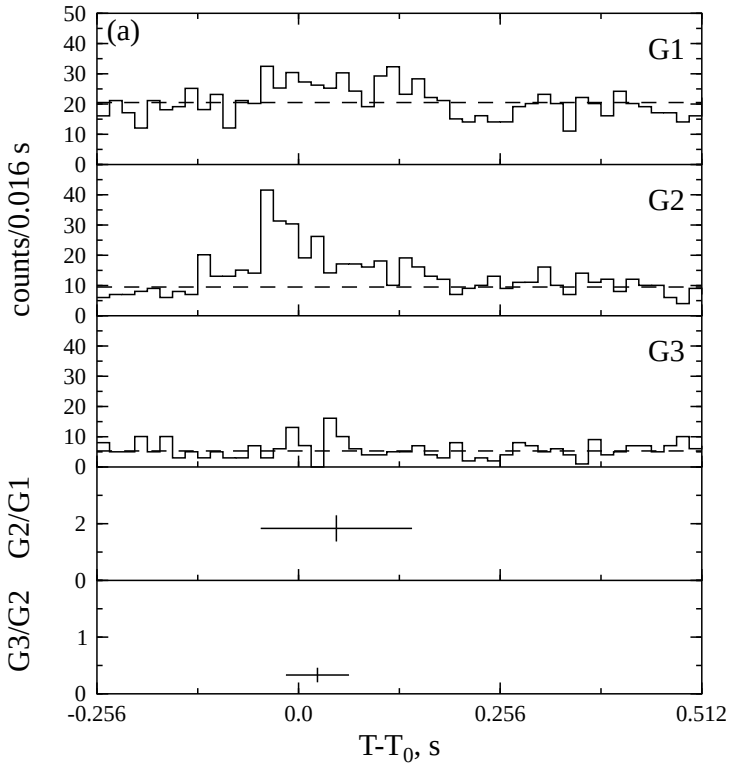

Fig. 155.— GRB 020426. T_0=39182.941 s UT.

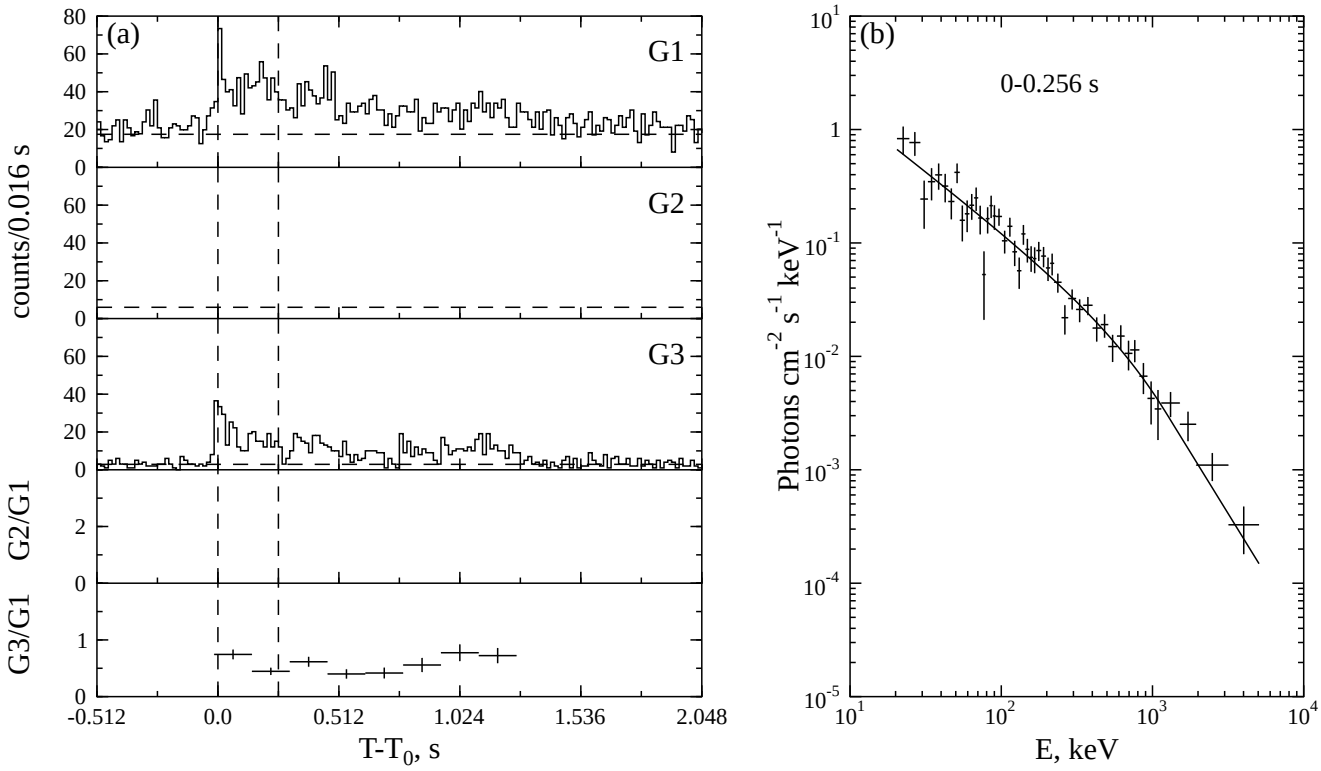

Fig. 156.— GRB 020504. T_0=55835.141 s UT.

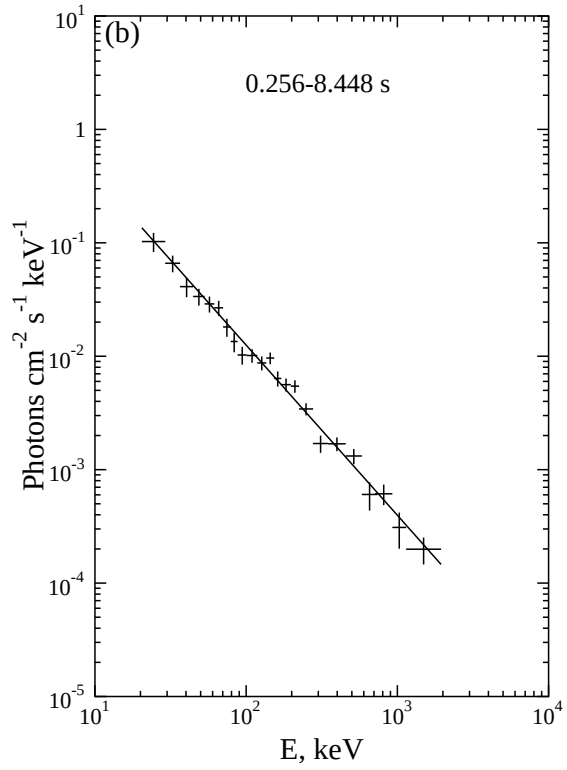

Fig. 157.— GRB 020504. T_0=55835.141 s UT (continued from Fig. 157).

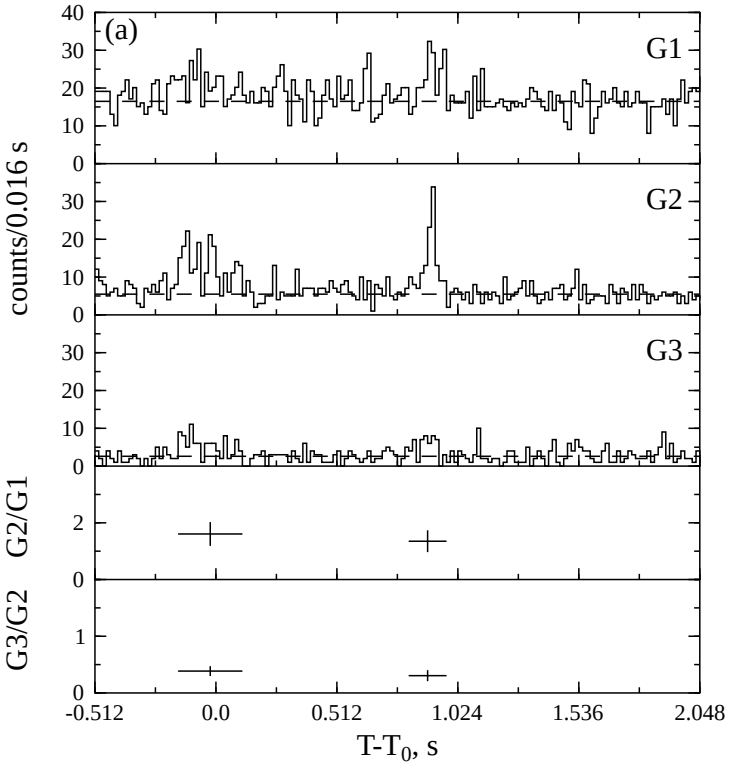

Fig. 158.— GRB 020509. T_0=74.563 s UT.

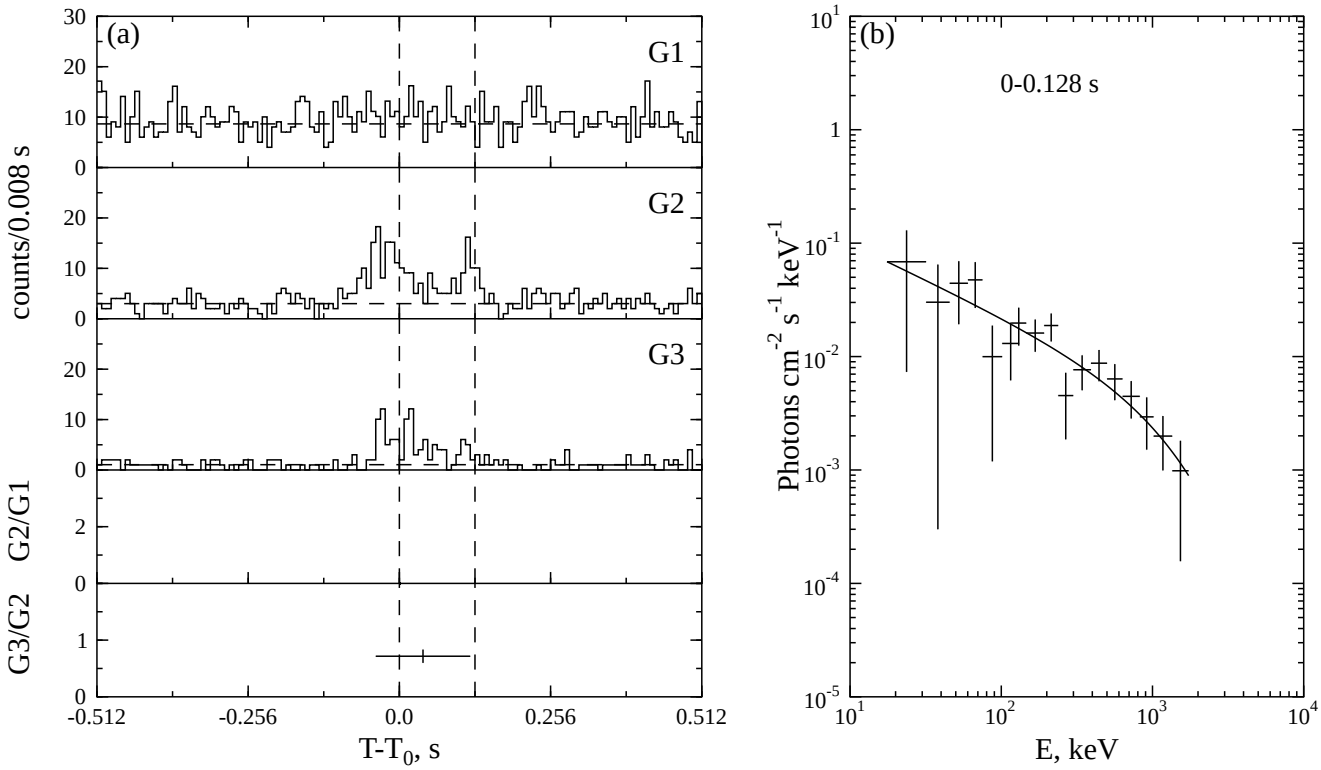

Fig. 159.— GRB 020525a. T_0=16014.630 s UT.

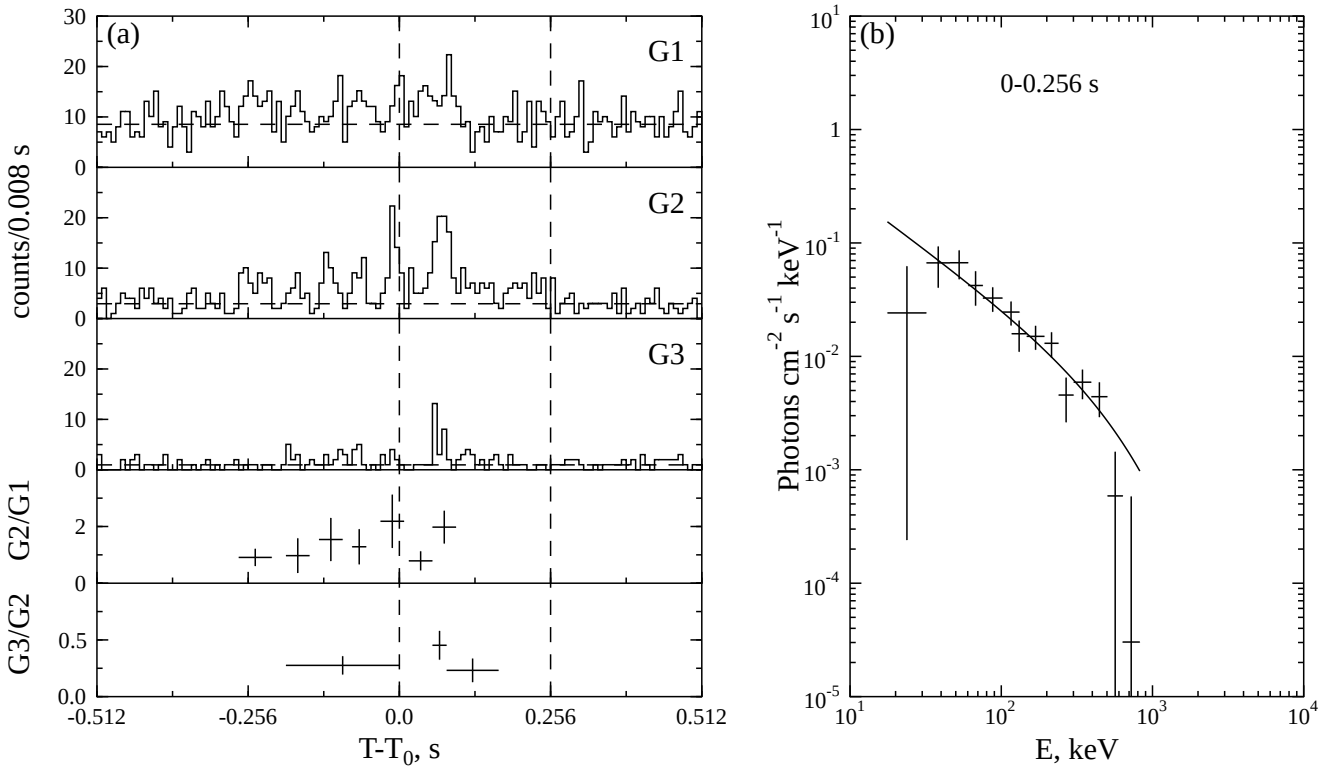

Fig. 160.— GRB 020602b. T_0=63030.315 s UT.

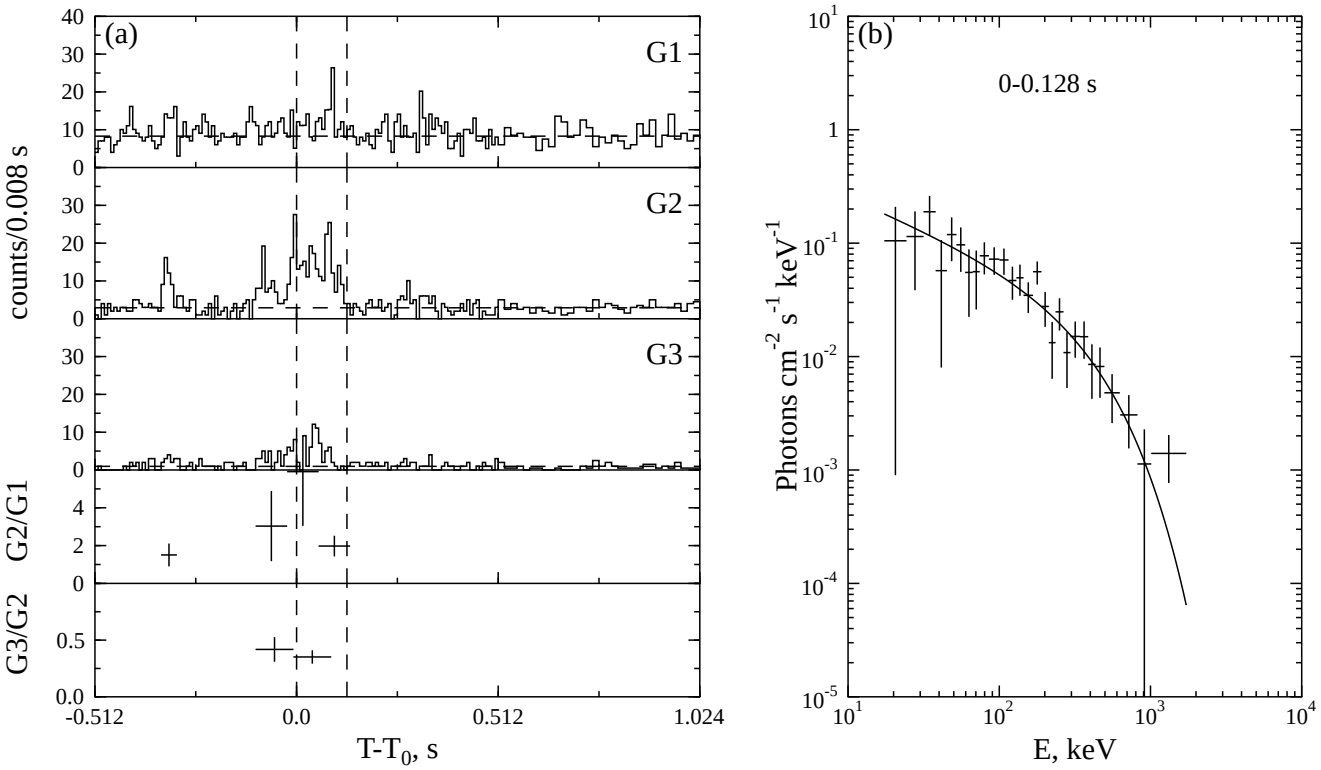

Fig. 161.— GRB 020715a. T_0=54866.135 s UT.

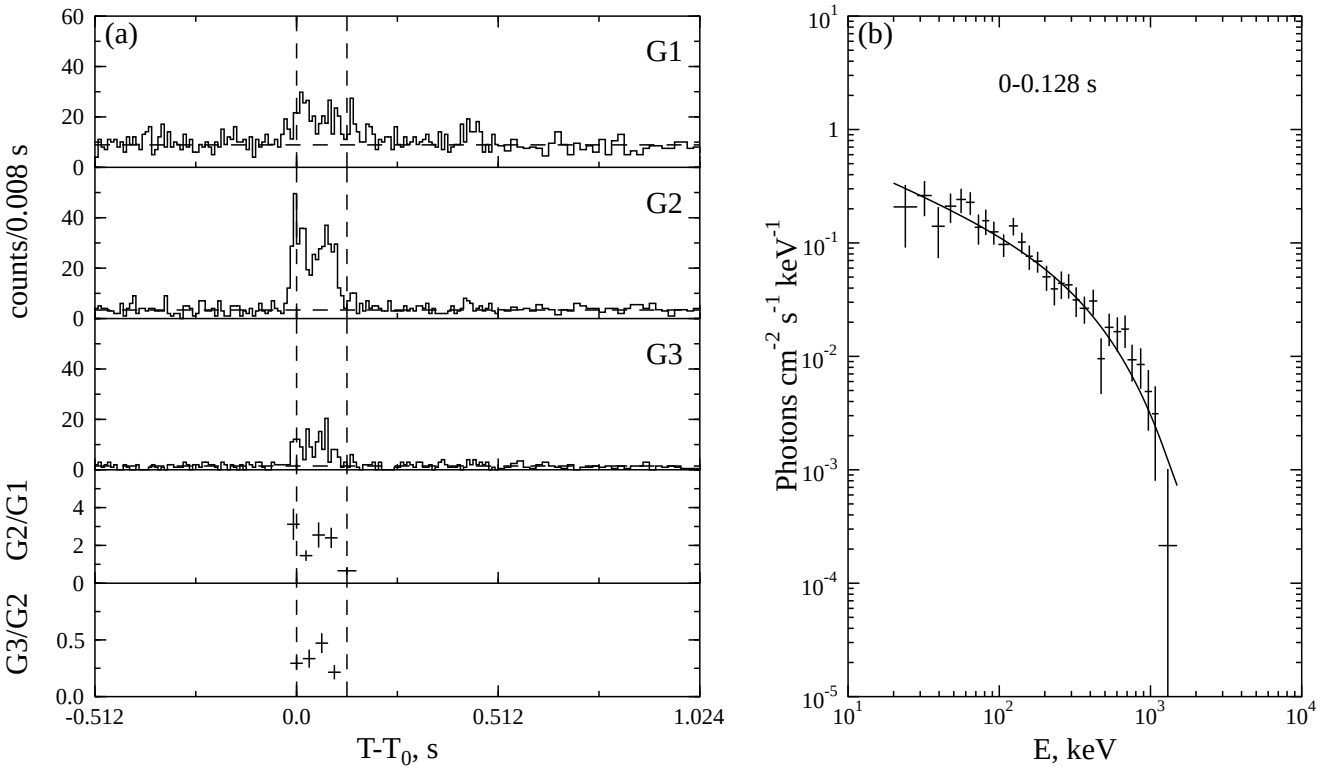

Fig. 162.— GRB 020731a. T_0=1635.905 s UT.

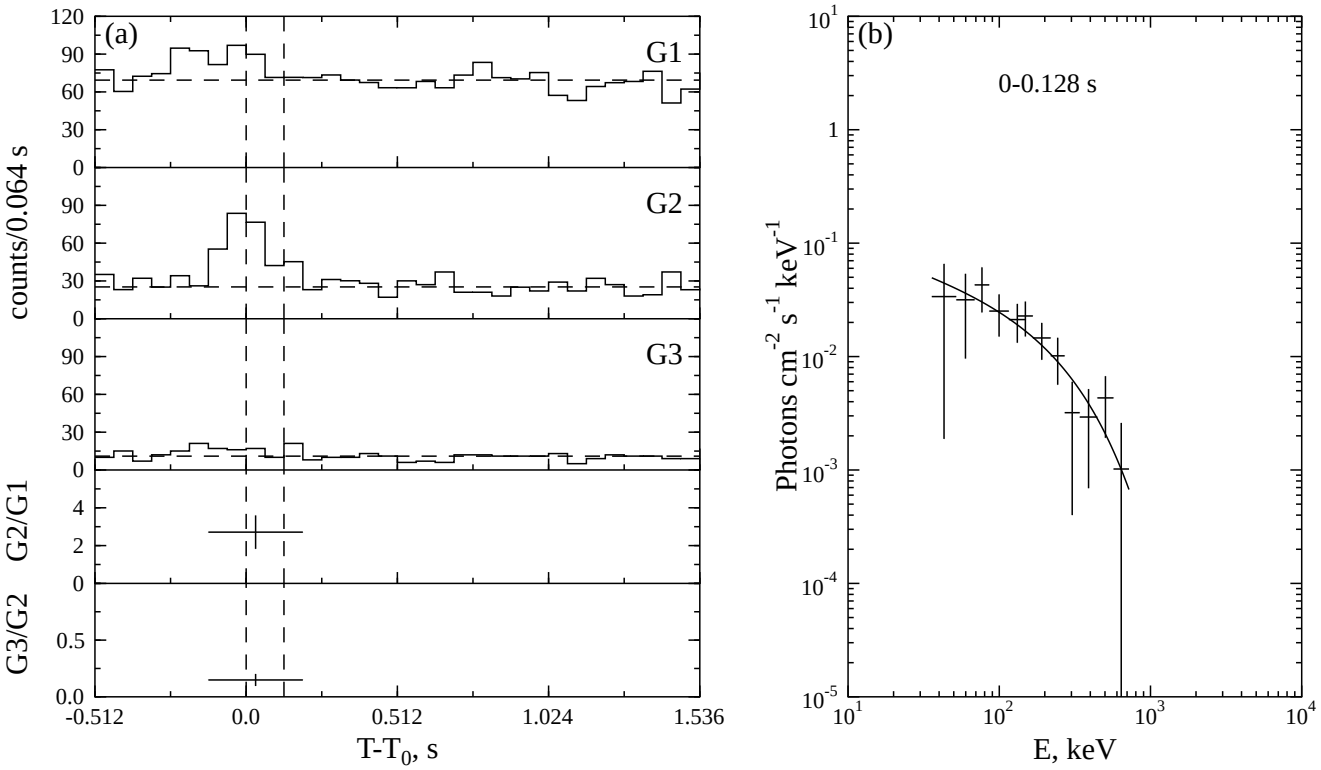

Fig. 163.— GRB 020731b. T_0=50231.739 s UT.

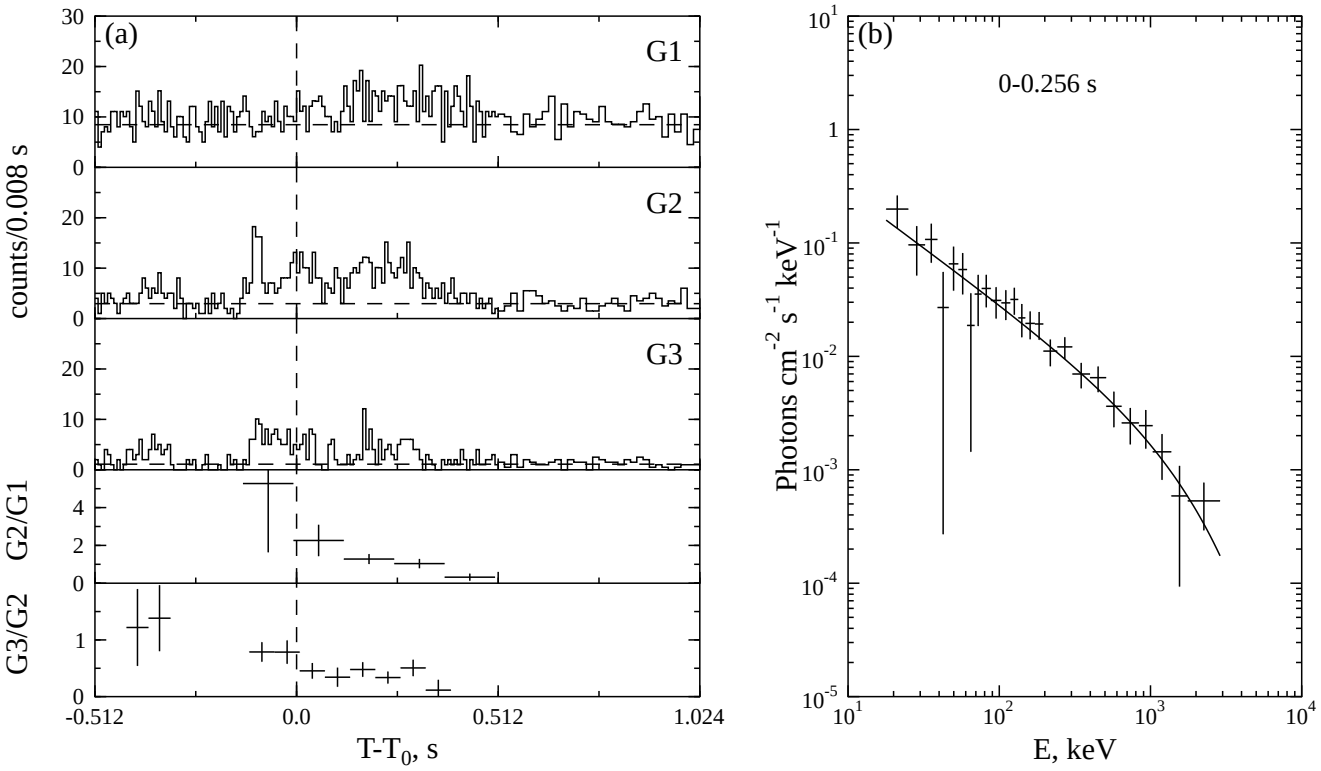

Fig. 164.— GRB 020828. T_0=20737.981 s UT.

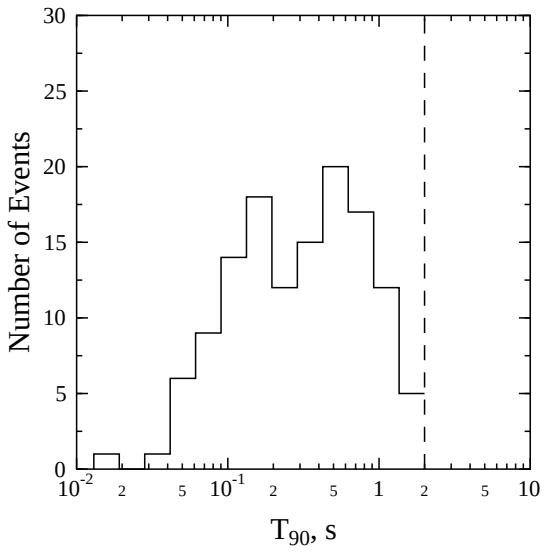

Fig. 165.— Duration distribution.

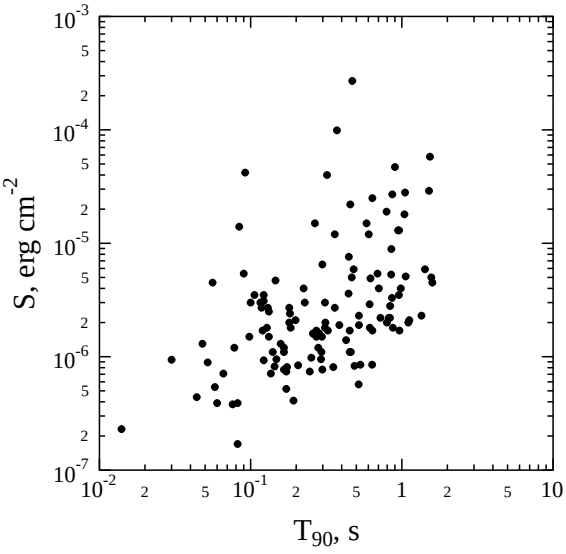

Fig. 166.— Fluence vs duration distribution.

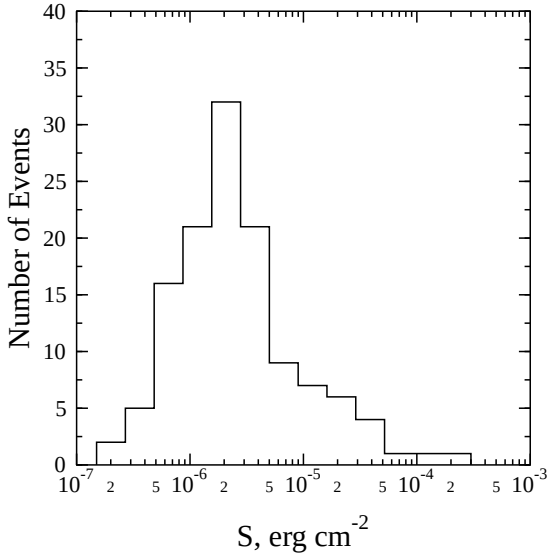

Fig. 167.— Fluence distribution.

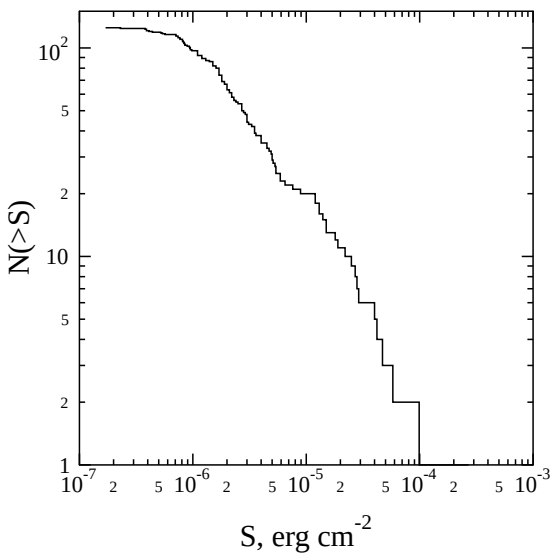

Fig. 168.— Cumulative fluence distribution.

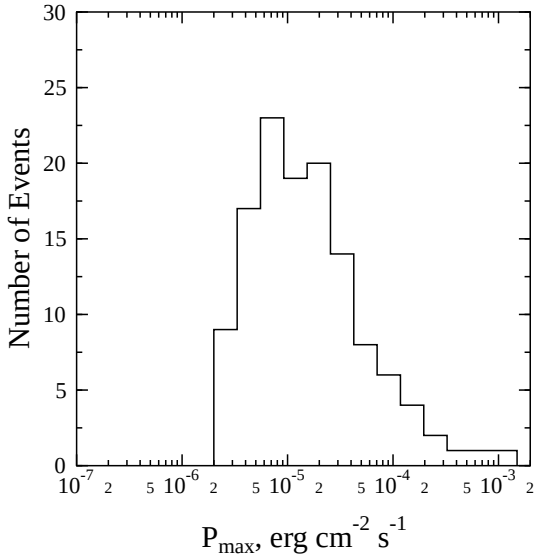

Fig. 169.— Peak flux distribution.

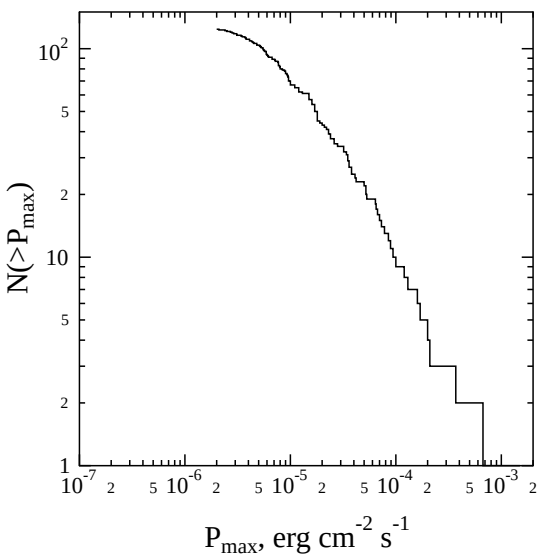

Fig. 170.— Cumulative peak flux distribution.

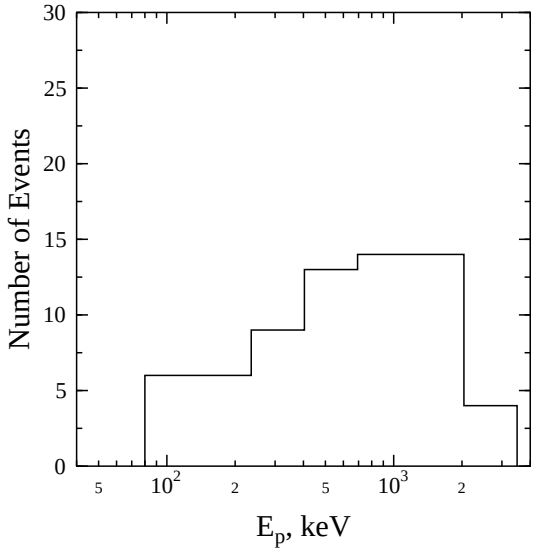

Fig. 171.— E_p distribution (E_p is the energy at which the EF_E-spectrum ($F_E = E\,\mathrm{d}N/\mathrm{d}E$) reaches its maximum).

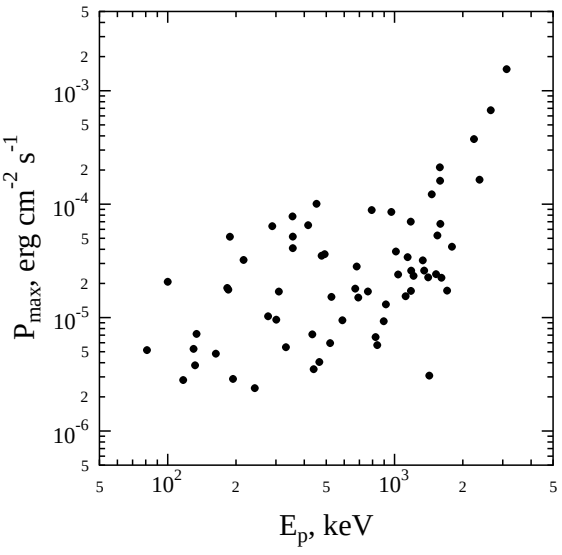

Fig. 172.— Peak flux vs E_p distribution.